Volume 6, Number 4
July–August 1998

ISSN: 0869-5938

STRATIGRAPHY AND GEOLOGICAL CORRELATION

Official English Translation of *Stratigrafiya. Geologicheskaya Korrelyatsiya*

Editor-in-Chief
Boris S. Sokolov

Member of the Russian Academy of Sciences
Counsellor of the Presidium of the Russian Academy of Sciences

Journal of the Fundamental and Applied Aspects of Stratigraphy and the Correlation of Geologic Events and Processes in Time and Space

МАИК НАУКА/INTERPERIODICA PUBLISHING

Stratigraphy and Geological Correlation

(Stratigrafiya, Geologicheskaya Korrelyatsiya)

ISSN: 0869-5938

Editor-in-Chief
Boris S. Sokolov
Member of the Russian Academy of Sciences,
Counsellor of the Presidium of the Russian Academy of Sciences

Address for correspondence: Staromonetnyi per. 22, Moscow, 109180 Russia
Phones: 7 (095) 951-2164; Fax: 7 (095) 233-5590.

Deputy Editor-in-Chief
Mikhail A. Semikhatov
Member of the Russian Academy of Sciences
Head of Laboratory, Geological Institute,
Russian Academy of Sciences

Assistant Editor
Aleksei B. Herman
Senior Scientist,
Geological Institute,
Russian Academy of Sciences

EDITORIAL BOARD

Mikhail A. Akhmet'ev
Dr. Sci. (Geol.–Min.),
Head of Laboratory, Geological Institute,
Russian Academy of Sciences

Aleksandr S. Alekseev
Professor, Department of Paleontology,
Moscow State University

Mikhail N. Alekseev
Dr. Sci. (Geol.–Min.),
Chief Scientist, Geological Institute,
Russian Academy of Sciences

Ivan A. Basov
Dr. Sci. (Geol.–Min.),
Deputy Director, Institute of the Lithosphere,
Russian Academy of Sciences

Michael G. Basset
Professor, National Museum of Wales,
Cardiff, UK

William A. Berggren
Professor, Department of Geology and
Geophysics, Woods Hole Oceanographic
Institute, USA

Elena V. Bibikova
Dr. Sci. (Geol.–Min.), Chief Scientist,
Vernadskii Institute of Geochemistry
and Analytical Chemistry,
Russian Academy of Sciences

Nikita A. Bogdanov
Corresponding Member of the Russian Academy
of Sciences, Director, Institute of the
Lithosphere, Russian Academy of Sciences

Kiyotaka Chinzei
Professor, Institute of Geology,
University of Tokyo, Tokyo, Japan

Nikolai M. Chumakov
Dr. Sci. (Geol.–Min.),
Chief Scientist, Geological Institute,
Russian Academy of Sciences

Yurii B. Gladenkov
Dr. Sci. (Geol.–Min.),
Head of Laboratory, Geological Institute,
Russian Academy of Sciences

Dmitrii L. Kaljo
Professor, Institute of Geology, Tallinn, Estonia

Victor E. Khain
Member of the Russian Academy of Sciences,
Chief Scientist, Institute of the Lithosphere,
Russian Academy of Sciences

Lidiya A. Nevesskaya
Dr. Sci. (Biol.), Laboratory Chief, Institute of
Paleontology, Russian Academy of Sciences

Aleksandr G. Ponomarenko
Dr. Sci. (Biol.), Chief Scientist, Institute of
Paleontology, Russian Academy of Sciences

Jurgen Remane
Professor, Institute de Géologie,
Université de Neuchâtel, Switzerland

Aleksei Yu. Rozanov
Dr. Sci. (Geol.–Min.),
Director, Institute of Paleontology,
Russian Academy of Sciences

Boris A. Sokolov
Dr. Sci. (Geol.–Min.),
Professor, Dean, Faculty of Geology,
Moscow State University

Otto Walliser
Professor,
Göttingen University, Göttingen, Germany

Sun Weigo
Professor, Nanjing Institute of Geology
and Paleontology, Academia Sinica, China

Victor A. Zakharov
Dr. Sci. (Geol.–Min.),
Head of Laboratory, Institute of Geology,
Geophysics, and Mineralogy,
Siberian Branch, Russian Academy
of Sciences, Novosibirsk

Aleksandr I. Zhamoida
Corresponding Member of the Russian Academy
of Sciences, Russian Geological Institute,
St. Petersburg

Staff Editor Tamara V. Trishkina

Editor of the English Translation Anatolii Ya. Sharas'kin, Dr. Sci. (Geol.–Min.)

SCOPE

Stratigraphy and Geological Correlation (Stratigrafiya, Geologicheskaya Korrelyatsiya) is the only journal in the world designed to provide comprehensive coverage of the fundamental and applied aspects of stratigraphy and the correlation of geological events and processes in time and space. Articles are based on the results of multidisciplinary research and are directed toward researchers, university professors, students, and geologists interested in understanding stratigraphy and the chronological features of the world's geological record.

Stratigraphy and Geological Correlation is abstracted and/or indexed in *Petroleum Abstracts*, *Research Alert*, *SciSearch*, *Current Contents* (*Physical, Chemical*, and *Earth Sciences*) and *World Translations Index*.

SUBSCRIPTION OFFICE
INTERPERIODICA
P.O. BOX 1831, BIRMINGHAM, AL 35201-1831 USA
PHONE: (800) 633-4931; (205) 995-1567 (outside US and Canada);
FAX: (205) 995-1588

PUBLISHER
МАИК НАУКА/INTERPERIODICA PUBLISHING
PROFSOYUZNAYA UL. 90, MOSCOW, 117864 RUSSIA
PHONE: 7 (095) 336-1600; FAX: 7 (095) 336-0666
E-mail: compmg@maik.rssi.ru
Web Site: http://www.maik.rssi.ru

SUBSCRIPTION PRICES (1998, Volume 6, 6 issues)
US $839.00 (North America), $964.00 (elsewhere). A 5% discount is given on 2-year orders. Subscriptions may be entered at any time. Orders may be placed at agencies or directly. There is a 5% discount to all subscription agencies. Cancellations not allowed except for duplicate payment. Prepayment required. Advance payment required in US$/US bank. MasterCard/Visa accepted. Make checks payable to *Stratigraphy and Geological Correlation* or Interperiodica.

Stratigraphy and Geological Correlation (ISSN: 0869-5938) is published bimonthly for US $839.00 (North America), outside North America for $964.00 per year by MAIK Nauka/Interperiodica Publishing, 5724 Hwy. 280 East, Birmingham, Alabama 35242-5724 USA. Periodical postage paid at Birmingham, Alabama, and additional mailing offices. POSTMASTER: Send address changes to *Stratigraphy and Geological Correlation*, P.O. Box 1831, Birmingham, Alabama 35201 USA.

The journal was founded in 1993.

Original Russian Edition Copyright © 1998 by the Russian Academy of Sciences
and Division of Geology, Geophysics, Geochemistry, and Mining Sciences.
English Translation Copyright © 1998 by МАИК Наука/Interperiodica Publishing (Russia).

Contents

Vol. 6, No. 4, 1998

Simultaneous English language translation of the journal is available from МАИК Наука/Interperiodica Publishing (Russia). *Stratigraphy and Geological Correlation* ISSN 0869-5938.

Carbonate Carbon Isotopic Composition in the Upper Riphean Stratotype, the Karatau Group, Southern Urals

V. N. Podkovyrov, M. A. Semikhatov, A. B. Kuznetsov, D. P. Vinogradov, V. I. Kozlov, and I. V. Kislova 319

U-Pb Systematics on Proterozoic Carbonate Rocks: The Inzer Formation of the Upper Riphean Stratotype (Southern Urals)

G. V. Ovchinnikova, I. M. Vasil'eva, M. A. Semikhatov, A. B. Kuznetsov, I. M. Gorokhov, B. M. Gorokhovskii, and L. K. Levskii 336

Silurian Stratigraphic Scale for East Siberia

Yu. I. Tesakov, N. N. Predtechenskii, V. G. Khromykh, and A. Ya. Berger 348

Large Ruscinian Mammalia in the Territory of the Former Soviet Union

E. A. Vangengeim, I. A. Vislobokova, and M. V. Sotnikova 368

The Late Oligocene of Belarus

L. I. Murashko, T. B. Rylova, and T. V. Yakubovskaya 383

Stratigraphy of the Upper Cenozoic Volcanosedimentary Sequence in the East Sayan Mountains Adjacent to the Baikal Region

N. A. Logachev, S. V. Rasskazov, A. V. Ivanov, V. A. Misharina, and G. P. Chernyaeva 397

Tectonostratigraphy of the Northern Olyutor Zone (Anastasiya Bay area of Koryak Highland)

A. V. Solov'ev, T. N. Palechek, and R. M. Palechek 408

Critics and Discussions

On the Taimyr Stage of the Continental Permian Deposits in Siberia

N. K. Mogucheva 422

Stratigraphy and Geological Correlation, Vol. 6, No. 4, 1998, pp. 319–335. Translated from Stratigrafiya. Geologicheskaya Korrelyatsiya, Vol. 6, No. 4, 1998, pp. 3–19.
Original Russian Text Copyright © 1998 by Podkovyrov, Semikhatov, Kuznetsov, Vinogradov, Kozlov, Kislova.
English Translation Copyright © 1998 by МАИК Наука/Interperiodica Publishing (Russia).

Carbonate Carbon Isotopic Composition in the Upper Riphean Stratotype, the Karatau Group, Southern Urals

V. N. Podkovyrov*, M. A. Semikhatov, A. B. Kuznetsov*, D. P. Vinogradov*, V. I. Kozlov***, and I. V. Kislova****

** Institute of Precambrian Geology and Geochronology, Russian Academy of Sciences, nab. Makarova 2, St. Petersburg, 199034 Russia*
*** Geological Institute, Russian Academy of Sciences, Pyzhevskii per. 7, Moscow, 109017 Russia*
**** Institute of Geology, Ufa Research Center, Russian Academy of Sciences, ul. K. Marksa 16/2, Ufa, 450000 Russia*
Received October 10, 1996

Abstract—The Karatau Group of the Southern Urals furnishes an opportunity to reveal the C-isotopic composition for the major part of the Upper Riphean in a single type succession comprising, according to radiometric and paleontological evidence, both the lower and upper horizons of this unit (1000 ± 50–650 ± 20 Ma). In the studied sections, the group is dominated by carbonate deposits, which in terms of cathodoluminescent, geochemical and isotopic–geochemical data can be considered insignificantly altered and retaining the primary C-isotopic signature. Limestones of the lower Katav Subformation, lowermost in the carbonate succession of the group, show the descending trend of $\delta^{13}C$ values from 4.4 down to –0.8‰ PDB, whereas limestones of the upper Katav Subformation and the lower part of the overlying lower Inzer Subformation demonstrate the ascending trend up to 3.9‰ with three positive excursions. The upper part of the lower Inzer limestones is characterized by low positive values of $\delta^{13}C$ and the upper Inzer limestones, by the low negative values. Limestones and dolomites of the overlying Min'yar Formation display the largest for the Karatau Group range of $\delta^{13}C$ variations from –2.2 to 5.9‰ with four peaks. The Uk Formation limestones, which terminate the Karatau carbonate succession, show again the low positive values of $\delta^{13}C$. Variations of $\delta^{13}C$ in the Karatau Group are basically consistent with the general Upper Riphean trend. However, contrary to other Upper Riphean sections, the Karatau Group is devoid of long intervals characterized by high (>6‰) values and demonstrates much smaller $\delta^{13}C$ range. These distinctions may be due to significant stratigraphic hiatuses in the Karatau carbonate succession.

Key words: *Proterozoic, Neoproterozoic, Upper Riphean, carbon isotopic chemostratigraphy, carbonate carbon isotopic composition, Southern Urals*

Secular $\delta^{13}C$ variations in carbonates reflecting the balance between the carbonate and organic carbon in the World Ocean have come into common use for the Upper Riphean and Vendian (Neoproterozoic) chemostratigraphy and for substantiating wide biochemical reconstructions in this part of the geological record (Brasier, 1992; Kaufman *et al.*, 1993, 1996; Kaufman and Knoll, 1995; Knoll *et al.*, 1995; Semikhatov, 1995 and references herein). The increased information shows that the Late Riphean and Vendian (especially the second half of this interval, 850–530 Ma) were characterized by very noticeable secular $\delta^{13}C$ variations in seawater in response to significant fluctuations in the global carbon cycle, biospheric oxygen budget, and climate.

However, the recent model for the $\delta^{13}C$ variations throughout the Neoproterozoic is based not on the long-ranged type successions of the Upper Riphean and Vendian, but on several discrete portions of Neoproterozoic sections exposed in distant regions. The correlation of these portions to each other and, especially, to the Upper Riphean and Vendian stratotypes, as well as their radiometric calibration, requires further investigations and, in some cases, a more strict approach than is done now.

An opportunity to obtain the C-isotopic chemostratigraphic characteristics for the most of the Upper Riphean deposits forming a single type succession is to study the Karatau Group of the Southern Urals, which is the Upper Riphean stratotype dominated in the western sections by insignificantly altered carbonates (*Stratotip...*, 1983). To realize this opportunity we investigated a representative collection of the Karatau carbonates in which we determined the strontium (Gorokhov *et al.*, 1996; Kuznetsov *et al.*, 1997) and carbon (Semikhatov *et al.*, 1995; Podkovyrov *et al.*, 1997) isotopic compositions and isochron Pb-Pb ages (Ovchinnikova *et al.*, 1995a, 1998). All obtained data on the $\delta^{13}C$ and $\delta^{18}O$ variations in the Karatau limestones and dolomites, as well as the characteristics of secondary alter-

ations of these rocks evaluated by using the integrated petrographic, cathodoluminescent, geochemical and isotopic-geochemical analyses are presented below.

LITHOSTRATIGRAPHY AND RADIOMETRIC AGE OF THE KARATAU GROUP

The Karatau Group represents a thick (3.0–5.5 km) sedimentary complex, which terminates the Riphean stratotype section exposed within the Bashkir meganticlinorium at the western slope of the Southern Urals. These deposits widespread in the western part of the meganticlinorium are underlain by the Middle Riphean type unit (the Yurmatin Group) and unconformably overlain by the Vendian strata. The succession and composition of the majority of formations within the Karatau Group were firmly established long ago (Garan', 1963; Kozlov, 1982; *Stratotip* ..., 1983), but spatial–chronological relationships between carbonate and siliciclastic lithostratigraphic units in its middle part were once a subject of controversy (Raaben, 1975; Komar, 1978; Kozlov, 1982; Raaben and Komar, 1983; Krylov, 1983). However, the recent works seem to resolve these contradictions (Kozlov *et al.*, 1991; Maslov and Krupenin, 1991; *Unifitsirovannye* ..., 1993). At present, the only matter of dispute is the relationships between the Karatau Group and the underlying Yurmatin Group. Some investigators share the traditional opinion suggesting an unconformity between these groups, whereas the others argue for their conformable relations (Kozlov, 1982; *Stratotip* ..., 1983; Maslov, 1990; Kozlov *et al.*, 1991; Shalaginov and Maslov, 1997).

According to the recent regional scales, the Karatau Group consists of six formations: the siliciclastic Zil'merdak Formation (1200–3300 m), the Katav Formation of variegated limestones (200–350 m), the Inzer Formation of variable carbonate–siliciclastic composition (300–800 m), the Min'yar Formation (350–650 m) composed of limestones and dolomites, the siliciclastic–carbonate Uk Formation (160–350 m) that terminates the succession in the western part of the Bashkir meganticlinorium, and the siliciclastic Krivaya Luka Formation (250–300 m), which survived the preVendian erosion in the eastern part of this structure (Kozlov *et al.*, 1991; Semikhatov *et al.*, 1991; *Unifitsirovannye* ..., 1993; Shalaginov and Maslov, 1997). Three lower formations grade upsection into each other everywhere, whereas there are erosion surfaces at the base of the Uk Formation and locally at the base of the Min'yar Formation (Bekker, 1961, 1988; Raaben, 1975; Kozlov, 1982; Kozlov *et al.*, 1991; Maslov and Krupenin, 1991).

We studied the carbonate-rich part of the Karatau Group (the Katav through Uk formations) in the following sections of the western Bashkir meganticlinorium (Fig. 1): (1) in the middle course of the Manaisu River streaming through the western slope of the Zil'merdak Ridge (the main lower part of the Katav Formation); (2) in the town of Min'yar and its vicinity, in the Mt. Krasnaya slopes and the Kashcheev Creek valley (the middle and upper Katav Formation and the lower Inzer Formation), as well as at the right bank of the Sim River and in the B'yanka quarry area (the upper Inzer Formation and the Min'yar Formation excluding the uppermost horizons); (3) at the right bank of the Yuryuzan' River upstream of the Shubino Village (the upper Min'yar Formation and the entire Uk Formation). These sections were easily correlated on the basis of lithostratigraphic criteria and the detailed mapping in the town of Min'yar area. Stratigraphic positions of samples used for C-isotopic analysis are shown in Fig. 2, and the aforementioned formations are briefly described below (for details see Kozlov, 1982; *Stratotip* ..., 1983; Kozlov *et al.*, 1991; Maslov and Krupenin, 1991).

The Katav Formation is subdivided into two subformations. The lower subformation begins with brick-red stromatolitic limestones locally clastic and clayey (65–70 m) and ends with variegated clayey thin-bedded limestones and marls (about 100 m) containing some horizons and lenses of flakestones. The upper subformation (95–100 m) is composed of gray clayey, locally dolomitized limestones with peculiar "striated" (microbial) lamination and rare flakestone interbeds.

The Inzer Formation in the Min'yar section, like everywhere in the western Bashkir meganticlinorium, has the two-unit structure. Its lower subformation (the Podinzer Beds, 190 m) is composed of dark-gray and black flaggy aphanitic limestones lacking siliciclastic admixture and of dolomitic limestones associated with stromatolitic limestones and abundant flakestones in the upper part of the unit. Interbeds of clayey limestones at the base of the Inzer Formation emphasize the gradual transition from the Katav Formation. The upper Inzer Subformation (about 200 m) has the three-member structure: two members of gray to variegated feldspar–quartz glauconitic sandstones, siltstones and rare shales (70 and 50 m) separated by a member of gray stromatolitic, microphitolitic and clastic limestones (80 m).

The studied Min'yar sections (360–380 m) predominantly consists of light-gray and gray mechanogenic and stromatolitic dolomites, subordinate limestones of similar habit confined to the basal and upper horizons of the formation, and lenses and interbeds of flakestones. In the upper half of the formation, the carbonate beds usually contain lenses and nodules of dark-gray early diagenetic cherts whose first occurrence level marks the boundary between the lower (210 m) and upper (160–180 m) subformations. Locally at the base of the formation, there is a thin (1–3.5 m) siliciclastic horizon suggesting, in Raaben's opinion (Raaben, 1975), the pre-Min'yar erosion.

The Uk Formation near the Shubino Village is represented by greenish-gray glauconite–quartz sandstones, siltstones and rare shales with interbeds (0.2–

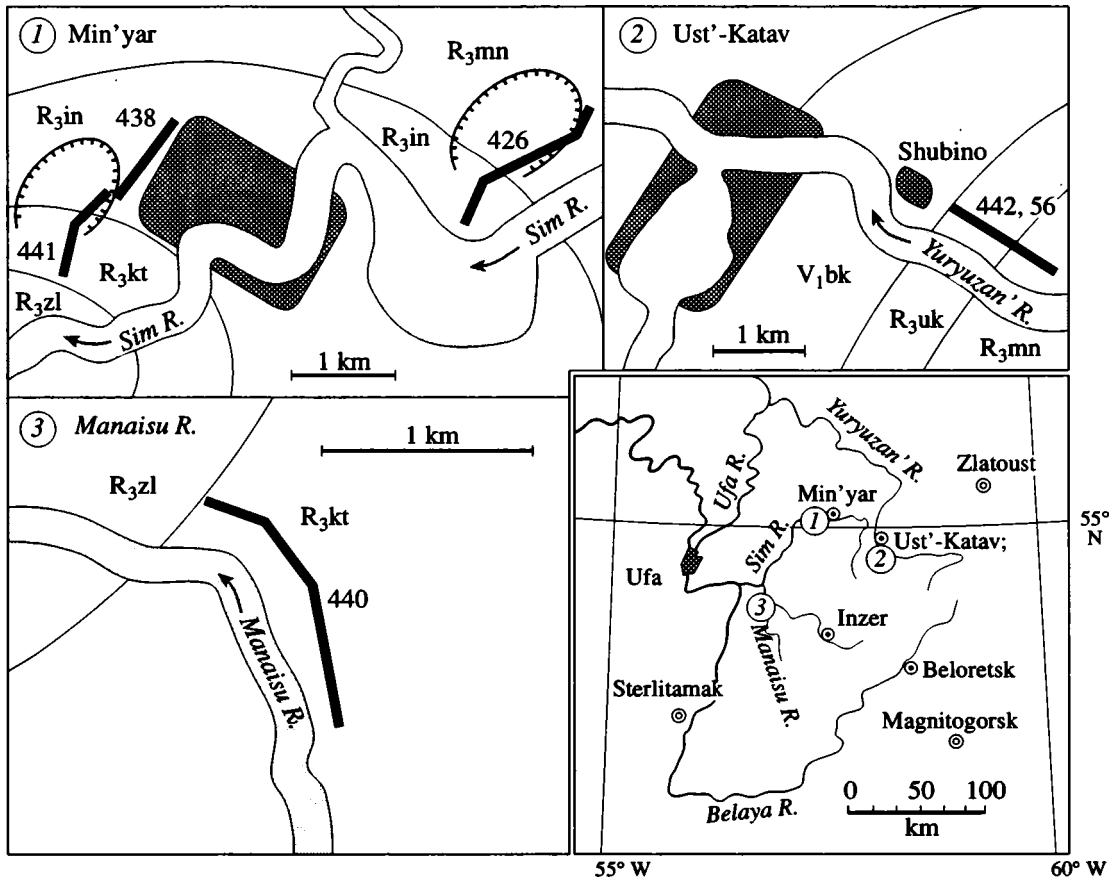

Fig. 1. Localities of the studied carbonate units of the Karatau Group: (*1*) town of Min'yar area; (*2*) Yuryuzan' River upstream near the Shubino Village; (*3*) middle course of the Manaisu River; (R_3zl) Zil'merdak Fm.; (R_3kt) Katav Fm.; (R_3in) Inzer Fm.; (R_3mn) Min'yar Fm.; (R_3uk) Uk Fm. of the Upper Riphean; (Vbk) Bakeevo Fm. of the Vendian.

0.4 m) and thicker members (5–8 m) of limestones in the lower part (70 m), and by gray stromatolitic and rare clastic limestones crowned by dolomites (20–25 m) in the upper part (140 m). The erosional surface can be observed at the base of the formation. This unconformity is likely responsible for the local pinch-out of the upper (Shubino) member of stromatolitic limestones of the Min'yar Formation (Bekker, 1988). Another unconformity at the top of the Uk Formation is much more evident: sandstones and conglomerates of the Vendian Bakeevo Formation overlie its different horizons and locally the Min'yar dolomites.

In the opinion of Maslov (1988, 1997), the described deposits were accumulated in a subtidal setting and document the transition from the shallow-water marine environment of the Katav–Inzer time to moderately deep open marine environment of the Min'yar time, and then to slight shallowing in the Uk time. However, structural features of the deposits indicate that the lower Katav, Podinzer and lower Min'yar carbonates were mostly accumulated in relatively deep-water settings near the storm wave base, whereas the stromatolitic and clastic carbonates of these and Uk formations predominantly represent sediments of the open shelf zones with active hydrodynamics.

Inferences on the isotopic age of the Karatau Group are based on determinations variable in methodical aspects. The most reliable is the isochron Pb-Pb age of 836 ± 25 Ma measured for the lower Inzer carbonates and apparently indicating the time of their early diagenesis (Ovchinnikova *et al.*, 1998). This conclusion is supported by the isochron Rb-Sr age determinations on the fine-grained (0.6–2 μm) fractions of authigenic illite from the Inzer Formation: their age range of 805–835 Ma corresponds to a later event of the burial diagenesis (Ovchinnikova *et al.*, 1995a). Mutually consistent K-Ar and isochron Rb-Sr ages of Al-glauconite from the lower siliciclastic member of the Uk Formation (688 ± 10 and 670 ± 10 Ma respectively) attract attention from the methodical viewpoint (Gorozhanin and Kutyavin, 1986). Significance of these dates is evident from the isochron Rb-Sr age (672 ± 22 Ma) for whole-rock samples of volcanics intercalated with sediments correlative to the uppermost part of the Karatau Group in the northern Urals (Semikhatov *et al.*, 1991). In addition, there are some outdated K-Ar age determi-

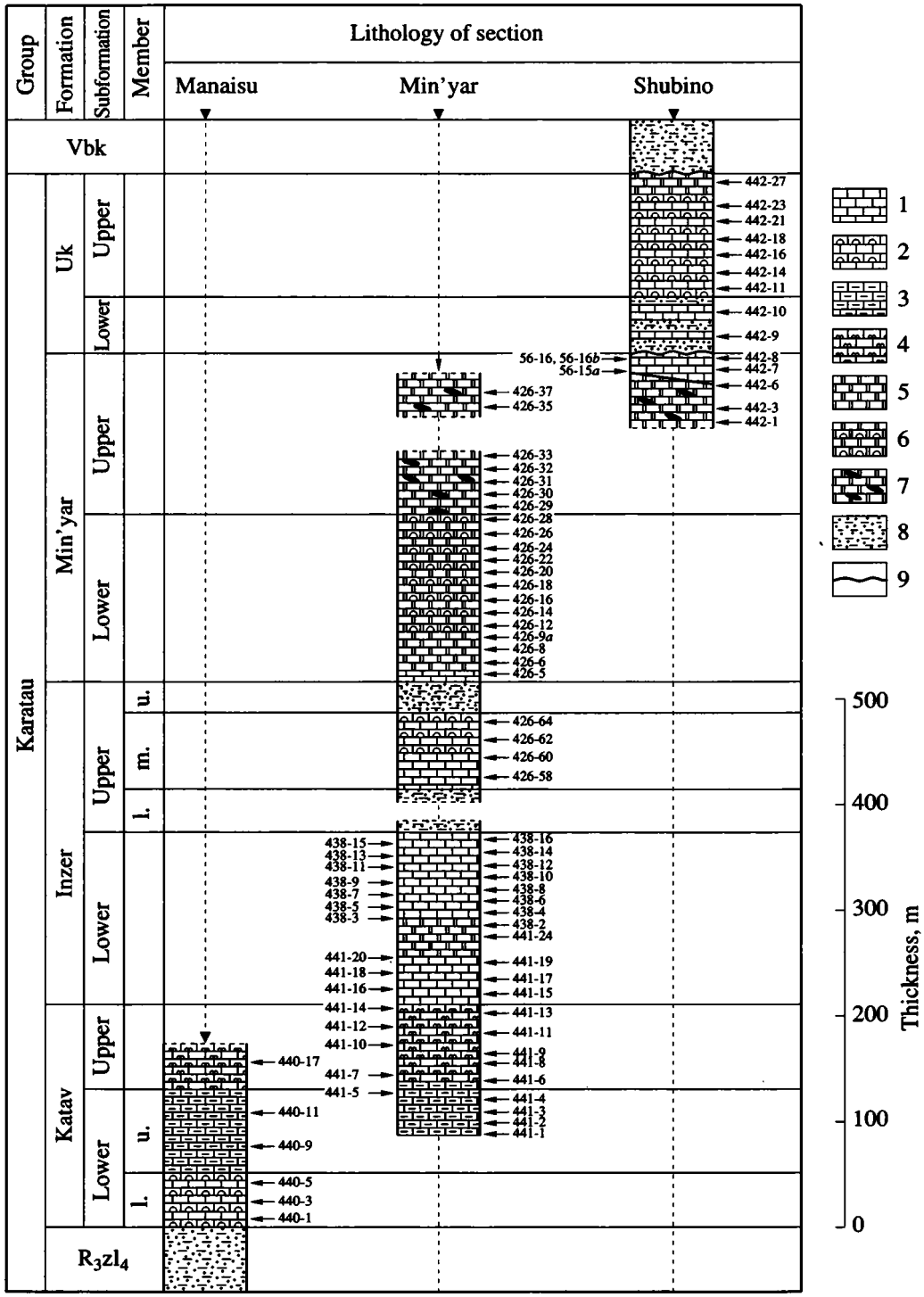

Fig. 2. Lithology of the studied sections and position of samples analyzed for the C- and O-isotopic composition.
(1) Micritic and clastic limestones, (2) stromatolitic limestone, (3) clayey limestone, (4) limestone with "striated" (microbial) lamination; (5) dolomite; (6) stromatolitic dolomite; (7) dolomite and stromatolitic dolomite with lenses and nodules of early diagenetic cherts; (8) siliciclastic rocks; (9) unconformities. Arrows with sample numbers show the position of analyzed rocks. Formation indexes as in Fig. 1.

nations on inadequately studied glauconites from various horizons of the group. These values regularly decrease upsection and correspond to 938 Ma in the upper part of the Katav Formation, to 896–853 Ma in the lower and middle parts of the Inzer Formation, to 791–683 Ma in the upper member of the latter, to 740 Ma in the lower part of the Min'yar Formation, and to 713–680 Ma in the upper part of the last unit (Garris, 1977; *Stratotip* ..., 1983).

The minimal age limit of the group is infered from the following set of consistent data: (1) the whole-rock K-Ar age of gabbro-diabases intruding the group is 620–660 Ma; (2) the U-Pb zircon age of the Barangulovo granites intruding the analogues of the Karatau Group to the east of the Bashkir meganticlinorium is estimated to be 660 ± 15 Ma; (3) the K-Ar ages on glauconites from the Vendian deposits unconformably overlying the Karatau Group and its analogues in the central Urals range from 625 to 560 Ma (*Stratotip* ..., 1983; Keller and Semikhatov, 1990; Koroteev *et al.*, 1997). Previously, the maximal age limit of the group was partly estimated on the basis of whole-rock K-Ar dating of gabbro-diabases, which were considered as pre-Karatavian in age, and yielded the age values of 1150–1000 Ma in addition to other, obviously rejuvenated values (Garris, 1977; *Stratotip* ..., 1983). However, the real relationships between these gabbro-diabases and the Karatau deposits have not been established.

According to these data, the time range of the Karatau Group was usually considered to be 1000 ± 50–650 ± 20 Ma (Kozlov *et al.*, 1991; Semikhatov *et al.*, 1991; Koroteev *et al.*, 1997). The first date evidently conventional is however supported by the available paleontological evidence.

The composition of organic-walled microfossils from the upper part of the Zil'merdak Formation and its analogues in the Volga–Urals area (*Stratotip* ..., 1982, 1983) indicates that the enclosing deposits are not older than 1000 Ma (Semikhatov, 1995; Knoll and Sergeev, 1995). The lower Karatau stromatolites (Raaben, 1975; Komar, 1978; *Stratotip* ..., 1982) include some characteristic taxa of interregional distribution, which are confined in Siberia, North Africa, North America, and Spitsbergen to the lower Upper Riphean deposits dated back to 1000–850 Ma (Semikhatov and Raaben, 1996). Stromatolites of the upper Karatau Group (the Min'yar and Uk formations) are similar in composition to their forms of the terminal Upper Riphean known in other regions, particularly in the Akademikerbreen Group of Spitsbergen (Raaben, 1975). The fact that the group under consideration contains the upper Upper Riphean deposits is confirmed by the occurrence of *Melanocerillium* in the Min'yar Formation (Maslov *et al.*, 1994), as these fossils appear in the geological record about 850–800 Ma ago. As for the microfossils from the post-Zil'merdak part of the Karatau Group, the assemblages of their silicified forms are deprived of stratigraphically valuable taxa (Sergeev, 1992), while a rich and diverse assemblage of organic-walled forms occurs only at the base of the Podinzer Beds (*Stratotip* ..., 1982). This assemblage is similar with that found in the middle horizons of the Akademikerbreen Group (Butterfield *et al.*, 1994). However, this similarity is of doubtful significance for detailed correlations, because the Podinzer Beds belong to the lower part of the Upper Riphean, whereas the Akademikerbreen Group undoubtedly represents its upper horizons (Butterfield *et al.*, 1994; Kaufman and Knoll, 1995).

Thus, the available paleontological and isotopic-geochronological data strongly suggest that the Karatau Group includes both the lower (1000–850 Ma) and upper (younger than 850 Ma) horizons of the Upper Riphean. Using the presented radiometric dates and admitting the linear correlation between the thickness and accumulation time of the deposits, we estimated radiometric ages for the boundaries between carbonate formations of the Karatau Group (Fig. 5). It is evident that the values obtained are by no means precise and may illustrate only general time ranges of the studied samples.

ANALYTICAL PROCEDURES

To study C- and O-isotopic compositions, we collected macroscopically uniform samples of limestones and dolomites without evident signs of recrystallization, schistosity, or weathering. Sampling intervals in the carbonate successions usually varied between 8 and 15 m being slightly smaller only in the Uk Formation. The samples were cut into two parts, one of which was used for chemical and isotopic analyses, the other for petrographic and cathodoluminencent investigations in thin sections and polished preparations.

The samples were dissolved in 1N HCl and contents of major components were determined by weight chemical analysis. Concentrations of Mn and Fe were measured by the atomic absorbtion spectroscopy using AAS-30 analyzer. In addition, the isotope dilution technique described in previous publications (Gorokhov *et al.*, 1995; Kuznetsov *et al.*, 1997) was used to determine the Sr content in the carbonate phases of the samples. The cathodoluminescent examination of limestones and dolomites was performed at the laboratory of the Mekhanobr-Analit Co. (St. Petersburg) by using the Comebax microanalyzer. The electron microscope CamScan supplemented with the spectrometer Link was used for the microprobe analysis of carbonate phases.

C- and O-isotopic compositions were measured in whole-rock samples of moderately or non-luminescent (dolo)micrites or (dolo)microsparites, as well as in other carbonate deposits with minimum signs of recrystallization and/or lowest content of the late carbonate segregations.

To extract the carbon dioxide for determining the O- and C-isotopic compositions, the powdered samples

were treated with the concentrated phosphoric acid (ρ = 1.89 g/ml) during two (limestones) or 72 (dolomites) hours at the temperature of 25°C. The obtained CO_2 volume was used to simultaneously determine C- and O-isotopic compositions applying mass spectrometer MI-2101 and using the laboratory standard of the Institute of Precambrian Geology and Geochronology çalibrated with respect to the PDB scale on the basis of international standards KH-2 and TKL. The analytical uncertainty for $\delta^{13}C$ and $\delta^{18}O$ measurements was not greater than ±0.2‰. All presented values of $\delta^{13}C$ and $\delta^{18}O$ were calculated relative to the PDB standard.

In order to evaluate the geological significance of the $\delta^{13}C$ values obtained, we paid special attention to the degree of epigenetical alterations of the samples. This was defined by using the commonly accepted geochemical and isotopic criteria, such as Mn/Sr and Fe/Sr ratios, $\delta^{18}O$ values, and the presence or absence of covariations of $\delta^{18}O$ versus Mn/Sr and $\delta^{18}O$ versus $\delta^{13}C$ (Veizer, 1983; Fairchild *et al.*, 1990; Kaufman *et al.*, 1993; Kaufman and Knoll, 1995; Sochava *et al.*, 1996; Podkovyrov and Vinogradov, 1996). These criteria are important because the initial $\delta^{13}C$ values in thermally unaltered carbonates are most frequently changed during the retrogressive catagenesis under the influence of meteoritic fluids. This process increases Fe and Mn concentrations in carbonates and simultaneously decreases Sr concentrations and $\delta^{18}O$ (Yudovich *et al.*, 1980; Brand and Veizer, 1980; Veizer, 1983; Kaufman and Knoll, 1995). At present, the critical value of the Mn/Sr ratio, which differentiates between the samples with initial and disturbed C-isotopic systems, is considered to be either ≤10 for limestones and dolomites (Kaufman *et al.*, 1993, 1996; Kaufman and Knoll, 1995; Knoll *et al.*, 1995), or <8 for limestones and <20 for dolomites (Sochava *et al.*, 1996; Podkovyrov and Vinogradov, 1996). In this article, we accepted the following critical Mn/Sr and Fe/Sr ratios: ≤4 and ≤10 for limestones and ≤6 and ≤15 for dolomites, respectively. The higher ratios for dolomites is accepted because the Sr incorporation into the crystal lattice of calcite is more significant than in the dolomite structure (Yudovich *et al.*, 1980; Veizer, 1983), and because the early diagenetic dolomitization in the Proterozoic time was accompanied by the carbonate enrichment in Mn (Brand and Veizer, 1980; Fairchild *et al.*, 1990).

As for the oxygen isotopic composition, the experience suggests that virtually unaltered samples of the Upper Proterozoic carbonates have $\delta^{18}O \geq -10‰$ PDB (Kaufman and Knoll, 1995; Knoll *et al.*, 1995; Gorokhov *et al.*, 1995). As a rule, O-isotopic composition is lighter in limestones than in dolomites as a consequence of isotopic fractionation during the early diagenesis and/or earlier diagenetic neomorphism of dolomites. The neomorphism led to the stabilization of isotopic systems of dolomites, whereas limestones remained permeable for diagenetic fluids (Kaufman and Knoll, 1995; Knoll *et al.*, 1995).

RESULTS AND DISCUSSION

Petrographic and Cathodoluminiscent Data. The Katav limestones are mainly represented by thin-laminated (20–150 μm) micrites with the finest microsparite lenses, which do not disrupt the primary rock structures. Less frequent submicroscopic segregations and millimeter-thick veins of secondary fine-grained sparite and local dolosparite can be observed. The thin lamination is emphasized by fine stylolites saturated with Fe-hydroxides. The cathodoluminescence of the studied samples (441-4, 441-5, and 441-13) is weak to moderate and patchy in reddish to yellowish rose colors in the micrites and microsparites and brigher in secondary (dolo)sparites.

The basal Inzer limestones are more recrystallized than the Katav carbonates (Samples 441-16, 441-17, and 441-18). Dominant among them are unclearly laminated micrites with thin lenses of microsparite and rare sparite. The rocks show the relic clastic textures and contain very fine lenses and/or nests of fine-grained blocky to firbous calcite and thin, usually blind veins of fine- to medium-grained calcite. The rare scattered or localized dolomitization resulted in appearance of microcrystalline (0.07–0.2 mm) aggregates of rhombohedral dolomite grains. Upsection (Samples 441-21, 441-22 and all samples of series 438), the limestones tend to be less recrystallized. Rocks of this level exhibit alternation of thin micrite and microsparite laminae among which there are the finest lenses of late microcrystalline calcite and laminae (1–3 mm) of microsparite and sparite with clastic texture, as well as rare inclusions of replaced firbous calcite. Despite these textural patterns, the Inzer limestones are mainly represented by non-luminescent varieties. Only zonal and aggregated calcites of later generations display the bright rosy-yellow luminescence. The moderate yellowish luminescence is characteristic of dolomite grains.

The Min'yar dolomites vary from dolomicrites to dolosparites in stromatolitic varieties and are mainly represented by fine-grained dolosparites in mechanogenic varieties. The rocks retain the primary lamination and clastic textures and include the variable amount of thin (0.5–2 mm) lenses and veinlets of light microcrystalline dolomite with unclear zoning. Rare limestones are represented here by micrites and microsparites with sparse late calcite veinlets. The dolomites are characterized by a weak to moderate, reddish, locally patchy cathodoluminescence pattern. The intensity of luminescence reveals cores and margins of zonal dolomite crystals.

The Uk limestones and dolomitized limestones are predominantly represented by microsparites with varying amount of secondary incorporational and/or firbous sparite. The formation includes rare micrites, which either alternate with microsparites or sparites in the stromatolitic structures or form individual interbeds. Clastic textures and/or microphytolites are typical of the nonstromatolitic limestones. Rocks of all kinds

contain veinlets of microcrystalline calcite and local dolomite. Dolomites at the top of the formation are distinct because of the finest films of iron hydroxides and abundant late dolosparite. The cathodoluminescent analysis of the Uk limestones shows that their nonluminescent microsparite–sparite matrix containing the recrystallization spots is closely associated with a variable amount (up to 12–15% of the rock volume) of late sparite and/or dolosparite of variably intensive luminescence. In other words, the Uk carbonate samples are distinctly heterogenous in composition.

Geochemical Characteristics of Samples. Abundances of Ca, Mg, Mn, Fe, and Sr, as well as Mg/Ca, Mn/Sr and Fe/Sr ratios in the studied samples are shown in table and allow us to make the following conclusions.

In the Katav samples, the carbonate phase is represented by virtually pure limestones with a low Sr content (119–236 μg/g, and about 160 μg/g in average), an elevated Mn content (160–420 μg/g, and 270 μg/g in average), and a high Fe concentration (3300 μg/g in average and up to 5400 μg/g in individual samples). The dominant early diagenetic calcite, when compared with its later generation, is depleted in Mn (usually less than 200 versus 400–650 μg/g, respectively) and especially Fe (1100–2500 versus 6800 μg/g, respectively) being simultaneously enriched in Sr (100–710 μg/g and less than 100 μg/g in later phases). The carbonate phase as a whole is generally characterized by the low Mn/Sr (no more than 3.53 and usually less than 2.0) and high Fe/Sr ratios (sometimes as high as 22.8–31.5), except that in three samples the latter is less than 10.0. No covariations between these ratios were recorded. It is noteworthy that all Katav limestones contain abundant (15.8 wt% in average and ranging from 6.3 to 29.1 wt%) siliciclastic fraction almost entirely composed of clay enriched in Fe (Gareev, 1982). Exactly this fraction contaminated the late diagenetic carbonate phase of the studied rocks with Fe, Mn, and Pb, as well as with the radiogenic ^{87}Rb, and that process consequently resulted in the disturbance of the Rb-Sr and U-Pb isotopic systems (Kuznetsov *et al.,* 19995; Ovchinnikova *et al.,* 1998). In contrast, the much more conservative C- and O-isotopic systems have not been considerably reset (see below), as it also follows from the low Mn/Sr ratios typical of the rocks.

Limestones and dolomitic limestones of the lower Inzer Subformation (the Podinzer Beds) are characterized by the high Sr content in the carbonate phase (418 μg/g in average for 12 samples and ranging from 254 to 605 μg/g). These rocks are constituents of the regional Sr-enriched geochemical horizon (Anfimov *et al.,* 1987; Gareev, 1988). Their carbonate phase is also distinct because of the very low Mn and frequently low Fe concentrations, which are commonly in the ranges of 14–45 and 210–870 μg/g, respectively. Only four samples (441-15, 441-16, 441-17, and 438-16) contain up to 73–100 μg/g of Mn and up to 1735–2640 and even 4490 μg/g of Fe. Using the first three samples from the basal part of the formation as a test case, it was demonstrated that their enrichment in Mn and Fe was caused by migration of these elements with diagenetic fluids from the underlying Katav limestones (Kuznetsov *et al.,* 1997; Ovchinnikova *et al.,* 1998). However, this process did not affect noticeably the Mn/Sr and Fe/Sr ratios in the studied rocks because they were initially enriched in Sr but depleted in the secondary low-Mn calcite with low Sr concentrations (80–100 μg/g), but with high Mn (up to 980 μg/g) and Fe content. The Mn/Sr and Fe/Sr ratios in these rocks are in the ranges of 0.15–0.28 and 3.6–7.8, respectively, i.e., they are much lower than the critical values accepted for selecting the "best" (least altered) samples suitable for the C-isotopic analysis. As for the main portion of the lower Inzer carbonates, which are not enriched in Mn and Fe, they show surprisingly low ratios of Mn/Sr (0.03–0.11) and Fe/Sr (0.4–3.4) in the Min'yar section. Similar ratios are characteristic of the Podinzer limestones and dolomitic limestones exposed in the adjacent section (Kuztentsov *et al.,* 1997).

An insignificant degree of secondary alterations in the Podinzer limestones evident from the presented data, is confirmed by the fact that their initial $^{87}Sr/^{86}Sr$ ratios are lower than any other known ratios for carbonates attributable to this time interval (Kuznetsov *et al.,* 1997). Probably, the excellent preservation state of primary isotopic systems of these carbonates was facilitated by the very early cementation of sediments, by a high content of organic matter in the rocks, and by the low content of silisiclastic admixture. In 22 studied samples, the content of the latter is 1.5% in average and usually ranges from 0.4 to 2.0%, being as high as 9.6 and 5.1% only in two samples (441-15 and 441-17) from the basal beds of the subformation. If we omit these two samples from consideration, the average content of insoluble residue decreases to 0.88%. It should be noted that both mentioned values are much lower than the average SiO_2 content (2.86%) calculated by Gareev (1988) for 28 samples of the Podinzer limestones from unidentified sections.

Carbonates from the upper Inzer Subformation differ from those of the lower subformation first of all in the lower Sr content (169–298 μg/g) and larger amount of the siliciclastic admixture (1.3–7.0% and 3.9% in average). However, similarly to the lower Inzer deposits, the limestones of the upper subformation show the difference between the basal and uppermost horizons in abundance of Mn (51–75 versus 32–45 μg/g), Fe (1510–2620 versus 390–900 μg/g), and siliciclastic material (5.7–7.0 versus 1.3–1.8%). Nevertheless, the basal horizons of the upper subformation did not show a meaningful increase in Mn/Sr and Fe/Sr ratios, which are in the ranges of 0.17–0.27 and 2.2–5.3, respectively, in all samples analyzed. By analogue with the Podinzer deposits, we suggest that the basal part of the upper Inzer limestones was contaminated with Fe and Mn, when these elements migrated from the underlying

Geochemical characteristics and carbon and oxygen isotopic composition in carbonates of the Karatau Group

Sample number	Ca	Mg	Mn	Fe	Sr	Mg/Ca	Mn/Sr	Fe/Sr	$\delta^{13}C$	$\delta^{18}O$
	wt %		μg/g						‰ PDB	
1	2	3	4	5	6	7	8	9	10	11
Katav Formation. Lower subformation										
440-1*	37.3	0.80	360	3360	167	0.021	2.15	20.1	4.3	−10.5
440-3*	39.8	0.24	160	1820	148	0.006	1.08	12.3	4.4	−9.7
440-5*	39.3	0.09	240	980	132	0.002	1.82	7.4	3.8	−9.2
440-9*	38.2	<0.09	420	3590	236	<0.002	1.78	15.2	2.8	−7.2
440-11*	38.3	0.12	420	820	119	0.003	3.53	6.9	1.1	−7.8
441-1	39.5	<0.09	310	1200	149	<0.002	2.08	8.1	2.8	−6.3
441-2	39.6	<0.09	234	1560	154	<0.002	1.52	10.1	2.3	−6.4
441-3	38.5	<0.09	160	2900	141	<0.002	1.13	20.6	1.3	−6.9
441-4	38.5	<0.09	206	4240	–	<0.002	–	–	−0.2	−6.8
441-5	38.0	<0.09	240	3970	126	<0.002	1.90	31.5	−0.8	−7.9
Upper subformation										
441-6	37.4	<0.09	200	5060	–	<0.002	–	–	−0.7	−8.6
441-7	38.6	<0.09	190	4790	162	<0.002	1.17	29.6	0.3	−6.7
441-8	38.4	<0.09	195	4430	–	<0.002	–	–	−0.1	−7.2
441-9	38.8	<0.09	220	4360	190	<0.002	1.16	22.9	0.2	−7.0
440-17*	37.5	<0.09	380	1980	138	<0.002	2.75	14.3	0.3	−7.8
441-10	37.8	0.43	325	4060	–	0.011	–	–	0.2	−7.8
441-11	35.2	2.67	385	5400	–	0.076	–	–	1.4	−7.2
441-12	36.6	1.98	280	4230	160	0.054	1.75	26.4	1.9	−7.0
441-13	38.3	0.38	270	3470	152	0.010	1.78	22.8	0.3	−7.6
441-14	38.5	0.53	220	3410	184	0.014	1.20	18.5	1.8	−6.5
Inzer Formation. Lower subformation (Podinzer Beds)										
441-15	38.8	0.18	100	2640	541	0.005	0.18	4.9	2.2	−7.5
441-16	39.2	0.11	75	1735	486	0.003	0.15	3.6	3.6	−7.5
441-17	39.3	0.11	96	2630	338	0.003	0.28	7.8	2.3	−8.3
441-18	39.5	0.11	44	420	411	0.003	0.11	1.1	2.5	−7.5
441-19	39.5	<0.09	14	380	–	<0.002	–	–	2.4	−7.2
441-20	39.7	<0.09	15	330	423	<0.002	0.04	0.8	2.4	−7.8
441-24	38.4	1.15	17	870	254	0.030	0.07	3.4	3.0	−8.2
438-2	38.6	1.12	14	520	–	0.029	–	–	3.9	−7.5
438-3	39.1	0.35	23	420	495	0.009	0.05	0.8	3.1	−7.3
438-4	39.6	0.13	29	720	–	0.003	–	–	1.1	−7.3
438-5	39.7	0.18	18	240	–	0.005	–	–	0.8	−9.0
438-6	40.0	0.26	19	220	512	0.006	0.04	0.4	0.8	−9.7
438-7	39.6	0.23	18	210	–	0.006	–	–	1.2	−8.2
438-8	39.7	0.24	16	355	–	0.006	–	–	0.7	−8.8
438-9	39.9	0.24	21	325	521	0.006	0.04	0.6	0.9	−8.4
438-10	39.7	<0.09	15	370	490	<0.002	0.03	0.8	1.0	−8.3
438-11	39.8	0.19	18	310	–	0.005	–	–	1.0	−8.5
438-12	40.0	0.19	21	310	605	0.005	0.03	0.5	1.2	−8.4
438-13	39.8	0.19	28	455	–	0.005	–	–	1.4	−8.3
438-14	39.7	0.19	30	360	–	0.005	–	–	0.9	−8.6
438-15	40.0	0.18	22	315	545	0.004	0.04	0.6	0.9	−8.5
438-16	29.1	7.16	73	4490	–	0.246	–	–	2.5	−8.3

Table. (Contd.)

1	2	3	4	5	6	7	8	9	10	11
					Upper subformation					
426-58	38.6	<0.09	51	1510	298	<0.002	0.17	5.1	−1.0	−8.0
426-60	37.3	1.17	75	2620	–	0.031	–	–	−1.0	−8.0
426-62	38.3	0.62	45	900	169	0.016	0.27	5.3	−0.6	−7.8
426-64	38.7	0.52	32	390	175	0.013	0.18	2.2	0.0	−8.0
					Min'yar Formation. Lower subformation					
426-5	38.5	1.35	137	1370	195	0.035	0.70	7.1	−0.2	−7.4
426-6	21.9	13.32	184	450	11	0.608	16.73	40.9	1.3	−6.1
426-8	22.0	13.30	96	620	28	0.604	3.43	22.1	0.9	−6.0
426-9a	22.3	13.19	163	90	14	0.592	11.64	6.4	0.8	−3.9
426-12	18.6	10.69	91	410	65	0.575	1.40	6.3	−0.1	−1.6
426-14	22.1	13.26	115	220	54	0.601	2.13	4.1	−0.1	−1.5
426-16	22.1	12.20	99	500	57	0.552	1.74	8.7	0.7	−1.8
426-18	21.7	13.20	44	140	55	0.608	0.80	2.6	1.8	−4.0
426-20	22.1	13.38	100	150	75	0.606	1.33	2.0	1.1	−4.3
426-22	22.0	13.36	73	144	–	0.607	–	–	2.4	−4.6
426-24	21.8	13.36	51	100	70	0.612	0.73	1.4	2.0	−4.8
426-26	21.5	13.25	45	550	–	0.616	–	–	0.3	−5.0
426-28	22.0	13.26	64	235	–	0.603	–	–	−0.3	−4.3
					Upper subformation					
426-29	21.7	13.20	230	320	28	0.608	8.21	11.4	0.2	−4.5
426-30*	22.0	13.26	55	80	–	0.602	–	–	3.4	−5.4
426-31	21.6	13.22	68	90	44	0.612	1.55	2.1	3.0	−4.6
426-32*	21.2	13.24	44	77	–	0.625	–	–	0.6	−5.4
426-33	20.9	13.28	63	150	103	0.634	0.61	1.5	0.3	−4.3
426-35	22.0	13.41	96	240	68	0.609	1.41	3.5	−0.9	−4.4
426-37	21.5	13.41	84	690	65	0.623	1.29	10.5	1.7	−4.5
442-1	22.1	13.40	100	440	113	0.607	0.88	3.9	−1.8	−3.4
442-3	21.7	13.45	340	1350	90	0.621	3.78	15.0	−2.2	−3.8
442-6	32.8	5.10	2960	1420	230	0.156	12.87	6.2	1.3	−6.1
442-7	39.2	0.27	1460	660	404	0.007	3.61	1.6	1.6	−6.7
56-15a*	40.0	<0.09	444	670	375	<0.002	1.18	1.8	1.9	−6.1
56-16*	40.3	<0.09	536	380	346	<0.002	1.55	1.1	1.4	−5.9
56-16b*	39.8	0.32	130	150	477	0.008	0.27	0.3	2.7	−5.1
442-8	38.9	0.75	385	1420	340	0.019	1.13	4.2	5.9	−5.0
					Uk Formation. Lower subformation					
442-9	39.3	0.45	220	1700	281	0.011	0.78	6.1	2.6	−7.2
442-10	38.9	0.38	603	3450	289	0.010	2.09	11.9	1.4	−5.9
					Upper subformation					
442-11	40.3	<0.09	100	1120	715	<0.002	0.14	1.6	2.4	−7.2
442-14	38.4	0.26	82	1010	110	0.007	0.75	9.2	0.9	−6.6
442-16	38.8	1.09	150	810	117	0.028	1.28	6.9	1.0	−6.0
442-18	39.8	0.31	34	250	106	0.008	0.32	2.4	1.0	−5.8
442-21	39.8	0.31	33	340	109	0.008	0.30	3.1	0.7	−5.7
442-23	39.8	0.54	22	130	313	0.014	0.07	0.4	2.5	−4.2
442-27	27.4	9.48	110	1120	12	0.346	9.33	93.3	1.1	−7.9

Note: Oxygen and carbon isotope composition analyzed by B.G. Pokrovskii (Geological Institute, Russian Academy of Sciences).

siliciclastic member. The proximity of this member was likely the cause of a sharp increase in Fe content in the uppermost limestones of the lower subformation (Sample 438-16). In addition, the higher content of siliciclastic material in some upper Inzer limestones may imply that their carbonate phase was enriched in Mn and Fe in the course of redistribution of these elements between rock phases during diagenesis or epigenesis. Anyway, the influence of Mn- and Fe-enriched fluids on these deposits, as well as on the Podinzer Beds was not sufficient to increase the Mn/Sr and Fe/Sr ratios up to the level indicative of noticeable secondary alterations in the rocks.

The Min'yar dolomites show variable, but generally low contents of Mn, Fe, and Sr (44–340, 77–1350, and 11–113 μg/g, respectively). As a result, the Mn/Sr ratio in their carbonate phase is usually in the range of 0.61–3.78, and three samples only (426-6, 426-9a, and 426-29) revealed values (8.2–16.7) higher than the accepted critical limit. The Fe/Sr ratio considerably fluctuating (1.4–40.9) in the Min'yar dolomites exceeds the critical value only in five samples (table), being in two of them (426-6 and 426-8) as high as 22.1 and 40.9. The percentage of insoluble residue in the Min'yar dolomites usually varies in the range of 0.5–4.1%. The values exceeding 6.1% are recorded only in five samples; one of them (426-12) contains 40.1% of this fraction. In contrast to the Katav carbonates, in which the insoluble residue can be attributed to the clayey admixture, the Min'yar dolomites have the non-carbonate admixture represented by siliciclastic sandy–silty material and authigenic silica.

The basal Min'yar limestones (Sample 426-5) are enriched in Mn and especially Fe (table), which can be caused by both the considerable amount of siliciclastic admixture (7.2%) and the influence of the upper Inzer sandy–clayey member. Anyway, because of the high Sr content (195 μg/g), Mn/Sr and Fe/Sr ratios in these limestones (0.70 and 7.1, respectively) are considerably lower than the critical values. The limestones from the Shubino Member, that is 12–15 m thick unit located at the top of the Min'yar Formation, demonstrate the wide ranges of Mn (130–2960 μg/g) and Fe (150–1420 μg/g) concentrations. The Sr content in these rocks varies from 230 to 477 μg/g. The maximal Mn and Fe concentrations characterize the basal dolomitic limestones (Sample 442-6) of the Shubino Member and the uppermost limestones (Sample 442-8) immediately beneath the pre-Uk unconformity. Except the last sample, where Mn/Sr ratio is as high as 12.87, other Mn/Sr and Fe/Sr values indicate a minor alteration degree for all Shubino carbonates. In the Min'yar limestones and dolomites, the rise of Fe/Sr ratio is not accompanied by increase of Mn/Sr ratio et vice versa. The high values of both parameters are recorded only in two dolomite samples (426-6 and 426-29).

These parameters are different in the limestones of the lower and upper Uk subformations. Samples from the lower Uk Subformation are more rich in siliciclastic admixture, Mn, and especially Fe displaying the relatively stable and slightly elevated content of Sr (table). Therefore, Mn/Sr and Fe/Sr ratios in the lower subformation are somewhat greater than those in the upper subformation: 0.78–2.09 versus 0.07–1.28 in the case of Mn/Sr and 6.1–11.9 versus 0.4–9.2 in the case of Fe/Sr. These features of the lower Uk limestones can be easily attributed to their tight association with siliciclastic deposits dominating in the subformation. As for dolomites at the top of the formation section, they have slightly elevated Mn and Fe contents and are strongly depleted in Sr (table). As a result, these deposits show high Mn/Sr (9.33) and particularly high Fe/Sr (93.3) ratios that is quite indicative of their stratigraphic position immediately beneath the pre-Vendian unconformity.

The summarized data on the geochemical parameters of the carbonate samples from the Karatau Group allow the following conclusions: (1) Samples with negative $\delta^{13}C$ do not show any correlation between this parameter and Mn, Fe and Sr concentrations and, hence, they were affected by catagenetic alternations not stronger than any other studied samples. (2) In the whole collection studied, only one sample (442-6) of the Min'yar limestones and four samples of the Min'yar (426-6, 426-9a, and 426-29) and Uk (442-27) dolomites have Mn/Sr ratios indicating their significant secondary alterations. (3) The chosen critical values of Fe/Sr ratio (≤10 for limestones and ≤15 for dolomites) appeared to be exceeded in 13 samples of the Katav (440-1, 440-3, 440-9, 440-17; 441-2, 441-3, 441-5, 441-7, 441-9, 441-12, 441-13, 441-14) and Uk (442-10) limestones, and in three samples of the Min'yar (426-6 and 426-8) and Uk (442-27) dolomites. (4) Both parameters (Mn/Sr and Fe/Sr ratios) simultaneously exceed the critical values only in two samples from the Min'yar (426-6) and Uk (442-27) formations. So, according to the geochemical criteria, only the listed samples, especially two latter, might be significantly affected by secondary alterations. As we shall see, the isotopic-geochemical data suggests that Sample 442-27 is the only one, where these alterations disturbed the C-isotopic system.

Oxygen Isotopic Composition. In the Katav limestones, $\delta^{18}O$ values vary from –6.3 to –10.5‰ PDB, tending to increase upsection (Fig. 5). The minimal value of $\delta^{18}O$ is recorded in Sample 440-1 showing the elevated Fe/Sr (20.1) and low Mn/Sr (2.15) ratios. In other Katav samples with the elevated Fe/Sr ratio, $\delta^{18}O$ where range from –6.4 to –9.7‰ and Mn/Sr ratio is not greater than 2.75. There is no correlation between $\delta^{18}O$ and Mn/Sr ratio in these deposits (Fig. 3), and only several samples display the approximately correlated $\delta^{13}C$ and $\delta^{18}O$ values. In other words, secondary alterations of the Katav limestones that disturbed their Rb-Sr and U-Pb systems (Kuznetsov *et al.*, 1995b; Ovchinnikova *et al.*, 1998), were insufficiently strong to meaningfully affect the C-isotopic systems.

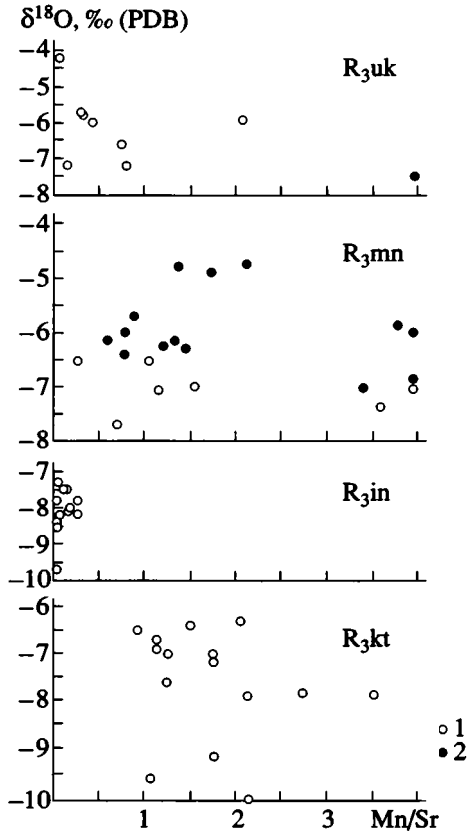

Fig. 3. $\delta^{18}O$–Mn/Sr diagram for carbonates of the Karatau Group: (1), limestones; (2), dolomites (formation indexes as in Fig. 1).

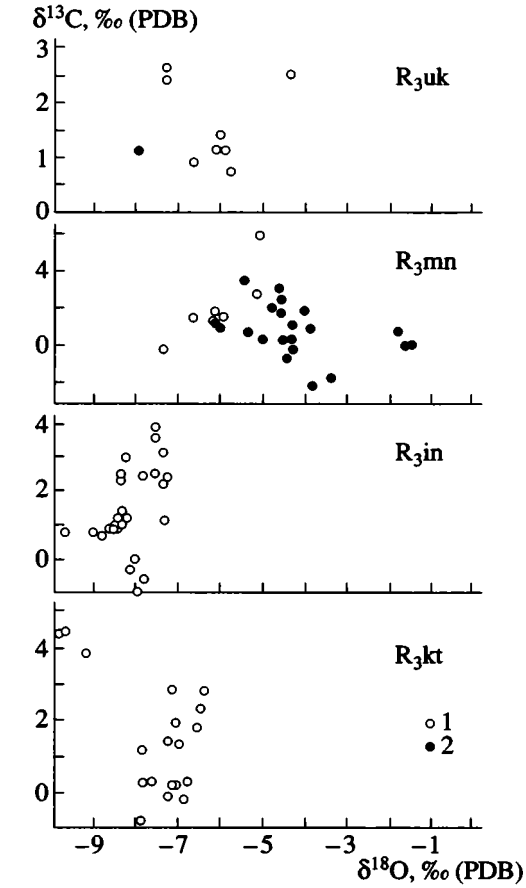

Fig. 4. $\delta^{18}O$–$\delta^{13}C$ diagram for carbonates of the Karatau Group: (1), limestones; (2), dolomites (formation indexes as in Fig. 1).

In samples of the Inzer limestones, $\delta^{18}O$ values commonly vary from –7.2 to –9.0‰ and drop to –9.7‰ in a single sample. As stated above, Mn/Sr and Fe/Sr ratios in these deposits are much lower than the critical values. In the Min'yar samples, $\delta^{18}O$ values do not drop below –7.9‰. These values in the Min'yar dolomites tend to be higher than in limestones (–6.1 to –1.5‰ and –7.4 to –5.1‰, respectively) and fall generally within the interval of –2 to –6‰ characteristic of the early diagenetic dolomites of the Upper Proterozoic (Veizer *et al.*, 1992). It should be stressed that the Min'yar samples with the elevated Mn/Sr and Fe/Sr ratios (426-6, 426-8, 426-9a, 426-29; 442-6, 442-7) appear to be appropriate in terms of the isotopic-geochemical criteria: their $\delta^{18}O$ is not lower than –6.7‰, and there is no correlation between $\delta^{18}O$ and Mn/Sr ratios, or between $\delta^{18}O$ and $\delta^{13}C$ (Figs. 3 and 4).

The Uk limestones are similar to the Min'yar limestones in the oxygen isotopic composition: $\delta^{18}O$ ranges from –7.9 to –4.2‰. There is no difference between $\delta^{18}O$ values measured in samples with a higher (the lower Uk Subformation) and lower (upper stratigraphic levels) Fe/Sr ratios. Only the uppermost Uk dolomites show signs of strong secondary alteration: in contrast to underlying limestones, they display much lesser $\delta^{18}O$ value (–7.9‰) together with higher Mn/Sr and especially Fe/Sr ratios (9.33 and 93.3, respectively). The $\delta^{18}O$ drop is accompanied in this case by a noticeable decrease in $\delta^{13}C$ (Fig. 4). All presented data as well as the petrographic features (see above) of the uppermost Uk dolomites indicate that their C-isotopic systems were disturbed.

Thus, the petrographic, cathodoluminiscent, and geochemical (Mn/Sr and Fe/Sr ratios) data indicate that in spite of secondary alterations all studied samples of Karatau carbonates, except the Sample 442-27 from the top of the Uk Formation, preserved their C- and O-isotopic systems insignificantly disturbed. This apparent contradiction can be understood if the volumes and concentrations of the diagenetic fluids, which were able to change the equilibrium of Mn, Fe, Sr, and other minor elements in carbonates, were insufficient to considerably affect compositions of the rock-forming components. In other words, all studied Karatau samples, except for one, can be considered as retaining their original C-isotopic signature.

Variations in the Carbon Isotope Composition. The Katav Formation initial in the carbonate part of the

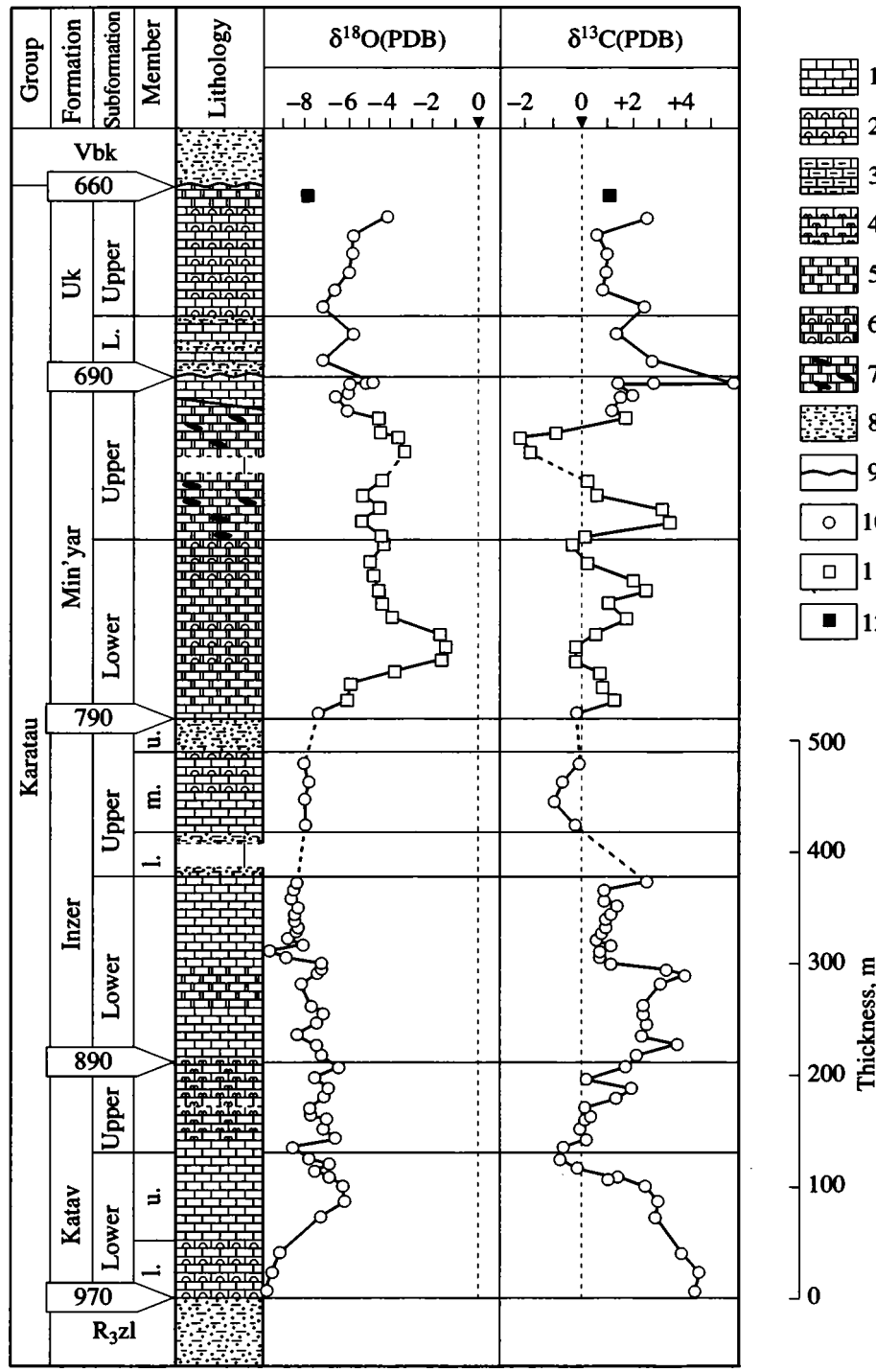

Fig. 5. $\delta^{13}C$ and $\delta^{18}O$ variation curves for carbonates of the Karatau Group: (1) micritic and clastic limestone, (2) stromatolitic limestone, (3) clayey limestone, (4) limestone with "striated" (microbial) lamination, (5) dolomite, (6) stromatolitic dolomite, (7) dolomite and stromatolitic dolomite with lenses and nodules of early diagenetic cherts, (8) siliciclastic rocks, (9) unconformities, (10) unaltered limestone, (11) unaltered dolomite, (12) altered dolomite (figures indicate the calculated radiometric ages of lithostratigraphic boundaries; formation indexes as in Fig. 1).

Karatau Group demonstrates noticeable variations in the carbonate C-isotopic composition. In its lower subformation, $\delta^{13}C$ rapidly decreases upsection from 4.3 or 4.4‰ at the base to negative values (–0.2 to –0.8‰) at the top. The upper subformation generally shows the low positive values of $\delta^{13}C$ (close to 1.8‰) slightly decreasing (down to 0.3‰) at the top of the unit (Fig. 5).

According to C-isotopic data, the Inzer Formation can be subdivided into three parts. In the lower part (108 m) of its lower subformation, $\delta^{13}C$ values vary from 2.3 to 3.9‰ and show two minor positive excursions (3.6‰ at the base of the interval and 3.9‰ at the top). The upper part of the lower subformation displays a sharp shift to lesser and uniform $\delta^{13}C$ values (0.7–1.4‰) with a minor positive excursion up to 2.5‰ at the top of the subformation. So, the lower Inzer limestones exhibit three successive peaks of $\delta^{13}C$ (3.6, 3.9, and 2.5‰) separated by intervals with predominant values of about 2 and 0.7–1.4‰. The upper Inzer limestones preceded by the 70-m-thick siliciclastic member demonstrate a further drop of $\delta^{13}C$ values, as compared with those in the underlying horizons of the formation. $\delta^{13}C$ approximates zero at the base and top of the upper Inzer carbonates and falls down to –1.0‰ in the middle part.

The Min'yar Formation is characterized by most significant variations in C-isotopic parameters observed in the Karatau Group: $\delta^{13}C$ ranges from –0.3 to +2.4‰ in its lower subformation and from –2.2 to +5.9‰ in the upper subformation. As a result, there are four peak values of $\delta^{13}C$, whose amplitudes increase upsection first from 1.3 to 2.4, and then to 3.0 and 5.9‰. (Unfortunately, the last value was recorded in a single sample.) The troughs separating these peaks become deeper (Fig. 5). So, the Min'yar Formation shows variations of $\delta^{13}C$ values increasing upward and having general amplitude of 8.1‰.

The unaltered Uk samples demonstrate the shift of $\delta^{13}C$ back to the low positive values (0.7–2.6‰). Against this background, there are two small positive excursions (2.4 and 2.5‰) separated by a zone of stable values (0.9–1.4‰) (Fig. 5).

Thus, without going into details, we can sum up the presented data in the following way: (1) According to the carbonate carbon isotopic composition, the continuous stratigraphic succession of the Katav and lower Inzer limestones can be divided into three parts: (a) the lower Katav deposits characterized by the descending trend of $\delta^{13}C$ variations from 4.4 to –0.8‰; (b) the upper Katav Subformation and the lower part of the lower Inzer Subformation with an ascending trend of $\delta^{13}C$ variations from –0.8 to 3.9‰; (c) the upper part of the lower Inzer Subformation marked by generally low positive values of $\delta^{13}C$. (2) The carbonate member of the upper Inzer Subformation bounded by siliciclastic members is characterized by minor negative $\delta^{13}C$ values. (3) The Min'yar Formation shows the most contrasting variations of $\delta^{13}C$ (from –2.2 to 5.9‰) as compared to other units of the Karatau Group. (4) The Uk limestones and dolomites display a shift of $\delta^{13}C$ back to the low positive values whose fluctuation is comparable with that observed in the lower part of the Min'yar Formation.

CONCLUSION

In its different parts, the current model of the Late Riphean $\delta^{13}C$ variations is substantiated by data of different validity. The model $\delta^{13}C$ variation curve for the second half of this erathem (younger than 850–800 Ma) is based on consistent data obtained from a series of successions in Spitsbergen, Greenland, Canada, Namibia, and Oman (Narbonne *et al.*, 1994; Faufman and Knoll, 1995; and references therein). It is unlikely that additional data may introduce significant modifications to this curve. However, the curve needs to be strictly calibrated against the chronometrical scale, especially because of the dual interpretation of radiometric age for the Varangerian (Laplandian) Glaciohorizon, whose base marks, by definition, the lower Vendian boundary (650 ± 20 Ma according to Keller and Semikhatov, 1990; Semikhatov *et al.*, 1991; Sokolov, 1995; Koroteev *et al.*, 1997, and 610 Ma according to Harland *et al.*, 1990; Knoll and Walter, 1992; Kaufman and Knoll, 1995).

As for the $\delta^{13}C$ variation curve for the early Late Riphean (from 1000 to 850–800 Ma), it was based for a long time on data from randomly selected samples representing, as evident now, the epigenetically altered carbonates (Schidlowski *et al.*, 1975, 1983; Fairchild *et al.*, 1990; Strauss and Moore, 1992). Representative C-isotopic parameters for this interval became available recently, when the better preserved samples from the Turukhansk and Uchur–Maia regions of Siberia were studied (Knoll *et al.*, 1995; Podkovyrov and Vinogradov, 1996). However these data should be reconciled to each other and chronologically correlated with data on the late Late Riphean in the aforementioned Arctic, North American, and African sections.

This article presents the first adequate information on the carbonate C-isotopic compositions in a single type succession of the Upper Riphean—the Katatau Group of the Southern Urals. In the western Bashkir meganticlinorium, this group is predominantly composed of carbonate deposits little affected by secondary alterations and retaining their primary C-isotopic signature. The group spans both the lower and upper parts of the Upper Riphean. For these reasons, the group represents a favorable object for reconstructing seculiar variations in the carbonate C-isotopic composition during the Late Riphean time.

The revealed $\delta^{13}C$ variations in the Karatau Group are in good agreement with the general trend of this parameter reported for the Late Riphean (Kaufman and Knoll, 1995; Knoll *et al.*, 1995) and depict several short-time negative excursions against the background

of positive $\delta^{13}C$ values and the growing amplitude of the C-isotopic variations upward the Karatau section. The $\delta^{13}C$ variation curve for the Katav–Inzer deposits is similar in configuration to that characterizing the middle part of the Riphean succession of the Turukhansk Uplift in Central Siberia (Knoll *et al.*, 1995), the interval from the Derevnya to Shorikha Formation inclusive. This interval is assigned to the lower Upper Riphean according to the integrated isotopic-geochronological, paleontological and chemostratigraphic records (Semikhatov and Serebryakov, 1983; Gorokhov *et al.*, 1995; Ovchinnikova *et al.*, 1995b; Knoll *et al.*, 1995). The coeval Lakhanda Group of the Uchur–Maia region of eastern Siberia shows in general the higher $\delta^{13}C$ values (Podkovyrov and Vinogradov, 1996) than in the correlative deposits of the Turukhansk region and the Southern Urals.

In the upper Karatau Group, i.e., in the Min'yar–Uk deposits, $\delta^{13}C$ values vary within a lesser range than it is envisaged in the mentioned model, and the curve configuration is different. The upper Upper Riphean successions, which served as a base for the model (Kaufman and Knoll, 1995), are characterized by long intervals of high positive $\delta^{13}C$ values (from 3-4 to 6–8‰ in the lower part and from 5–6 to 8–9‰ in the upper one) separated by short interludes of moderate negative (as low as –2.0‰) values. In contrast, as it was shown above, the upper Karatau carbonates demonstrate the less considerable $\delta^{13}C$ variations. They range commonly from –0.3 to 3.4‰, being more variable (from –2.2 to 5.9‰) in the upper Min'yar deposits only and the positive excursions are confined to very short intervals of the Karatau succession (Fig. 5).

To explain such a discrepancy between the C-isotopic characteristics of the upper Karatau Group and upper Upper Riphean deposits in the Arctic, Canada, and other regions, the following reasons can be suggested: (1) significant secondary alterations of the Karatau deposits, (2) a specific character of the late Karatavian basin, (3) a lack of the upper Upper Riphean horizons in the Karatau Group, (4) unsufficient sampling density of the studied carbonates, and (5) stratigraphic incompleteness of the Karatau carbonate succession.

The first of these causes must be rejected in the light of geochemical and isotopic-geochemical characteristics given above. The second cause is impossible because sedimentological data exclude a deep-water anoxic character of the late Karatavian basin (Maslov, 1988, 1997) and the initial $^{87}Sr/^{86}Sr$ ratios in the Inzer–Uk carbonates (Gorokhov *et al.*, 1996; Kuznetsov *et al.*, 1997; Podkovyrov *et al.*, 1997) suggest this basin to have been connected with the past World Ocean.

The third cause seems improbable in the light of available isotopic-geochronological and paleontological materials. It should be reminded that the Min'yar–Uk deposits are younger than 836 ± 25 Ma (Ovchinnikova *et al.*, 1995a, 1998), and glauconites from their upper horizons yielded the isochron Rb-Sr and K-Ar ages of 688 ± 10 and 670 ± 10 Ma (Gorozhanin and Kutyavin, 1986). Moreover, the Min'yar Formation contains *Melanocerillium* (Maslov *et al.*, 1994) characteristic of the upper Upper Riphean, and the succession of the Karatavian stromatolitic assemblages is comparable with that observed in the Upper Riphean of Spitsbergen (Raaben, 1975). The late Karatavian stromatolitic assemblages show similarity to the assemblages of the Akademikerbreen Group that was used, along with other successions, to elaborate the $\delta^{13}C$ variations model for the late Late Riphean.

At first sight, the inadequate sampling density seems to be an important factor, because the strongest positive $\delta^{13}C$ excursions in the Min'yar Formation are only recorded in one or two samples (Fig. 5). However, the careful analysis does not suggest this assumption to be correct. Actually, the upper Upper Riphean successions in the Arctic display the high positive $\delta^{13}C$ values not in descrete thin members, but within extended intervals few hundred meters thick (Kaufman and Knoll, 1995). So, if there were such intervals in the Karatau Group, they should have been recognized with the accepted sampling interval (in the Min'yar Formation each 13.5 m in average). Nevertheless, we do not exclude the necessity to use more closely spaced samples to detail the $\delta^{13}C$ variation trend in the Karatau Group, particularly near the excursion peaks.

Thus, the fifth cause, namely the possible stratigraphic incompleteness of the upper Karatau carbonate succession, seems to be most important. This incompleteness can be attributed to the presence of siliciclastic members and/or stratigraphic unconformities (hiatuses).

In the studied part of the Karatau Group, noticeable siliciclastic members are located at the base and top of the upper Inzer Subformation (50 and 70 m) and at the base of the Uk Formation (80 m). Time ranges of these units corresponding to regressive stages in the basin development are uncertain but unlikely large. All facts and stratigraphic position of siliciclastic members (Fig. 5) tempt us to suppose that intervals of siliciclastic sedimentation corresponded in time to three short-term negative excursions of $\delta^{13}C$, which are regarded as indicators of the glacial events and associated paleooceanographical changes of the late Late Riphean time (Kaufman *et al.*, 1993; Kaufman and Knoll, 1995). However, in the case of the lower Uk siliciclastic member, this supposition in incompatible with $\delta^{13}C$ values measured in its carbonate interbeds (1.4–2.6‰).

The problem of significant stratigraphic hiatuses in the Karatau succession have not been discussed in recent publications. The group is commonly considered as a continuous succession, and stratigraphic unconformities at the base of the Min'yar and Uk formations are usually attributed to local erosion events at the slopes of synsedimentary uplifts. Only sometimes, the pre-Uk unconformity was supposed to mark an important event

of erosion that eliminated the upper (Shubino) member of the Min'yar Formation in some sections (Bekker, 1961, 1988). The obtained C-isotopic data suggests that there are noticeable hiatuses in the upper part of the Karatau Group, and that the extended intervals of the succession are missing because of the pre-Uk, pre-Vendian, and, probably pre-Min'yar, events. To test this suggestion, we are going to analyze the representative collection of the upper Karatau carbonates for their C- and Sr-isotopic parameters. However, the C-isotopic data already obtained rise the problem concerning the time ranges of the Min'yar and Uk formations and noticeable hiatuses below them. Particularly, the Uk Formation is likely to correspond, according to its stratigraphic position and moderate positive $\delta^{13}C$ values, to a short time interval after the Sturtian glaciation.

Finally, the evaluation of all available C-isotopic chemostratigraphic data for the Riphean points to the necessity of strict calibrating the Late Riphean $\delta^{13}C$ variation curve in isotopic–geochronological (chronometric) terms and of correlating those parts of the curve which were established in different regions, in order to characterize the lower Upper Riphean in some areas and the upper Upper Riphean in others. As a result, we may obtain a uniform chronometrically calibrated curve of $\delta^{13}C$ variations in the Late Riphean time, which will be adequate for the purpose of global C-isotopic chemostratigraphy.

ACKNOWLEDGMENTS

We sincerely thank B.G. Pokrovskii for C- and O-isotopic analyses of some samples used in this paper. We are grateful to A.J. Kaufman and M.E. Raaben for a valuable discussion of problems considered above, to T.L. Turchenko for the X-ray diffraction analysis of insoluble residue from the Karatau carbonates, to G.V. Konstantinova and E.P. Kutyavin for determining the Sr content by the isotope dilution technique. The work was supported by the Russian Foundation for Basic Research, projects nos. 96-05-64329 and 97-05-65506.

Reviewer B.S. Sokolov

REFERENCES

Anfimov, L.V., Sul'man, A.M., and Petrishcheva, V.G., Strontium in the Riphean Carbonates from Southern Urals, in *Geochimiya osadochnykh formatsii Urala* (Geochemistry of Sedimentary Formations of the Urals), Sverdlovsk: Ural. Nauch. Tsentr Akad. Nauk SSSR, 1987, pp. 22–28.

Bekker, Yu.R., *Molassy dokembriya* (The Precambrian Molasses), Leningrad: Nedra, 1988.

Bekker, Yu.R., Age and Rock Succession in the Upper Part of the Karatau Group, Southern Urals, *Izv. Akad. Nauk SSSR, Ser. Geol.*, 1961, no. 9, pp. 49–60.

Brand, U. and Veizer, J., Chemical Diagenesis of Multicomponent Carbonate System, 1. Trace Elements, *J. Sed. Petrol.*, 1980, vol. 50, no. 5, pp. 1219–1236.

Brasier, M.D., Global Ocean–Atmosphere Change across the Precambrian–Cambrian Boundary, *Geol. Mag.*, 1992, vol. 129, no. 2, pp. 161–168.

Butterfield, N.J., Knoll, A.H., and Swett, K., Paleobiology of the Neoproterozoic Svanbergfjellet Formation, Spitsbergen, *Fossils and Strata* (Oslo), 1994, no. 34, pp. 1–84.

Fairchild, I.L., Marshall, J.D., and Bertrand-Sarfati, J., Stratigraphic Shifts in Carbon Isotopes from Proterozoic Stromatolite Carbonates, Mauritania: Influence of Primary Mineralogy and Diagenesis, *Am. J. Sci.*, 1990, vol. 290-A, pp. 46–79.

Garan', M.I., The Western Slope of the Urals and Central Zone of the Southern Urals, in *Stratigrafiya SSSR: Verkhnii dokembrii*, (Stratigraphy of the USSR: Upper Precambrian), Moscow: Gosgeoltekhizdat, 1963, pp. 114–161.

Gareev, E.Z., Geochemical Features of Carbonate Rocks from Reference Sections of the Riphean Katav and Uk Formations of Southern Urals, in *Verkhnii dokembrii i paleozoi Yuzhnogo Urala* (Upper Precambrian and Paleozoic of the Southern Urals), Ufa: Bashkir Fil. Akad. Nauk SSSR, 1982, pp. 36–46.

Gareev, E.Z., Geochemical Features and Depositional Environments of the Inzer Formation from the Riphean Stratotype, Southern Urals, in *Verkhnii dokembrii Yuzhnogo Urala i vostoka Russkoi plity* (The Upper Precambrian of the Southern Urals and the East Russian Plate), Ufa: Bashkir. Nauch. Tsentr Ural. Otd. Akad. Nauk SSSR, 1988, pp. 29–35.

Garris, M.A., *Etapy magmatizma i metamorfizma v doyurskoi istorii Urala i Priural'ya* (Stages of Magmatism and Metamorphism in the pre-Jurassic History of the Urals and Adjucent Regions), Moscow: Nauka, 1977.

Gorokhov, I.M., Semikhatov, M.A., Baskakov, A.V., Kutyavin, E.P., Mel'nikov, N.N., Sochava, A.V., and Turchenko, T.L., Isotopic Composition of Strontium in Carbonate Rocks of the Riphean, Vendian and Lower Cambrian of Siberia, *Stratigr. Geol. Korrelyatsiya*, 1995, vol. 3, no. 1, pp. 3–33.

Gorokhov, I.M., Semikhatov, M.A., Ovchinnikova, G.V., *et al.*, Lead and Strontium Isotopes in Ancient Carbonates from the Urals and Siberia: Evolution of Seawater $^{87}Sr/^{86}Sr$ over the Late Proterozoic, Abstracts of Papers, *6th Goldschmidt Conference, Heidelberg, Germany*, 1996, vol. 1, no. 1, p. 207.

Gorozhanin, V.M. and Kutyavin, E.P., Rubidium-Strontium Dating on Glauconites, from the Uk Formation, in *Dokembrii i paleozoi Yuzhnogo Urala* (Precambrian and Paleozoic of the Southern Urals), Ufa: Bashkir. Nauch. Tsentr Ural. Otd. Akad. Nauk SSSR, 1986, pp. 60–63.

Harland, W.B., Armstrong, R.L., Cox, A.V., *et al.*, *A Geologic Time Scale*, 1989, Cambridge: Cambridge Univ., 1990.

Kaufman, A.J. and Knoll, A.H., Neoproterozoic Variations in the C-isotopic Composition of Seawater: Stratigraphic and Biogeochemical Implications, *Precambrian Res.*, 1995, vol. 73, nos. 1–4, pp. 27–49.

Kaufman, A.J., Jacobsen, S.B., and Knoll, A.H., The Vendian Record of Sr and C Isotopic Variations in Seawater: Implication for Tectonics and Paleoclimate, *Earth Planet. Sci. Lett.*, 1993, vol. 120, nos. 3–4, pp. 409–430.

Kaufman, A.J., Knoll, A.H., Semikhatov, M.A., *et al.*, Integrated Chronostratigraphy of Proterozoic–Cambrian Boundary Beds in the Western Anabar Region, Northern Siberia, *Geol. Mag.*, 1996, vol. 133, no. 5, pp. 509–533.

Keller, B.M. and Semikhatov, M.A., Isotopic Geochronology for the Vendian of the USSR, *The Vendian System. Vol. 2:*

Geology, Sokolov, B.S. and Fedonkin, M.A., Eds., Berlin: Springer, 1990, pp. 184–190.

Knoll, A.H. and Sergeev, V.N., Taphonomic and Evolutionary Changes across the Mezoproterozoic–Neoproterozoic Transition, *Neues Jahrb. Paleontol. Abh.,* 1995, vol. 195, nos. 1–3, pp. 289–302.

Knoll, A.H. and Walter, M.R., Latest Proterozoic Stratigraphy and Earth History, *Nature,* 1992, vol. 356, pp. 673–678.

Knoll, A.H., Kaufman, A.J., and Semikhatov, M.A., The Carbon Isotopic Composition of Proterozoic Carbonates: Riphean Successions from Northwestern Siberia (Anabar Massif, Turukhansk Uplift), *Am. J. Sci.,* 1995, vol. 295, no. 6, pp. 823–850.

Komar, V.A., On the Structure and Stromatolites of the Upper Riphean Type Sections (Southern Urals), *Izv. Akad. Nauk SSSR, Ser. Geol.,* 1978, no. 8, pp. 50–60.

Koroteev, V.A., Krasnobaev, A.A., and Necheukhin, V.M., Geochronology and Geodynamics of the Upper Proterozoic of Northern Eurasia, in *Rifei Severnoi Evrazii: Geologiya, Obshchie problemy stratigrafii* (The Riphean of Northern Eurasia: Geology, General Problems of Stratigraphy), Yekaterinburg: Ural. Otd. Ross. Akad. Nauk, 1997, pp. 28–36.

Kozlov, V.I., *Verkhnii rifei i vend Yuzhnogo Urala* (The Upper Riphean and Vendian of the Southern Urals), Moscow: Nauka, 1982.

Kozlov, V.I., Krasnobaev, A.A., Kozlova, E.B., Sergeeva, N.D., Genina, L.A., Larionov, N.N., and Mikhailov, P.N., *Stratigrafiya rifeya v stratotipicheskom razreze Yuzhnogo Urala* (Stratigraphy of the Riphean Stratotype in the Southern Urals), Ufa: Bashkir Nauch. Tsentr Akad. Nauk SSSR, 1991.

Krylov, I.N., Stratigraphy and Microfossils from the Riphean Min'yar Formation in the Southern Urals, *Sov. Geol.,* 1983, no. 6, pp. 60–72.

Kuznetsov, A.B., Gorokhov, L.M., Mel'nikov, N.N., *et al.,* Rb-Sr Systematics of Postdepositional Alterations of Carbonates from the Karatau Group, Southern Urals, Abstracts of Papers, *XIV Symp. po geokhimii izotopov* (XIV Symp. on Isotopic Geochemistry), Moscow: Inst. Geochim. Analit. Chim. Ross. Akad. Nauk, 1995a, pp. 126–127.

Kuznetsov, A.B., Gorokhov, I.M., Ovchinnikova, G.V., *et al.,* Postsedimentary Alteration of Upper Riphean Limestones of the Katav Formation, the South Urals: Chemical and Isotopic Evidence, in *Precambrian of Europe: Stratigraphy, Structure, Evolution and Mineralization, MAEGS-9. Abstr.,* St. Petersburg, 1995b, p. 60.

Kuznetsov, A.B., Gorokhov, I.M., Semikhatov, M.A., Mel'nikov, N.N., and Kozlov, V.I., Strontium Isotope Composition in Limestones of the Inzer Formation, the Upper Riphean Type Section, Southern Urals, *Dokl. Akad. Nauk,* 1997, vol. 353, no. 2, pp. 249–254.

Maslov, A.V., *Litologiya verkhnerifeiskikh otlozhenii Bashkirskogo megantiklinoriya* (Lithology of the Upper Riphean Deposits of the Bashkir Meganticlinorium), Moscow: Nauka, 1988.

Maslov, A.V., On the Problem in the Middle–Upper Riphean Boundary in the Southern Urals, in *Stratigrafiya verkhnego proterozoya SSSR: Rifei i vend,* (The Upper Proterozoic Stratigraphy of the USSR: Riphean and Vendian), Ufa: Bashkir Nauch. Tsentr Ural. Otd. Akad. Nauk SSSR, 1990, pp. 76–78.

Maslov, A.V., Riphean Sedimentary Basins of the Western Slope of the Southern Urals: Facies, Lithological–Facial Complexes, Paleogeography, Evolution, *Doctorate Sci. (Geol.–Min.) Dissertation,* Yekaterinburg: Inst. Geol. Geochem. Ural Division Rus. Acad. Sci., 1997, p. 44.

Maslov, A.V., Abduazimova, Z.M., Karsten, L.A., and Puchkov, V.N., First Occurrences of *Melanocerillium* in the Riphean Type Sections of the Southern Urals, in *Sostoyanie, problemy i zadacha geologicheskogo kartirovaniya oblastei razvitiya dokembriya na territorii Rossii* (State, Problems, and Goal of the Geological Mapping of the Precambrian Areas in Russia), St. Petersburg: Vseross. Geol. Inst., 1994, p. 90.

Maslov, A.V. and Krupenin, M.T., *Razrezy rifeya Bashkirskogo meganticlinoriya (zapadnyi sklon Yuzhnogo Urala)* (Riphean Sections of the Bashkir Meganticlinorium, Western Slope of the Southern Urals), Sverdlovsk: Ural. Otd. Akad. Nauk SSSR, 1991.

Narbonne, G.M., Kaufman, A.J., and Knoll, A.H., Integrated Chemostratigraphy and Biostratigraphy of the Windermere Supergroup, Northwestern Canada: Implications for Neoproterozoic Correlation and Early Evolution of Animals, *Bull. Geol. Soc. Am.,* 1994, vol. 106, no. 10, pp. 1281–1292.

Ovchinnikova, G.V., Gorokhov, I.M., Semikhatov, M.A., *et al.,* Timing of Formation and Alteration of Deposits of the Upper Riphean Inzer Formation, Upper Riphean, Southern Urals, in *Obshchie problemy stratigrafii i geologicheskoi istorii rifeya Severnoi Evrasii* (General Problems of the Riphean Stratigraphy and Geological History of Northern Eurasia), Yekaterinburg: Ural. Otd. Ross. Akad. Nauk, 1995a, pp. 73–75.

Ovchinnikova, G.V., Semikhatov, M.A., Gorokhov, I.M., *et al.,* U-Pb Systematics of the Precambrian Carbonates: the Riphean Sukhaya Tunguska Formation, Turukhansk Uplift, Siberia, *Litol. Polezn. Iskop.,* 1995b, no. 5, pp. 525–536.

Ovchinnikova, G.V., Vasil'eva, I.M., Semikhatov, M.A., *et al.,* U-Pb Systematics of Proterozoic Carbonate Rocks: the Inzer Formation of the Upper Riphean Stratotype (Southern Urals), *Stratigr. Geol. Korrelyatsiya,* 1998, vol. 6, no. 4, pp. 336–347.

Podkovyrov, V.N. and Vinogradov, D.P., Epigenesis and Preservation of Carbon and Oxygen Isotopic Systems in Carbonates of the Lakhanda and Yudoma Groups of the Upper Riphean–Vendian Sections at the Belaya River, Southeastern Sakha, *Litol. Polezn. Iskop.,* 1996, no. 5, pp. 541–551.

Podkovyrov, V.N., Kuznetsov, A.B., Semikhatov, M.A., *et al.,* C- and Sr-Isotopic Composition in Carbonates of the Upper Riphean Stratotype: the Karatau Group, Southern Urals, in *Dokembrii Severnoi Evrazii* (The Precambrian of Northern Eurasia), St. Petersburg: Inst. Geol. Geochronol. Dokembr., 1997, p. 84.

Raaben, M.E., *Verkhnii rifei kak edinitsa obshchei stratigraficheskoi shkaly* (The Upper Riphean as a Unit of the Srandard Stratigraphic Scale), Moscow: Nauka, 1975.

Raaben, M.E. and Komar, V.A., The Lower–Upper Karatavian Boundary in the Uralian Stratotype, *Izv. Akad. Nauk SSSR, Ser. Geol.,* 1983, no. 9, pp. 86–96.

Schidlowski, M., Eichmann, R., and Junge, C., Precambrian Sedimentary Carbonates: Carbon and Oxygen Isotope Geochemistry and Implications for the Terrestrial Oxygen Budget, *Precambrian Res.,* 1975, vol. 2, no. 1, pp. 1–69.

Schidlowski, M., Hayes, I.M., and Kaplan, I.R., Isotopic Inference of Ancient Biochemistries: Carbon, Sulfur, Hydrogen, and Nitrogen, *Earth's Earliest Biosphere,* Schopf, J.W., Ed., Princeton: Princeton Univ., 1983, pp. 149–187.

Semikhatov, M.A., Methodic Principles of the Riphean Stratigraphy, *Stratigr. Geol. Korrelyatsiya,* 1995, vol. 3, no. 6, pp. 33–50.

Semikhatov, M.A. and Raaben, M.E., Dynamics of the Global Diversity of Proterozoic Stromatolites. Article 2. Africa, Australia, North America and General Synthesis, *Stratigr. Geol. Korrelyatsiya,* 1996, vol. 4, no. 1, pp. 26–54.

Semikhatov, M.A. and Serebryakov, S.N., *Sibirskii gipostratotip rifeya* (The Siberian Hypostratotype of the Riphean), Moscow: Nauka, 1983.

Semikhatov, M.A., Podkovyrov, V.N., Vinogradov, D.V., *et al.,* A Carbon Isotopic Composition of the Riphean Carbonate: the Type Upper Riphean Succession, the South Urals, in *MAEGS-9: Preambrian of Europe: Stratigraphy, Structure, Evolution, and Mineralization,* St. Petersburg, 1995, p. 101.

Semikhatov, M.A., Shurkin, K.A., Aksenov, E.M., *et al.,* New Stratigraphic Scale for the Precambrian of the USSR, *Izv. Akad. Nauk SSSR, Ser. Geol.,* 1991, no. 4, pp. 3–16.

Sergeev, V.N., *Okremnennye mikrofossilii dokembriya i kembriya Urala i Srednei Azii* (Precambrian and Cambrian Silicified Microfossils from the Urals and Central Asia), Moscow: Nauka, 1992.

Shalaginov, V.V. and Maslov, A.V., The Riphean of the Urals, Problems of Stratigraphy and Correlation, in *Rifei Severnoi Evrazii: Geologiya, obshchie problemy stratigrafii* (The Riphean of Northern Eurasia: Geology, General Problems of Stratigraphy), Yekaterinburg: Ural. Otd. Ross. Akad. Nauk, 1997, pp. 78–85.

Sochava, A.V., Podkovyrov, V.N., and Vinogradov, D.P., Variations in the Carbon and Oxygen Isotope Compositions in the Vendian–Lower Cambrian Carbonates of the Ura Anticlinorium, the South Siberian Platform, *Litol. Polezn. Iskop.,* 1996, no. 3, pp. 279–289.

Sokolov, B.S., The Vendian System and "Neoproterozoic III," *Stratigr. Geol. Korrelyatsiya,* 1995, vol. 3, no. 6, pp. 51–67.

Stratotip rifeya: Paleontologiya. Paleomagnetizm (The Riphean Stratotype: Paleontology, Paleomagnetism), Keller, B.M., Ed., Moscow: Nauka, 1982.

Stratotip rifeya: Stratigrafiya. Geokhronologiya (Stratotype of the Riphean: Stratigraphy, Geochronology), Keller, B.M. and Chumakov, N.M., Eds., Moscow: Nauka, 1983.

Strauss, H. and Moore, T.B., Abundance and Isotopic Composition of Carbon and Sulfur Species in Whole Rock and Kerogen Samples, *The Proterozoic Biosphere: Multidisciplinary Study,* Schopf, J.W. and Klein, C., Eds., Cambridge: Cambridge Univ., 1992, pp. 583–600.

Unifitsirovannye regional'nye stratigraficheskie skhemy Urala (The Unified Regional Stratigraphic Schemes of the Urals), Yekaterinburg: Ural. Otd. Ross. Akad. Nauk, 1993.

Veizer, J., Trace Elements and Isotopes in Sedimentary Carbonate, *Rev. Mineral.,* 1983, no. 11, pp. 260–299.

Veizer, J., Plumb, K.A., Clayton, R.N., *et al.,* Geochemistry of Precambrian Carbonates. 5. Late Paleoproterozoic Seawater, *Geochim. Cosmochim. Acta,* 1992, vol. 56, no. 6, pp. 2487–2501.

Yudovich, Ya.E., Maidl', T.V., and Ivanova, T.I., *Geokhimiya strontsiya v karbonatnykh otlozheniyakh* (Strontium Geochemistry in Carbonate Rocks), Leningrad: Nauka, 1980.

Stratigraphy and Geological Correlation, Vol. 6, No. 4, 1998, pp. 336–347. Translated from Stratigrafiya. Geologicheskaya Korrelyatsiya, Vol. 6, No. 4, 1998, pp. 20–31.
Original Russian Text Copyright © 1998 by Ovchinnikova, Vasil'eva, Semikhatov, Kuznetsov, Gorokhov, Gorokhovskii, Levskii.
English Translation Copyright © 1998 by МАИК Наука/Interperiodica Publishing (Russia).

U-Pb Systematics of Proterozoic Carbonate Rocks: The Inzer Formation of the Upper Riphean Stratotype (Southern Urals)

G. V. Ovchinnikova*, I. M. Vasil'eva*, M. A. Semikhatov, A. B. Kuznetsov*, I. M. Gorokhov*, B. M. Gorokhovskii*, and L. K. Levskii***

** Institute of Precambrian Geology and Geochronology, Russian Academy of Sciences, nab. Makarova 2, St. Petersburg, 199034 Russia*
*** Geological Institute, Russian Academy of Sciences, Pyzhevskii per. 7, Moscow, 109017 Russia*
Received December 30, 1996

Abstract—U-Pb and Pb-Pb isotopic systems were studied in limestones of the Inzer Formation representing the middle part of the Karatau Group of the Urals, whose section is authorized as the Upper Riphean stratotype. Carbonate rock samples selected to study the U-Pb and Pb-Pb systematics are apparently lacking indications of significant secondary alterations. Geochemical criteria applied to select the least altered samples were ratios Mn/Sr ≤ 0.2, Fe/Sr ≤ 5, and Rb/Sr ≤ 0.001, and also the minimum difference between $^{87}Sr/^{86}Sr$ ratios in primary and secondary carbonate phases separated by sample treating in 1 N solution of ammonium acetate (NH_4OAc). Carbonate fractions, some preliminary treated in NH_4OAc to remove secondary carbonate components, were dissolved in 1 N HCl under the room temperature before extracting U and Pb. Samples of the lower Inzer limestones satisfying the above criteria yielded Pb-Pb age value of 836 ± 25 Ma. This value corresponds to the time of early diagenesis in sediments and represents the isotopic date for the Upper Riphean stratotype best substantiated at present in methodical aspects. Diagenetic alterations in the lower Inzer sediments occurred when U and Pb systems in the latter were open under the influence of fluids derived from the underlying deposits of the Katav Formation. The inferred μ value and Pb isotope composition in the fluid are close to these parameters in siliciclastic fractions of the last formation. The parallel study of U-Pb and Pb-Pb systems of carbonate rocks is useful for detecting conditions of diagenesis and for elucidating the composition and possible source of diagenetic fluids.

Key words: *isotopic age, U-Pb systematics, carbonate rocks, diagenesis, Upper Proterozoic, Riphean, southern Urals.*

INTRODUCTION

Isotopic dates for the Karatau Group of southern Urals, the authorized stratotype of the Upper Riphean, were represented for a long period by K-Ar dates for glauconites poorly studied in mineralogical aspect and for whole-rock samples of gabbro-diabases, which are considered to be pre-Karatavian in age. The dating of glauconites yielded age values decreasing upward from 970–938 Ma in the lower part of the group to 658–600 Ma near its top, whereas dates for gabbro-diabases, except the evidently rejuvenated values, were approaching 1150–1000 Ma (Garris *et al.*, 1964; Garris, 1977; *Stratotip rifeya,* 1983). Later, the Rb-Sr isochron method applied to the Upper Karatau glauconites yielded the age value of 688 ± 10 Ma (Gorozhanin and Kutyavin, 1986). On the basis of these and other dates for overlying deposits, the time range of the Karatau Group was estimated as ranging either from 1050 ± 50 to 650 ± 50 (680 ± 20) Ma (Garris, 1977; Keller *et al.*, 1977; *Stratotip rifeya,* 1983, and references in these publications), or from 1000 ± 50 to 650 ± 20 Ma (Keller *et al.*, 1984; Bibikova *et al.*, 1989; Semikhatov *et al.*, 1991). However, these inferences require some verification in the light of recent data on stability of K-Ar and Rb-Sr systems in the above geochronometers.

The current progress in dating the carbonate rocks by using the U-Pb and Pb-Pb methods (for review and references, see Moorbath *et al.*, 1987; Jahn and Cuvellier, 1994; Ovchinnikova *et al.*, 1995b) opens a new possibility for the determination of the isotopic age of the Karatau Group predominantly composed of limestones and dolomites. In this work, we focused our attention on the Inzer Formation constituting a middle part of the group and represented by limestones, whose secondary alterations are very weak.

The practice of using the U-Pb and Pb-Pb methods for dating the carbonate rocks shows that isochron relations between measured values cannot be observed everywhere, and when this is the case, the calculated isotopic age does not always corresponds to the stratigraphic age of the studied samples. The basic reason here is the reorganization of U-Pb and Pb-Pb systems in

carbonates during their postsedimentation history. Accordingly, one of the essential procedures used in this study was a selection of the least altered rock samples appropriate for the U-Pb dating; we used a series of petrographic, geochemical, and isotopic-geochemical criteria to select them.

STRATIGRAPHIC POSITION AND COMPOSITION OF STUDIED SAMPLES

The Karatau Group, which is terminal in the Riphean type section, includes six formations exposed in the western and central areas of the Bashkir anticlinorium of southern Urals, where the total thickness of these deposits is 3.0 to 5.5 km. The lower (Zil'merdak) and upper (Krivaya Luka) formations are siliciclastic in composition, while four other units of the studied section (Katav, Inzer, Min'yar, and Uk formations) are predominantly or completely composed of carbonate deposits (*Stratotip rifeya*, 1983; Keller *et al.*, 1984; Kozlov *et al.*, 1991). The siliciclastic-carbonate Inzer Formation, whose samples have been analyzed in this study, constitutes the middle part of the sequence. Some time ago, lithostratigraphy of this interval, particularly the relations between its carbonate and siliciclastic members, have been variably interpreted (Komar, 1978; Raaben and Komar, 1983; Krylov, 1983; *Stratotip rifeya*, 1983), but now (Kozlov *et al.*, 1991) it is firmly established that in the western part of the anticlinorium, where we collected our samples, carbonates constitute the lower subformation and the middle member in the upper subformation of the Inzer Formation.

Secondary alterations in carbonate rocks of the Inzer Formation usually are insignificant (Kuznetsov *et al.*, 1997; Podkovyrov *et al.*, 1998). Despite this, in the procedure of U-Pb dating, we used only the samples from the lower subformation representing a monotonous limestone sequence, where the rare beds only experienced dolomitization. We excluded from analysis the upper Inzer limestones occurring as a minor member amid sandy to clayey units of the upper subformation, because their Pb system could be contaminated due to the close proximity to siliciclastic rocks.

The studied samples were collected from two sections (Fig. 1). One of them exhibits the entire Inzer succession and is located at the right-hand side of the Sim River in outskirts of town of Min'yar. The lower Inzer Subformation (Podinzer Beds in terminology of Goryainova and Fal'kova, 1933) represents here the 190-m-thick sequence of dark-gray and black, chiefly aphanic limestones with fine horizontal or rare cross-bedded lamination, and interbeds and lenses of carbonate breccias and flakestones. Within the 35-m-thick horizon in the middle part of the sequence, these rocks experienced dolomitization (Fig. 2). Interbeds of clayey limestone analogous to the same rock types in the underlying Katav Formation occur in the basal part of the subformation. Another section is exposed along the highway Ufa–Beloretsk near the settlement of Kulmas. This exposure corresponds to the 60-m-thick middle fragment of the lower Inzer Subformation comprising the aforementioned horizon of dolomitic rocks and the limestone member below it. These rocks do not differ in composition and structural features from their counterparts exposed in the Min'yar section.

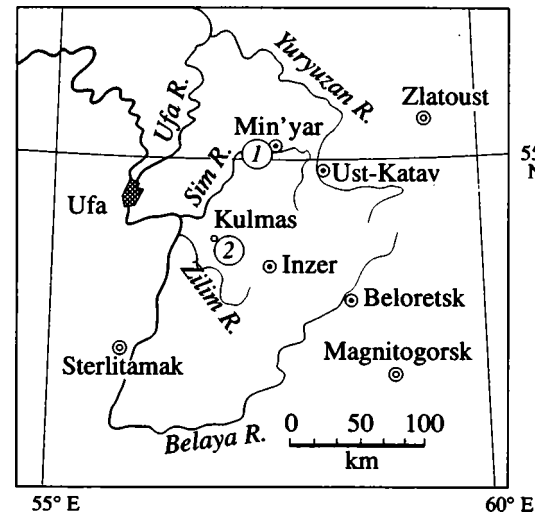

Fig. 1. Geographic map showing the position of the studied Min'yar (*1*) and Kulmas (*2*) sections of the Inzer Formation.

The recrystallization degree of the lower Inzer carbonates, predominantly represented by micrite and microsparite, is low. In its basal portion, the subformation consists of micritic limestones with thin microsparite lenses and small sparite inclusions. In the upper part, it shows frequently alternating laminae of micrite and microsparite with relict clastic structures and miniature fragments of replaced fibrous calcite. In addition, the fine-grained calcite may form sporadic nests of crystals and occurs as a mineral filling of microfractures in the rock that is characteristic of the Kulmas rather than the Min'yar section. The carbonate fraction of the rocks usually consists of quite pure calcite (Mg content up to 0.35%, Table 1), but in the aforementioned horizon of dolomitic rocks the Mg concentration rises up to 2.5% (Kuznetsov *et al.*, 1997). The low content of residual fraction insoluble in HCl is a characteristic feature of all the rocks. In the studied samples, it is usually 0.2–0.8%; higher values of 1.9 and 4.4% were measured in two cases only (Table 1). The X-ray diffraction data show that the insoluble residue incorporates quartz, less frequent feldspar, and traces of illite. The cathodoluminescent analysis demonstrates that our limestone samples are dominated by nonluminescent calcite, and only rare inclusions of zonal calcite grains of the late generation and their aggregates display the pink to yellow luminescence.

Accumulation of sediments of the lower Inzer Subformation occurred after the paleogeographic rearrangement in the Late Riphean basin of the southern Urals. This event resulted in the following conse-

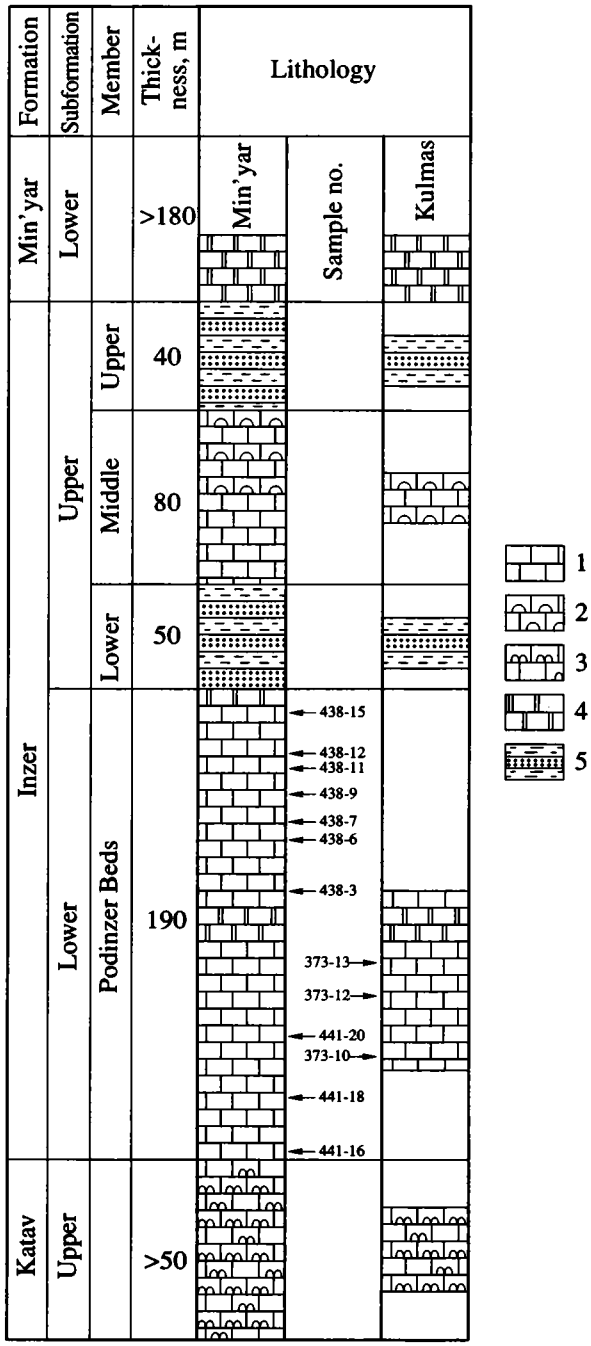

Fig. 2. Lithology and labeled positions of samples in the studied sections: (1) limestones; (2) stromatolitic limestones; (3) clayey limestones; (4) dolomitic limestones and dolomites; (5) siliciclastic deposits.

quences: in reduction of the western provenance, the main source of clastic material during the Zil'merdak–Katav time; in accumulation of thick carbonate and siliciclastic successions in the open-sea settings; and in appearance of the eastern provenance, whose influence on the study region was perceptible only in the late Inzer time (Maslov, 1988). Thus, the studied lower Inzer deposits of the Min'yar and Kulmas localities accumulated in an open-sea environments outside a zone of active influx of siliciclastic material.

INVESTIGATION METHODS

To study chemostratigraphy (Kuznetsov *et al.*, 1997; Podkovyrov *et al.*, 1998) and isotopic-geochronological parameters of the Karatau carbonates (this work), we selected homogeneous rock samples lacking signs of secondary recrystallization. Each of them was sawed into two parts, one for the chemical and isotopic analysis, and another for studying petrography and cathodoluminescence.

By chemical analysis, samples were dissolved using 1 N HCl. We used the standard weight method to determine contents of Ca and Mg in the carbonate fraction, and the atomic absorption spectrometry to measure concentrations of Mn and Fe. The isotopic dilution mass spectrometry was used to determine concentrations of Rb and Sr.

Selection of samples intended for investigation of U-Pb systematics was performed in two stages. Initially, we selected those samples of 27 available which were known to have low values of Mn/Sr, Fe/Sr, and Rb/Sr ratios, because one of the factors resetting isotopic systems in carbonates is the mineral interaction with fresh-water fluids that rises concentrations of Mn and Fe in carbonates and also is responsible for their depletion in Sr (Brand and Veizer, 1980; Gorokhov, 1996). It should be stressed that we used strict geochemical criteria indicative of low alteration degree, such as $Mn/Sr \leq 0.2$, $Fe/Sr \leq 5$, and $Rb/Sr \leq 0.001$ (Kuznetsov *et al.*, 1997). Another criterion used to verify the low alteration degree of samples was the $\delta^{18}O$ parameter that ranges in unaltered limestones from –7.5 to –8.5‰ PDB (Podkovyrov *et al.*, 1998).

During the next step of selection, we took into account that Precambrian limestones and dolomites consist of carbonate phases different in age and geochemical parameters, among which only one phase corresponds to the primary carbonate, whereas another (or others) is related in origin to secondary (catagenetic) stages of the rock alteration (Gorokhov *et al.*, 1995b; Ovchinnikova *et al.*, 1995b). Accordingly, we selected for U-Pb dating only those samples, which were found to display the lowest alteration degree in terms of Rb-Sr systematics (Kuznetsov *et al.*, 1997). In practice, we classified our samples as appropriate when they showed a minimum difference between $^{87}Sr/^{86}Sr$ ratios of the primary and secondary phases.

Some of the samples selected for analysis of U-Pb and Pb-Pb isotopic systems were preliminary treated in 1 N solution of ammonium acetate (NH_4OAc) in order to separate their heterogeneous carbonate phases (Gorokhov *et al.*, 1995b; Ovchinnikova *et al.*, 1995b). The samples were dissolved in 1 N HCl under the room temperature for subsequent extraction of U and Pb.

Table 1. Chemical composition of carbonate fractions in limestones of the lower Inzer Subformation

Sample no.	Insoluble residue, wt %	Ca, %	Mg, %	Mn, μg/g	Fe, μg/g	Rb, μg/g	Sr, μg/g	Ca/Sr	Mn/Sr	Fe/Sr
373-10	0.57	39.3	0.13	18	460	0.11	439	900	0.04	1.1
373-12	0.63	39.5	0.51	14	395	0.09	417	950	0.03	0.9
373-13	4.41	39.1	0.43	11	160	0.12	570	660	0.02	0.3
438-3	0.82	39.1	0.35	23	420	0.07	495	790	0.05	0.8
438-6	0.21	40.0	0.26	19	220	0.07	512	780	0.04	0.4
438-7	0.58	39.6	0.23	18	210	–	–	–	–	–
438-9	0.67	39.9	0.24	21	325	0.04	521	770	0.04	0.6
438-11	0.14	39.8	0.19	18	310	–	–	–	–	–
438-12	0.33	40.0	0.19	21	310	0.07	605	660	0.03	0.5
438-15	0.25	40.0	0.18	22	315	0.21	545	730	0.04	0.6
441-16	1.91	39.2	0.11	75	1735	0.33	486	940	0.15	0.8
441-18	0.77	39.5	0.11	44	420	0.15	411	960	0.11	1.1
441-20	0.54	39.7	0.01	15	330	0.19	423	810	0.04	3.6

Abbreviations used below to designate the analyzed rock fractions are as follows: PCC-1 is for the carbonate residue after the sample treatment with NH_4OAc, and this fraction is assumed to be enriched in the primary carbonate component; PCC-2 is for the whole-rock carbonate material untouched by treatment with NH_4OAc; and ISR is for the residue insoluble in HCl.

Pb isotope composition and concentrations of U and Pb were analyzed in aliquots using the mixed $^{235}U + ^{208}Pb$. tracer. U and Pb were separated from bromide solutions using the ion-exchange technique with Bio-Rad 1 × 8 as described by Manhes *et al.* (1978). U and Pb isotope compositions were analyzed on Finnigan MAT-261 multicollector mass spectrometer using a regime of simultaneous measurement of all isotope ion currents. The measured Pb isotope ratios were corrected for mass fractionation of 0.11% per atomic mass unit calculated from replicate measurements of Pb isotope composition in NBS SRM-982 standard. The procedure blank during the period of our investigation was 0.05 ng for U and 0.5 ng for Pb. Raw U-Pb data were processed using the PBDAT program, and isochron regressions were calculated using the Isoplot v. 2.0 package of Ludwig (1989, 1990). All uncertainty values are quoted in the paper at the 2σ level.

RESULTS

The studied sections with labeled positions of the analyzed samples are illustrated graphically in Fig. 2. Data of chemical analysis are summarized in Table 1, and U-Pb isotopic results for different rock fractions are shown in Table 2.

In the $^{207}Pb/^{204}Pb$–$^{206}Pb/^{204}Pb$ diagram (Fig. 3), all data points for PCC-1 and PCC-2 plot along a linear array producing two groups with different ranges of isotopic ratios. Samples 438-6, 438-9, 438-11, and 438-12 from the upper part of the lower Inzer Subformation (the Min'yar locality) represent the first group and reveal the higher values of $^{207}Pb/^{204}Pb$ and $^{206}Pb/^{204}Pb$ ratios. The second group of data points is displaced toward the origin of the coordinates and corresponds to three samples from the same part of the Min'yar section (438-3, 438-7, and 438-15) and to all samples from lower beds of the above locality (441-16, 441-18, and 441-20) and from the Kulmas section (373-10, 373-12, and 373-13).

The combination of all PCC-1 and PCC-2 data points (n = 19) defines the Pb-Pb errorchron corresponding to a date of 891 ± 46 Ma with the MSWD value of 21.9. Omission of five data points most obviously deviating from the regression line (PCC-1 and PCC-2 phases of samples 438-9 and 441-16, and PCC-2 phase of Sample 438-3) reduces the date to 836 ± 25 Ma (MSWD = 3.9, n = 14). The low MSWD value allows us to consider the last date as statistically reliable. Within the admissible error, this date is concordant with the Pb-Pb age value for the lower Inzer Subformation calculated on the basis of a lesser group of samples (848 ± 48 Ma according to Ovchinnikova *et al.*, 1995a). The result is also well compatible with the succession of K-Ar dates on glauconites from the middle horizons of the Karatau Group: 938 Ma for the upper part of the Katav Formation underlying the Inzer beds; 896–853 Ma for the lower–middle interval of the Inzer Formation; 791–683 Ma for the upper member of this formation; and 740–680 Ma for deposits of the overlying Min'yar Formation (Garris, 1977; *Stratotip rifeya*, 1983).

The U-Pb age values calculated on the basis of selected 14 data points turn out to be much older, as compared to the Pb-Pb date, and characterized by much

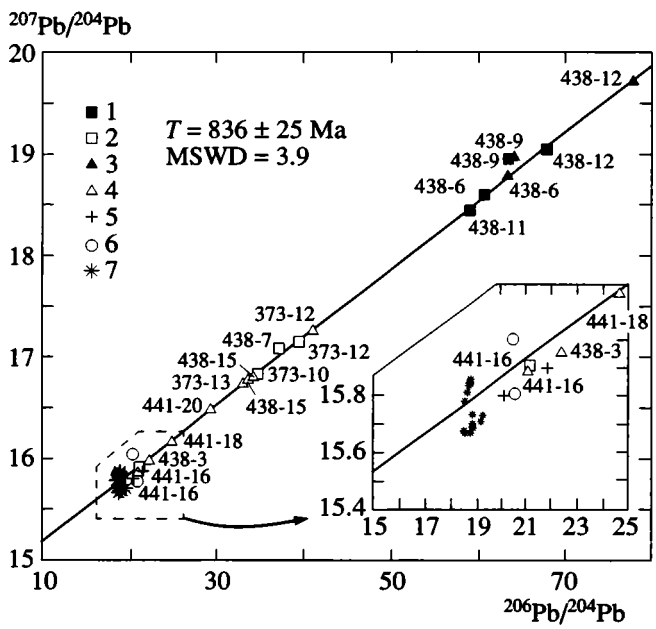

Fig. 3. $^{207}Pb/^{204}Pb$–$^{206}Pb/^{204}Pb$ diagram for carbonate rocks from the Inzer and Katav formations: (1–5) data points for the Inzer Formation indicating PCC-1 phases of the first (1) and second (2) groups, PCC-2 phases of the first (3) and second (4) groups, and (5) ISR phases of the studied samples; (6–7) data points for the Katav Formation indicating ISR (6) and carbonate (7) phases of limestones (abbreviations are explained in the text).

higher uncertainties and MSWD magnitudes: $T(^{206}Pb/^{238}U) = 1160 \pm 150$ Ma with the MSWD value of 7110 and $T(^{207}Pb/^{235}U) = 1060 \pm 50$ Ma with the MSWD value of 219. This remark concerns in full measure to U-Pb dates calculated for the second group of samples from the Inzer Formation (Figs. 4, 5). The high magnitude of uncertainties and MSWD indicates a distortion of U-Pb isotopic systems in the studied limestones, especially in the second group of our samples.

The overstated U-Pb ages may be a consequence of the U loss from, and/or Pb introduction into the isotopic system. The migration ability of U under conditions of hypergenesis is well known (Asmersom and Jacobsen, 1993; Jahn and Cuvellier, 1994; Hoff *et al.*, 1995; Jones *et al.*, 1995; Ovchinnikova *et al.*, 1995b), whereas the principal possibility of low-radiogenic Pb introduction into limestones of the lower Inzer Subformation is discussed below. Taking into account all these factors, we consider the U-Pb age values calculated for the whole set of samples as meaningless in the geological aspect and exclude them from the subsequent geochronological considerations. As for the U-Pb ages calculated separately for the first group of our samples (see Figs. 4, 5), they are concordant within the error limits to the Pb-Pb date calculated for the whole group of the analyzed samples. However, the age uncertainty and MSWD estimated for the last group are also high, and these U-Pb dates are excluded from consideration as well.

DISCUSSION

U-Pb systematics of carbonate rocks. Geochemical parameters of the studied Inzer limestones show that their samples attributed to the second group are more rich in U and Pb, as compared to the first sample group, and they are also characterized by the less radiogenic Pb isotope composition and by low measured values of $\mu = {}^{238}U/{}^{204}Pb$ (Table 2). This situation may be either a consequence of initial geochemical variations in sedimentation environments, or a result of postdepositional disturbances in U-Pb systems of our samples that is the more likely case.

Difference in U-Pb systematics between both groups of carbonates is well evident in $^{206}Pb/^{204}Pb$–$^{238}U/^{204}Pb$ and $^{207}Pb/^{204}Pb$–$^{235}U/^{204}Pb$ diagrams (Figs. 4, 5). Whereas data points of the second sample group plot along a single trend together with ISR phases of Inzer limestone and with all studied phases of the Katav rocks, those of the first group plot a little above this trend. In addition, MSWD value characterizing the data point dispersion relative to the regression line is much higher for the second group, than for the first one. This suggests that in one rock group the disturbance of U-Pb systems was more significant than in another.

In terms of U-Pb systematics, $\mu_1 = {}^{238}U/{}^{204}Pb$ is a decisive parameter of environment (geochemical reservoir), under which the carbonate sediments were accumulated or recrystallized. This parameter is usually calculated in accordance with the one-stage model of Pb evolution. The model suggests that radiogenic Pb isotopes reside in a closed system with a definite μ_1 value at the time ($T = 4.55$ Ga) of the Earth formation (Tatsumoto *et al.*, 1973). In the $^{207}Pb/^{204}Pb$–$^{206}Pb/^{204}Pb$ diagram, the Pb growth curves corresponding to different μ_1 values take their origin from one point characterizing the isotopic composition of primordial Pb of the Earth. Hypothetical data points of the growth curves illustrating the Pb isotope composition in systems with different μ_1 values at the time t plot along a single line (the so-called primary isochron) connecting these points with the point of primordial Pb (whose age is T). Intersection of the primary isochron, whose age is t, and the secondary one, which is plotted on the basis of experimental Pb-Pb data and also corresponds to the age t, defines the model μ_1 value. Such an intersection point belongs to a particular Pb growth curve, and its μ_1 value is characteristic of both this curve and environments of rock formation (Faure, 1986).

Jahn and Cuvellier (1994) demonstrated that the mean μ_1 value calculated in accordance with the one-stage model for carbonates of a wide stratigraphic range (from 2.6 to 0.18 Ga old) is equal to 8.4 ± 0.4, i.e., it is several orders of magnitude lower than in recent marine carbonates (>50000). Our limestones are not an exception, because the model μ_1 value calculated for the lower Inzer Subformation is equal to 8.4. This striking uniformity of μ_1 values calculated for carbonates highly variable in age indicate that their U-Pb sys-

Table 2. Element concentrations and U-Pb isotopic ratios measured in different rock fractions of the Inzer limestones

Sample no.	Rock fraction	Pb, μg/g	U, μg/g	μ	$^{206}Pb/^{204}Pb$	$^{207}Pb/^{204}Pb$	$^{208}Pb/^{204}Pb$
441-16	PCK-2	1.009	0.247	16.20	21.088	15.887	38.294
441-16	PCK-1	0.971	–	–	21.172	15.907	38.369
441-16	HPO	6.810	3.59	33.99	20.137	15.805	37.697
441-18	PCK-2	–	–	–	24.664	16.164	37.781
441-20	PCK-2	–	–	–	29.397	16.481	37.393
438-3	PCK-2	0.377	0.124	22.09	22.395	15.956	38.165
438-6	PCK-2	0.154	0.346	234.2	63.504	18.808	37.521
438-6	PCK-1	0.167	0.350	213.2	60.694	18.599	37.535
438-7	PCK-1	–	–	–	37.164	17.070	38.765
438-9	PCK-2	0.202	0.488	256.8	64.230	18.982	39.140
438-9	PCK-1	0.209	0.488	247.0	63.493	18.965	39.197
438-11	PCK-1	0.200	0.394	197.4	58.923	18.456	38.146
438-12	PCK-2	0.158	0.435	325.1	77.800	19.732	38.570
438-12	PCK-1	0.177	0.423	261.5	68.162	19.058	38.415
438-15	PCK-2	0.583	0.542	71.49	33.376	16.748	37.892
438-15	PCK-1	0.516	0.628	94.74	34.313	16.809	37.925
373-10	PCK-2	0.639	0.779	96.17	34.092	18.814	39.520
373-12	PCK-2	0.419	0.744	151.5	41.113	17.271	39.514
373-12	PCK-1	0.415	–	–	39.539	17.151	39.330
373-13	PCK-2	0.624	0.586	72.67	32.902	16.714	38.992
373-13	HPO	16.50	5.73	22.76	21.851	15.905	37.099

tems were reset at the similar stages of lithogenesis in response to the Pb introduction and, possibly, to the U loss. Accordingly, the U-Pb and Pb-Pb isotopic dates for carbonates, which did not suffer catagenetic and metamorphic alteration, reflect the age of this process. The known experience of dating shows that in the case of nonmetamorphosed marine carbonates their U-Pb systems were reset in the course of early diagenesis, when carbonate minerals incorporated the mixed leads consisting of fractions derived from sediments themselves and introduced by diagenetic fluids (Haglund *et al.*, 1969; Russell *et al.*, 1994; Jahn and Cuvellier, 1994; Ovchinnikova *et al.*, 1995b; Johnes *et al.*, 1995; Jahn and Simonson, 1995).

The calculated $^{207}Pb/^{204}Pb$–$^{206}Pb/^{204}Pb$ age is correct only then, when the U-Pb systems in a series of studied samples either remained closed since the moment of early diagnesis, or episodically opened at the very beginning of the rock history and/or in the recent time. It is likely that these systems of the Inzer carbonates opened two times. However, such an opening in the course of the early diagenesis (the initial stage of the rock history) and the U loss during the recent hypergenesis do not discredit the correctness of the Pb-Pb dating.

Naturally, a case of mixing the materials with different Pb isotope composition could also produce a straight regression line in the $^{207}Pb/^{204}Pb$–$^{206}Pb/^{204}Pb$ diagram. In this case however, we should expect the same correlation between data points in the $^{208}Pb/^{204}Pb$–$^{206}Pb/^{204}Pb$ coordinates. For the Inzer carbonates, the last assumption is invalid, and the mixing model seems to be hardly appropriate to the occasion. Therefore, we may consider the straight line in Fig. 3 as an isochron, whose inclination angle is meaningful in the geochronological aspect.

Thus, the Pb-Pb age value of 836 ± 25 Ma calculated on the basis of 14 data points apparently corresponds to the time of early diagenesis of carbonate sediments of the lower Inzer Subformation. This inference is supported by Rb-Sr isochron age values of 805–835 Ma measured for the fine-grained mineral fractions of the Inzer shales and corresponding to a later geological event of burial diagenesis (Ovchinnikova *et al.*, 1995a; Gorokhov *et al.*, 1995a).

Source of diagenetic fluids. Comparing the U-Pb systematics of the lower Inzer carbonates and underlying limestones of the Katav Formation (unpublished data of Ovchinnikova and Vasil'eva), we may get an insight into the essence of postsedimentation geochemical processes in the studied part of the Karatau Group. As one can see in $^{238}U/^{204}Pb$–U and $^{238}U/^{204}Pb$-Pb diagrams (Figs. 6, 7), in the carbonate phase of the Inzer samples have higher μ values and are enriched in U, but significantly depleted in Pb (2–10 times of magnitude) as compared to the carbonate phase of the Katav limestones. This is especially characteristic of the first group of the Inzer carbonates, while data points of the second group plot closer to siliciclastic phases of the studied rock samples from both formations. As one would expect, U and Pb concentrations in the last

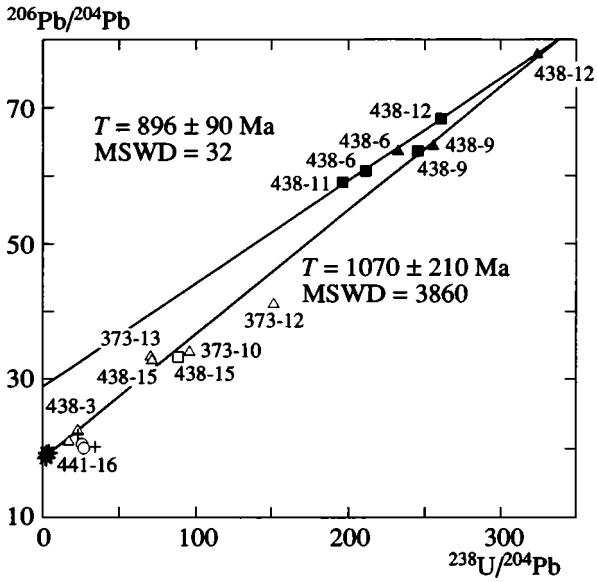

Fig. 4. $^{206}Pb/^{204}Pb$–$^{238}U/^{204}Pb$ diagram for carbonate rocks from the Inzer Formation (symbols as in Fig. 3).

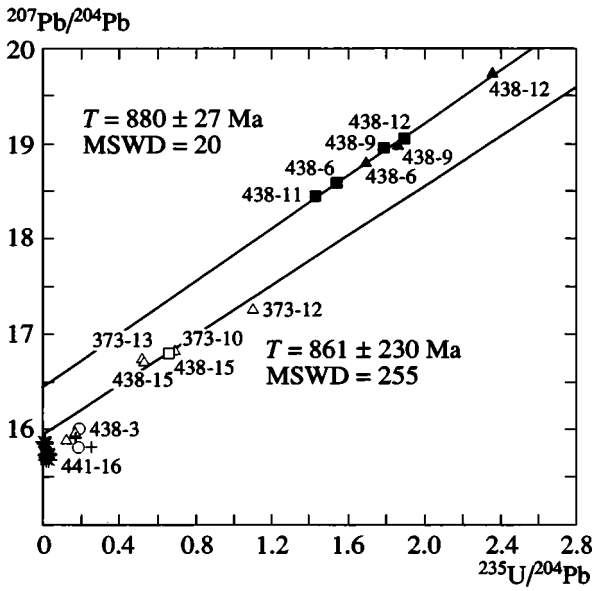

Fig. 5. $^{207}Pb/^{204}Pb$–$^{235}U/^{204}Pb$ diagram for carbonate rocks from the Inzer Formation (symbols as in Fig. 3).

phases are much higher than in carbonates, but their measured μ values are lower.

A significant exchange of Pb isotopes between carbonate and noncarbonate phases (siliciclastic material including) is shown to be a feature of diagenesis and metamorphism (Moorbath *et al.*, 1987; Farquhar *et al.*, 1994; Jahn and Cuvellier, 1994; Babinski *et al.*, 1995; Ovchinnikova *et al.*, 1995b). Consequently, one may assume that a high content of siliciclastic (mostly clayey) fraction in the Katav limestones (14.4% in average according to data published by Kuznetsov *et al.* (1995a), was the main factor responsible for enrichment of diagenetic fluids in U and Pb, and for a lower $^{238}U/^{204}Pb$ ratio in the fluids as compared to carbonate sediments. This resulted not only in a radical disturbance of Rb-Sr and U-Pb systems of the Katav limestones whose PCC-1 phases were enriched in Pb and radiogenic ^{87}Sr (Kuznetsov *et al.*, 1995b), but also in a partial growth of low-radiogenic Pb content in the overlying Inzer carbonates (especially in the second group of our samples). This assumption appears to be supported by the relative stratigraphic position of samples attributed to the first and second groups (Fig. 2), and by data implying that during the compaction of sediments, fluids predominantly migrate in the vertical direction (Choquette and James, 1987). Nevertheless, among samples whose data points highly deviate from the isochron regression line (Fig. 3), two (438-3 and 438-9) are located in the upper horizons of the subformation, and only one (441-16) is collected from its lower part. This situation may indicate that local factors contributed as well to changes in U-Pb systems of the studied samples.

The early diagenetic disturbance of U-Pb systems of the studied Inzer carbonates are responsible for a significant dispersion of data points relative to the regression lines in Figures 4 and 5. Consequently, the intersection points between these lines and axes of ordinates, i.e., the initial Pb isotope composition, can be defined with a considerable uncertainty. As we calculated at the confidence level of 95%, $(^{206}Pb/^{204}Pb)_0$ and $(^{207}Pb/^{204}Pb)_0$ ratios range within 25.5–32.2 and 16.3–16.5, respectively, for the first group of samples, and within 16.6–23.6 and 15.6–16.1, for the second one. Despite the high uncertainty, the calculated ranges suggest that the initial Pb isotope composition was somewhat different in the first and second group of carbonates, though they do not prove this directly. Nevertheless, the Pb-Pb age values calculated separately for each group are concordant within the error limits with the age value estimated on the basis of all data points. Consequently, a difference in the initial composition of Pb isotopes, if possible at all, was not greater than the analytical error.

At the same time, both groups of carbonates are clearly different in their ranges of ^{208}Pb and ^{206}Pb content (Fig. 8). In the studied limestones, any correlation between isotopic ratios of ^{206}Pb, the decay product of ^{238}U, and ^{208}Pb, the decay product of ^{232}Th, is lacking, and this is a consequence of the extremely low (approaching zero) value of $^{232}Th/^{238}U$ ratio in the sea water and recent carbonate sediments. Dispersion of data points in this diagram reflects the variable $^{208}Pb/^{206}Pb$ ratios in the diagenetic fluid whose isotopic composition was controlled by Pb derived from the siliciclastic ISR phase of the Katav limestones. A separate position of data point areas illustrating the ^{208}Pb distribution in siliciclastic ISR phases of the Katav limestones, on the one hand, and of the Inzer limestones, on the other (Fig. 8), sug-

gest a primary difference in composition of siliciclastic material in both formations. In their $^{208}Pb/^{204}Pb$ ratios, the Inzer carbonate phases of the second group of our samples (sample series 373 and some samples from series 441) are more similar to ISR phases of the Katav limestones (Fig. 8), and this similarity favors the assumption that silicate components of the latter affected the chemical and isotopic composition of diagenetic fluids responsible for the distortion of Pb-Pb systems in the Inzer carbonates.

Considering the aforementioned geochemical factors, we may understand why data points of three studied samples (PCC-1 and PCC-2 phases of samples 438-9 and 441-16, and PCC-2 phase of sample 438-3) significantly deviate from the linear regression line shown in $^{207}Pb/^{204}Pb$–$^{206}Pb/^{204}Pb$ diagram (Fig. 3).

In the $^{206}Pb/^{204}Pb$–$^{238}U/^{204}Pb$ and $^{207}Pb/^{204}Pb$–$^{235}U/^{204}Pb$ diagrams (Figs. 4, 5), data points of both carbonate phases from samples 438-3 and 441-16 plot close to data points of ISR phases and thus demonstrate that carbonates have been contaminated with Pb derived from the silicate fractions. This conclusion well accords with a high content of siliciclastic material, Fe, and Mn in Sample 441-16 (Table 1), and also with its stratigraphic position directly above the thick Katav carbonate succession containing a considerable admixture of fine clayey material enriched in Fe (Gareev, 1982).

Sample 438-3 was collected in the upper part of the lower Inzer Subformation above a horizon of dolomitic limestone that separates the sample series 441 and 438 (see Fig. 2). As this sample, when compared to many others, is enriched in ISR and Fe and shows a higher Fe/Sr ratio (Table 1), we may suspect that in this case the U-Pb system was also distorted because of the isotopic exchange between siliciclastic and carbonate fractions of the rock. However, Sample 373-13 shows a higher ISR content than Sample 438-3 (4.41 versus 0.82%), but the data point of the former plots on the isochron line. This controversial situation may reflect some peculiar features of ISR phases of these samples.

PCC-1 and PCC-2 phases of Sample 438-9 plot significantly above the Pb-Pb isochron (Fig. 3), and this may be a consequence of several factors: (1) the sample may be older than others; (2) Pb isotope composition in diagenetic fluid could be unusual; (3) there was the U loss from the system, or the ^{238}U decay chain was disturbed in response to Rn loss; (4) the initial Pb isotope composition in this carbonate phase was different as compared to that in others.

We can easily exclude the first factor, because the sample under consideration is one in a series collected from the continuous stratigraphic succession of deposits (Fig. 2). The second factor also appears to be unrealistic. The carbonate fraction of Sample 438-9 exhibits higher $^{207}Pb/^{204}Pb$ and $^{206}Pb/^{204}Pb$ ratios than all studied ISR phases, and this eliminates a possibility of contamination with Pb derived from the silicate compo-

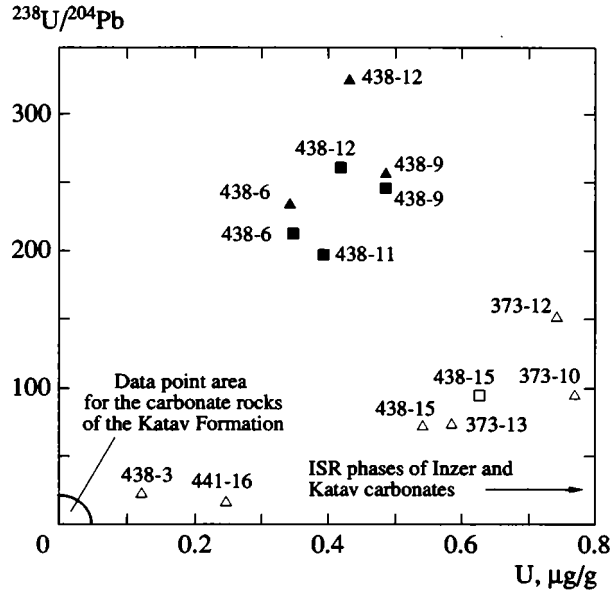

Fig. 6. $^{238}U/^{204}Pb$ ratios and U concentrations in the first and second group of the Inzer carbonates (symbols as in Fig. 3).

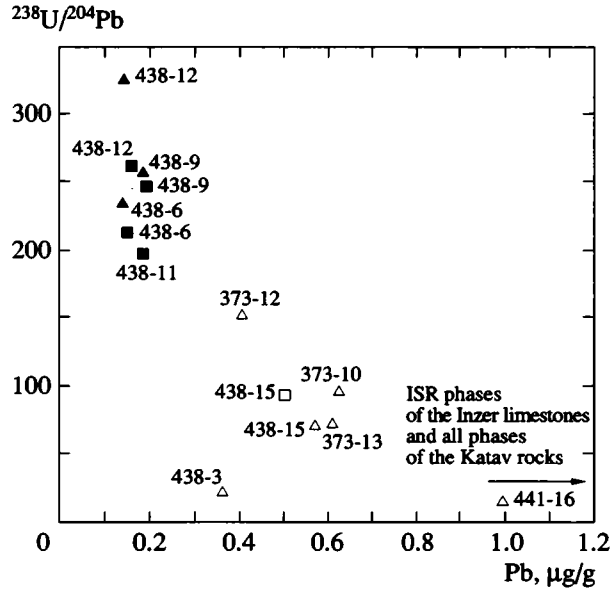

Fig. 7. $^{238}U/^{204}Pb$ ratios and Pb concentrations in the first and second group of the Inzer carbonates (symbols as in Fig. 3).

nents. In addition, low concentrations of Mn and Fe in the sample together with low Mn/Sr and Fe/Sr ratios exclude a chance that some exotic Pb entered the system with meteoric waters.

In contrast, the third and fourth factors appear to be quite real. Displacement of data points upward from the isochron (and accordingly, the greater Pb-Pb age) may result from both the U loss from the rock (Moorbath and Taylor, 1985), and the degassing of ^{222}Rn, an intermediate decay product of ^{238}U. The half-life of ^{222}Rn is

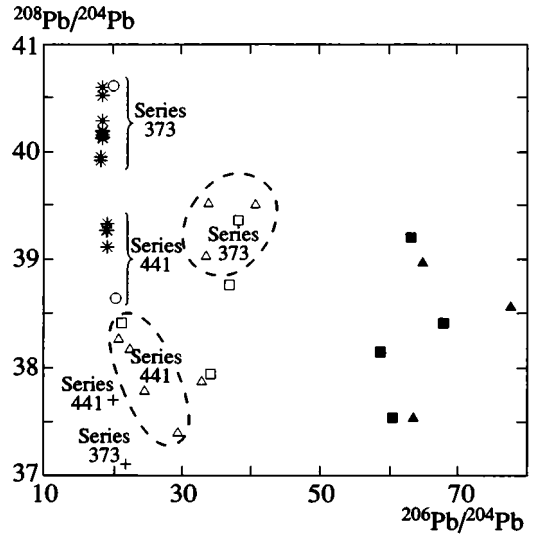

Fig. 8. $^{207}Pb/^{204}Pb$–$^{206}Pb/^{204}Pb$ diagram for carbonates from the Inzer Formation (symbols as in Fig. 3).

several orders of magnitude greater than this parameter of ^{219}Rn, one of isotopes in the decay chain of ^{235}U (3.82 days versus 3.92 seconds), and hence the potential diffusion loss is much higher for the former, than for the latter. After a considerable period of time, this factor may and must significantly increase isotopic ratios of ^{207}Pb and ^{206}Pb, the final decay products of ^{235}U and ^{238}U. Disturbance of U-Pb systems in response to diffusion loss of ^{222}Rn was revealed in the course of investigation of the uranium ores (Ludwig *et al.*, 1981; Holliger *et al.*, 1989) and Proterozoic carbonates (Jahn and Cuvellier, 1994). In such a case, the Pb-Pb age turns out to be overstated, whereas the age value calculated on the basis of $^{206}Pb/^{238}U$ ratio is understated. In contrast, the ^{235}U–^{207}Pb system in the same sample retains a quasi-closed state, because the diffusion loss of ^{219}Rn is neglectfully small. Distribution of data points corresponding in Figs. 5 and 6 to PCC-1 and PCC-2 phases of Sample 438-9 is consistent with these considerations.

The last opportunity that Sample 438-9 is unusual with respect to the initial Pb isotope composition cannot be disregarded as well. Because of a short residence time of Pb in the sea water (≈50 years), isotopic ratios of this element in a sea basin could vary in space and with time depending on the Pb isotope composition in the continental runoff. From this viewpoint, our Sample 438-9 may correspond, though not necessarily, to the stratigraphic level of carbonates incorporating the more radiogenic, and consequently the older initial Pb.

Comparison of the behavior of U-Pb and Rb-Sr systems in carbonates of the lower Inzer Subformation. The sample series used to analyze the Rb-Sr systematics (Kuznetsov *et al.*, 1997) includes 11 samples considered in this work along with one sample from the horizon of dolomitic limestones in the middle part of the subformation, and Sample 441-15 from its basal portion in the Min'yar section. The initial $^{87}Sr/^{86}Sr$ ratios for PCC-1 phases of samples from the Min'yar section are within the range of 0.70525–0.70538, i.e., they are lower than any values previously published for coeval deposits. The last named fact and aforementioned strict criteria used to select the least altered samples allow us to consider the above range as adequately characterizing the Sr isotope composition in the sea water of the middle Late Riphean time. In other words, the primary carbonate phases of these samples attained first an isotopic equilibrium with the sea-water Sr, and afterward their Rb-Sr systems stood closed at the stage of early diagenesis and during the subsequent geological history. Only two samples from the base of the Min'yar section (441-15 and 441-16) represent an exception, since they show higher values of Fe/Sr, Rb/Sr, Mn/Sr, and initial $^{87}Sr/^{86}Sr$ ratios, and this is interpreted as a result of influence of fluids derived from the underlying clayey carbonates of the Katav Formation (Kuznetsov *et al.*, 1997).

The lower Inzer carbonates of the Kulmas section differ from coeval rocks of the Min'yar sequence in having greater magnitudes of the initial $^{87}Sr/^{86}Sr$ ratios, although they also satisfy all the criteria used to select the least altered samples. This disturbance of their Rb-Sr isotopic systems was interpreted as a result of secondary alterations, which were not reflected in the geochemical parameters but still were manifested in a higher recrystallization degree of the rocks (Kuznetsov *et al.*, 1997).

Thus, the initial Rb-Sr signature is generally preserved in the analyzed Inzer carbonates of the Min'yar section, whereas it is changed in the rocks of the Kulmas locality. At the same time, the U-Pb systems of limestones from both localities turned out to be open at the early diagenetic stage. This is evident from μ_1 values characteristic of all samples and from enrichment of carbonates of the second group in the common Pb derived from the silicate components of the underlying Katav deposits. Analyzing the behavior of U-Pb and Rb-Sr isotopic systems in the Inzer limestones, we may divide the studied samples into three categories, each corresponding to a particular state of stability of the above systems.

The first category is classed with samples collected from the upper part of the Min'yar section, whose PCC-1 phases are enriched in radiogenic Pb and show lower values of the initial $^{87}Sr/^{86}Sr$ ratios (the first of groups considered above). The Rb-Sr systems of these samples stood closed after the sedimentation stage, whereas the U-Pb systems experienced transformations at the early diagenetic stage ($\mu_1 = 8.4$) and evolved under the quasi-closed conditions afterward.

The second category is represented by several limestone samples (438-3, 438-7, and 438-15) from the lower and, partly, from the upper parts of the Min'yar section, which preserve the initial Rb-Sr signature, but are enriched in U and Pb. The Pb isotope composition

in these samples is less radiogenic, and measured μ values are lower than in carbonates of the first category.

In both cases, the behavior of U-Pb and Rb-Sr systems appears to be understandable, if we accept the above conclusion that the composition of diagenetic fluids in the Inzer sediments was formed under the influence of the underlying clayey limestones of the Katav Formation. The Pb content in the latter is 2–10 times higher than in the Inzer carbonates, whereas the Sr concentration is 4–5 times lower (Anfimov *et al.*, 1987; Kuznetsov *et al.*, 1997). It is quite likely that the Rb/Sr ratio in the diagenetic fluid, which migrated into the Inzer deposits, was close in average to its value in the whole-rock samples of the Katav limestones. This fluid with high Pb and low Sr concentrations significantly transformed the U-Pb systems in a large volume of the Inzer deposits, and to a lesser extent affected their Rb-Sr systems. The latter were noticeably transformed only in the lowermost beds of the subformation (samples 441-15 and 441-16). In this connection, we should remember that the PCC-1 phase of the last sample plots clearly away from the Pb-Pb isochron in Fig. 3.

Finally, all samples from the Kulmas section represent the third category. Like in the second category, these samples reveal the lowered $^{206}Pb/^{204}Pb$ and $^{207}Pb/^{204}Pb$ ratios, the rather high concentrations of U and Pb, and low measured values of μ, but they display a somewhat higher range of the initial $^{87}Sr/^{86}Sr$ ratios. As we believe, the postdiagenetic recrystallization that transformed the Rb-Sr systems of the rocks (Kuznetsov *et al.*, 1997) occurred soon after the early diagenesis. Otherwise, the samples from the Kulmas section would not plot at the same isochron together with other samples of the Inzer limestones. Unfortunately, any reliable geological information about the recrystallization time of the Kulmas carbonate deposits is unknown.

Thus, the degree of diagenetic transformations in U-Pb and Rb-Sr systems of the Inzer carbonates was dependent on the isotopic composition and concentrations of Pb and Sr in these deposits and diagenetic fluids. All the factors are obviously variable and may differently influence the migration ability of components of both isotopic systems under particular conditions of diagenesis. The comparative analysis of U-Pb and Rb-Sr systematics is a useful approach, if the objective is to understand the geochemical features of lithogenesis in the history of marine carbonates.

CONCLUSION

(1) The isochron Pb-Pb age of the lower Inzer Subformation is calculated as equal to 836 ± 25 Ma on the basis of 14 data points of the limestone samples collected near the town of Min'yar and at the Kulmas locality. This value corresponds to the time of the early diagenetic stage in sediments; it currently represents the most reliable isotopic date for the Upper Riphean type section—the Karatau Group of the southern Urals.

(2) Deposits of the subformation experienced the diagenetic alteration under influence of fluids that distorted their initial U-Pb systems. The fluids migrated from the underlying deposits of the Katav Formation and were close in the μ value and Pb isotope composition to the siliciclastic fraction of these deposits. Based on the comparative analysis of U-Pb systematics of the Inzer and Katav limestones, this inference is well compatible with the stratigraphic position of samples whose U-Pb systems have been disturbed to a different extent.

(3) The considered data on U-Pb and Rb-Sr systems in carbonate deposits show that these systems are variably resistant against various postsedimentary alterations. They elucidate conditions of the rock diagenesis, and also the likely source and composition of diagenetic fluids.

ACKNOWLEDGMENTS

We are very grateful to Yu.A. Shukolyukov whose comments on the manuscript were very valuable, to V.I. Kozlov whose sample collection of the Karatau Group was used in this study, to T.L. Turchenko who investigated mineralogy of silicate components in the studied samples by means of X-ray diffractometry, and to V.N. Podkovyrov who performed the cathodoluminescent analysis of our samples. The work was financially supported by the Russian Foundation for Basic Research, project nos. 96-05-64928 and 96-05-64329.

Reviewers E.V. Bibikova and Yu.A. Shkolyukov

REFERENCES

Anfimov, L.V., Sul'man, A.M., and Petrishcheva, V.G., Strontium in Riphean Carbonates from Southern Urals, in *Geokhimiya osadochnykh formatsii Urala* (Geochemistry of Sedimentary Formation in the Urals), Sverdlovsk: Ural. Nauchn. Tsentr Akad. Nauk SSSR, 1987, pp. 22–28.

Asmerom, I. and Jacobsen, S.B., The Pb Isotopic Evolution of the Earth: Inferences from River Water Suspended Loads, *Earth Planet. Sci. Lett.*, 1993, vol. 115, pp. 245–256.

Babinski, M., Chemale, F., Jr., and van Schmus, W.R., The Pb/Pb Age of the Mines Supergroup Carbonate Rocks, Quadrilatero Ferrifero, Brazil, *Precambrian Res.*, 1995, vol. 72, pp. 235–245.

Bibikova, E.V., Lobach-Zhuchenko, S.B., Semikhatov, M.A., *et al.*, Geochronological Scale of the Precambrian in the East European Platform and Framing Structures, *Izv. Akad. Nauk SSSR, Ser. Geol.*, 1989, no. 4, pp. 8–22.

Brand, U. and Veizer, J., Chemical Diagenesis of Multicomponent Carbonate System: 1. Trace Elements, *J. Sediment. Petrol.*, 1980, vol. 50, no. 5, pp. 1219–1236.

Choquette, P.W., James, N.P., Diagenesis 12: Diagenesis in Limestones—the Deep Burial Environment, *Geosci. Can.*, 1987, vol. 14, no. 1, pp. 3–35.

Farquhar, P.M., Smith, P.E., and Hancock, R.G., Variable U-Pb Time Domains in a Devonian Limestone, *8th Internal. Conference on Geochronol., Cosmochronol., and Isotope*

Geology. U.S. Geol. Surv., Circular 1107, Berkeley, 1994, p. 95.

Faure, G., *Principles of Isotope Geology*, New York: Wiley and Sons, 1986. Translated under the title *Osnovy isotopnoi geologii*, Moscow: Mir, 1989.

Gareev, E.Z., Geochemical Features of Carbonate Rocks from Reference Sections of the Riphean Katav and Uk formation of Southern Urals, in *Verkhnii dokembrii i paleozoi Yuzhnogo Urala* (Upper Precambrian and Paleozoic of the Southern Urals), Ufa: Bashkir. Fil. Akad. Nauk SSSR, 1982, pp. 36–46.

Garris, M.A., *Etapy magmatizma i metamorfizma v doyurskoi istorii Urala i Priural'ya* (Stages of Magmatism and Metamorphism in the Pre-Jurassic History of the Urals and Adjacent Regions), Moscow: Nauka, 1977.

Garris, M.A., Kazakov, G.A., Keller, B.M., *et al.*, Geochronological Scale of the Upper Proterozoic (Riphean and Vendian), in *Absolyutnyi vozrast geologicheskikh formatsii* (Absolute Age of Geological Formations), Moscow: Nauka, 1964, pp. 431–455.

Gorokhov, I.M., Diagenesis of Carbonate Sediments: Behavior of Trace Elements and Strontium Isotopes, *Litologiya i paleogeografiya* (Lithology and Paleogeography), Verba, Yu.L., Ed., St. Petersburg: Geol. Upr., 1996, pp. 141–164.

Gorokhov, I.M., Melnikov, N.N., Turchenko, T.L. *et al.*, Two Illite Generations in an Upper Riphean Shale: The Rb-Sr Isotope Evidence, *EUG 8, Strasbourg, France, 9–13 April, 1995. Abstracts Supplement no. 1 to Terra Nova*, 1995a, vol. 7, pp. 330–331.

Gorokhov, I.M., Semikhatov, M.A., Baskakov, A.V., *et al.*, Strontium Isotope Composition in Riphean, Vendian, and Lower Cambrian Carbonates from Siberia, *Stratigr. Geol. Korrelyatsiya*, 1995b, vol. 3, no. 1, pp. 3–33.

Goryainova, O.P. and Fal'kova, E.A., Report on Geological Study in the Bol'shoi Inzer and Zilim River Basins, *Tr. Vses. Geol.-Razved. Ob'edin.*, 1933, vol. 272, pp. 1–36.

Gorozhanin, V.M. and Kutyavin, E.P., Rubidium-Strontium Dating on Glauconite from the Uk Formation, in *Dokembrii i paleozoi Yuzhnogo Urala* (Precambrian and Paleozoic of the Southern Urals), Ufa: Bashkir. Nauchn. Tsentr Ural. Otd. Akad. Nauk SSSR, 1986, pp. 60–63.

Haglund, D.S., Friedman, G.M., and Miller, D.S., The Effect of Fresh Water on the Redistribution of Uranium in Carbonate Sediments, *J. Sediment. Petrol.*, 1969, vol. 39, pp. 1283–1296.

Hoff, J.A., Jemeson, J., and Hanson, G.N., Application of Pb Isotopes to the Absolute Timing of Regional Exposure Events in Carbonate Rocks: An Example from U-rich Dolostones from the Wahoo Formation (Pennsylvanian), Prudhoe Bay, Alaska, *J. Sediment. Res.*, 1995, vol. A65, no. 1, pp. 225–233.

Holliger, P., Pagel, M., and Pironon, J., A Model for ^{238}U Radioactive Daughter Loss from Sediment-Hosted Pitchblende Deposits and the Late Permian–Early Triassic Depositional U-Pb Age of the Muellenbach Uranium Ore (Baden-Wuerttenberg, FRG), *Chem. Geol. (Isot. Geosci. Sect.)*, 1989, vol. 80, pp. 45–53.

Jahn, B.M. and Cuvellier, H., Pb-Pb and U-Pb Geochronology of Carbonate Rocks: An Assessment, *Chem. Geol. (Isot. Geosci. Sect.)*, 1994, vol. 115, no 1/2, pp. 125–151.

Jahn, B. M. and Simonson, B. M., Carbonate Pb-Pb Ages of the Wittenoom Formation and Carawine Dolomite, Hamersley Basin, Western Australia (With Implications for Their Correlation with the Transvaal Dolomite of South Africa), *Precambrian Res.*, 1995, vol. 72, pp. 247–261.

Johnes, C.E., Halliday, A.N., and Lohmann, K.C., The Impact of Diagenesis of High-Precision U-Pb Dating of Ancient Carbonates: An Example from the Late Permian of New Mexico, *Earth Planet. Sci. Lett.*, 1995, vol. 134, pp. 409–423.

Keller, B.M., Kratz, K.O., Mitrofanov, F.P., *et al.*, Advances in the Standard Stratigraphic Scale of the Precambrian in the USSR, *Izv. Akad. Nauk SSSR, Ser. Geol.*, 1977, no. 11, pp. 16–21.

Keller, B.M., Semikhatov, M.A., and Chumakov, N.M., Type Sections of the Upper Proterozoic Erathem, *Geologiya dokembriya. Doklady 27 Mezhdunarodnogo geol. kongressa* (Geology of the Precambrian. Reports 27th Intern. Geol. Congress), Moscow, 1984, vol. 5, pp. 56–76.

Komar, V.A., On the Structure and Stromatolites of the Upper Riphean Type Section (Southern Urals), *Izv. Acad. Nauk SSSR, Ser. Geol.*, 1978, no. 8, pp. 50–60.

Kozlov, V.I., Krasnobaev, A.A., Kozlova, E.V., *et al.*, *Stratigrafiya rifeya v stratotipicheskom razreze Yuzhnogo Urala* (Stratigraphy of the Riphean Stratotype in the Southern Urals), Ufa: Bashkir. Nauchn. Tsentr Akad. Nauk SSSR, 1991.

Krylov, I.N., Stratigraphy and Microfossils from the Riphean Min'yar Formation of the Southern Urals, *Sov. Geol.*, 1983, no. 6, pp. 60–72.

Kuznetsov, A.B., Gorokhov, I.M., Mel'nikov, N.N., *et al.*, Rb-Sr Systematics of Postdepositional Alterations in Carbonates from the Karatau Group, Southern Urals, Abstracts of Papers, *XIV Symposium on Isotopic Geochemistry*, Moscow: Inst. Geochim. Analit. Khim. Ross. Akad. Nauk, 1995a, pp. 126–127.

Kuznetsov, A.B., Gorokhov, I.M., Ovchinnikova, G.V., *et al.*, Postsedimentary Alteration of Upper Riphean Limestones of the Katav Formation, the South Urals: Chemical and Isotopic Evidence, *Precambrian of Europe: Stratigraphy, Structure, Evolution, and Mineralization, MAEGS-9*, St. Petersburg, 1995b, p. 60.

Kuznetsov, A.B., Gorokhov, I.M., Semikhatov, M.A., *et al.*, Strontium Isotope Composition in Limestones from the Inzer Formation, the Upper Riphean Stratotype in Southern Urals, *Dokl. Akad. Nauk*, 1997, vol. 353, no. 2, pp. 249–254.

Ludwig, K.R., PBDAT for MS-DOS. A Computer Program for IBM-PC Compatibles for Processing Raw Pb–U–Th Isotope Data. Version 1.06, *U.S. Geol. Surv. Open File Rep. 88-542*, 1989, pp. 1–40.

Ludwig, K.R., Isoplot for MS-DOS. A Plotting and Regression Program for Radiogenic Isotope Data for IBM-PC Computers. Version 2.00, *U.S. Geol. Surv. Open File Rep. 88-557*, 1990, pp. 1–40.

Ludwig, K.R., Nash, J.T., and Naeser, C.W., U-Pb Isotope Systematics and Age of Uranium Mineralization, Midnite Mine, Washington, *Econ. Geol.*, 1981, vol. 76, pp. 89–110.

Manhes, G., Minster, J.E., and Allegre, C.J., Comparative Uranium-Thorium Lead and Rubidium-Strontium Study of the Severin Amphoterite: Consequences for Early Solar System Chronology, *Earth Planet. Sci. Lett.*, 1978, vol. 39, no. 1. pp. 14–21.

Maslov, A.V., *Litologiya verkhnerifeiskikh otlozhenii Bashkirskogo megantiklinoriya* (Lithology of the Upper Riphean

Deposits of the Bashkir Meganticlinorium), Moscow: Nauka, 1988.

Moorbath, S. and Taylor, P.N., Precambrian Geochronology and Geological Record, in *Petrology of Igneous and Metamorphic Rocks,* New York: Wiley, 1985.

Moorbath, S., Taylor, P.N., Orpen, J.L., *et al.,* First Direct Radiometric Dating of Archaean Stromatolite Limestone, *Nature,* 1987, vol. 326, no. 6116, pp. 865–867.

Ovchinnikova, G.V., Gorokhov, I.M., Semikhatov, M.A., *et al.,* Timing of Formation and Alterations of Deposits of the Upper Riphean Inzer Formation, Southern Urals, *Obshchie problemy stratigrafii i geologicheskoi istorii rifeya Severnoi Evrazii* (General Problems of Riphean Stratigraphy and Geological History of Northern Eurasia), Ekaterinburg, 1995a, pp. 73–75.

Ovchinnikova, G.V., Semikhatov, M.A., Gorokhov, I.M., *et al.,* U-Pb Systematics of Precambrian Carbonates: The Riphean Sukhaya Tunguska Formation of the Turukhansk Uplift in Siberia, *Litol. Polezn. Iskop.,* 1995b, no. 5, pp. 525–536.

Podkovyrov, V.N., Semikhatov, M.A., Kuznetsov, A.B., Vinogradov, D.P., Kozlov, V.I., and Kislova, I.V., Carbonate Carbon Isotopic Composition in the Upper Riphean Stratotype, Karatau Group, Southern Urals, *Stratigr. Geol. Korrelyatsiya,* 1998, vol. 6, no. 4, pp. 319–335.

Raaben, M.E. and Komar, V.A., The Lower–Upper Karatavian Boundary in the Uralian Stratotype, *Izv. Akad. Nauk SSSR, Ser. Geol.,* 1983, no. 9, pp. 86–96.

Russell, J., Grey, K., Whitehouse, M., and Moorbath, S., Direct Pb/Pb Determination of the Ashburton and Nablerm Basins, Western Australia, Abstracts of Papers, *8th Internal. Conference on Geochronol., Cosmochronol., and Isotope Geology, Berkeley, CA, USA, 1994,* 1994, U.S. Geol. Surv., Circular 1107, p. 275.

Semikhatov, M.A., Shurkin, K.A., Aksenov, E.M., *et al.,* New Stratigraphic Scale for the Precambrian of the USSR, *Izv. Akad. Nauk SSSR, Ser. Geol.,* 1991, no. 4, pp. 3–13.

Stratotip rifeya. Stratigrafiya. Geokhronologiya (Stratotype of the Riphean: Stratigraphy, Geochronology), Keller, B.M. and Chumakov, N.M., Eds., Moscow: Nauka, 1983.

Tatsumoto, M., Knight, R.J., and Allegre, C.J., Time Differences in the Formation of Meteorites as Determined from the Ratio of Lead-207 to Lead-206, *Science,* 1973, vol. 180, no. 3991, pp. 1279–1283.

Stratigraphy and Geological Correlation, Vol. 6, No. 4, 1998, pp. 348–367. Translated from Stratigrafiya. Geologicheskaya Korrelyatsiya, Vol. 6, No. 4, 1998, pp. 32–51.
Original Russian Text Copyright © 1998 by Tesakov, Predtechenskii, Khromykh, Berger.
English Translation Copyright © 1998 by МАИК Наука/Interperiodica Publishing (Russia).

Silurian Stratigraphic Scale for East Siberia

Yu. I. Tesakov*, N. N. Predtechenskii, V. G. Khromykh*, and A. Ya. Berger***

**Joint Institute of Geology, Geophysics, and Mineralogy, Siberian Division, Russian Academy of Sciences, Universitetskii pr. 3, Novosibirsk, 630090 Russia*

***All-Russia Research Institute of Geology, Srednii pr. 74, St. Petersburg, 199026 Russia*

Received June 27, 1996

Abstract—Principles of stratigraphic regionalizing and chronozonal characteristics of global and regional stratigraphic scale for East Siberia are presented. The stratigraphic regionalizing resulted in recognition of five subregions (North Taimyrskii, North Prieniseiskii, Tungusskii, Nyuya–Berezovskii, and Irkutskii) and 15 stratigraphic areas (Middendorf, Norilsk, Turukhansk, Igarka, Kochumdek, Vorogovka, South Taimyr, Ledyanka, Maimecha, Moiero, Morkoka, Vilyui, Nyuya–Berezovka, Ilim, and Baltura). The global scale is divided into stages and substages are subdivided into 54 global chronozones with indicated first and last occurrence levels of guide fossils, such as graptolites, brachiopods, conodonts, and tabulates. The regional scale of East Siberia is divided into six horizons (Moiero, Khaastyr, Agidy, Khakoma, Tukal, and Postnichnyi) and 13 subhorizons ranging through 54 regional chronozones, whose stratigraphic intervals correspond to those of global chronozones. In East Siberia, the first and last occurrence levels are established for guide species of graptolites, chitinozoans, acritarchs, cephalopods, trilobites, brachiopods, scolecodonts, conodonts, bryozoans, tentaculites, ostracodes, gastropods, crinoids, rugoses, tabulates, stromatoporoids, algae, pelecypods, vertebrates, chiolites, and conularians. Stratotypes are selected for all chronozones (global and regional).

Key words: *stratigraphy, Silurian, scale, stratotype, Siberia.*

An integrated epicontinental (platform type) basin that existed in East Siberia during the Silurian time accumulated the whole spectrum of sediments varying from the terrigenous graptolite facies of a deep shelf in the northwestern Siberian platform and northern Taimyr to the halide deposits of shallow-water lagoons in the southeast and south of the platform. Most significant exposures of Silurian deposits are known in the median sublatitudinal zone of Taimyr, in the western and northeastern periphery of the Tunguska syneclise, in the western and southeastern parts of the Vilyui syneclise, and in the Irkutsk amphitheater. In central areas of the Tunguska and Vilyui syneclises, Silurian beds are overlain by thick sequences of younger deposits, but they are penetrated by numerous boreholes. In the marginal areas of the Siberian platform these beds are either completely eroded, or preserved only in separate blocks inside the field of Lower Paleozoic and Precambrian rocks.

Investigation history of Silurian System in East Siberia is divisible into three periods (Nikiforova, 1955; Nikiforova and Andreeva, 1961; Tesakov *et al.*, 1979; Tesakov and Obut, 1984). The initial period was related to episodic works on general geology at the end of 19th and beginning of 20th centuries, when Silurian deposits were first discovered in this territory and their fauna was locally described. Next period lasted until the terminal 1960s and corresponded to a time of geological survey of a medium scale that also included the route studies of Silurian rocks along the main rivers of Siberia. Many principal sections were nearly completely studied at this time, and many faunal groups were comprehensively investigated. The recent period commenced at the end of the 1970s and included the detailed and ingenious lithologic, paleontologic, and ecosystem investigations of all natural and borehole sections of Silurian rocks in East Siberia. In many cases, the latter are characterized by 100% of core recovery, because the drilling was aimed to evaluate the potential of the region with respect to mineral, petroleum, and gas resources. At present, many sections are described and correlated in a bed-by-bed manner, and the regional (horizons) to local (formations) stratigraphic units are recognized in all areas of East Siberia. Regional and local scales are elaborated up to the chronozonal level, and the preparation of adequate schemes of Silurian stratigraphy and lithopaleogeographic maps based on ecosystem analysis is now in progress (Tesakov *et al.*, 1979, 1980, 1985, 1986, 1992; Tesakov, 1981; *Silur*, 1982; Tesakov and Obut, 1984). We used all available data to substantiate the chronozonal stratigraphic scale of Silurian deposits in East Siberia and to coordinate it with the global scale for the Silurian System in accordance with principles of stratigraphic regionalizing and recognition of global, regional, and local stratigraphic units.

Stratigraphic regionalizing (Tesakov *et al.*, 1975) was used as an approach to the ordering of stratigraphic

schemes, scales, and units different in their applied significance. Usual procedures of facial, structural–facial, formational, tectonic (for recent and ancient time slices), and geographic regionalizing do not offer an unambiguous interpretation of the whole stratigraphic section usable for correlation of chronostratigraphic intervals corresponding to periods and epochs. Due to persistent time-dependent changes in geological structures and facies, it is impossible to regionalize a given territory for a considerable stratigraphic interval on the basis of above criteria. Moreover, the structural and facial boundaries do not coincide in general, and, consequently, the facial and structural regionalizing can be used (in combination or separately) only in the paleogeographic reconstructions for a certain time slice. Recent geological structures and geography do not reveal sedimentation environments in the past basins, and stratigraphic regionalizing based on combination of chronostratigraphic units is the only approach to an adequate elucidation of stratigraphy in any part of the globe. Hierarchy of categories used in stratigraphic regionalizing is as follows: globe, region, subregion, district, area, and locality. When necessary, we may also distinguish zones and provinces, or concrete points for the purpose of small- to large-scale regionalizing. The principal categories are globe, region, and district, where we may distinguish the global, regional, and local stratigraphic subdivisions. Relations between the adopted categories of stratigraphic regionalizing and stratigraphic units different in rank are shown in Table 1.

Point is the lowest unit for the stratigraphic regionalizing. It characterizes a section, where we may recognize the partial segments (copulae), i.e., the stratigraphic subdivisions monofacial in the vertical direction, which are of unknown geographic range, as it is the case, for instance, in the borehole section. During the subsequent study in a wider area these subdivisions may serve as a basis for distinguishing beds, lenses, biostromes, bioherms, and other geothems.

Locality corresponds to a distribution area of the concrete beds, which may be grouped into packets.

Area represents the geographic territory, where we distinguish a particular combination of stratigraphic members.

District is a territory, where a certain number of stratigraphic formations is recognized. This category is one of the principal in the stratigraphic regionalizing, since the district (local) stratigraphic scheme depicts a succession of principal cartographic units.

Subregion unites several districts displaying the same type of sedimentation cycles. In geographic range, it corresponds to the distribution area of particular subregional rock groups. In a given subregion, some formations (stratigraphic levels) are detectable everywhere. The named beds represent principal units in subregions.

Region is a territory displaying the concrete set of stratigraphic horizons and usually coinciding with contours of a sedimentary basin spanning the type series of facial zones from the deep shelf to the shallow coastal zone. Any region is usually situated inside the closed contour outlining coastal boundaries of a large sedimentary basin.

Provinces or zones unite several regions similar in the type of sedimentation and biota. Special stratigraphic units are undetermined in this case.

Globe is characterized by the global stratigraphic subdivisions traceable all over the Earth. Stage is the principal stratigraphic unit in this category.

At present, the international stratigraphic classification is not uniform. To avoid this disadvantage, we introduce the concept of global, regional, and local (district) series and chronozones (Table 1). In accordance with international terminology, we consider the term superstage as corresponding to the group, the regional stage as an equivalent of the horizon, and the formation, if it is isochronous, as a unit identical to the local stage. The diachronous formations are interpreted as formations proper in understanding of American stratigraphers.

Figure 1 illustrates the stratigraphic regionalizing of Silurian deposits in East Siberia. In the type areas, there are shown the stratotype localities and parastratotypes of regional and local stratigraphic units.

Global Silurian chronostratigraphic scale (Table 2). At present, the Silurian System is clearly divided into parts (subsystems) and four superstages (global series): Llandovery, Wenlock, Ludlow, and Přidoli. The Llandoverian Series is subdivided into Rhuddanian, Aeronian, and Telychian stages; the Wenlock consists of Sheinwoodian and Homerian stages, while the Ludlow includes Gorstian and Ludfordian stages. The Přidoli Series is still undivided into stages (Holland, 1989). This scheme of stage subdivisions was officially approved by the International Commission on Stratigraphy of the International Union of Geological Science in 1985. All the stages are substantiated on the basis of boundary stratotypes studied in sections of England and Czechia (Holland, 1980a, 1980b, 1985, 1989: Basset, 1985). Elaboration of more detailed chronostratigraphic subdivisions corresponding to substages and global chronozones (*International ...*, 1976, p. 10, Table 1) is still in progress. A first attempt to distinguish the global Silurian chronozones was in 1975, when the Homerian Stage was divided into Whitwellian and Gleedonian chronozones (Basset *et al.*, 1975). When correlating the regional standard scale of Silurian deposits in East Siberia with the global standard of the system, we (Tesakov *et al.*, 1985, 1992) also made an effort to distinguish the substages and 54 global chronozones in the Silurian System. Working on this model, where the global chronozone is considered as a principal elementary unit, we used data from the following publications: Jones (1925, 1949), *Silurian ...*, (1961), Holland *et al.* (1963, 1980), Toghill (1968), Cocks *et al.* (1970, 1971, 1983, 1984), Basset *et al.*

Table 1. Basic units used for stratigraphic regionalizing and principal chrono- and biostratigraphic subdivisions of different geographic significance

Units of stratigraphic regionalizing													
Globe		Region		Subregion		District		Area		Locality		Point	
Principal chronostratigraphic and biostratigraphic subdivisions													
Global chronostratigraphic units	Global biostratigraphic units	Regional chronostratigraphic units	Regional biostratigraphic units	Subregional chronostratigraphic units	Subregional biostratigraphic units	District chronostratigraphic units	District biostratigraphic units	Areal chronostratigraphic units	Areal biostratigraphic units	Local chronostratigraphic units	Local biostratigraphic units	Partial chronostratigraphic units	Partial biostratigraphic units
System													
Series													
Superstage		Superhorizon		Subregional Group		District Group							
Stage	Global Biointerval (Biochron)	Horizon	Regional Biointerval (Biophase)	Beds	Subregional Biointerval	Formation	District Biointerval		Areal Biointerval		Local Biointerval		Partial Biointerval
Substage		Subhorizon				Subformation		Member		Packet			
Chronozone (Global Chronozone)		Regional Chronozone		Subregional Chronozone		District Chronozone		Areal Chronozone		Bed		Copula (Segment)	

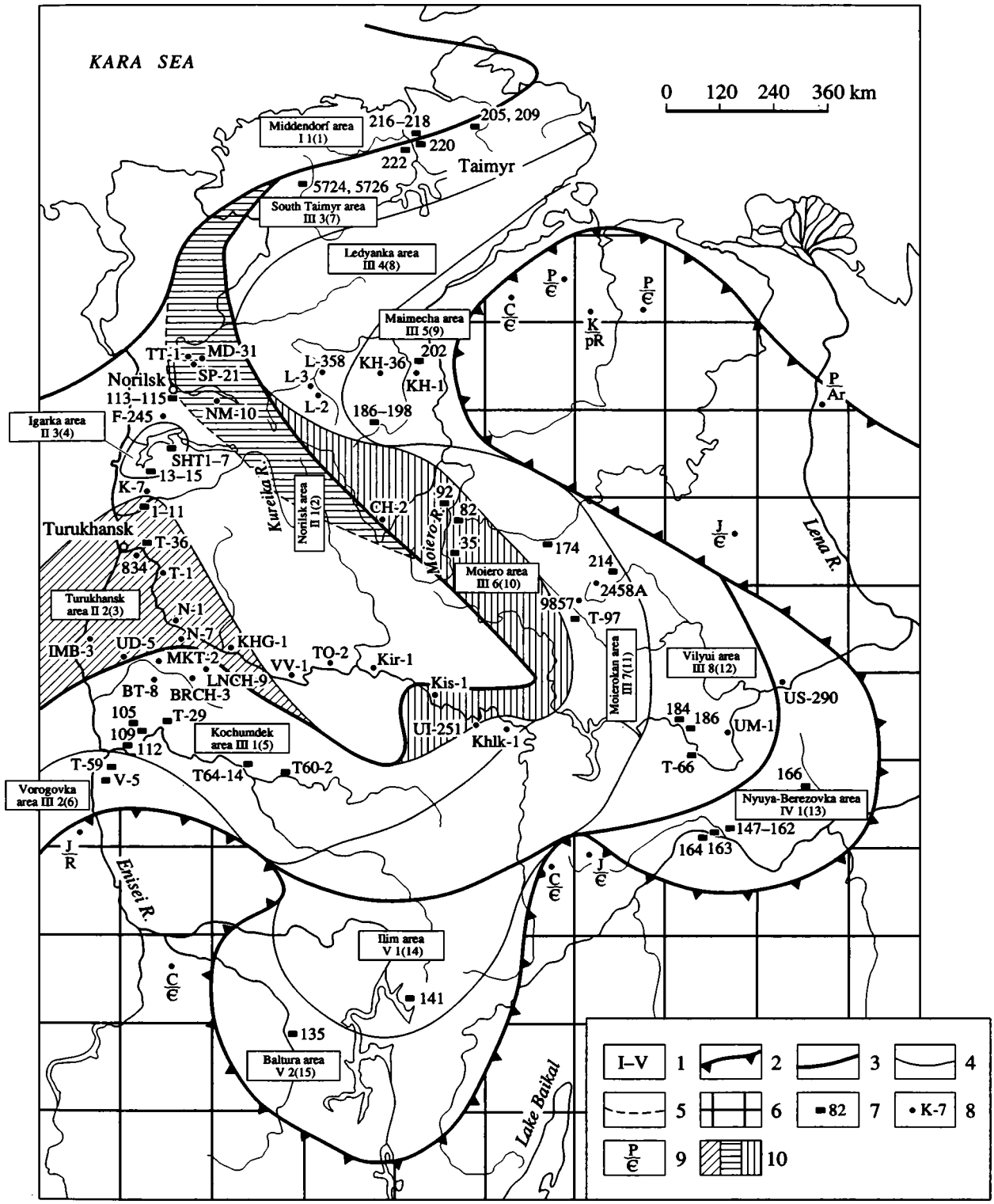

Fig. 1. Stratigraphic regionalizing of East Siberia for the Silurian System: (1) subregions— North Taimyrskii (I), North Prieniseiskii (II), Pritungusskii (III), Nyuya-Berezovskii (IV), Irkutskii (V); (2) boundaries of Silurian basin in East Siberia; (3) boundaries of subregions; (4) boundaries of districts; (5) boundaries of areas; (6) land; (7) number of exposure; (8) number of borehole; (9) hiatus in sedimentation; (10) type districts.

(1975), White and Lawson (1978), Basset (1979, 1985, 1989), Holland (1980a), Kříž *et al.* (1983, 1986), Williams and Ingham (1989), Cocks (1989), Lawson and White (1989), and Kříž (1989). These works include all essential data about sections selected as stratotypes for the global chronozones and substages.

Our version of the global Silurian chronostratigraphic scale (Table 2) includes the time reference marks. The time scale was initially used to establish the number of global chronozones spanning about 500 k.y. each (Tesakov *et al.*, 1985). It is based on the scale of McKerrow *et al.* (1980) who compiled the age data available at that time for boundaries between the global series or superstages (Llandovery, Wenlock, Ludlow, and Přidoli). Afterward, the boundary dates for global series were revised (McKerrow *et al.*, 1985; Tucker and McKerrow, 1995). For instance, these dates were displaced in the following manner: from 438 (1980) to 435 (1985) and 443 Ma (1995) for the Llandovery; from 425.5 (1980) to 425 (1985) and 428 Ma (1995) for the Wenlock; from 420 (1980; 1985) to 423 Ma (1995) for the Ludlow; from 413.5 (1980) to 414 (1985) and 419 Ma (1995) for the Přidoli; and from 411 (1980) to 412 (1985) and 417 Ma (1995) for the Lochkovian Stage. In general, the error of age determination can be as high as ±3–7 Ma, and we consider it unnecessary to change the time scale accepted previously and in this paper (Table 2).

Superstages (global series) and stages correspond in full measure to those approved by the International Commission on Stratigraphy (Holland, 1989, Fig. 16). At the same time, the problem of the basal Silurian boundary is lacking an adequate solution (Lesperance *et al.*, 1987). The former idea (Cocks *et al.*, 1970, 1971) to place the lower Rhuddanian boundary at the base of the Llandovery and *persculptus* Biozone appears to be more correct because this level is related to many global events and represents a high-rank boundary in the evolution history of lithosphere and biosphere. The officially approved boundary (Williams and Ingham, 1989) is substantiated by a single biological event and corresponds to the first occurrence level of *Akidograptus acuminatus* postdating the global reorganization of biota.

Substages. Some of them, such as Eltonian, Bringewoodian, Leintwardinian, Whitecliffian (Holland *et al.*, 1963), and Fronian (Cocks *et al.*, 1970), have been already substantiated in the rank of stages, or as the Whitwellian and Gleedonian chronozones (Basset *et al.*, 1975). The lower and middle substages of the Rhuddanian are named respectively as Bronid and Crechan after the synonymous formations distinguished in the same stratotypes.

Global chronozones are synonyms of zones (Renevier, 1901), standard chronozones (*Report* ..., 1967), and chronozones merely (*International* ..., 1976, Table 1). They are indicated as stratotypes of subdivisions confined, if possible, by distinct stratigraphic boundaries and successively replacing one another in the type regions of the Silurian System (England and Czechia).

Stratotypes *i2* are used for the global chronozones of the lower (Bronid) and middle (Crechan) Rhuddanian (Cocks *et al.*, 1984; transect i2, Figs. 3, 4, and 6).

Stratotypes *h1* are selected for the global chronozones of the upper Rhuddanian and lower Aeronian (Cocks *et al.*, 1984; transect h1, Figs. 3, 4, 6, 60, and 63).

Stratotypes *f3* are used for the global chronozones of the middle Aeronian (Cocks *et al.*, 1984; transect f3, Figs. 3, 4, and 6).

Stratotypes *d3–d4* are accepted for the global chronozones of the upper Aeronian and Telychian (Cocks *et al.*, 1984; transect d, Figs. 2, 4, 6, 64, and 67).

Stratotypes of the "Wenlock area" are applied for the global chronozones of the Wenlock Series (Basset *et al.*, 1975), locality Hughley Brook, x–x', bed G-i, Fig. 5; locality Whitwell Coppice, 58–68, Figs. 2, 6, and 8; locality Rushbury, 31–45, Figs. 2, 8; locality Eaton Track, 19–25, Figs. 2, 7, and 8; locality Longville-Stanway RD, 46–50, Figs. 2, 8).

Stratotypes *A* are used for the global chronozones of the Eltonian Substage and for the global chronozone 1 of the Bringewoodian Substage (White and Lawson, 1978, transect A, Figs. 1–3). In the transect A, the lower part of the upper Eltonian is truncated by a fault (White and Lawson, 1978, Fig. 3). As the upper Eltonian sequence is 45 m thick in the Ludlow area (Cocks *et al.*, 1971, Table XIV, section J), the lower part of the upper Eltonian is considered to be 25 m thick. The base of the Elton Formation in the transect A (A1) is correlated with the Ludlow boundary stratotype and with stratotypes of the Gorstian Stage and Eltonian Substage in the stratotype Pitch Coppice section (P.C./bed F1 of Lawson and White, 1989, Figs. 54, 55).

Stratotypes *B* are used for the global chronozones 2 and 3 of the Bringewoodian Substage (White and Lawson, 1978, Figs. 4, 5).

Stratotypes *C* are implemented for the global chronozone of the Leintwardinian Substage (White and Lawson, 1978, Figs. 4, 5).

Stratotypes *B* are applied for the global chronozones of the Whitecliffian Substage (White and Lawson, 1978, Figs. 4, 5). The Whitecliffian Chronozone 2 is unexposed in the transect B. Its thickness is defined as equal to 30 m (Cocks *et al.*, 1971, Table XIV, section J).

The Pozari stratotypes are used for the substages and global chronozones of the Přidoli Stage or global group (Kříž, 1989, Figs. 65–67).

Lithological and paleontological characteristics of beds corresponding to all aforementioned stratotypes of global chronozones are presented together with the indicated transect descriptions in works of Cocks *et al.* (1984), Basset *et al.* (1975), White and Lawson (1978), and Kříž (1989).

When selecting stratotypes of global chronozones, we primarily paid attention to those sections, where the boundary stratotypes of formerly approved global units were strictly identified. Some stratotypes (particularly those of the Rhuddanian Stage) are poorly exposed and do not satisfy all the standard requirements (*International...*, 1976, p. 27, section C). They need an additional revision and may be replaced. The composite bed sequence (the standard for the Silurian) consisting of global chronozone stratotypes successively replacing one another is a real basis for correlation of geological sections in various regions with the concrete global chronozones.

Global biointervals (biochrons as biogeochronological equivalents of global chronozones), which are shown in the global scale (Table 2) to illustrate the paleontological characteristics of the units, are not independent subdivisions. From the viewpoint of biostratigraphy, all 54 global chronozones are characterized in accordance with Oppel's principles, i.e., by the first and last occurrence levels of species within a particular global chronozone. However, any biointerval is restricted beforehand by the time range of boundary stratotypes of chronozones, which cannot be changed depending on stratigraphic ranges of species. Consequently, the amount of global chronozones is always identical to the amount of global biointervals. Ideally, the scale of biochrons supplementary to the global chronozonal scale must reveal moments of origin and extinction of all important Silurian species, and any global chronozone will be characterized in this case by faunal assemblages, which have been born and died out within it. These concurrent-range zones will be changing with time, because the available data on stratigraphic ranges of species are incomplete and may be replenished and refined in the course of further studies. The local (district) biointervals include only species recognized in individual districts. Therefore, paleontological contents of global and local biointervals are highly dissimilar despite their identical enumeration, because the local biointervals include only the faunas from a particular area, whereas global units of this type incorporate all regional faunas. In the scale of global biointervals, stratigraphic ranges of species are always wider than in local subdivisions, because the former should finally contain the complete information about the phylogenetic origin of species and their extinction, while the particular district merely reveals their local distribution ranges. Thus, correlation between individual sections can be based on local biointervals with their correction relative to global stratigraphic ranges of species depicted in the scale of biochrons.

The suggested global chronostratigraphic scale is designed for the chronozonal correlation of all section through the standard of successive global units firmly established in accordance with global chronozone stratotypes, and also for the distribution control of all Silurian species within the global chronozones. At present, biozones of unclear stratigraphic range find their use in solving this kind of problems, for instance, this is done in "Global Standard of the Silurian System" (Williams and Ingham, 1989, Fig. 21; Cocks, 1989, Figs. 26, 31, and 35; Basset, 1989, Fig. 45).

Figure 2 shows distribution of some Tabulata species versus the chronozonal scale and principles of distinguishing the global biointervals on the basis of the first and last occurrence levels of these forms. It is plotted by using data from previous publications (Tesakov *et al.*, 1980, 1985; *Silur* ..., 1982; Sokolov and Tesakov, 1963, 1984).

The global chronozonal scale is also useful for calibration of all biozones and for estimation of their stratigraphic and age ranges. As an example, we may consider the Přidoli Series. At various times, this series was subdivided into graptolite zones (Rickards, 1995, Fig. 2), varying in amount from seven (*parultimus, ultimus, pridolensis, lochkovensis, bouceki, perneri,* and *transgrediens*) to three (*parultimus–ultimus, branicensis–lochkovensis*, and *bouceki–transgrediens*). In the Pozari stratotype section, the base of *bouceki* Zone corresponds to the base of Bed 106. Consequently, biozones *parultimus, ultimus, pridolensis,* and *lochkovensis* correspond, in accordance with our Table 2, only to the first global chronozone of the lower Přidoli, and this interval defines their geochronological range. In addition, Table 2 shows the first and last occurrence levels of graptolites, brachiopods, conodonts, and tabulates used to substantiate boundaries between the global chronozones.

Regional Silurian chronostratigraphic scale for East Siberia (Table 3) is completely correlated with the global (standard, international) scale (Table 2). Both scales were elaborated on the basis of the same principles using the time units of about 500 k.y. per each chronozone interpolated from the time scale of McKerrow *et al.* (1980). Boundaries between the regional chronozones were fixed when sections of the Silurian type areas in East Siberia were thoroughly correlated with those of England and Czechia. Accordingly, the time ranges and amount (54) of global and regional chronozones are identical. The first version of the regional Silurian scale for East Siberia was published in 1992 (Tesakov *et al.*, 1992), and afterward it was refined in many aspects. The new version presented in this paper is to be approved by the Regional Siberian Stratigraphic Commission and by the Interdepartmental Stratigraphic Committee of Russia (ISCR).

The main chronostratigraphic subdivisions of the scale are the Prianabarskii (Llandovery) and Prieniseiskii (Wenlock, Ludlow, and Přidoli) superhorizons divided into the Moierokan (Rhuddanian and lower Aeronian), Khaastyr (middle–upper Aeronian), Agidy (Telychian), Khakoma (Wenlock), Tukal (Gorstian), and Postnichnyi (Ludfordian and Přidoli) horizons, the latter formerly known as Kholyukhan Horizon. Each of the horizons includes two to three subhorizons consisting of regional chronozones. The horizons are officially

Table 2. Global Silurian stratigraphic scale

Global Silurian stratigraphic scale																										
Global chronostratigraphic units										Standard global chronostratigraphic units (sections in England and Czechia)																
System	Series	Superstage	Stage	Substage			Global Chronozone	Global Biointerval	Time scale, Ma (interpolation after McKerrow, 1980)	Regional Group	Formation (in a range of stratotype)			Subformation	District Chronozone	District Biointerval	Stratotype	Copulae (Beds), Observation points	Thickness, m	Correlation level (biochron)						
Approved by IUGS (Basset, 1985)				Workable																						
Devonian			Lochkovian						411									159 = K/20								
Silurian	Upper	Ludlow (ld)	Přidoli (p)	upper	Bitov		2	54		Přidoli (p)	Pozari		38.0	II	2	54	Pozari	150–158	8.0	54						
							1	53	412						1	53		141–149	11.5	53						
				lower			3	52						I	3	52		127–140	8.5	52						
							2	51	413						2	51		106–126	7.5	51						
					Jarov		1	50							1	50		96–105	4.0	50						
			Ludford-ian (ldf)	Whitecliffian			2	49	414	Ludlow	Whitecliff		53.0	II	1	49	B'	II.1	30.0	49						
							1	48						I	1	48		39–46	23.0	48						
				Leintwardinian			1	47	415		Leintwardine		33.0	I, II	1	47	C	9–31	33.0	47						
			Gorstian (gor)	Bringewoodian			3	46			Bringewood		54.0	II	1	46	B	7–20	17.0	46						
							2	45	416					I	2	45		1–6	20.0	45						
							1	44							1	44	"Wenlock area"	29–31	17.0	44						
				Eltonian			7	43	417		Elton			III	2	43		24–28	20.0	43						
							6	42							1	42		III.1	25.0	42						
							5	41	418					II	3	41		16–23	30.0	41						
							4	40							2	40		12–15	28.0	40						
							3	39	419						1	39		7–11	27.0	39						
							2	38						I	2	38		6	23.0	38						
							1	37	420				174.0		1	37		1–5 = P.C./F	22.0	37						
	Lower		Homerian (hom)	Gleedonian			2	36		Wenlock	Much Wenlock		25.0	I	1	36		47–50	25.0	36						
							1	35	421		Farley			III	1	35		24–25; 46	22.0	35						
				Whitwellian			4	34			Coalbruckdail			II	4	34		19–23	22.0	34						
							3	33	422						3	33		43–45	22.0	33						
							2	32							2	32		34–42	22.0	32						
							1	31	423						1	31		66–68; 31–33	22.0	31						
			Shein-woodian (she)	upper			3	30						I	4	30		63–65	21.0	30						
							2	29	424						3	29		61–62	21.0	29						
							1	28							2	28		10	21.0	28						
				lower			2	27	425				219.0		1	27		58–60	21.0	27						
							1	26			Buildwas		26.0	I	1	26		X–X'/G–1	26.0	26						
		Llandovery (l)	Telychian (tel)	upper			1	25	426	Llandovery	Serig (Cc)	C_6		II	1	25	d_4	C_6	45.0	25						
							3	24							3	24		107	45.0	24						
				middle			2	23	427			C_5		I	2	23	d	$C_5$2	45.0	23						
							1	22					180.0		1	22		163	45.0	22						
				lower			1	21	428		Wormwood (Cb)	C_4		II	3	21	d_3	187	32.0	21						
			Aeronian (aer)	upper			2	20						I	2	20		160–162	42.0	20						
							1	19	429				116.0		1	19		158–159	42.0	19						
				middle (Fron)			5	18				C_3		III	1	18	f_3	5a	42.0	18						
							4	17	430		Ridings (Ca)	C_2		II	2	17		103	42.0	17						
							3	16							1	16		102	42.0	16						
							2	15	431			C_1		I	2	15		4	42.0	15						
							1	14					210.0		1	14		101–139	42.0	14						
				lower		Idvian	2	13	432		Trifavour (B)	B_3		II	2	13	h_1	77–40–76	40.0	13						
							1	12							1	12		72–39	40.0	12						
				upper			2	11	433			B_2		I	2	11		70–71	40.0	11						
							1	10				B_1	170.0		1	10		38–38a	50.0	10						
			Rhudda-nian (rhu)	middle (Crechan)			6	9	434		Crechan (Ac)	A_4		II	3	9	i_2	34–35	42.0	9						
							5	8							2	8		65	42.0	8						
							4	7	435						1	7		186–64	42.0	7						
							3	6						I	3	6		32; 63	42.0	6						
							2	5	436						2	5		62	42.0	5						
							1	4					252.0		1	4		28	42.0	4						
				lower (Bronid)			3	3	437		Bronid (Ab)			III	1	3		27	40.0	3						
							2	2				A_3		II	1	2		61–26–26a	40.0	2						
							1	1	439			A_2	120.0	I	1	1		88 = B/46	40.0	1						
Ordovician			Ashgillian					0			Scratch (Aa)	A_1				0		24								

Table 2. (Contd.)

Correlation level (biochron)	First (+) and last (–) occurrence levels of species of global significance							
	Graptolites	Brachiopods		Conodonts		Tabulataes		
D	(+) *Monograptus uniformis*	(+)	–	(+)	–	(+) *Favosites kozlowskii*		
54	(–) *Monograptus transgrediens*	–		(+) *Icriodus woschmidti*		(+) *Riphaeolites sokolovi*	P85/6	
53	(+) *Monograptus perneri*	(+) *Dayia bohemica*	Brit.	–		(+) *Roemeria infundibulifera*	P219/4	
52	–	–		–		(+) *Scalites tschernovi*	P43/25	
51	(+) *Monograptus bouceki*	–		–		(+) *Mesosolenia reliqua*	P35/116	
50	(+) *Monograptus parultimus*	(+) *Gracianella graciosa*	Brit.	–		–		
49	(+) *Monograptus formosus*	–		(+) *Ozarkodina crispa*		–		
48	(+) *Neocucullograptus kozlowskii*	–		(+) *Ozarkodina snajdri*		–		
47	(+) *Saetograptus leintwardinensis*	–		(+) *Polygnathoides siluricus*		(+) *Squameofav. incredibilis*	P27/37	
46	–	(+) *Conchidium hnighti*	Brit.	–		(+) *Scalites prostratus*	P44/15	
45	–	–		–		–		
44	–	–		–		(+) *Laceripora cribrosa*	P186/13	
43	(+) *Lobograptus invertus*	–		(+) *Lonchodina greilingi*	10/16	–		
42	–	(+) *Chonetes lepisma*	Brit.	–		(+) *Mesofavosites bonus*	P186/1a	
41	(+) *Monograptus scanicus*	–		(+) *Ancoradella ploeckensis*		(+) *Barrandeolites bowerbanki*	P186/1	
40	–	(+) *Conchidium biloculare*	218/8b	(+) *Spathognathodus primus*	3/14	–		
39	–	(+) *Dayia navicula*	Brit.	–		–		
38	(+) *Monograptus tumescens*	–		–		–		
37	(+) *Monograptus nilssoni*	(+) *Atrypa reticularis*	Brit.	(+) *Kockelella staurodus*		–		
36	–	–		–		(+) *Desmidopora alveolaris*	P19/15	
35	(+) *Monograptus ludensis*	–		–		–		
34	(+) *Monograptus deubeli*	–		–		–		
33	(+) *Gothograptus nassa*	–		–		(+) *Thecia minor spinosa*	P16/1	
32	–	–		(+) *Ozakkodina bohemica*		–		
31	(+) *Cyrtograptus lundgreni*	–		(+) *Ozarkodina sagitta sagitta*		–		
30	(+) *Cyrtograptus ellesae*	–		(+) *Neoprioniodus ezcavatus*	64/15	–		
29	(+) *Cyrtograptus linnarssoni*	–		(–) *Trichonodella symmetrica*	58/16	(+) *Subalveolites panderi*	P96/11a	
28	(+) *Cyrtograptus rigidus*	–		(+) *Kockelella variabilis*	58/10	(+) *Thecia minor minor*	P96/11	
27	(+) *Monograptus riccartonensis*	–		(+) *Ozarkodina sagitta rhenana*		–		
26	(+) *Cyrtograptus sentrifugus*	(+) *Eocoelia angelini*	Brit.	(+) *Huddella johni*	60/3	–		
25	–	(+) *Omnutakhella bazenovae*	114/64	–		(+) *Sapporipora favositoides*	114/64	
24	(+) *Monograptus crenulatus*	(+) *Eocoelia sulcata*	Brit.	–		–		
23	(+) *Monograptus griestoniensis*	(+) *Costistricklandia lirata*	Brit.	(+) *Ozarkodina gaertneri*	SP21/97	(+) *Mesosapporipora porosa*	87/38	
22	(+) *Monograptus crispus*	(+) *Eocoelia curtisi*	Brit.	(+) *Spathognathodus sp.*	86/30	(+) *Mesosolenia festiva*	87/35	
21	(+) *Monograptus turriculatus*	(+) *Stricklandia laevis*	Brit.	(+) *Pter. amorphognathoides*	84/11	–		
20	–	(+) *Anabaria rara*	77/39	(+) *Trichonodella symmetrica*	14/101	–		
19	–	(–) *Septatrypa antiquata*	77/31	(+) *Carniodus carnulus*	178/17	(+) *Subalveolites subulosus*	113/30	
18	–	(+) *Plectatrypa wenlockiana*	13/16	(+) *Icriodella sandersoni*	114/17	(+) *Tuvaelites hemisphaericus*	77/22	
17	(+) *Monograptus elegans*	(+) *Pentlandina subcostatuls*	77/13	(+) *Pterospathozdus celloni*	14/75	–		
16	–	(+) *Cryptothyrella norilica*	77/4	(+) *Oulodus kentuckyensis*	113/7	–		
15	(–) *Demirastrites triangulatus*	–		(+) *Icriodella inconstans*	78/26	(+) *Parastriatopora rhizoides*	TT1/28a	
14	(+) *Monograptus sedgwicki*	(+) *Kulumbella biconvexa*	FT3/14	(+) *Icriodella deflecta*	78/16	(+) *Cystihalysites mirabilis*	LNCH9/11	
13	(+) *Cephalograptus cometa*	(+) *Pentamerus oblongus*	13/11	(+) *Apsidognathus tuberculatus*	13/6	–		
12	(+) *Monograptus convolutus*	(+) *Strickl lens intermedia*	Brit.	(+) *Kockelella ranuliformis*	216/3b	–		
11	(+) *Monograptus leptotheca*	(+) *Alispira tenuicostata*	82/21	(+) *Hadr. staurognathoides*	184/42	(+) *Paleofavosites asper*	82/23	
10	(+) *Demirastrites delicatulus*	(+) *Eocoelia hemisphaerica*	82/19	–		(+) *Multisolenia tortuosa*	82/20	
9	(+) *Dipligaptus magnus*	(+) *Septatrypa magna*	82/17	–		(+) *halysites catenularius*	LNCH9/8	
8	(–) *Rastrites norilskensis*	(+) *Stricklandia salteri*	82/16	–		(+) *F. gothland. gothlandicus*	82/16	
7	(–) *Lagarograpt. inexpeditus*	(+) *Meifodia recta*	82/13	–		–		
6	(+) *Demirastrites triangulatus*	(+) *Coolinia gracilic*	BT8/5	(+) *Pterospathodus tenuis*		–		
5	(+) *Coronograptus gregarius*	–		(+) *Decoriconus fragilis*	184/11	–		
4	(+) *Coronograptus cyphus*	(+) *Stricklandia lens lens*	Brit.	–		–		
3	(+) *Metabologr. moyeroensis*	(+) *Clorinda undata*	Brit.	–		–		
2	(+) *Cystograptus vesiculosus*	(+) *Stricklandia lens prima*	Brit.	(+) *Distomodus kentuckyensis*	79/6	–		
1	(+) *Parakidograptus acuminatus*	(+) *Alispira gracilis*	SP21/14	(+) *Oulodus nathani*	147/2	–		
O	(–) *Glyptograptus persculptus*	(–)	–	(–)	–	(–) *Tollina keiserlingi*		

approved by ISCR (*Resheniya ...*, 1983) as the regional Silurian subdivisions of the Siberian platform. Subhorizons and regional chronozones so far do not have official status.

Deposits of the *Prianabarskii Superhorizon* characterize, in general, the marine sedimentation cycle, while sediments of the *Prieniseiskii Superhorizon,* except the rocks of the North Taimyr subregion, are of the lagoonal-marine type. Both superhorizons are named after the synonymous subregional series. Names of horizons are derived from synonymous formations distinguished in Silurian type areas of East Siberia, and subdivisions of both types are characterized by the same stratotypes. The original succession of horizons (Tesakov *et al.,* 1979) included the Kholyukhan Horizon, whose stratotype at the Moiero River was later discredited and replaced by another one, and the unit was restored afterward under the name of Postnichnyi Horizon (Tesakov *et al.,* 1992).

Moierokan Horizon (Rhuddanian and lower Aeronian). The stratotype is located near the mouth of the Moierokan River. From the northwest toward the southeast, deposits of the horizon grade from normal marine graptolite shales first to marine calcareous shales rich in benthic organic remains, and then to gray dolomites and variegated evaporites of the past coastal zone.

Khaastyr Horizon (middle–upper Aeronian). The stratotype is situated between the first and second Moierokan rapids. Graptolite and calcareous shales, the latter rich in benthic fossils, together with dolomites and sandstones, widespread in the south of Siberian platform, are major sedimentary facies of the horizon.

Agidy Horizon (Telychian). The stratotype is established at the Moiero River right below the second Moierokan Rapids. In the northwest of the platform, the horizon consists of marls and limestones bearing marine faunas. In the central area, the unit is generally composed of dolomites, while variegated gypsum-bearing dolomites and sandstones are its main rock types in the southeast.

Khakoma Horizon (Wenlock). The stratotype locality is at the Moiero River near the Khakoma River mouth. Nearly everywhere in the Siberian platform and southern Taimyr, the horizon is represented by massive limestones and dolomites enclosing the coral–stromatoporoid biostromes, bioherms, and reefal buildups. Normal marine marls and limestones bearing graptolites, brachiopods, and ostracodes occur in the northern zone of Taimyr and in the southwest of the platform.

Tukal Horizon (Gorstian). Stratotype sections are located at the Kureika River between the Nizhnie Shcheki and Verkhnie Shcheki localities. The horizon consists of marls and limestones in the northern Taimyr and southwestern area of the platform; association of limestones and dolomites is typical of the central platform areas, and variegated dolomite, marl, and gypsum beds are widespread in the southeast. The low species diversity and frequent biostromes of algal stromatolites are characteristic of the unit.

Postnichnyi Horizon (Ludfordian and Přidoli). The stratotype was recovered by drilling at the eastern coast of the Pyasino Lake (Borehole TT-1 with 100% of core recovery). The core section is stored at the Museum of the Norilsk Geological-Prospecting Expedition. In the northern Taimyr, the unit is composed of limestones and shales. In the Siberian platform, it consists of gray dolomites and variegated dolomitic marls with gypsum inclusions in the southwest, and of variegated dolomite, marl, and gypsum beds in the southeast. The stratotype is lacking fauna, and we selected another section as the parastratotype (Tesakov *et al.,* 1995). This section bearing marine fossils is located near the Middendorf Caves (Exposure 218) at the Nizhnyaya Taimyra River.

Stratotypes of all subhorizons and regional chronozones are established within the horizon stratotypes located in the districts Moiero (Fig. 3a; Moierokan, Khaastyr, Agidy, and Khakoma horizons), Turukhansk (Fig. 3b; Tukal Horizon), and Norilsk (Fig. 3c; Postnichnyi Horizon). They are listed below in the stratigraphic succession.

Stratotype 82 for all regional chronozones of the lower Moierokan, and for regional chronozones 1–3 of the upper Moierokan subhorizons: the right-hand bank of the Moierokan River 2.0 km upstream from the mouth.

Stratotype 83 for the regional chronozones 4–5 of the upper Moierokan Subhorizon: upper exposures in the right-hand bank of the Moierokan River 6.0 km upstream from the mouth.

Stratotype 78 for the regional chronozone 1 in combination with the lower part of the chronozone 2 of the lower Khaastyr Subhorizon: the left-hand bank of the Moiero River 4.0 km downstream from the Khaastyr River mouth.

Stratotype 90 for the upper part of the regional chronozone 2 together with the lower part of the regional chronozone 3 of the lower Khaastyr Subhorizon: middle and upper part of the exposure at the right-hand bank of the Moiero River 6.5 km downstream from the Moierokan River mouth. The exposure corresponds to the covered interval of the sequence between stratotypes 78 and 77.

Stratotype 77 for the upper part of the regional chronozone 3 and entire chronozone 4 of the lower Khaastyr Subhorizon, and also for the regional chronozones of the upper Khaastyr Subhorizon: the left-hand bank of the Moiero River 1.5 km downstream from the Moierokan Rapids.

Stratotypes 84 and 85 for the lower regional chronozone of the lower Agidy Subhorizon: the continuous exposure at the left-hand bank of the Moiero River 1.0–1.5 km upstream from the Moierokan River mouth. The exposure is formally divided at the level of the red interlayer.

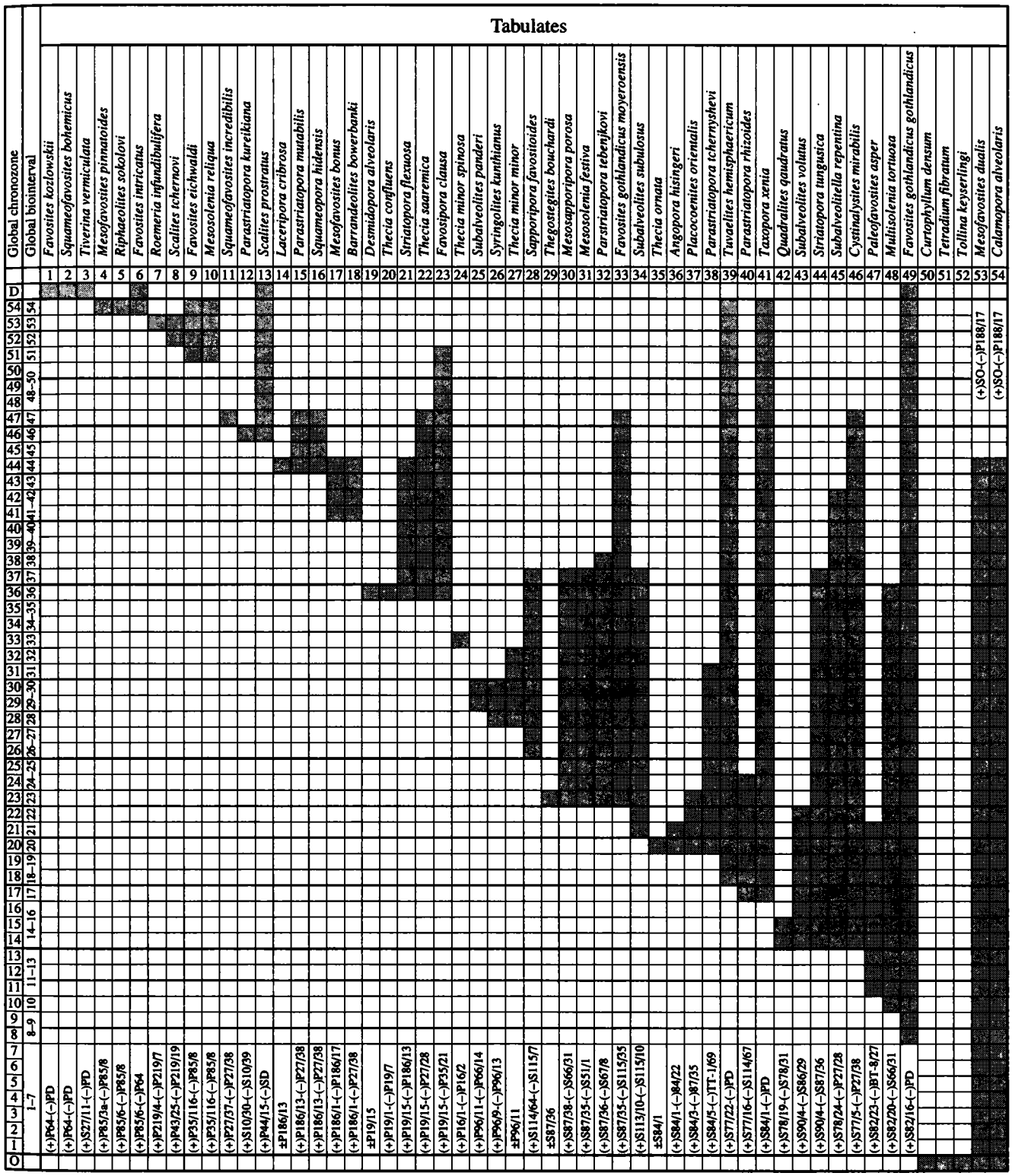

Fig. 2. Global distribution of Tabulata species and their global biointervals.

Stratotype 86 for the regional chronozone 2 of the lower Agidy Subhorizon: the middle part of an exposure at the right-hand bank of the Moiero River 3.2 km upstream from the Moierokan River mouth.

Stratotype 87 for the regional chronozones of the upper Agidy Subhorizon: the left side of a small canyon with two waterfalls at the right-hand bank of the Moiero River 4.0 km upstream from the Moierokan River mouth.

Table 3. Regional Silurian stratigraphic scale for East Siberia

Global Silurian stratigraphic scale					Regional Silurian chronostratigraphic scale for East Siberia													
					Regional chronostratigraphic units					Standard regional chronostratigraphic units								
Superstage	Stage	Substage	Global Chronozone	Global Biointerval	Superhorizon	Horizon	Subhorizon	Regional chronozone	Regional biointerval	Group	Formation	Subformation	District chronozone Observation points	District biointerval	Stratotype	Partial Copula (Bed)	Thickness, m	Correlation level
1	2	3	4	5	6	7	8	9	10	11	12	13	14	15	16	17	18	19
D_1	Lochkovian					Yampakhtinskii				–	Yampakhta				TT-1	141–144	8.2	–
Přídoli (pr)	Přídoli	upper	2	54	Prieniseiskii (prn)	Postnichnyi (ps)	upper	2	52–54		Postnichnaya 81.0	upper 20.5	2	47–54		136–140	11.2	54
			1	53				1					1			129–135	9.1	53
		lower	3	52			middle	3				middle 31.5	3			125–128	11.2	52
			2	51				2	51				2			120–124	11.8	51
			1	50				1	50				1			116–119	8.5	50
Ludlow (ld)	Ludfordian	upper	2	49			lower	3	47–49			lower 29.0	3			114–115	7.9	49
			1	48				2					2			112–114‡	11.2	48
		lower	1	47				1					1			106–111	9.8	47
	Gorstian	upper	3	46		Tukal (tk)	upper	6	46	Prieniseiskaya	Tukal 67.5	upper 40.5	6	46	10	28–40	7.7	46
			2	45				5	45				5	45	4	13–14	5.1	45
			1	44				4	44				4	44		4–12	7.9	44
		lower	7	43				3	43				3	43	1	10–16; 2–3	6.7	43
			6	42				2	42				2	42	2	16–18; 1–9	6.0	42
			5	41				1	41				1	41		29–30; 4–15	6.8	41
			4	40			lower	4	40			lower 27.0	4	40	3	14–28	6.4	40
			3	39				3	39				3	39		2–13	6.2	39
			2	38				2	38				2	38	11	14–17	6.4	38
			1	37				1	37				1	37		3–13	7.9	37
Wenlock (w)	Homerian	upper	3	36	Prianabarskii (pr)	Khakoma (hk)	upper	6	36	Prieniseiskaya	Khakoma 82.0	upper 40.0	6	36	66	26–31	8.0	36
			2	35				5	35				5	35		19–25	8.2	35
			1	34				4	34				4	34		15–18	4.8	34
		lower	3	33				3	33				3	33		9–14	5.1	33
			2	32				2	32				2	32		7–8	6.1	32
			1	31				1	31				1	31		1–6	8.0	31

Table 3. (Contd.)

1	2	3	4	5	6	7	8	9	10	11	12	13	14	15	16	17	18	19
Wenlock (w)	Sheinwoodian	upper	3	30	Prieniseiskii (prn)	Khakoma (hk)	lower	5	30	Prieniseiskaya	Khakoma 82.0	lower 42.0	5	30	64	12–18	9.8	30
			2	29				4	29				4	29	58	16–22	8.5	29
			1	28				3	28				3	28		7–15	6.2	28
		lower	2	27				2	27				2	27	58A	4–8; 2–6	8.3	27
			1	26				1	26				1	26	60	3–4; 2–3	9.2	26
Llandovery (l)	Telychian	upper	1	25	Prianabarskii (pr)	Agidy (ag)	upper	3	25	Prianabarskaya	Agidy 84.5	upper 42.0	3	25	87	53–56	9.4	25
		middle	3	24				2	24				2	24		41–52	14.8	24
			2	23				1	23				1	23		35–40	17.6	23
			1	22			lower	2	22			lower 42.5	2	22	86	23–34	20.9	22
		lower	1	21				1	21				1	21	84; 85	8–22	21.6	21
	Aeronian	upper	2	20	Prianabarskii (pr)	Khaastyr (hs)	upper	3	20	Prianabarskaya	Khaastyr 129.5	upper 50.0	3	20	77	36–43	20.0	20
			1	19				2	19				2	19		27–35	13.6	19
		middle	5	18				1	18				1	18		20–26	16.5	18
			4	17			lower	4	17			lower 79.5	4	17		11–19	21.0	17
			3	16				3	16				3	16	90	22–23; 1–10	18.0	16
			2	15				2	15				2	15		25–31; 18–21	20.3	15
			1	14				1	14				1	14	78	18–24	20.3	14
		lower	2	13		Moierokan (mr)	upper	5	13		Moierokan 111.0	upper 57.0	5	13	83	27–28	13.0	13
			1	12				4	12				4	12		24–26	11.4	12
	Rhuddanian	upper	2	11				3	11				3	11	82	21–23	10.2	11
			1	10				2	10				2	10		19–20	10.5	10
		middle	6	9				1	9				1	9		17–18	11.8	9
			5	8			lower	8	8			lower 54.0	8	8		14–16	13.7	8
			4	7				7	7				7	7		13	11.0	7
			3	6				6	6				6	6		11–12	8.3	6
			2	5				5	5				5	5		9–10	8.5	5
			1	4				4	4				4	4		8	5.0	4
		lower	3	3				3	3				3	3		4–7	5.0	3
			2	2				2	2				2	2		2–3	1.8	2
			1	1				1	1				1	1		1	0.5	1
O_3	Ashgillian				Kety	Burskii				Bura					–	–	–	–

Table 3. (Contd.)

Correlation level (biophase)	Silurian fauna and flora from East Siberia Regional levels of the first (+) and last (–) occurrences of species in East Siberia							
	Graptolites		Chitinozoans		Acritarchs		Cephalopods	
D	–		–		–		–	
54	–		–		(–) *Leiosphaeridia plicata*	SP21/228	–	
53	–		–		–		–	
52	–		–		–		–	
51	(–) *Monograptus rarus*	218/22	–		–		–	
50	(+) *Monograptus rarus*	218/20	–		–		(–) *Hemicosm. semiannulatum*	218/18
49	–		–		–		–	
48	–		–		–		–	
47	(–) *Monograptus priodon*	220/36	–		–		–	
46	(–) *Bohemograp. bohemicus*	218/11	(–) *Desmochitina densa*	10/38	(–) *Favososph. kozlowskii*	10/28	–	
45	–		–		(–) *Leiosphaeridia cerina*	115/44	–	
44	–		–		(–) *Leiosphaeridia laevigata*	4/4	–	
43	–		(–) *Sphaeroch. sphaerocephala*	115/39	(+) *Trachysph. raryplicatum*	SP21/160	–	
42	–		–		(–) *Cymatiosphaera pavimenta*	2/18	–	
41	–		–		(–) *Cymatiosphaera nebulosa*	43/2	–	
40	–		(–) *Eisenackitina bohemica*	115/25	–		(+) *Hemicosm. semiannulatum*	218/8
39	(+) *Monograptus uncinatus*	218/8	–		–		–	
38	–		(–) *Conochitina conulus*	SP21/132	(–) *Lophosphaerid. citrinum*	10/28	–	
37	(+) *Bohemograp. bohemicus*	218/6	(+) *Sphaeroch. sphaerocephala*	114/98	(–) *Favos. heterobrochatum*	SP21/131	–	
36	–		–		–		(–) *Armenoceras bachtense*	66/31
35	(+) *Monograptus ludensis*	218/5a	–		–		–	
34	–		–		–		–	
33	(–) *Monograptus testis*	217/15g	(–) *Eisenack. lagenomorpha*	66/12	–		–	
32	(+) *Monograptus testis*	217/15c	–		–		–	
31	–		–		(–) *Comasphärid. willierеae*	114/89	(–) *Huroniella inflecta*	114/89
30	(+) *Cyrtograptus lundgreni*	217/15a	–		–		(–) *Arm. sauthamptonense*	MD31/104
29	–		–		–		–	
28	–		(+) *Desmochitina densa*	58/7	–		(–) *Sactoceras richteri*	58/9
27	(+) *Pristiograptus dubius*	217/11	(+) *Ancyroch. pachyderma*	114/82	(–) *Lophosphaer. turulosum*	114/85	(+) *Kochoceras cunciforme*	TT1/7
26	(+) *Monograpt. riccartonensis*	217/9	–		(–) *Comasph. sequestratus*	114/72	(+) *Sactoceras richteri*	60/3
25	–		(–) *Linochitina longa*	178/40	(+) *Favososph. polybrochatum*	87/55	(+) *Armenoceras backtense*	178/42
24	(–) *Streptograptus nodifer*	SP21/100	(–) *Conochitina rossica*	114/46	(–) *Leiosphaeridia voigti*	114/53	(+) *Kulinnia hyperborea*	114/48
23	(–) *Monograptus spiralis*	216/6	(–) *Calpichitina acollaris*	178/41	(–) *Trachysph. universalum*	PE43/84	(–) *Hiregirocer. costalatum*	PE43/86
22	–		(–) *Conochitina edjelensis*	PE43/77	(+) *Nucellosphaer. deunffii*	86/25	(–) *Rizoceras acutum*	114/37
21	(+) *Streptograptus nodiger*	SP21/71	(+) *Conochitina conulus*	SP21/71	(+) *Multiplic. oligofurcatum*	MD31/62	–	
20	–		(–) *Eisenackitina conica*	PE43/46	(+) *Dactylofusa estilis*	SP21/65	–	
19	–		–		(+) *Baltisph. granuliferum*	PE43/36	–	
18	–		–		(+) *Trachysph. formosum*	PE43/26	–	
17	(+) *Monograptus elegans*	216/5a	–		(+) *Favososph. kozlowskii*	14/78	(–) *Armenoceras clarum*	177/20
16	–		(+) *Conochitina elegans*	178/4	(+) *Comasphaerid. willierеae*	77/9	(–) *Geisonoceras kureikense*	113/4
15	(–) *Demirastrit. triangulatus*	216/3d	(+) *Eisenack. lagenomorpha*	SP21/47	(+) *Leiosphaeridia plicata*	MD31/20	(+) *Wadeoceras sibiricum*	TT1/28a
14	(+) *Monograptus sedgwicki*	13/12	–		(+) *Micrhystrid. coronatum*	PE43/1	(+) *Armenoceras clarum*	177/12
13	–		(+) *Eisenackitina protracta*	MD31/11	(+) *Trachysph. universalum*	SP21/34	–	
12	(+) *Monograptus distans*	NM10/4	–		(+) *Leiofusa granulacutis*	83/26	(+) *Huroniella inflecta*	83/26
11	–		(+) *Calpichitina acollaris*	175/3	–		(–) *Kentronites conulus*	TT1/21
10	(+) *Demirastrit. delicatulus*	TT1/19	–		–		–	
9	–		(+) *Eisenackitina oviformis*	SP21/33	(+) *Lophosph. parverarum*	MD31/5	(+) *Rizoceras acutum*	175/5
8	(–) *Rastrites norilskensis*	SP21/26	(+) *Linochitina longa*	174/9	–		(+) *Arm. sauthamptonense*	82/16
7	(–) *Lagarograpt. inexpeditus*	TT1/19a	–		(+) *Leiosphaeridia voigti*	SP21/28	–	
6	(+) *Demitastrit. triangulatus*	TT1/13	(+) *Eisenackitina conica*	SP21/27	(+) *Baltisph. echinodermum*	MD31/2	(+) *Hiregiroceras costalatum*	174/3
5	(+) *Coronograptus gregarius*	TT1/9	–		–		–	
4	(+) *Coronograptus cyphus*	82/8	–		–		–	
3	(+) *Metabology. moyeroensis*	82/4	(+) *Ancyrochitina ancyrea*	85/2	–		–	
2	(+) *Cystograptus vesiculosus*	216/1c	–		–		(+) *Geisonoceras kureikense*	82/2
1	(+) *Parakidogr. acuminatus*	216/1a	(+) *Conochitina edjelensis*	SP21/14	–		–	
O	–		–		–		–	

Table 3. (Contd.)

Correlation level (biophase)	Silurian fauna and flora from East Siberia							
	Regional levels of the first (+) and last (–) occurrences of species in East Siberia							
	Trilobites		Brachiopods		Scolecodonts		Conodonts	
D	–		–		–		–	
54	–		–		–		–	
53	–		–		–		–	
52	–		–		–		–	
51	–		–		–		–	
50	–		–		–		–	
49	–		–		–		–	
48	–		–		–		–	
47	–		–		–		–	
46	–		(–) *Morinorhynchus proprius*	115/55	–		(–) *Ozarkodina typica*	10/38
45	–		(–) *Eohowellella vadrenkinae*	4/14	–		(–) *Spathognathodus primus*	10/28
44	–		(–) *Howellel. elevataeformis*	MD31/148	–		(–) *Oulodus siluricus*	MD31/143
43	–		(–) *Dalejina ribnayaensis*	LNCH9/39	–		(+) *Lonchodina greilingi*	10/16
42	–		–		–		–	
41	–		(–) *Protatrypa lepidota*	115/39	(–) *Xaniprion sibiricus*	SP21/133	–	
40	–		(+) *Conchidium biloculare*	218/8b	(–) *Polychaetaspis latus*	115/26	(+) *Spathognathodus primus*	3/14
39	–		(–) *Anabaria rara*	3/13	–		–	
38	–		–		(–) *Mochtyella angelini*	115/20	–	
37	–		–		(–) *Kettnerites aspersus*	114/102	(+) *Oulodus siluricus*	TT1/79
36	–		–		–		(–) *Kockelella variabilis*	52/10
35	–		(–) *Stegerhynch. mojeroensis*	66/22	–		(–) *Huddlella johni*	66/20
34	(–) *Encrinurus creber*	114/94	(–) *Alispira rotundata*	62/8	–		–	
33	–		–		–		–	
32	–		–		–		–	
31	–		(–) *Plectatrypa wenlockiana*	MKT2/52	–		(+) *Ozarkodina excavata*	64/20
30	–		–		–		(+) *Neoprioniodus excavatus*	64/15
29	–		–		–		(–) *Trichonodella symmetrica*	58/16
28	–		–		(–) *Vistulella kozlowslii*	114/87	(+) *Kockelella variabilis*	58/10
27	–		–		–		–	
26	–		(–) *Eoplectodonta pumila*	217/6	–		(+) *Huddlella johni*	60/3
25	(+) *Encrinurus creber*	114/66	(+) *Omnutakhel. bazhenovae*	114/64	–		(–) *Distomodus kentuckyensis*	114/65
24	–		(–) *Alispira tenuicostata*	87/50	–		(–) *Icriodella sandersi*	114/51
23	–		(+) *Morinorhynchus proprius*	114/38	–		(+) *Ozarkodina gaertneri*	SP21/97
22	(–) *Eophacops quadrillineatus*	FT3/24	(–) *Pentamerus oblongus*	FT3/24	–		(+) *Spathognathodus* sp.	86/30
21	(–) *Acernaspis incerta*	14/117	(+) *Pratatrypa lepidota*	ff7/54	–		(+) *Pter. amorphognathoides*	84/11
20	(–) *Acernaspis nanus*	178/24	(+) *Anabaria rara*	77/39	–		(+) *Trichonodella symmetrica*	14/101
19	–		(–) *Septatrypa antiquata*	77/31	(–) *Mochtyella fragilis*	178/15	(+) *Carniodus carnulus*	178/17
18	(+) *Bumastus barriensis*	77/24	(+) *Plectatrypa wenlockiana*	113/16	(+) *Mochtyella angelini*	115/20	(+) *Icriodella sandersi*	114/17
17	(+) *Encrinurus punctatus*	ff7/35	(+) *Pentlandina subcostatula*	77/13	(+) *Kozlowskipr. brevialatus*	113/11	(+) *Pterospathodus celloni*	14/75
16	(+) *Stenopareia bowmanni*	177/19	(+) *Crytothyrella norillica*	77/4	(+) *Multiprion trapezoideus*	MD31/26	(+) *Oulodus kentuckyensis*	113/7
15	(+) *Eophacops quadrilineatus*	ff7/24	(–) *Brevilamnul. undatiformis*	FT3/16	(+) *Polychaetaspis latus*	MD31/20	(+) *icriodella inconstans*	78/26
14	(+) *Eobronteus norilskensis*	78/23	(+) *Kulumbella biconvexa*	FT3/14	(+) *Kettnerites aspersus*	SP21/37	(+) *Icriodella deflecta*	78/16
13	(+) *Acernaspis pulcher*	175/8	(+) *Pentamerus oblongus*	13/11	–		(+) *Apsidognath. tubersulatus*	13/6
12	(–) *Acernaspis superciliexcelsis*	83/24	(+) *Howellel. elevataeformis*	216/3d	–		(+) *Kockelella ranuliformis*	216/3·
11	(+) *Unguliproetus enodis*	78/8	(+) *Alispira tenuicostata*	82/21	–		(+) *Hadrogn. starognathoides*	184/42
10	(+) *Pseudoproetus tertius*	82/19	(+) *Borealis nanus*	82/20	–		–	
9	(+) *Stenopareia angulata*	82/18	(+) *Septarypa magna*	82/17	–		–	
8	–		(+) *Stricklandia salteri*	82/16	–		–	
7	–		(+) *Clorinda undata*	83/13	–		–	
6	(+) *Acernaspis superciliexcelsis*	82/11	(+) *Coolinia gracilis*	BT8/5	–		(+) *Icriodella discreta*	174/2
5			–		–		(+) *Decoriconus fragilis*	184/11
4	–		(+) *Strophomena sibirica*	FT3/3	–		–	
3	(+) *Pseudoproetus bellus*	FT3/2	(+) *St. decemplicatus duplex*	82/4	–		–	
2	(–) *Cyphoproetus externus*	82/3	(+) *Eridorthis siluriensis*	LNCH9/1	–		(+) *Distomodus kentuckyensis*	79/6
1	(+) *Cyphoproetus externus*	82/1	(+) *Alispira gracilis*	SP21/14	(+) *Vistulella kozlowskii*	SP21/14	(+) *Oulodus nathani*	147/2
O	–		–		–		–	

Table 3. (Contd.)

Correlation level (biophase)	Silurian fauna and flora from East Siberia							
	Regional levels of the first (+) and last (–) occurrences of species in East Siberia							
	Bryozoan		Tentaculitids		Ostracodes		Gastropods	
D	–		–		–		–	
54	–		–		–		–	
53	–		–		–		–	
52	–		–		–		–	
51	–		–		–		–	
50	–		–		–		–	
49	–		–		–		–	
48	–		–		–		–	
47	–		–		–		–	
46	(–) *Monotrypa benjamini*	10/34	–		(±) *Schrenkia nulta*	4/5	(–) *Prosolarium cirrhosa*	10/28
45	–		–		(–) *Beyrichia parva*	115/44	–	
44	(–) *Lioclema crustulum*	4/9	–		(–) *Beyrichia kureikiana*	F245/140	–	
43	(+) *Lioclema crustulum*	1/11	–		(+) *Beyrichia parva*	115/39	–	
42	(+) *Mesotrypa alashensis*	1/8	–		(+) *Healdianella inornata*	1/16	–	
41			–		–		–	
40	–		–		(+) *Eukloed. kureikensis*	115/25	–	
39	(+) *Monotrypa benjamini*	3/7	–		(+) *Sighetopsis cardinata*	115/23	–	
38	–		–		–		–	
37	–		–		–		–	
36	–		–		–		–	
35	(–) *Homotrypa hondelensis*	6/24	–		(+) *Leperditia lumaea*	66/21	(–) *Lophospira sinuosa*	66/20
34	–		–		–		–	
33	–		–		(+) *Beyrichia kureikiana*	66/9	(–) *Trochonema transformis*	114/94
32	(–) *Eridotrypa callosa*	114/90	–		–		(–) *Lophospera alta*	114/90
31	–		–		–		–	
30	–		–		(–) *Cytherellina ovifirmis*	K1010/26	–	
29	–		–		–		–	
28	(–) *Batostoma microcellata*	114/86	–		–		(+) *Lophospira alta*	114/86
27	–		–		(–) *Sibiritia wiluiensis*	LNCH9/41	(+) *Oriostoma varvara*	114/83
26	(+) *Monotrypa padiculata*	60/3	–		–		–	
25	–		–		–		–	
24	(+) *Eridotrypa callosa*	114/50	–		(–) *Bollia cardinis*	K1010/21	(–) *Holopea transversa*	114/48
23	–		–		(–) *Imandites ambiquus*	TT7/68	(–) *Pararaph. qualteriatum*	114/43
22	(+) *Batostoma microcellata*	114/36	(–) *Costatulites corniformis*	114/37	(–) *Norilskinia cuspidata*	86/31	(–) *Murchisonia insignis*	TT7/55
21	(–) *Moyerella stallata*	MKT2/26	–		(+) *Herrmannina nana*	85/20	(+) *Murchisonia cingulata*	114/18
20	(–) *Strictopora markhensis*	178/26	–		(+) *Beyrichia mirabilis*	PE43/40	(–) *Bucanopsis sibiricus*	178/27
19	(–) *Hennigopora florida*	14/96	(–) *Costatulites homogenus*	89/1	(+) *Sibiritia eurina*	F245/18	(–) *Poleumita mashkovae*	178/9
18	(–) *Prilodictya lanceolata*	77/25	–		(+) *Norilskinia norilica*	SP21/59	(–) *Poleumita anabarica*	83/28
17	(+) *Strictopora markhensis*	14/74	–		(+) *Hatangeus armatus*	TT7/33	(+) *Trochonema transformis*	113/9
16	(+) *Stictoporella lamellata*	180/4	(+) *Evenkyites rarus*	77/1	(+) *Cyrterellina oviformis*	K1010/21	–	
15	(+) *Hennigopora florida*	113/1	–		(+) *Daleiella decorata'*	SP21/47	(+) *Loxoplocus vostokovae*	177/20
14	(+) *Rhinidictya bifurcata*	13/12	(–) *Costatulites undatus*	78/23	(+) *Costaegara hastata*	78/24	(+) *Gyronema quadricarina*	175/15
13	(+) *Helopora spiralis*	83/27	–		–		(+) *Poleumita anabarica*	83/28
12	(+) *Ensipora erecta*	83/24	–		–		(+) *Ruedemannia lirata*	177/10
11	–		(+) *Costatulites homogenus*	78/11	–		–	
10	(+) *Monotr. amplexoformis*	82/20	–		–		(+) *Umbonellina infrasilurica*	82/19
9	–		–		(+) *Eurychilina fragilis*	82/17	(+) *Cyclonema bilix*	82/17
8	(+) *Moyerella stellata*	82/15	–		(+) *Thrallella alveolata*	LNCH9/7	(+) *Straparollus alacer*	UD5/7
7	–		–		(+) *Sibiritia wiluiensis*	82/13	(+) *Eotomaria supracingulata*	175/2
6	–		–		(+) *Silenis sibiricus*	174/1	–	
5	–		–		–		(+) *Gyronema multangulata*	TT1/16
4	–		(+) *Costatulites undatus*	82/8	–		(+) *Murchisonia insignis*	UD5/4
3	–		–		–		–	
2	–		–		–		(+) *Prosoptychus globulus*	LNCH9/4
1	–		–		–		–	
O	–		–		–		–	

Table 3. (Contd.)

Correlation level (biophase)	Silurian fauna and flora from East Siberia Regional levels of the first (+) and last (–) occurrences of species in East Siberia							
	Crinoids		Rugose corals		Tabulates		Stromatoporoid	
D	–		–		(+) *Tiverina cermiculata*	SHT27/11	–	
54	–		–		–		–	
53	–		–		–		–	
52	–		–		–		–	
51	–		–		–		–	
50	–		–		–		–	
49	–		–		–		–	
48	–		–		–		–	
47	–		–		–		–	
46	(–) *Bazaricrinus parvulus*	10/34	–		(–) *Parastriat. kureikiana*	10/39	(–) *Clathrodictyon mohicanum*	10/36
45	–		–		(+) *Parastriat. kureikiana*	4/13	–	
44	(–) *Bystrow. quinquelobatus*	2/11	–		(–) *Syringop. fascicularis*	115/40	(–) *Densastroma astroites*	4/12
43	(–) *Bystrowicrinus biobatus*	115/44	–		–		–	
42	–		(–) *Tryplasma flexuosum*	1/6	–		(+–) *Strom. dzvenigorodensis*	1/6
41	–		–		–		–	
40	–		(–) *Miculiella annae*	3/13	–		–	
39	–		(–) *Entelophyllum articulatum*	3/5	(–) *Subalveol. subulosus*	3/13	(–) *Ecclimad. sibiricum*	115/10b
38	–		–		–		(+) *Ecclimad. sibiricum*	115/7
37	–		(+) *Tryplasma flexuosum*	11/6	(–) *Multisolenia tortuosa*	SP21/127	(–) *Ecclimad. fastigiatum*	114/104
36	(–) *Egiasar. egiasarowi*	114/96	(–) *Yassia enormis*	66/31	(–) *Mesosolenia festiva*	87/35	(+) *Plexodictyon savaliense*	66/31
35	–		–		–		–	
34	–		–	TT1/69	–		(+) *Yavorskiina njuilensis*	163/3
33	–		(–) *Cyathastis typus*	66/8	–		(–) *Rosenella hakomiense*	53/7
32	–		(+) *Cystiphyllum culindricum*	TT1/69	–		(–) *Clathrodictyon muriei*	BT8/61
31	–		(+) *Miculiella compacta*	54/1	–		(–) *Labechia conferta*	BT8/60
30	–		(+) *Kymocystis papillaris*	58/16	(–) *Halysites catenularius*	K1010/26	(+) *Yabeodictyon crispatim*	UD5/35
29	(–) *Crotalocrinites borealis*	FT3/23	(+) *Neocystiphyl. holtedahli*	58/7	–		–	
28	–		(+) *Miculiella crassiseptata*	58A/4c	(+) *Parastriatopora mutabilis*	114/86	–	
27	–		(+) *Neocystiphyll. mac'coyi*	60/3	(+–) *Desmidopora alveolaris*	114/85	–	
26	(–) *Turuch. turuchanensis*	114/80	(+) *Protopiloph. cylindricum*		–		(+) *Ecclimad. fastigiatum*	114/104
25	(+) *Dastaricr. petaloideus*	114/67	–		(+) *Sapporipora favositoides*	114/64	(+) *Clavidictyon cylindricum*	114/62
24	(–) *Tajmirocr. tajmirensis*	78/21	–		(–) *Mesofavosites dualis*	SP21/26	(+) *Neobeatricea nikiforovae*	BT8/44
23	(+) *Sibiricrinus helenae*	114/44	(+) *Cyathactic typus*	TT1/58	–		(+) *Stromatopora lenensis*	85/35
22	(+) *Megalocrinus latiobatus*	112/7	(+) *Yassia enormis*	86/2	(+) *Mesosolenia festiva*	87/35	–	
21	(+) *Turuch. turuchanensis*	114/24	(–) *Entelophyllum medius*	TT1/46	(+) *Mesofavosites planus*	84/12	(+) *Pachystylost. sibiricum*	84/22
20	(+) *Scalaricr. scalariformis*	77/43	(–) *Crass. crassiseptatum*	178/26	(+) *Placocoenites orientalis*	77/39	(+) *Plümatalinia densa*	77/39
19	(+) *Bystrowicrinus bilobatus*	TT1/34	(–) *Streptelasma whittardi*	178/16	(+) *Vaenopora kaljoi*	77/29	(–) *Labechia obrouchevi*	112/3
18	(+) *Megalocrinus pentalobatus*	TT1/31	(+) *Streptelasma whittardi*	178/9	(+) *Tuvael. hemisphaericus*	77/22	–	
17	–		(+) *Cystilasma sibiricum*	TT1/92	(+) *Subalveolites subulosus*	114/30	(+) *Plectost. tenuipalum*	UD5/16
16	(+) *Crotalocrinites borealis*	SP21/48	(+) *Cyathactis euryone*	77/9	(+) *Coenites juniperinus*	UD5/13	–	
15	–		(+) *Helicealasma whittardi*	TT1/28a	(+) *Subalveolitella repentina*	L3/22	(+) *Labechia obrouchevi*	101/1
14	(+) *Myelodactylus flexibilis*	90/3	(+) *Entelophyl. articulatum*	78/21	(+) *Cystihalysites mirabilis*	LNCH9/11	(+) *Clathrodict. variolare*	9857/17
13	–		–		–		–	
12	–		–		(+) *Angopora hisingeri*	L3/13	–	
11	(+) *Glyptocrinus elegans*	TT1/21	(+) *Crassilasma completum*	82/19	(+) *Paleofavosites asper*	82/23	–	
10	–		(+) *Brachyelasma sibiricum*	175/4	(+) *Multisolenia tortuosa*	82/20	–	
9	–		–		–		(+) *Clath. microundilatum*	BT8/11b
8	–		(+) *Kodonoph. complanatum*	82/16	(+) *F. goth. gothlandicus*	82/16	–	
7	–		–		–		–	
6	–		–		–		(+) *Labechia venusta*	LNCH9/8
5	–		–		–		–	
4	–		–		–		–	
3			–		–		–	
2	(+) *Dentiferocr. dentiferus*	LNCH9/1	–		–		–	
1	–		–		–		–	
O	–		–		(–) *Tollina keyserlingi*	205/24	(–) *Aulacera nodulosa*	

Table 3. (Contd.)

Correlation level (biophase)	Silurian fauna and flora from East Siberia											
	Regional levels of the first (+) and last (–) occurrences of species in East Siberia											
	Algae			Pelecypods			Fishes			Hyolithids and conulariids		
D	–			–			–			–		
54	–			–			–			–		
53	–			–			–			–		
52	–			–			–			–		
51	–			–			–			–		
50	–			–			–			–		
49	–			–			–			–		
48	–			–			–			–		
47	–			–			–			–		
46	–			–			–			–		
45	(–) *Hedstroem. halimedoidea*		115/46	–			–			–		
44	–			–			–			–		
43	–			–			–			–		
42	–			–			–			–		
41	–			–			–			–		
40	–			(+–) *Cardinia signata*		118/8b	–			–		
39	–			–			–			–		
38	–			–			–			–		
37	–			–			–			–		
36	–			(–) *Megalomus* sp.			–			–		
35	–			–			–			–		
34	–			–			–			–		
33	–			–			–			–		
32	–			–			–			–		
31	–			–			–			–		
30	–			(+) *Megalomus* sp.			–			–		
29	–			–			–			–		
28	–			–			–			–		
27	–			–			–			–		
26	(+–) *Solenopora concentrica*		114/75	–			(–) *Loganellia scotica*		135/64	–		
25	(+) *Rothpletzella gotlandoca*		114/70	–			–			–		
24	(+) *Hedstroem. halimedoidea*		114/56	–			–			–		
23	–			–			(+) *Helenolepis trifurcata*		135/57	–		
22	–			–			–			–		
21	–			–			–			–		
20	–			–			(–) *Tubia bergeri*		135/48	–		
19	–			–			(+) *Udalepis forata*		135/44	–		
18	–			–			(+–) *Tesakoviasp. concentrica*		135/42	(–) *Conulata*		9857/41
17	–			–			–			–		
16	–			–			(+) *Loganellia scotica*		140/24	–		
15	–			–			–			(–) *Hyolitoidea*		SP21/44
14	–			–			(+) *Elegestolepis conica*		156/30	–		
13	–			–			–			–		
12	–			–			–			–		
11	–			–			–			–		
10	–			(–) *Actinopteria pumila*		FT3/12	(+) *Ilimia predtechenskii*		135/12	–		
9	–			–			–			–		
8	–			–			(+) *Loganellia moskalenkoae*		140/8	–		
7	–			–			–			–		
6	–			–			(+) *Loganellia sibirica*		156/2	(+) *Conulata*		82/11
5	–			–			–			–		
4	–			–			–					
3	–			–			–			–		
2	–			(+) *Actinopteria pumila*		FT3/1	–			(+) *Hyolitoidea*		SP21/20
1	–			–			–			–		
O	–			–			–			–		

Stratotype 60 for the lower part of the regional chronozone 1 of the lower Khakoma Subhorizon: the right-hand bank of the Moiero River 3.0 km downstream from the Khakoma River mouth.

Stratotype 58A for the boundary interval between the regional chronozones 1 and 2 of the lower Khakoma Subhorizon: the left-hand bank of the Moiero River 0.7–1.0 km downstream from the Khakoma River mouth.

Stratotype 58 for the upper part of the regional chronozone 2 and for chronozones 3 and 4 of the lower Khakoma Subhorizon. This and previous stratotypes constitute one section exposed at the left-hand bank of the Moiero River and extending for 1.8 km downstream from the Khakoma River mouth.

Stratotype 64 for the regional chronozone 5 of the lower Khakoma Subhorizon: the middle part of an exposure at the right-hand bank of the Moiero River 3 km downstream from the Mramornyi Rapids.

Stratotype 66 for the regional chronozones of the upper Khakoma Subhorizon: the bluff at the left-hand side of the Moiero River 6.2 km downstream straight away from the Mramornyi Rapids.

Stratotype 11 for the regional chronozones 1 and 2 of the lower Tukal Subhorizon: the Nizhnie Shcheki locality at the right-hand side of the Kureika River.

Stratotype 3 for the regional chronozones 3 and 4 of the lower Tukal Subhorizon and for the basal portion of the regional chronozone 1 of the upper Tukal Subhorizon: the Verkhnie Shcheki locality at the left-hand bank of the Kureika River 10 m downstream from the exposure 2 in the footwall of normal fault.

Stratotype 2 for the boundary interval of the regional chronozones 1 and 2 of the upper Tukal Subhorizon: the Verkhnie Shcheki locality at the left-hand bank of the Kureika River 300 m downstream from the exposure 1.

Stratotype 1 for the boundary interval of the regional chronozones 2 and 3 of the upper Tukal Subhorizon: first outcrops of the Verkhnie Shcheki locality at the left-hand bank of the Kureika River 340 m downstream from the Bannyi Creek.

Stratotype 4 for the upper part of the regional chronozone 3 and for the regional chronozones 4 and 5 of the upper Tukal Subhorizon: the left-hand bank of the Kureika River 100 m downstream from the exposure 1.

Stratotype 10 for the regional chronozone 6 of the upper Tukal Subhorizon: the northern side of the Verkhnie Shcheki locality at the left-hand bank of the Kureika River (more detailed characteristics of stratotype localities at the Kureika River have been reported by Tesakov *et al.*, 1980, Figs. 14, 15).

Stratotype TT-1 for subhorizons and regional chronozones of the Postnichnyi Horizon: Borehole TT-1 at the eastern coast of the Pyasino Lake, 69°93′3″N and 88°13′8″E (core samples are stored at the Museum of the Norilsk Geological-Prospecting Expedition).

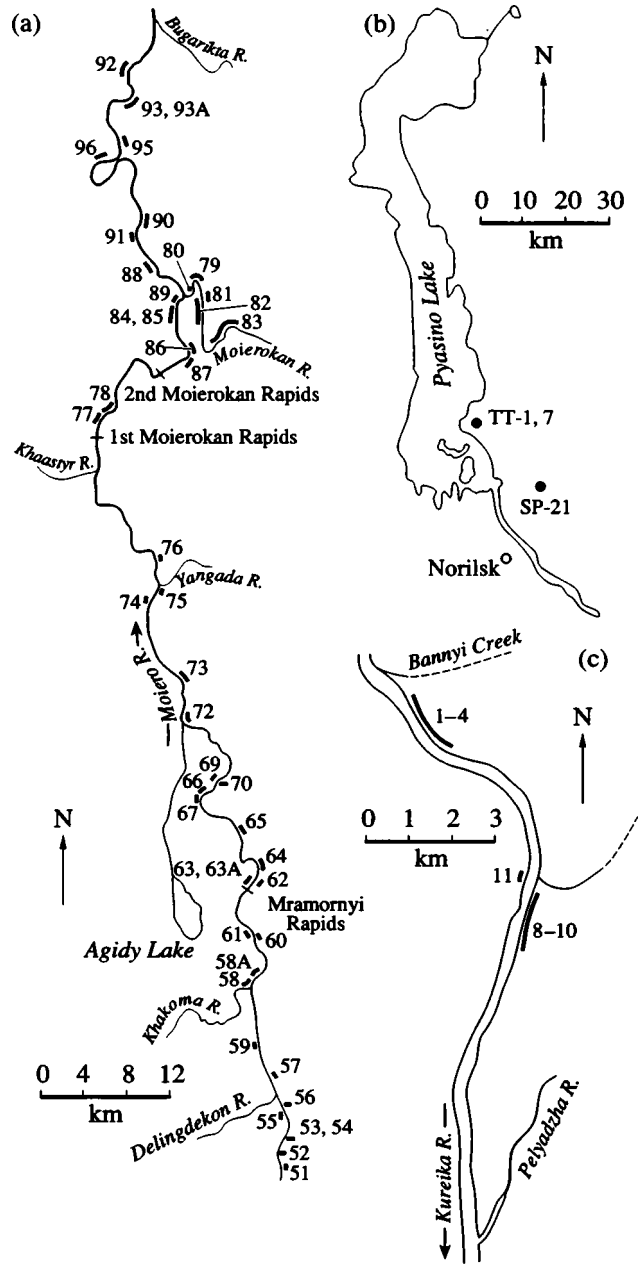

Fig. 3. Localities of stratotypes for regional chronozones of East Siberia: (a) Moiero district, Moiero River basin; (b) Turukhansk district, Kureika River basin; (c) Norilsk district, borehole TT-1.

Sedimentary beds earlier described in detail (Tesakov *et al.*, 1980; *Silur*, 1982) are perfectly exposed in all listed stratotypes. The stratotype-to-stratotype increment of the obtained composite section was verified by means of the correlation of individual beds in adjacent exposures satisfying the requirements of stratigraphic succession. Exceptions to this rule are the lower boundaries of the Tukal and Postnichnyi horizons, because in this case we had to correlate the isolated stratotypes on the basis of fauna and regional

cycles of sedimentation. The base of the Tukal Horizon is marked by the transition from coral–stromatoporoid limestones to algal dolomites, and that of the Postnichnyi Horizon separates the algal dolomites from halide-dolomitic marls.

The chronozonal standard of the Silurian System (Table 3) elaborated on the basis of this composite section was used to calibrate chronozonal subdivisions in most East Siberian localities of Silurian deposits naturally exposed or penetrated by drilling. All 54 isochronal (chronozonal) levels were traced throughout the East Siberia and used to reveal geographic ranges of all species and to fix the first and last occurrence levels of regional significance for basic guide species (Table 3).

Using the same methodical approach in our elaboration of the global and regional (East Siberian) scales of the Silurian System we got the chance to correlate both standards at the chronozonal level and to coordinate stratigraphic ranges of global and regional chronozones (Table 3).

ACKNOWLEDGMENTS

This work was financially supported by the Russian Foundation for Basic Research, project no. 95-05-15564.

Reviewer B.S. Sokolov

REFERENCES

Basset, M.G., Lithostratigraphy, Biostratigraphy, and Chronostratigraphy: Silurian of England as an Example, *Izv. Akad. Nauk Kazakh. SSR, Ser. Geol.*, 1979, nos. 4–5, pp. 115–122.

Basset, M.G., Towards a "Common Language" in Stratigraphy, *Episodes*, 1985, no. 8, pp. 87–92.

Basset, M.G., The Wenlock Series in the Wenlock Area, *Geol. Ser. Nat. Mus. Wales*, 1989, no. 9, pp.51–73.

Basset, M.G., Cocks, L.R.M., Holland, C.H., *et al.*, The Type Wenlock Series, *Rep. Inst. Geol. Sci.*, 1975, no. 75/13, pp. 1–19.

Cocks, L.R.M., The Llandovery Series in the Llandovery Area, *Geol. Ser. Nat. Mus. Wales*, 1989, no. 9, pp. 36–50.

Cocks, L.R.M., Holland, C.H., Rikards, R.B., and Strachan, I., A Correlation of Silurian Rocks in the British Isles, *J. Geol. Soc. London*, 1971, vol. 127, pp. 103–136.

Cocks, L.R.M., Lane, P.D., Rikards, R.B., *et al.*, The Llandovery Area as the Type for the First Series of the Silurian System, *Report to the Subcommission on Silurian Stratigraphy, April 1983*, pp. 1–30.

Cocks, L.R.M., Toghill, P., and Ziegler, A.M., Stage Names within the Llandovery Series, *Geol. Mag.*, 1970, vol. 107, pp. 79–87.

Cocks, L.R.M., Woodcock, N.M., Rikards, R.B., *et al.*, The Llandovery Series of the Type Area, *Bull. Brit. Mus. Nat. History, Geol.*, 1984, vol. 38, pp. 131–182.

Holland, C.H., Silurian Series and Stage: Decision Concerning Chronostratigraphy, *Lethaia*, 1980a, vol. 13, p. 238.

Holland, C.H., Silurian Subdivisions, *Lethaia*, 1980b, vol. 13, p. 366.

Holland, C.H., Series and Stages of the Silurian System, *Episodes*, 1985, no. 8, pp. 101–103.

Holland, C.H., Classification, *Geol. Ser. Nat. Mus. Wales*, 1989, no. 9, pp. 23–26.

Holland, C.H., Lawson, J.D., and Walmsley, V.G., The Silurian Rocks of the Ludlow District, Shropshire, *Bull. Brit. Mus. Nat. History, Geol.*, 1963, vol. 8, pp. 93–171.

Holland, C.H., Lawson, J.D., Walmsley, V.G., and White, D.T., Ludlow Stage, *Lethaia*, 1980, no. 13, p. 268.

International Stratigraphic Guide: A Guide to Stratigraphic Classification, Terminology, and Procedure, Hedberg, H.D., Ed., New York: Wiley and Sons, 1976.

Jones, O.T., The Geology of the Llandovery District. Part 1: the Southern Area, *Quart. J. Geol. Soc. London*, 1925, vol. 81, pp. 344–388.

Jones, O.T., The Geology of the Llandovery District. Part 2: the Northern Area, *Quart. J. Geol. Soc. London*, 1949, vol. 105, pp. 43–64.

Kříž, J., The Přidoli Series in the Prague Basin (Barrandien Area, Bohemia), *Geol. Ser. Nat. Mus. Wales*, 1989, no. 9, pp. 90–100.

Kříž, J., Jaeger, H., Paris, F., *et al.*, The Přidoli Series as the Fourth Series of the Silurian System, *A supplementary Submission to the Subcommission on Silurian Stratigraphy, March 1983*, pp. 1–59.

Kříž, J., Jaeger, H., Paris, F., and Schönlaub, H.P., Přidoli—the Fourth Subdivision of the Silurian, *Jahrb. Geol., B.-A.*, 1986, vol. 129, pp. 291–360.

Lawson, J.D. and White, D.E., The Ludlow Series in the Ludlow Area, *Geol. Ser. Nat. Mus. Wales*, 1989, no. 9, pp. 73–90.

Lesperance, P.J., Barnes, C.R., Berry, W.B.N., *et al.*, The Ordovician–Silurian Boundary Stratotype: Consequences of Its Approval by the IUGS, *Lethaia*, 1987, vol. 20, pp. 217–222.

McKerrow, W.S., Lambert, R.St.J., Berry, W.B.N., *et al.*, The Ordovician, Silurian, and Devonian Time Scales, *Earth Planet. Sci. Lett.*, 1980, vol. 51, no. 1, pp. 1–8.

McKerrow, W.S., Lambert, R.St.J., and Cocks, L.R.M., The Ordovician, Silurian, and Devonian Periods, *Mem. Geol. Soc. London*, 1985, no. 10, pp. 73–80.

Nikiforova, O.I., New Data on Ordovician–Silurian Stratigraphy and Paleogeography in the Siberian Platform, *Tr. Vses. Geol. Inst., Nov. Ser.*, 1955, vol. 7, pp. 50–106.

Nikiforova, O.I. and Andreeva, O.N., *Stratigrafiya ordovika i silura Sibirskoi platformy i ee paleontologicheskoe obosnovanie* (Ordovician–Silurian Stratigraphy of the Siberian Platform and Paleontological Substantiation) Leningrad: Gostoptekhizdat, 1961.

Renevier, E., Commission internationale de classification stratigraphique, *8-e Congress Geologique Internationale*, Paris, 1901, no. 1, pp. 201–203.

Report of the Stratigraphical Code Subcommittee, Proc. Geol. Soc. London, 1967, no. 1638, pp. 75–87.

Resheniya Vsesoyuznogo stratigraficheskogo soveshchaniya po dokembriyu, paleozoyu i chetvertichnoi sisteme Srednei Sibiri (Resolutions of the All-Union Stratigraphic Conference on the Precambrian, Paleozoic, and Quaternary in Central Siberia), Novosibirsk: Sib. Inst. Geol. Geofiz. Mineral. Syr'ya, 1983.

Rikards, R.B., Utility and Precision of Silurian Graptolite Biozones, *Lethaia*, 1995, vol. 28, pp. 129–137.

Silurian: Lexique Stratigraphique International. Europe, Fascicule 3a; England, Wales and Scotland, Part 3a V, Whittard, W.E. and Simpson, S., Eds., Paris: Anatole-France, 1961.

Silur Sibirskoi platformy. Razrezy, fauna i flora severo-zapadnoi chasti Tungusskoi sineklizy (Silurian in the Siberian Platform: Sections, Fauna and Flora from the Northwestern Tunguska Syneclise), Sokolov, B.S., Ed., Moscow: Nauka, 1982.

Sokolov, B.S. and Tesakov, Yu.I., *Tabulyaty paleozoya Sibiri* (Paleozoic Tabulata from Siberia), Moscow: Akad. Nauk SSSR, 1963.

Sokolov, B.S. and Tesakov, Yu.I., *Populyatsionnyi, biotsenoticheskii i biostratigraficheskii analiz tabulyat. Podol'skaya model'* (Analysis of Tabulata Population, Biocoenoses, and Biostratigraphy: The Podol'sk Model), Novosibirsk: Nauka, 1984.

Tesakov, Yu.I., Ecosystem Evolution of Ancient Platform Sedimentary Basins, in *Problemy evolyutsii geologicheskikh protsessov* (Problems of Evolution of Geological Processes), Novosibirsk: Nauka, 1981, pp. 186–199.

Tesakov, Yu.I., Malich, N.S., Zanin, Yu.N., *et al., Stratigrafiya ordovika Sibirskoi platformy* (Ordovician Stratigraphy of Siberian Platform), Novosibirsk: Nauka, 1975.

Tesakov, Yu.I. and Obut, A.M., The Silurian, in *Fanerozoi Sibiri, T. 1, Vend, Paleozoi* (Phanerozoic of Siberia: vol. 1, Vendian and Paleozoic), Novosibirsk: Nauka, 1984, pp. 88–108.

Tesakov, Yu.I., Predtechenskii, N.N., Bazarova, L.S., *et al., Silur Sibirskoi platformy. Novye regional'nye i mestnye stratigraficheskie podrazdeleniya* (Silurian of the Siberian Platform: New Regional and Local Stratigraphic Subdivisions), Novosibirsk: Nauka, 1979.

Tesakov, Yu.I., Predtechenskii, N.N., Bazarova, L.S., *et al., Silur Sibirskoi platformy. Opornye razrezy severo-zapada Sibirskoi platformy* (Silurian of the Siberian Platform: Reference Sections in the Northwestern Siberian Platform), Novosibirsk: Nauka, 1980.

Tesakov, Yu.I., Predtechenskii, N.N., Berger, A.Ya., *et al., Opornyi razrez reki Moiero silura Sibirskoi platformy* (The Moiero Reference Section of the Silurian in the Siberian Platform), Novosibirsk: Nauka, 1985.

Tesakov, Yu.I., Predtechenskii, N.N., Berger, A.Ya., *et al.,* Silurian Stratigraphy in the Taimyr Mountain Area, in *Nedra Taimyra* (Earth Interior of Taimyr), St. Petersburg: Vseross. Geol. Inst., 1995, pp. 123–140.

Tesakov, Yu.I., Predtechenskii, N.N., Khromykh, V.G., *et al., Fauna i flora silura Zapolyar'ya Sibirskoi platformy* (Silurian Fauna and Flora from Polar Regions of the Siberian Platform), Novosibirsk: Nauka, 1986.

Tesakov, Yu.I., Predtechenskii, N.N., Khromykh, V.G., *et al., Razrezy i fauna silura severa Tungusskoi sineklizy* (Sections and Silurian Fauna from the Northern Tunguska Syneclise), Novosibirsk: Nauka, 1992.

Toghill, P., The Graptolite Assemblages and Zones of the Birkhill Shales (Lower Silurian) at Dob's Linn, *Paleontology,* 1968, no. 11, pp. 654–668.

Tucker, R.D. and McKerrow, W.S., Early Paleozoic Chronology: A Review in Light of New U–Pb Zircon Ages from Newfoundland and Britain, *Can. J. Earth Sci.,* 1995, vol. 32, pp. 368–379.

White, D.E. and Lawson, J.D., The Stratigraphy of New Sections in the Ludlow Series of the Type Area, Ludlow, Salop, England, *Rep. Inst. Geol. Sci.,* 1978, vol. 78/30, pp. 1–10.

Williams, S.H. and Ingham, J.K., The Ordovician–Silurian Boundary Stratotype at Dob's Linn, Southern Scotland, *Geol. Ser. Nat. Mus. Wales,* 1989, no. 9, pp. 27–35.

Stratigraphy and Geological Correlation, Vol. 6, No. 4, 1998, pp. 368–382. Translated from Stratigrafiya. Geologicheskaya Korrelyatsiya, Vol. 6, No. 4, 1998, pp. 52–66.
Original Russian Text Copyright © 1998 by Vangengeim, Vislobokova, Sotnikova.
English Translation Copyright © 1998 by MAIK Nauka/Interperiodica Publishing (Russia).

Large Ruscinian Mammalia in the Territory of the Former Soviet Union

E. A. Vangengeim*, I. A. Vislobokova, and M. V. Sotnikova***

** Geological Institute, Russian Academy of Sciences, Pyzhevskii per. 7, Moscow, 109017 Russia*
*** Paleontological Institute, Russian Academy of Sciences, Profsoyuznaya ul. 123, Moscow, 117647 Russia*

Received May 29, 1996; in final form August 21, 1996

Abstract—The presented review of data on large Ruscinian Mammalia from different areas of the former Soviet Union shows that in most localities this fauna correlates with the second half of MN Zone 14 and with MN Zone 15. Single finds in the south of West Siberia are attributed to the initial Ruscinian. The boundary between zones is marked by quantitative changes in proportions of individual forms. A biostratigraphic boundary noticeable in the middle of MN Zone 15 appears to correspond to the lower limit of the Csarnotian in the scheme of M. Kretzoi. The farther to the east, the greater was influence of Asian elements on the fauna evolution in response to continental climatic parameters progressing in this direction.

Key words: *large Mammalia, Ruscinian, biostratigraphy.*

INTRODUCTION

About 80 localities of Ruscinian fauna are known in the territory of the former Soviet Union. In the geographic aspect, they are distributed irregularly: about 60 localities are reported from southern areas of the European part, nearly 20 occur in West Siberia and Kazakhstan, one (the Ol'khon locality) is situated in the south of East Siberia, and another one (the Adycha River) in the extreme northeast of Siberia. Remains of small Mammalia are the main components in most localities, especially in Asian part of the territory, where only a few finds of large Mammalia are known (Fig. 1).

Stratigraphic parameters of these localities are also variable. The early Ruscinian is characterized by fauna (mostly by small mammals) in the south of West Siberia and in northern Kazakhstan. In the European part of the territory, fauna of the initial early Ruscinian is extremely scarce and represented by a few finds in Moldova, where single forms occur in the Stol'nicheny Alluvium resting on the lower Pontian deposits; these forms appear to be characteristic of the Turolian–Ruscinian boundary interval.

In the European part of the territory, many localities characterize the terminal early Ruscinian (Pevzner *et al.*, 1996). Most localities in Ukraine and Moldova occur in two rather thick sedimentary units of alluvial plains, namely in the Kuchurgan and Karboliya alluvial deposits. Remains of small mammals, which are collected from individual beds of both sequences, show that each of the indicated units accumulated in a rather long period of time (Vangengeim *et al.*, 1995). However, remains of large mammals are not related to particular beds and characterize these deposits in general. The Kuchurgan Alluvium ("Gravel") is dated back to the terminal early and middle Kimmerian, or to the upper portion of MN Zone 14 and initial part of MN Zone 15. The Karboliya Alluvium corresponds in age to the late Kimmerian and MN Zone 15. Fauna of the terminal Ruscinian and transitional Ruscinian–Villafranchian period is reported from the well-known locality "Catacombs of Odessa," where it occurs in red beds filling karst cavities in the lower Pontian limestones.

In addition, there are single finds of fauna, whose stratigraphic position on the early Pliocene time scale is unknown. For instance, the precise stratigraphic position is unknown for the famous Kosyakino locality (Stavropol region), which includes some Ruscinian forms and spans the bone-bearing beds ranging in age from the Turolian to Villafranchian. In this work, we use data on those forms from this locality, which can be attributed, though conventionally, to the Ruscinian.

The irregular stratigraphic and geographic distribution of large mammalian fauna is an obstacle for understanding its evolution in a greater part of northern Eurasia during the early Ruscinian. Some aspects of this history can be understood, however, on the basis of data concerning the adjacent regions and earlier stages of the fauna evolution.

It should be also mentioned that we know very little about the early history of large Ruscinian Mammalia in western and central Europe. The oldest Ruscinian localities, which are dated justly, are coeval with early stages of the Zanclean transgression, but there is a considerable time gap between them and late Turolian (Messinian) localities. This gap is most likely responsible for an impression that Turolian and Ruscinian large

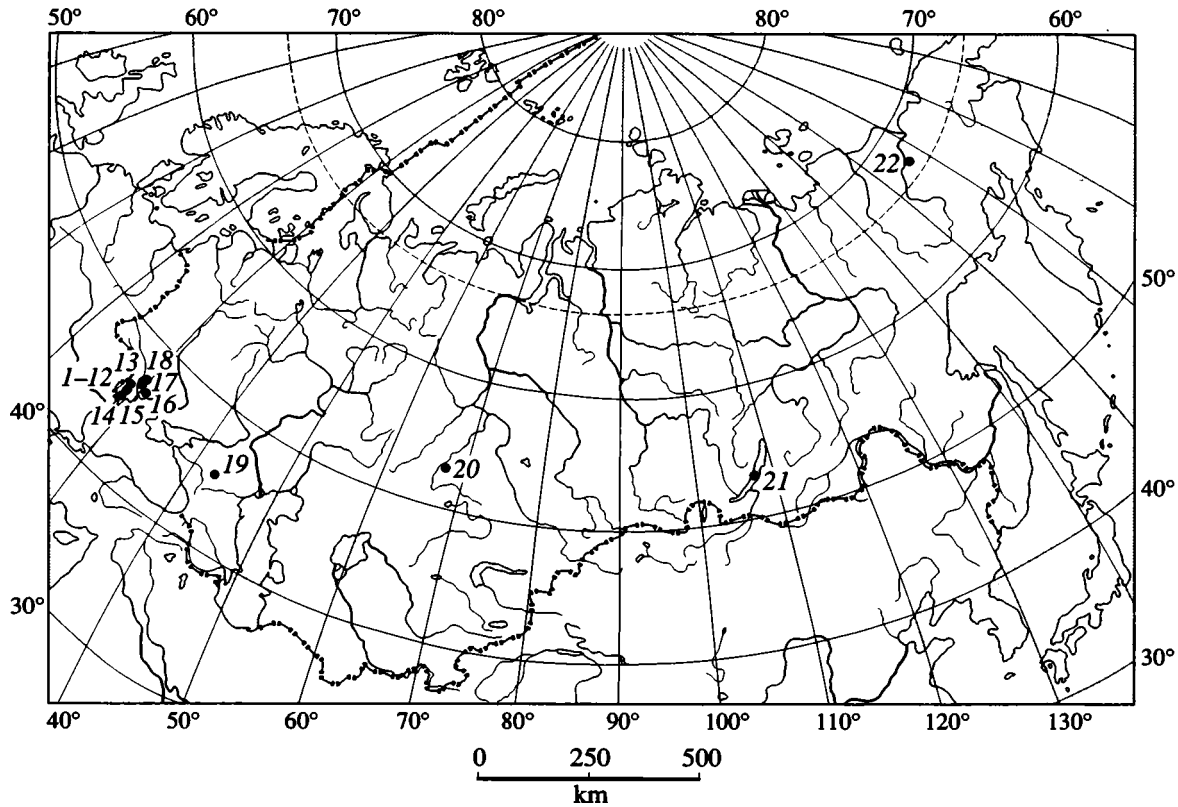

Fig. 1. Main localities of Ruscinian Mammalia in the territory of the former Soviet Union: (*1*) Kagul; (*2*) Moskovei; (*3*) Budei; (*4*) Musait; (*5*) Lucheshty; (*6*) Tatareshty; (*7*) Pilenei-Moldavian; (*8*) Gavanosy; (*9*) Trifoneshty; (*10*) Valeny; (*11*) Fagadyl; (*12*) Khadzhi-Abdul; (*13*) Sagaidak; (*14*) Etuliya; (*15*) Kotlovina; (*16*) Catacombs of Odessa; (*17*) Grebeniki; (*18*) Kuchurgan; (*19*) Kosyakino; (*20*) Biteke; (*21*) Ol'khon; (*22*) Krestovka.

mammals are disunited by an important event in the fauna evolution.

Our objective in this work was to integrate all available data on large mammals from Ruscinian localities in the territory of the former Soviet Union, and to get an insight, if possible, into the evolution of Ruscinian mammal assemblages in the European part of the region, because such assemblages (in a strict sense) are unknown at present in the Asian part. In addition to published data, the used materials include the unpublished results of L.I. Khozatskii about fauna from Bol'shaya Sal'cha and Kagul river basins (kindly submitted to us by L.A. Nesov), and also new results, which we obtained by revising collections stored at the Geological and Paleontological Institutes of Russian Academy of Sciences and at the Odessa State University.

SYSTEMATICS OF LARGE RUSCINIAN MAMMALIA

(see table for list of species from principal localities)

Order Primates

Few remains of Ruscinian primates are known from the northern Black Sea region (southwestern Ukraine and Moldova), where they are correlated in age with the upper part of MN Zone 14 and MN Zone 15. They all belong to family Cercopithecidae.

Remains of *Macaca* sp. were encountered in the Novopetrovka, Voinichevo, and Grebeniki 2 localities. Khomenko (1915) listed this form among species of the "Moldavian Roussillion," but he did not indicate the locality.

Dolichopithecus ruscinensis Dep. is recorded in the Novopetrovka locality, *D.* cf. *ruscinensis* in the Budei locality, and *D.* sp. in the Kotlovina locality (Delson, 1974; Alekseeva, 1977; Tesakov and Mashchenko, 1992). In the lower Karboliya Beds of Romania (Malusteni locality, the boundary between MN zones 14/15), these forms coexist with *"Dolichopithecus"* cf. *arvernensis* Dep. (Delson, 1974).

In central and western Europe, data on primates correlative in age with the lower part of MN Zone 14 are unknown. Reported finds of *Macaca* cf. *sylvana* L., *Mesopithecus monspessulanus* Gerv., and *Dolichopithecus ruscinensis* occur beginning from the second half of the Ruscinian (Delson, 1974).

In Asian part of the territory under consideration, Turolian or Ruscinian primates are undiscovered.

Order Carnivora

Family Canidae

The oldest Ruscinian form *"Canis"* sp.[1] is recovered from the Rytovo Formation section near the town of Pavlodar in Kazakhstan (Pavlodar 2 locality, the lowermost part of MN Zone 14). Fragmentary remains of the same form are discovered from upper Ruscinian deposits of the following localities: the Novaya Andriashevka, Budei, Novaya Karboliya, Lucheshty, and Etuliya in Moldova, and the Ol'khon Island in the Lake Baikal. A small canid from the locality Catacombs of Odessa, which was described as *Vulpes odessana* by Odintsov, should be also attributed to this genus. The same form occurs in the Etuliya and Lucheshty localities.

Outside the former Soviet Union, *"Canis"* remains were recovered from a series of Ruscinian localities of Europe, China (Flynn *et al.*, 1991; Rook, 1993), and Mongolia (localities Khirgiz Noor and Chono-Khariakh).

First representatives of the *"Canis"* group appear in Eurasia at the end of the Turolian (*"Canis" monticinensis,* Rook, 1992). It is likely that in the Ruscinian there was the adaptive radiation of these carnivores. Their distribution area initially spread over Eurasia and then was reduced to central Asian areas (China, Transbaikal region, northern Mongolia, Tajikistan, and Kazakhstan) in the Villafranchian time. The most abundant and diverse *"Canis"* species occur in the Villafranchian deposits of China (Tedford and Qui, in press).

Two other groups of Canidae (genera *Nyctereutes* and *Vulpes*) are known from terminal Ruscinian deposits of the Catacombs of Odessa. *Vulpes* sp. is reported from the Etuliya locality.

Family Ursidae

The Catacombs of Odessa locality of the terminal Ruscinian is known to bear *Agriotherium* sp., the form occurring in both the lower and upper Ruscinian deposits of western Europe (Alberdi, 1974a; Wolsan, 1989). The history of *Agriotherium* can be traced in Eurasia from the Turolian to terminal early Villafranchian time. At the end of the Turolian, representatives of the genus migrated from Eurasia to North America (Tedford *et al.*, 1987) and also to Africa, where a rather primitive *Agriotherium* form, transitional between Miocene and Pliocene species, was found in the Langebaanweg locality (Hendey, 1977).

The remains of *Ursus* ex gr. *minimus* occur in the Catacombs of Odessa deposits of the upper Ruscinian and in the Kosyakino locality, whose precise position inside the Ruscinian interval is unknown. *Ursus* sp. is discovered at the Etuliya locality. In western and central Europe, bears of the genus *Ursus* are known to occur beginning from the mid-Ruscinian time (Erdbrink, 1953).

In Europe, the genus *Ursus* demonstrates a wide adaptive radiation during the Ruscinian, when its species colonized new ecological niches. Accordingly, its early Pliocene forms were very diverse and had a variable dental system characteristic in general to carnovorous ursids. These forms are described as *U. boeki, U. ruscinensis, U. pyrenaicus, U. arvernensis, U. minimus,* and *U. wenzensis*. Baryshnikov (1991) considers them as representatives of the earliest "Tibetoid" stage in the evolution of the genus *Ursus*. In general, the Ruscinian history of the family Ursidae is characterized by considerable taxonomic changes. Typical Turolian genera *Ursavus* and *Indarctos* became extinct in the Miocene–Pliocene boundary period and were replaced by genera *Ursus* and *Agriotherium.*

Family Mustelidae

The remains of *Promephitis* sp. are known from the Etuliya locality of Moldova (MN Zone 15, unpublished data of Khazatskii), and the presence of *P. malustenensis* is recorded in the Malusteni locality of Romania (the boundary between MN zones 14/15, Simionescu, 1930). Information about Ruscinian skunks from Europe is limited only by these two finds, however they were more widespread in Eurasia during the Turolian (late Miocene). *P. alexejewi* Schlosser is a component of the early Ruscinian Ertemte fauna from Asia. Skunks of Turolian and Villafranchian ages occur in a series of Chinese localities (Teilhard and Leroy, 1945; Flynn *et al.*, 1991), but in Mongolia (locality Hirgiz Noor 2) their remains are Ruscinian in age.

Martes sp. and *Mustela* sp. are found in the late Ruscinian localities Etuliya and Catacombs of Odessa. The species of both genera are usual elements of Ruscinian faunas from Europe and Asia.

The late Ruscinian Etuliya locality is also known to contain remains of *Pannonictis pliocaenica* Korm. A similar form was recovered from early Villafranchian deposits of China (the Yushe basin; Teilhard and Leroy, 1945) and Mongolia (Shamar locality, Sotnikova, 1980). In Ukraine, a primitive representative of this carnivore is known from the middle Turolian Cherevichnoe fauna (Yu.A. Semenov, personal communication). In western Europe, a single find of the late Ruscinian *Pannonictes* form is reported from the Wölfersheim locality, but in younger Villafranchian deposits this genus is widespread.

The very small wolverine *Gulo minor* Sotnikova presumably Ruscinian in age is an oldest representative of the genus *Gulo* in Siberia (Adycha River basin, Sotnikova, 1982). Other Ruscinian species of this genus are so far unknown in Eurasia. Wolverines of the next evolutionary stage are present in the early Villafranchian Udunga locality (Transbaikal region). The last representatives of Neogene wolverines, such as *Plesi-*

[1] We use the conventional name *"Canis"* for a series of primitive forms of Canidae from Miocene–Pliocene deposits of North America and Eurasia. At present (Tedford and Qui, in press), they are classed with a new genus.

Fauna of large Ruscinian mammals from the former Soviet Union

Species	Ukraine and Moldova																
	MN 13/14			MN 14						MN 14/15	MN 15						
	Stol'nicheny Alluvium			Kuchurgan Alluvium							Karboliya Alluvium						
	Surik	Sagaidak	Mikhailovka	Novopetrovka	Novaya Andriashevka	Voinichevo	Yurovka	"Kuchurgan Gravel"	Grebeniki-2	Budei	Musait	Novaya Karboliya	Novye Kirgany	Valeny	Gavanosy	Moskovei
Primates																
Macaca sp.				+		+			+							
Dolichopithecus cf. *ruscinensis*				+						+						
Dolichopithcus sp.																
Carnivora																
"Canis" odessanus																
"Canis" sp.					+			+		+		+				
Nyctereutes sp.																
Vulpes praecorsac																
Agriotherium sp.																
Ursus ex gr. *minimus*								+								
Promephitis sp.								+								
Martes sp.																
Mustela sp.								+								
Pannonictis pliocaenicus																
Gulo minor																
Arctomeles ferus																
Pliohyaena perrieri pyrenaica								sp.								
Chasmaporthetes lunensis odessanus																
Machairodus sp.		+														
Megantereion sp.																
Homotherium sp.																
Lynx ex gr. *brevirostris-issiodorensis*								+								
Proboscidea																
Anancus arvernensis															+	
Zygolophodon borsoni								+	+?							
Perissodactyla																
Tapirus cf. *arvernensis*																
Dicerorhinus (=*Stephanorhinus*) *megarhinus*								+								

Table. (Contd.)

Species	Ukraine and Moldova																
	MN 13/14			MN 14						MN 14/15	MN 15						
	Stol'nicheny Alluvium			Kuchurgan Alluvium							Karboliya Alluvium						
	Surik	Sagaidak	Mikhailovka	Novopetrovka	Novaya Andriashevka	Voinichevo	Yurovka	"Kuchurgan Gravel"	Grebeniki-2	Budei	Musait	Novaya Karboliya	Novye Kirgany	Valeny	Gavanosy	Moskovei
Dicerorhinus sp.	+	+	+								+					
Hipparion sp.	+	+	+													
Hipparion cf. *longipes*								+								
H. tchikoicum																
Artiodactyla																
Propotamochoerus provincialis								+					+			
Hippopotamus sp.																
Paracamelus alexejevi											+				+	+
Paracamelus sp.																
Muntiacus pliocaenicus				+												
Eostyloceros pidoplitchkoi				+		+	+									
E. maci																
Paracervulus australis				+										+		
Pliocervus kutchurganicus				+												
P. sp.		+														
Croizetoceros ramosus								+					+			
Cervus warthae													+	+		
C. pardinensis																
C. perrieri																
Procapreols wenzensis																
P. cf. *cusanus*				+												
P. sp.																
Pseudalces mirandus																
Sivatheriinae																
Plioportax ukrainicus				+												
Paleoreas sp.		+														
Gazella borbonica		+														
G. sp.			+	+												
Parabos boodon																
?Ioribos sp.											+					

Table. (Contd.)

Species	Ukraine and Moldova										Northern Caucasus	Siberia				
	MN 15									MN 15		MN 14			MN 15	?
	Karboliya Alluvium															
	Dermenzhi	Lucheshty	Tatareshty	Trifeshty	Khadzhi-Abdul	Trifoneshty	Etuliya	Kotlovina	"Moldavian Roussillion"	Catacombs of Odessa	Kosyakino	Pavlodar-2	Ol'khon	Biteke (Kuskol Formation)	Biteke (Algabas assemblage)	Adycha
Primates																
Macaca sp.									+							
Dolichopithecus cf. *ruscinensis*																
Dolichopithcus sp.								+								
Carnivora																
"Canis" odessanus		+					+			+						
"Canis" sp.												+	+			
Nyctereutes sp.										+						
Vulpes praecorsac							+			+						
Agriotherium sp.										+						
Ursus ex gr. *minimus*		+					sp.			+	+					
Promephitis sp.							+									
Martes sp.							+									
Mustela sp.										+						
Pannonictis pliocaenicus							+									
Gulo minor																+
Arctomeles ferus										+						
Pliohyaena perrieri pyrenaica		+								+						
Chasmaporthetes lunensis odessanus										+						
Machairodus sp.																
Megantereion sp.										+						
Homotherium sp.					+					+						
Lynx ex gr. *brevirostris-issiodorensis*		sp.		+						+	+					
Proboscidea																
Anancus arvernensis		+	+	+			+			+	+					
Zygolophodon borsoni									+							
Perissodactyla																
Tapirus cf. *arvernensis*	+										+					
Dicerorhinus (=*Stephanorhinus*) *megarhinus*											+					
Dicerorhinus sp.							+									

Table. (Contd.)

Species	Ukraine and Moldova										Northern Caucasus	Siberia				
	MN 15									MN 15		MN 14			MN 15	?
	Karboliya Alluvium															
	Dermenzhi	Lucheshty	Tatareshty	Trifeshty	Khadzhi-Abdul	Trifoneshty	Etuliya	Kotlovina	"Moldavian Roussillion"	Catacombs of Odessa	Kosyakino	Pavlodar-2	Ol'khon	Biteke (Kuskol Formation)	Biteke (Algabas assemblage)	Adycha
Hipparion sp.									+	+	+					
Hipparion cf. *longipes*																
H. tchikoicum															+	
Artiodactyla																
Propotamochoerus provincialis		+									+					
Hippopotamus sp.									+							
Paracamelus alexejevi							+		+	+						
Paracamelus sp.														+		
Muntiacus pliocaenicus																
Eostyloceros pidoplitchkoi						+										
E. maci													+			
Paracervulus australis																
Pliocervus kutchurganicus																
P. sp.																
Croizetoceros ramosus		+														
Cervus warthae																
C. pardinensis							?+									
C. perrieri							?+									
Procapreols wenzensis					+											
P. cf. *cusanus*									+							
P. sp.		+	+													
Pseudalces mirandus											+					
Sivatheriinae											+					
Plioportax ukrainicus																
Paleoreas sp.																
Gazella borbonica																
G. sp.			+							+						
Parabos boodon									+							
?Ioribos sp.																

Note: In columns "Kuchurgan Gravel" and "Moldavian Roussillion" we quote data on fauna whose concrete localities have not been indicated.

ogulo monspessulanus Viret and *P. major* Teilh., existed in Europe and China during the Ruscinian (Kurten, 1970; Flynn *et al.*, 1991). The appearance of archaic *Gulo* in northern Eurasia may indicate that this genus originated and initially evolved in the boreal, or even in the subarctic landscape-climatic zone, precisely in Beringia.

Arctomeles (=Parameles) ferus (Roshchin) is described as a component of fauna from the Catacombs of Odessa (Roshchin, 1949). *A. gennevauxi* (Viret), the oldest species of the genus, is recorded at the Montpellier locality (MN Zone 14) of western Europe. Remains of *A. pliocaenicus* Stach occur at the level of MN Zone 15, the Weze locality (Wolsan, 1989), but this genus is unknown in Europe above the Ruscinian beds. *A. suillus* (Teilhard) is listed as a species of the early Ruscinian Ertemte fauna from China (Li *et al.*, 1984). In the early Villafranchian, this genus spread over China, Mongolia, and Transbaikal region. We consider it possible to relate the appearance of *Arctomeles* forms in Europe with a migration wave from southern and southeastern areas of Asia that happened in the first half of the Ruscinian.

Family Hyaenidae

The family is represented only by two forms *Chasmaporthetes lunensis* (Camp.) and *Pliohyaena (=Pachycrocuta) pyrenaica* (Dep.) recovered from the late Ruscinian localities Catacombs of Odessa and Lucheshty. The genus *Chasmaporthetes* includes species of hunting hyenas, whereas hyenas proper belong to genus *Pliohyaena* known since the Ruscinian time. The first group dominated in *Hipparion* faunas of Eurasia up to the end of the Turolian. In the Ruscinian, an abundance of both groups was close to the balance, and real hyena-like forms prevailed since the early Pleistocene. Hyaenidae thrived in the Turolian, and the generic composition of the family was completely changed at the Turolian–Ruscinian boundary (or at the beginning of the Ruscinian), when all ancient genera except two became extinct. The latter two genera are *Chasmaporthetes* that existed till the end of the Villafranchian (Werdelin and Solounias, 1991) and *Thalassictis* that survived up to the end of Ruscinian in China (Flynn *et al.*, 1991). The former diversity of Hyaenidae considerably decreased in the Ruscinian and Villafranchian presumably because of a wide adaptive radiation of Canidae. Remains of *Chasmaporthetes* (= *Hyaena*) *borissiaki*, which have been described by Khomenko in the composition of the Moldavian Roussillion, are likely recovered from older (Pontian) deposits (Sotnikova, 1994).

Family Felidae

Subfamily Machairodontinae. Transitional Turolian–Ruscinian beds of the Sagaidak locality in Moldova yielded remains of *Machairodus* sp., *Homotherium* sp., and *Megantereon* sp., all known from the uppermost Ruscinian deposits (localities Catacombs of Odessa and Khadzhi-Abdul). They are more archaic in characteristic features than the Villafranchian forms. Subfamily Machairodontine is present in many Ruscinian localities of Europe and Asia. However, it is difficult to classify its forms at the genus level because the remains are fragmentary. In Eurasia, the subfamily seems to be autochthonous. Beuamont (1975) has suggested that the late Miocene dirk-tooth *Paramachairodus* and sabre-tooth *Machairodus* genera may represent the primitive sister taxa of the Pliocene genera *Megantereon* and *Homotherium.* The assumed North American origin of *Megantereon* can be hardly accepted at present as valid (Turner, 1987). Unfortunately, the available data do not elucidate when the Miocene grouping of *Paramachairodus* and *Machairodus* was replaced by the Pliocene *Megantereon–Homotherium* assemblage, and what happened to the subfamily Machairodoninae in the Ruscinian. In both Europe and Asia, all known finds from the uppermost Miocene (Turolian) deposits represent genus *Machairodus. Megantereon* and *Homotherium*, forms that are confidently defined in Asia, Africa, central and western Europe are known to occur beginning from the early Villafranchian.

Subfamily Felinae. This taxon is represented by most usual Ruscinian form *Lynx* ex gr. *brevirostris-issiodorensis.* It has been reported as occurring in the Kuchurgan Gravel, in Kosyakino (Vereshchagin, 1959; Korotkevich, 1988), and Catacombs of Odessa localities, and in a series of late Ruscinian sites of Moldova. The Ruscinian is the first occurrence level of genus *Lynx.*

Order Proboscidea

In central and western Europe, proboscideans are represented by two forms: *Zygolophodon borsoni* (Hays) and *Anancus arvernensis* (Cr. et Job.). Stratigraphic position of their remains within the Ruscinian interval is unrestrained. The remains are dated, at best, back to the Kimmerian. Some of the *Z. borsoni* remains are correlative in age with the second half of MN Zone 14 (localities Novopetrovka and Grebeniki 2), but one is recorded in MN Zone 15 (the Kagul region). Rather abundant remains of *Anancus arvernensis* occur in the upper Ruscinian beds. It appears that population of *Zygolophodon* forms decreased by the late Ruscinian (Godina and David, 1973; Alekseeva, 1977; Dubrovo and Kapelist, 1979). *Z. borsoni* existed in Europe until the middle early Villafranchian, and *A. arvernensis* presumably became extinct at the end of this stage.

Some published data about the early Pliocene occurrences of *Deinotherium* remains seem erroneous, since either stratigraphic inferences are incorrect, or the remains are redeposited from older beds.

In Asian part of the territory in question, remains of Ruscinian mastodonts are unknown, but *Zygolophodon borsoni* fauna and forms resembling *Anancus arvern-*

ensis are reported from China (Tobien, 1978). Based on data about possible migration of zygodont mastodonts through Beringia into North America (Tobien, 1976), we assume that their remains may be also discovered in northern Asia.

Order Perissodactyla

Family Tapiridae

In the published literature, there is reference to two finds of *Tapirus* cf. *arvernensis* Cr. et Job. from the Ruscinian deposits in European part of the former Soviet Union, namely from the Kosyakino locality of northern Caucasus and from the Kuchurgan Gravel of Ukraine, although in the last case the particular locality has not been indicated (Vereshchagin, 1959; Korotkevich, 1988). Tapirid remains are also known in the Malusteni locality of Romania that is coeval to the lower part of the Karboliya Alluvium (Samson and Radulesco, 1973). These data indicate that tapirs formerly occurred, though rarely, in eastern Europe, where their remains are confined to the later interval of MN Zone 14 and initial interval of MN Zone 15. In the pre-Ruscinian or younger faunas of this region, tapirid bones are unknown. In western and central Europe, Ruscinian tapirs were more usual and survived until the early–middle Villafranchian (Guerin and Eisenmann, 1982). The oldest Ruscinian remains of tapirs seem to be recovered from the Hauterives locality in southern France that is attributed to the early Zanclean (Guerin and Mein, 1971). Apparently, the northern Black Sea region represented a marginal zone of distribution area of European tapirs. More arid landscape-climatic conditions prevented their migration further to the east.

Family Rhinocerotidae

Remains of Ruscinian rhinocerotids are quite rare in the former Soviet Union. They generally belong to genus *Dicerorhinus*. Their identification at the species level is usually impossible because of the fragmentary state of remains. In some localities only, there was detected *D. megarhinus* (De Christol), a characteristic form of the Ruscinian faunas from Europe.

Family Equidae

This family is represented by genus *Hipparion* s.l., whose remains are rare, fragmentary, and hardly identifiable at the species level. Korotkevich (1967) reported remains of a rather large and well-proportioned hipparion with underdeveloped lateral dactyls in the unnamed locality of the Kuchurgan Alluvium. In size and structure of its metapodia, this form resembles to a certain extent the late Turolian *Hipparion longipes* W. Grom. from the Pavlodar locality of Kazakhstan. Some fragmentary remains unidentifiable at the species level are known in several Ruscinian localities. In opinion of Alberdi (1989), who has studied this material, the remains can be attributed to her Morphotype 5 characteristic of late Ruscinian localities La Galera, Villalba Alta, and Layna.

As stated by Gabuniya (1959, p. 120), remains of a large *Hipparion* from the Kosyakino locality display "a combination of highly specialized and archaic morphological features." This form is cited in the literature under different names: *H.* sp.; *H. stavropolense* Macarovici; and *H. malustenense* Rad. et Samson. According to Zhegallo (1978), the Kosyakino hipparion is a transitional form from the *H. sefvei–H. crassum* lineage. Remains of a very graceful medium-sized hipparion (metapodium bones, first phalanx, and fragments of pelvis bone) from the Catacombs of Odessa are still undescribed.

In western and central Europe, remains of the early Ruscinian *Hipparion* fauna are also rare and fragmentary. They are more abundant here in the late Ruscinian localities. In the East Mediterranean (Greece and Turkey), there are known at least two species: the massive and large *Hipparion crassum* Gervais and similar graceful hipparion close to *H. longipes* (van der Meulen and van Kolfschoten, 1986; Eisenmann and Sondaar, 1989). It is likely that there was another coeval form originally described as *H. crassum* (the Ptolemais locality), but Eisenmann and Sondaar consider it as different from the type species. In the West Mediterranean (the Teruel basin of Spain), there are known remains of three hipparions: *H. fissurae* Crus. et Sond. well-proportioned and medium in size, and two other forms still lacking description (Alberdi and Alcala, 1989–1990).

H. crassum and similar forms (*H. malustenense* Rad. et Sams.) are recorded in southern France, Hungary, and the Malusteni locality of Romania (Guerin and Mein, 1971; Eisenmann and Sondaar, 1989). Eisenmann and Sondaar consider *H. crassum* as a typical late Ruscinian form and doubt its presence in the early Ruscinian Alcoy locality of Spain (Alberdi, 1974b).

The late Ruscinian fauna from Asian regions (the Algabas assemblage after Zazhigin and Zykin, 1984) includes a peculiar species *H. tchikoicum* Ivan. This form displaying several archaic features, such as brachydont dental system and well-developed lateral dactyls, was widespread together with *H. houfenense* Teilh. et Young in the early Villafranchian faunas of central Asia (Transbaikal region and northern Mongolia; Zhegallo, 1978). Forsten (1992) also detected *H. tchikoicum* in several localities of China. According to her data, this species appeared in China in the second half of the Ruscinian and was a component of the earliest Villafranchian faunas. In opinion of Zhegallo (1978), *H. tchikoicum* is a species of the Asian lineage *H. thleobaldi–H. sefvei*. *H. crassum* is considered to be a form related with *H. sefvei* and *H. tchikoicum*, and we assume that this species appeared in the mid-Ruscinian faunas of Europe as a result of the first Pliocene migration from Asia. Afterward, the early Villafranchian

migration wave resulted in geographic expansion of *Hipparion houfenense* and closely related *H. crusafonti-rocinantis*.

Order Artiodactyla

Suborder Suiformes

Family Suidae

Representatives of Ruscinian Suidae are known in the northern Caucasus and northern Black Sea region. *Propotamochoerus provincialis* Gerv. is recorded in the Kosyakino fauna (Vereshchagin, 1959) and also in the Kuchurgan Alluvium (Korotkevich, 1988) and localities Lucheshty and Novye Kirgany of the Moldavian Roussillion (Alekseeva, 1977). The same species occurs in the Malusteni locality of Romania correlative with the Karboliya Beds (Simionescu, 1930).

In southwestern and southeastern Europe, remains of Ruscinian *P. provincialis* are more frequent and confined to stratigraphic interval ranging from MN Zone 13 to MN Zone 15 (Made, 1989–1990). Accordingly, the distribution area of the species extended during the Ruscinian from Spain to the northern Caucasus. The youngest remains of *P. provincialis* are recovered from the lower Villafranchian deposits of the Transcaucasia (Vekua, 1972) and Slovakia (Fejfar, 1964). In western Europe, genus *Propotamochoerus* coexisted with widespread *Sus* representatives.

Family Hippopotamidae

A single find of *Hippopotamus* sp. representing the family in Moldova has been listed by Khomenko (1915) as an element of the Moldavian Roussillion (MN Zone 15). The first occurrence of the genus in Europe is recorded in MN Zone 13. Mediterranean faunas include the widespread species *Hippopotamus crusafonti* (Faur and Meon, 1984). Villafranchian hippopotamids were more diverse and populated Europe, India, and Africa.

Suborder Tylopoda

Family Camelidae

In the northern Black Sea region, *Paracamelus alexejevi* Havesson is the dominant form of late Ruscinian Camelidae. Its abundant remains (hundreds of individuals) are recovered from the locality Catacombs of Odessa. The same or very close form is also known from the late Ruscinian Musait, Moskovei, Lucheshty, Etuliya, Gavanosy, and Kagul localities of Moldova (Godina and David, 1973; Alekseeva, 1977).

In western Siberia, the oldest remains of *Paracamelus* sp. occur in the Kuskol Formation near the Biteke River (Ishym River basin) and are dated back to the earliest Ruscinian (Zykin *et al.*, 1991). In China, the oldest *Paracamelus* form from the Gaozhuang fauna is of the middle Ruscinian age (Flynn *et al.*, 1991).

The first wave of camelid migration in Eurasia from North America took place at the terminal Miocene time (Turolian). In the northern Black Sea region, their remains are buried in the lower Pontian limestones (Alekseeva, 1977). During this period, they migrated further to the west up to Spain (Morales *et al.*, 1980). In the post-Ruscinian time, camels were quite usual members of mammal communities in Kazakhstan, southwestern Siberia, southern areas of the East European plain, and northern Caucasus. The genus existed until the end of the early Pleistocene (Alekseeva, 1977).

Suborder Ruminantia

Family Cervidae

In the territory of the former Soviet Union, Ruscinian Cervidae were very diverse. The family included at least 12 species from eight genera and four subfamilies.

Subfamily Muntiacinae. In the former Soviet Union, all representatives of the subfamily do not cross limits of the Ruscinian. Radiation of genera *Muntiacus* and *Paracervulus* commenced at the beginning of the Ruscinian. The first genus is represented by an endemic species *M. pliocaenicus* Korotkevich whose remains are reported from the Novopetrovka locality (MN Zone 14) of Ukraine (Korotkevich, 1988). This and other localities corresponding to this zone (Yurovka and Voinichevo) also yielded muntjak remains of the genus *Eostyloceros* classed with the endemic species *E. pidoplitchkoi* Korotkevich. The same species is recorded in the late Ruscinian locality Trifoneshty of Moldova (Korotkevich, 1988). *E. maci* Vislobokova is discovered from the Ruscinian horizon of the Ol'khon Island of the Lake Baikal. *E. blainvillei* Zdansky from the Paote fauna of China is a progenitor of all these species.

During the late Ruscinian, *Paracervulus australis* (Serres) (= *Cervus ruscinensis* Dep., = *Capreolus ruscinensis* Dep.) inhabited the south of Ukraine (localities of the Kuchurgan Alluvium), Moldova (Valeny locality) and Romania (Simionescu, 1930; Korotkevich, 1988). During the Ruscinian, this form was also quite widespread in central and western Europe.

Subfamily Cervinae. Its genus *Pliocervus* is represented by *P. kutchurganicus* Korotkevich from the Novopetrovka and adjacent localities corresponding to MN Zone 14 (Korotkevich, 1988). *Pliocervus* sp. is a component of fauna from the Sagaidak locality of the Stol'nicheny Alluvium (the initial Ruscinian or Turolian–Ruscinian boundary). In Europe, the stratigraphic distribution of *Pliocervus* forms spans a considerable time interval from MN Zone 11 to MN Zone 16.

Croizetoceros ramosus (Croizet et Jobert) is present in late Ruscinian localities (Korotkevich, 1988). Its stratigraphic range in Europe corresponds to the Ruscinian–early Villafranchian interval (range of MN zones 14–16). Remains of a deer similar to *Cervus (Rusa) warthae* Czyzewska occur only in the late Ruscinian localities of Moldova (Valeny and Novye Kir-

gany). In central Europe, the stratigraphic range of *C. warthae* is limited by MN Zone 15. Appearance of *Croizetoceros* and *Cervus* genera in Europe seems to be related to the adaptive radiation of cervines at the Turolian–Ruscinian boundary time, or at the very beginning of the Ruscinian.

Particularly important is the Etuliya locality bearing remains of deer species *Cervus pardinensis* (Cr. et Job.) and closely related *C. perrieri* (Cr. et Job.). *C. pardinensis* is known to occur in Europe from the initial Ruscinian (Gdl locality) up to the lower Villafranchian. *C. perrieri* is known only from the lower Villafranchian deposits. At the same time, remains of both forms are buried in the uppermost horizon of deposits referred to the Moldavian Roussillion, and two versions of data interpretation appear to be possible. (1) The Etuliya locality is situated to the south of the Bol'shaya Sal'cha River valley, where most Ruscinian mammals are discovered. The observed geological relations show that the Karboliya (late Ruscinian) Beds are overlain by sequentially younger members of the alluvial plain deposits accumulated in the region up to the middle of the late Pliocene, the initial period of formation of recent river valleys, and stratigraphic members of these deposits become younger in the southerly direction. The oldest river terrace in the southern Moldova yielded fauna of the middle Villafranchian mammals. Consequently, the Etuliya section may include the lower Villafranchian beds of the alluvial plain. In this case, the deer fauna in question is the early Villafranchian in age. (2) If deposits bearing remains of *C. pardinensis* and *C.* cf. *perrieri* represent the Karboliya Beds proper, then we must admit that *C. perrieri* appeared in Europe earlier that it was formerly suggested.

Subfamily Odocoileinae. In Moldova, its species *Procapreolus wenzensis* (Czyzewska) has been recovered from the Khadzhi-Abdul locality, and the same species is known from the Weze 1 locality (MN Zone 15) of Poland. This form appears to be a descendant of the late Miocene species *P. florovi* Korotkevich. It shows phylogenetic relations with *Capreolus constantini* Visl. et Kalm. from the lower Villafranchian beds of the Transbaikal region and may represent the direct ancestor of genus *Capreolus*. *Procapreolus* cf. *cusanus* is described from the Novopetrovka locality, and according to Khomenko (1915) it is a component of the Moldavian Roussillion fauna from the Bol'shaya Sal'cha and Kagul river valleys. *P. cusanus* was widespread in the Villafranchian faunas of Europe. *Procapreolus* sp. (= *Cervus moldavicus* Janovskaya) is detected in localities Fagadyl, Lucheshty, and Tatareshty (MN Zone 15) of Moldova.

Subfamily Alcinae. This subfamily is represented only by *Pseudalces mirandus* Flerov from the Kosyakino fauna of northern Caucasus. The species belongs to an indirect evolutionary line of the group. The data available suggest that representatives of the subfamily migrated into Eurasia from North America at the very end of Miocene, i.e., about 6 Ma ago (Vislobokova, 1990).

Family Giraffidae

A form from the subfamily Sivatheriinae is detected at the Kosyakino locality. In the territory under consideration, Sivatheriinae appeared since the Vallesian time. The latest remains of *Sivatherium* sp. have been recognized in the middle Villafranchian deposits of Tajikistan.

Family Bovidae

The Boselaphini tribe of the family is represented by *Plioportax ukrainicus* Korotkevich from the Novopetrovka locality (Korotkevich, 1988).

Palaeoreas sp. has been detected by E.L. Dmitrieva in the Stol'nicheny Alluvium of the Sagaidak locality (boundary between MN zones 13/14). This genus is widespread in the Turolian faunas of the East Mediterranean. Its remains from Moldova seem to be youngest in geological aspect. Few remains of *Gazella* sp. are known from several late Ruscinian localities. *Gazella borbonica* Dep. was recovered together with *Palaeoreas* bones identified by Dmitrieva from the Stol'nicheny Alluvium of the Sagaidak locality. In Europe, this genus is known as spanning the stratigraphic range of MN Zone 15 to the middle Villafranchian inclusive. Its remains from Moldova seem to be the oldest among all others known in Europe. According to Khomenko (1915), *Parabos boodon* (Christol) from the Moldavian Roussillion fauna inhabited an area from the Atlantic coast to the northern Black Sea region, where it replaced the late Turolian *P. cordieri* (Gerv.).

The late Ruscinian Musait locality of Moldova yielded remains of ? *Joribos* sp. (Godina and David, 1973). Representatives of this genus are also known from the lower Villafranchian deposits of Georgia (Vekua, 1972).

GENERAL CHARACTERISTICS OF RUSCINIAN MAMMAL ASSEMBLAGES FROM EUROPEAN PART OF THE FORMER SOVIET UNION

A comparison between Ruscinian mammal assemblages from European part of the former Soviet Union and central to western Europe shows that they are rather similar in general composition. However, as evident from the occurrence frequency, the quantitative proportions between some groups of animals were different. For instance, monkeys from genus *Dolichopithecus*, tapirs, Suidae, and *Parabos* forms used to be frequent members of Ruscinian mammal communities in the west, whereas their remains are extremely rare in the east. Hippopotamids that existed in the Mediterranean region since the terminal Turolian are represented in the east by a single find. In contrast, the northern Black Sea region was a habitat area of plentiful muntjaks whose

Fig. 2. Stratigraphic position of reference localities of large Ruscinian mammals.

remains are abundant. This group was represented by three genera, whereas only one species *Paracervulus australis* is known in central and western Europe.

Apparently, eastern Europe represented a marginal zone of the distribution area of European genera *Dolichopithecus, Tapirus, Propotamochoerus,* and *Parabos,* and deers from genus *Pliocervus* migrated to this zone at the end of the Turolian. Another peculiar feature of Ruscinian faunas from eastern Europe is manifested in presence of endemic species, such as muntjaks *Muntiacus pliocaenicus* and *Eostyloceros pidoplitchkoi,* and also *Plioportax ukrainicus.* It is similarly remarkable that camels abundant in the eastern region did not migrated to the west during the Ruscinian–Villafranchian. Genera *Muntiacus, Eostyloceros,* and *Paracamelus* are immigrants from eastern and central Asia, whereas *Arctomeles, Plioportax,* and presumably *Pannonictis* may be originated in southern or southeastern Asia.

Some western taxa, such as Viverridae, *Metailurus,* and *Plesiogulo* are unknown in the eastern region. However at present, this cannot be interpreted as a distinctive feature of this area, because we know here only few rich burials and may suspect that paleontological records are incompletely revealed.

Thus, the considered data suggest that the Ruscinian fauna of eastern Europe was formed on the basis of West European population of mammals (in a broad sense), but it also included a considerable number of Asian elements. The outlined difference between East and West European faunas was apparently controlled by environmental changes toward the more continental type of climate in the easterly direction, and, consequently, by progressively growing influence of Asian fauna. A comparison between Ruscinian and older Turolian faunas of eastern Europe shows that the later period is characterized by the decreased abundance and lower diversity of *Hipparion* forms, giraffes, and antelopes, and by parallel diversification of large progressive muntjaks and small real deers. The same changes were characteristic of West European faunas, and this indicates that the Ruscinian climate was more humid than in the terminal Turolian time.

When compared with Ruscinian assemblages, the Villafranchian faunas of eastern Europe demonstrate that muntjaks and small deers were replaced by larger real deers from genera *Axis, Arvernoceros,* and *Eucladoceras.* Simultaneously, roe deers of genus *Procapreolus* were replaced by *Capreolus* species. In contrast to Villafranchian faunas of western Europe, tapirs and hippopotamids were missing in the eastern region.

As for the Ruscinian mammals from Asian regions of the former Soviet Union, the available information about them is limited and implies that this fauna included *"Canis"* forms widespread in Eurasia and

representatives of typical Asian taxa *Eostyloceros, Hipparion tchikoicum,* and *Paracamelus.*

When European and Asian faunas are compared as a whole, it becomes evident that many Ruscinian mammals existed for a longer period in China and Mongolia than in Europe. First of all, this was characteristic of small carnivores from family Viverridae (genera *Metailurus, Promephitis*, and *Agriotherium*). Small *"Canis"* forms and *Hipparion* species remained rather widespread even in the Villafranchian time. In Europe, their remains in the Villafranchian deposits are very scarce, whereas in central Asia they appear to be the main and dominant taxa in the early Villafranchian faunas. These data suggest that climatic changes throughout the Pliocene period were not as considerable in central Asia as in Europe.

As shown recently (Pevzner *et al.*, 1996), the Ruscinian mammal faunas from European part of the former Soviet Union (mainly from the northern Black Sea region) are correlative with two units of the continental stratigraphic scheme by P. Mein: with an upper part of MN Zone 14 and MN Zone 15. This correlation is based on data about the taxonomic composition and evolutionary level of small mammals, and also on geological and magnetostratigraphic observations. The boundary between zones is at the level of the Kochiti event inside the Gilbert Chron (Fig. 2).

With respect to taxonomic composition of large mammals, there is no principal difference between these zones. Nevertheless, like in the fauna of rodents, there are certain changes in proportions of some Mammalia taxa at the lower boundary of MN Zone 15. These changes are as follows: abundance of muntjaks sharply decreases; *Zygolophodon borsoni* becomes less widespread; frequency of *Anancus arvernensis* occurrences grows; and camels appear once again after the Pontian time. As for small mammals, ochotonids dominant in the Ruscinian become replaced by voles.

All these events were apparently related to changes in climatic environments and landscapes at the boundary between early and late Ruscinian, when obviously humid climate of the initial period was converted then into more arid.

Inside the late Ruscinian, there is a noticeable biostratigraphic boundary presumably corresponding to the lower limit of Csarnotian in the scheme of M. Kretzoi. Above this boundary, deers enter a new phase of adaptive radiation and get a higher degree of diversity. At the same time, their new forms (*Cervus (Rusa)* cf. *warthae*, ? *C. pardinensis,* and *Procapreolus wenzensis*) migrated to the east from western Europe. The boundary is also marked by appearance of genera *Pliomys* and *Dolomys* in the vole fauna. Finally, the very end of the Ruscinian (locality Catacombs of Odessa corresponding to the terminal interval of Gilbert Chron) is the first occurrence level of two machairodontine genera *Megantereon* and *Homotherium,* which evolved further in the Villafranchian time. In other regions of Eurasia, these genera do not occur before the Villafranchian, and it is still unclear whether they are immigrants or autochthonous in origin. As it follows from data available at present, the transition from Ruscinian to Villafranchian faunas was very gradual.

ACKNOWLEDGMENTS

This work was supported by the International Science Foundation (grant nos. MQD 000 and MQD 300).

Reviewer M.A. Akhmet'ev

REFERENCES

Alberdi, M.T., Las *"faunas de Hipparion"* de los yacimientos espanoles, *Estud. Geol.*, 1974a, vol. 30, pp. 189–212.

Alberdi, M.T., El genero *Hipparion* en Espana, *Trab. sobre. Neogeno–Quatern.*, 1974b, vol. 1, pp. 1–146.

Alberdi, M.T. and Alcala, L., El genero *Hipparion* en la fosa de Alfambra–Teruel, *Paleontol. Evol.*, 1989–1990, vol. 23, pp. 105–109.

Alekseeva, L.I., *Teriofauna rannego antropogena Vostochnoi Evropy* (Early Anthropogene Teriofauna of Eastern Europe), Moscow: Nauka, 1977.

Baryshnikov, G.F., *Ursus mediterraneus v pleistotsene Kavkaza i zamechaniya po istorii melkikh medvedei Evrazii* (*Ursus mediterraneus* of the Pleistocene from the Caucasus and Comments on History of Small Ursids in Eurasia), Moscow: Nauka, 1991.

Beaumont, G., Recherches sur les Follides (Mammiferes, Carnivores) du Pliocene inférieur des sables à *Dinotherium* des environs d'Eppelsheim (Rheinhessen), *Arch. Sci.*, 1975, vol. 28, pp. 369–404.

Delson, E., Preliminary Review of Cercopithecid Distribution in the Circum Mediterranean Region, *V Congress du Néogéne Méditerranéen, Mem. BRGM*, 1974, vol. 1, no. 78, pp. 131–135.

Dubrovo, I.A. and Kapelist, K.V., *Katalog mestonakhozhdenii tretichnykh pozvonochnykh USSR* (Catalogue of Tertiary Vertebrate Localities in the Ukrainian SSR), Moscow: Nauka, 1979.

Eisenmann, V. and Sondaar, P., *Hipparion* and the Mio–Pliocene Boundary, *Boll. Soc. Paleontol. Ital.*, 1989, vol. 28, nos. 2–3, pp. 217–226.

Erdbrink, D.P., *A Review of Fossil and Recent Bears of the Old World,* Deventer: Jan de Lange, 1953, vol. 1.

Faur, M. and Meon, H., *L'Hippopotamus crusafonti* de la Mosson (press Montpellier). Premiere reconnaissance d'un Hippopotame neogene en France, *C. R. Acad. Sci. France,* 1984, vol. 298, no. 3, pp. 93–98.

Feifar, O., The Lower Villafranchian Vertebrates from Hajnachka near Fialkovo in Southern Slovakia, *Rozpr. Praha Svazck.*, 1964, vol. 30, pp. 1–115.

Flynn, L.J., Tedford, R.H., and Qiu, Z., Enrichment and Stability in the Pliocene Mammalian Fauna of North China, *Paleobiol.*, 1991, vol. 17, no. 3, pp. 246–265.

Forsten, A., *Hipparion tchicoicum* Ivanjev une forme particulière d'Equidae tridactyle Pliocéne d'Asie, *Geobios,* 1992, vol. 25, pp. 161–173.

Gabuniya, L.K., *K istorii gipparionov* (On History of *Hipparion*), Moscow: Akad. Nauk SSSR, 1959.

Godina, A.Ya. and David, A.I., *Neogenovye mestonakhozhdeniya pozvonochnykh na territorii Moldavskoi SSR* (Neogene Vertebrate Localities in the Moldavian SSR), Kishinev: Shtiintsa, 1973.

Guerin, C. and Eisenmann, V., Repartition stratigraphique des tapirs (Mammalia, Perissodactyla) dans le Néogéne et le Quaternaire d'Europe occidentale, *9 Reunion Annuelle des sciences de la terre*, Paris, 1982, p. 298.

Guerin, C. and Mein, P., Les principaux gisements de mammiferes miocenes et pliocenes de domaine Rhodanien, *Docum. Lab. Geol. Univ. Lyon, H. S.,* 1971, pp. 131–170.

Hendey, Q.B., Fossil Bear from South Africa, *South. Afr. J. Sci.,* 1977, vol. 73, pp. 112–116.

Khomenko, I.N., The Roussillion Stage of the Middle Pliocene in Bessarabia and Its Significance for Understanding Geochronology of Balta Sand and Kuyalnitskii Deposits, *Tr. Bessarab. O-va Estestvoispyt.,* 1915, vol. 6, pp. 1–28.

Korotkevich, E.L., Fauna of Large Mammals from Pliocene Deposits of the Kuchurgan River Valley, in *Mesto i znachenie iskopaemykh mlekopitayushchikh Moldavii v kainozoe SSSR* (Position and Significance of Fossil Mammals in the Cenozoic of the USSR), Kishinev: Akad. Nauk. Mold. SSR, 1967, pp. 77–84.

Korotkevich, E.L., *Istoriya formirovaniya gipparionovoi fauny Vostochnoi Evropy* (Formation History of *Hipparion* Fauna in Eastern Europe), Kiev: Naukova Dumka, 1988.

Kurten, B., The Neogene Wolwerine *Plesiogulo* and the Origin of *Gulo* (Carnivora, Mammalia), *Acta Zool. Fennica,* 1970, vol. 131, pp. 1–22.

Li, C., Wu, W., and Qui, Z., Chinese Neogene: Subdivision and Correlation, *Vertebr. Palasiat.*, 1984, vol. 22, no. 3, pp. 1–178.

Made, J.V.D., A Range-Chart for European Siudae and Tayassuidae, *Palaeontol. Evol.*, 1989–1990, vol. 23, pp. 99–104.

Meulen van der, A.J. and Kolfschoten von, T., Review of the Late Turolian to Early Biharian Mammal Faunas from Greece and Turkey, *Mem. Soc. Geol. Ital.,* 1986, no. 31, pp. 201–211.

Morales, J., Soria, D., and Aguirre, E., Camelido finimioceno en Venta del Moro, primera cita para Europa occidental, *Estud. Geol.,* 1980, vol. 36, pp. 139–142.

Odintsov, I.A., *Volpes odessana* sp. nov.: A New Species of Pliocene Carnivore from Karst Caves of Odessa, *Paleontol. Sborn. Lvov. Univ.*, 1967, no. 4/1, pp. 130–137.

Pevzner, M.A., Vangengeim, E.A., Vislobokova, I.A., Sotnikova, M.V., and Tesakov, A.S., Ruscinian of the Territory of the Former Soviet Union, *Newslett. Strat.,* 1996, vol. 33, no. 2, pp. 77–97.

Rook, L., *"Canis" monticiensis* sp. nov., a New Canidae (Carnivora, Mammalia) from the Late Messinian of Italy, *Boll. Soc. Paleontol. Ital.,* 1992, vol. 31, pp. 151–156.

Rook, L., I cani dell Eurasia dal Miocene Superiore al Pleistocene Medio, *Doctoral Thesis,* Roma: La Sapienza Univ., 1993, p. 154.

Roshchin, A.D., A New Genus of Fossil Mustelidae from Pliocene Deposits near Odessa, *Tr. Odess. Univ.,* 1949, vol. 1, pp. 97–110.

Samson, P. and Radulescu, C., Les faunes des mammiferes et la limite Pliocene–Pleistocene en Roumanie, *Trav. Inst. Speol.,* 1973, vol. 12, pp. 191–228.

Simionescu, I., Vertebratele Pliocene de la Malusteni (Covurlui), *A. R. Publ. Adamachi*, 1930, vol. 9, no. 49, pp. 84–148.

Sotnikova, M.V., Late Pliocene Mustelidae from the Shamar Locality (Mongolian Peoples Republic), *Byull. Komiss. Izuch. Chetvertich. Perioda Akad. Nauk SSSR,* 1980, no. 50, pp. 138–145.

Sotnikova, M.V., On History of Genus *Gulo* in Eurasia, *Tr. Zool. Inst. Akad. Nauk SSSR,* 1982, vol. 3, pp. 138–145

Sotnikova, M.V., Genus *Chasmaporthetes* Hay, 1921, from Pliocene Deposits of Russia, Ukraine, Mongolia, and Tajikistan, *Paleoteriologiya* (Paleoteriology), Tatarinov, L.P., Ed., Moscow: Nauka, 1994, pp. 113–139.

Tedford, R.H. and Qui, Z., A New Canid Genus from the Pliocene of Yushe, Shanxi Province (in press).

Tedford, R.H., Skinner, M.E., Fields, R.W., *et al.,* Faunal Succession and Biochronology of the Arikareen through Hemphillian Interval (Late Oligocene through Earliest Pliocene Epochs in North America), *Cenozoic Mammals of North America: Geochronology and Biostratigraphy,* Woodburne, M.D., Ed., Berkeley: Univ. of California, 1987, pp. 153–210.

Teilhard de Chardin, P. and Leroy, P., Les Mustelides de Chine, *Publ. Inst. Geobiol. Peking*, 1945, no. 12, pp. 1–56.

Tesakov, A.S. and Mashchenko, E.N., The First Confident Find of *Macaca* Remains (Cercopthecodae, Primates) in Pliocene Deposits of Ukraine, *Paleontol. Zh.,* 1992, no. 4, pp. 47–52.

Tobien, H., Migration of Proboscideans and Lagomorphs through the Beringia Land during Cenozoic, *Beringiya v kainozoe* (Beringia of Cenozoic Time), Kontrimavichus, V.L., Ed., Vladivostok: Dal'nevost. Tsentr Akad. Nauk SSSR, 1976, pp. 249–262.

Tobien, H., On the Evolution of Mastodonts (Proboscidea, Mammalia), Part 2, *Geol. Jahrb.,* 1978, vol. 106, pp. 159–208.

Turner, A., *Meganterion cultridens* (Cuvier) (Mammalia, Felidae, Machairodontinae) from Plio-Pleistocene Deposits in Africa and Eurasia, with Comments on Dispersal and the Possibility of a New World Origin, *J. Paleontol.,* 1987, vol. 61, no. 6, pp. 1256–1268.

Vangengeim, E.A., Pevzner, M.A., and Tesakov, A.S., Chronological Relationship of Pliocene Deposits in Fluviatile Plains between Prut and Southern Bug Rivers, *Stratigr. Geol. Korrelyatsiya,* 1995, vol. 3, no. 1, pp. 61–72.

Vekua, A.K., *Kvabebskaya fauna akchagyl'skikh pozvonochnykh* (The Kvabeb Fauna of Akchagylian Vertebrates), Moscow: Nauka, 1972.

Vereshchagin, N.K., *Mlekopitayushchie Kavkaza* (Mammals of the Caucasus), Moscow: Akad. Nauk SSSR, 1959.

Vislobokova, I.A., *Iskopaemye oleni Evrasii* (Fossil Deers of Eurasia), Moscow: Nauka, 1990.

Werdelin, L. and Solounias, N., *The Hyaenidae: Taxonomy, Systematics and Evolution, Ser. Fossils and Strata*, Oslo, 1991.

Wolsan, M., Drapiezne Carnivora, *Folia Quatern.*, 1989, vols. 59–60, pp. 177–196.

Zazhigin, V.S. and Zykin, V.S., New Data on Pliocene Stratigraphy in the South of West Siberian Plain, in *Stratigrafiya pogranichnykh otlozhenii neogena i antropogena Sibiri* (Stratigraphy of Neogene–Anthropogene Boundary Deposits in Siberia), Novosibirsk: Sib. Otd. Akad. Nauk SSSR, 1984, pp. 29–53.

Zhegallo, V.I., *Gippariony Tsentral'noi Asii* (*Hipparion* Fauna of Central Asia), Moscow: Nauka, 1978.

Zykin, V.S., Zazhigin, V.S., and Kazanskii, A.Yu., Late Neogene in the South of the West Siberian Plain: Stratigraphy, Paleomagnetism, and Principal Climatic Events, *Geol. Geofiz.*, 1991, no. 1, pp. 78–86.

Stratigraphy and Geological Correlation, Vol. 6, No. 4, 1998, pp. 383–396. Translated from Stratigrafiya. Geologicheskaya Korrelyatsiya, Vol. 6, No. 4, 1998, pp. 67–80.
Original Russian Text Copyright © 1998 by Murashko, Rylova, Yakubovskaya.
English Translation Copyright © 1998 by МАИК Наука/Interperiodica Publishing (Russia).

The Late Oligocene of Belarus

L. I. Murashko, T. B. Rylova, and T. V. Yakubovskaya

Institute of Geosciences, Belarussian Academy of Sciences, ul. Zhodinskaya 7, Minsk, 220141 Belarus

Received December 7, 1995

Abstract—The upper Oligocene continental deposits are widespread in the southern Belarus. They are represented by the liman-deltaic sand and clay beds of the Starodubka Formation associated with monomineral lacustrine quartz sands, alluvial sediments of the Krupeiki Formation, and coeval brown coal deposits in karst depressions, which are accumulated after the Kharkov sea regression. Mineralogical and geochemical study of these deposits in the stratotype areas elucidated their genesis and provided grounds for the lithostratigraphic subdivision of their upper Oligocene interval. Eight spore–pollen assemblages of this interval were unraveled from seven section and supplemented with paleocarpological data obtained from 20 section representing eight groups of localities. The spore–pollen diagram from Well 3 near the village of Smolyarka is most complete and used to study for the first time the Oligocene–Miocene boundary floras correlative with floral assemblages known in Poland and Germany.

Key words: *Oligocene, geological structure, mineral composition, pollen assemblages, megaflora, stratigraphy, correlation, Belarus.*

The initial late Oligocene marks the emergence of the geocratic environment in Belarus. This event of geological history is manifested as a distinct lithologic boundary indicating the transition from marine glauconite-bearing sediments of the terrigenous–regressive stage to the accumulation of continental coaliferous deposits.

The upper Oligocene continental deposits of Belarus were originally distinguished on the basis of palynological data by Manykin (1959, 1966, 1973), who placed them at the base of the Oligocene–Miocene Poltava Group. In the period of the 1960s to the early 1990s, Oligocene beds were under intense geological (L.F. Azhgirevich, L.N. Bogomolova, B.N. Gurskii, R.A. Zinova), paleontological (A.F. Burlak, P.I. Dorofeev, Yu.V. Zosimovich, T.B. Rylova, T.V. Yakubovskaya), and lithological (Ya.I. Anoshko, A.G. Ber, V.A. Vecher, N.V. Zaitseva, L.I. Murashko) investigations used for a regional syntheses of results (*Geologiya* ..., 1971; *Resheniya* ..., 1983). However, data of the latest period about deposits bearing floral remains provided grounds for a better understanding of Belarussian paleogeography during the final (continental) stage of the Paleogene.

At the beginning of the late Oligocene, a vast early Oligocene sea of the southern Belarus with a rather uniform type of sedimentation was replaced by several lesser basins with more differentiated sedimentation environments. Sediments of that time were accumulated in coastal marine and properly continental settings, such as limans cut off the sea, remnant lakes, river valleys, and closed karst-lake depressions (Fig. 1). Judging from the accumulated deposits, lakes of tectonic depressions were as deep as 20–30 m in the southwestern Belarus near the Stolin and Mikashevichi–Zhitkovichi salient, and as deep as 50 m in the southwestern part of the Pripyat depression. The lakes recurrently varied in size representing at times a mingled water system and degrading at other times up to the complete disappearance.

In Belarus, like everywhere in Europe (Okinshevich, 1973; Azhgirevich and Levkov, 1979), the late Oligocene was favorable for the karst formation. The most prominent manifestations of this process are related here to the underground leaching of either the Cretaceous carbonates (in the Podlyaska–Brest basin), or the Devonian saliferous deposits (in the western Pripyat depression). Depending on the leaching rate, the karst holes were either filled with clastic sandy to silty sediments or transformed into marshy basins. A slow subsidence of these basins under warm and humid climatic conditions was favorable for the brown coal accumulation. This Cenozoic stage of intense coal formation suggests that Belarus was a part of the northern subtropical belt that existed in the late Oligocene–middle Miocene time.

LIMAN-DELTAIC DEPOSITS OF THE STARODUBKA FORMATION

The liman-deltaic deposits in question rest on the marine Kharkov Formation of the lower Oligocene. They are well exposed and perfectly studied in the Starodubka, Peredelka, Loev, and Krupeiki localities of

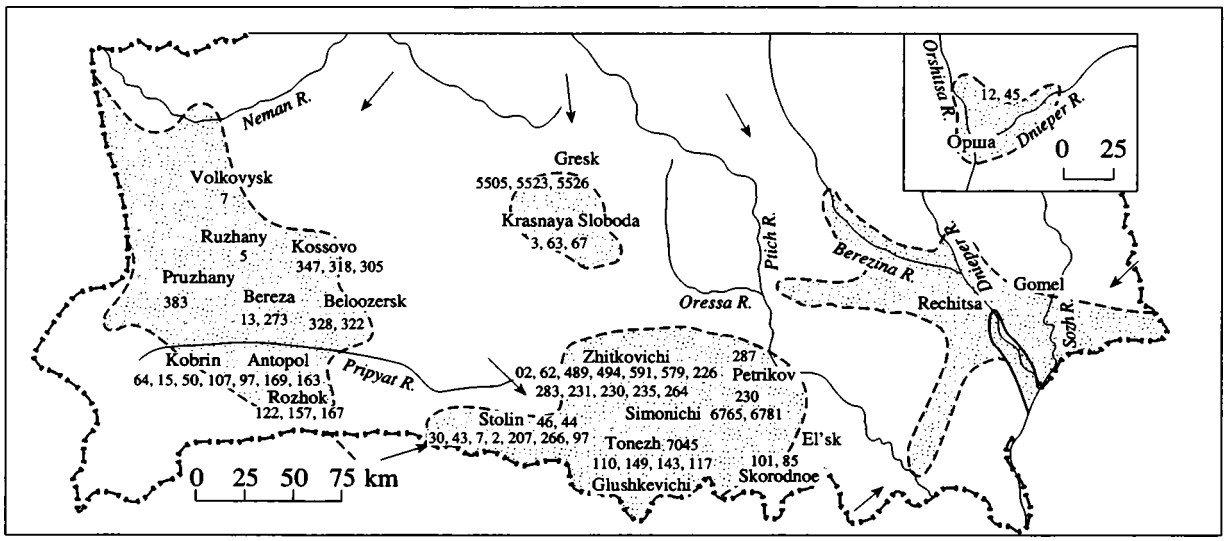

Fig. 1. Distribution areas of the upper Oligocene deposits in Belarus and numbers of drill holes, where paleontological remains were studied (scale 1 : 2 500 000).

the Bragin–Loev saddle and display here a three-member structure (Zinova and Burlak, 1980). The lower member (2 m) is composed of greenish white fine-grained glauconite–quartz sand enclosing interlayers of dark gray clay (up to 5 cm). These units yielded three spore–pollen assemblages.

Assemblage I (Starodubka-I) is macerated from the lower member of the Starodubka Formation exposed near the villages of Peredelka and Krupeiki (Krasnaya Gora), albeit near the village of Starodubka it is confined to the middle member. The assemblage shows predominance of conifers (Fig. 2) represented by diverse *Pinus* species, especially by pollen of subgenus *Haploxylon,* and also by *Podocarpus* specimens. *Sciadopitys, Picea, Tsuga*, and *Cedrus* were encountered as additional components of conifers sporadically associated with *Alnus, Betula, Ulmus, Tilia, Myrica, Artemisia,* and Chenopodiaceae (Zinova and Rylova, 1985).

Assemblage II (Starodubka-II) is distinguished in the middle member of the formation at the Starodubka and Peredelka localities (Dorofeev and Manykin, 1969; Zinova and Burlak, 1980; Zinova and Rylova, 1985; Rylova, 1993). Pollen of gymnosperms is again dominant here, although in contrast to Assemblage I it is mixed with considerably more abundant pollen of angiosperms (Fig. 2). Conifers are exemplified by pollen of *Pinus* (mostly by grains of *Haploxylon* subgenus) and *Podocarpus*. Taxodiaceae and Cupressaceae (up to 25%) along with *Sciadopitys* (up to 7%) turn to be more abundant in this group also incorporating *Tsuga* and *Cedrus.* Pollen of *Rhus* (up to 23%) and *Engelhardtia* (up to 5.5%) dominant among angiosperms is associated with also abundant representatives of formal genera *Tricolporopollenites* Pfl. et Thoms. and *Tricolpopollenites* Pfl. et Thoms. (up to 13% in sum), whose species include *Tricolporopollenites pseudocingulum* (R. Pot.) Pfl. et Thoms., *T. cingulum* ssp. *fusus* (R. Pot.) Pfl. et Thoms., *Araliaceoipollenites edmundi* (R. Pot.) R. Pot., and also with *Quercoidites microhenrici* (R. Pot.) R. Pot., Thoms. et Thierg., and some other palynomorphs. Pollen of *Quercus, Ulmus, Betula, Carya, Tilia, Carpinus, Alnus, Castanea, Myrica, Pterocarya, Acer, Nyssa, Vitis,* Araliaceae, Sterculiaceae, Clethraceae, and Arecaceae is less abundant. Content of herbaceous palynomorphs is not higher than 3.5%. Rare spores are those of *Sphagnum,* Cyatheaceae, Gleicheniaceae, and Polypodiaceae. This assemblage resembles palynoflora from the upper Oligocene Bereka Formation of Ukraine (Zosimovich and Rotman, 1976; Zinova and Rylova, 1985; Zosimovich, 1992).

The same member of the Starodubka Formation also yielded paleocarpological remains classified by Dorofeev (Dorofeev and Manykin, 1969; *Materialy,* 1973; Zinova and Rylova, 1985). The list of respective taxa, to which we apply a somewhat refined nomenclature, is presented in the table. All species of the Starodubka flora are of the extinct type. Seven (18%) of its 39 genera are also of this type (*Caricoidea, Eoeuryale, Microdiptera, Protosequoia, Spirimatospermum, Urospathites,* and *Tubela*). Nineteen (49%) genera disappeared from Belarus in the Neogene, but were preserved in North America and Southeast Asia (*Decodon, Liriodendron, Aralia, Glyptostrobus, Taxodium, Saururus, Sciadopitys, Magnolia,* and others), and only 23 genera (33%) survived in the recent flora of Belarus. Many genera, such as *Ampelopsis, Aralia, Brasenia, Cunninghamia, Glyptostrobus, Liriodendron, Magnolia,* and others, compose the subtropical group, whereas *Haloragis* and *Spirimatospermum* are elements of tropical flora. They all represent at least 50% of the assemblage, and mainly exemplify the deciduous arboreal

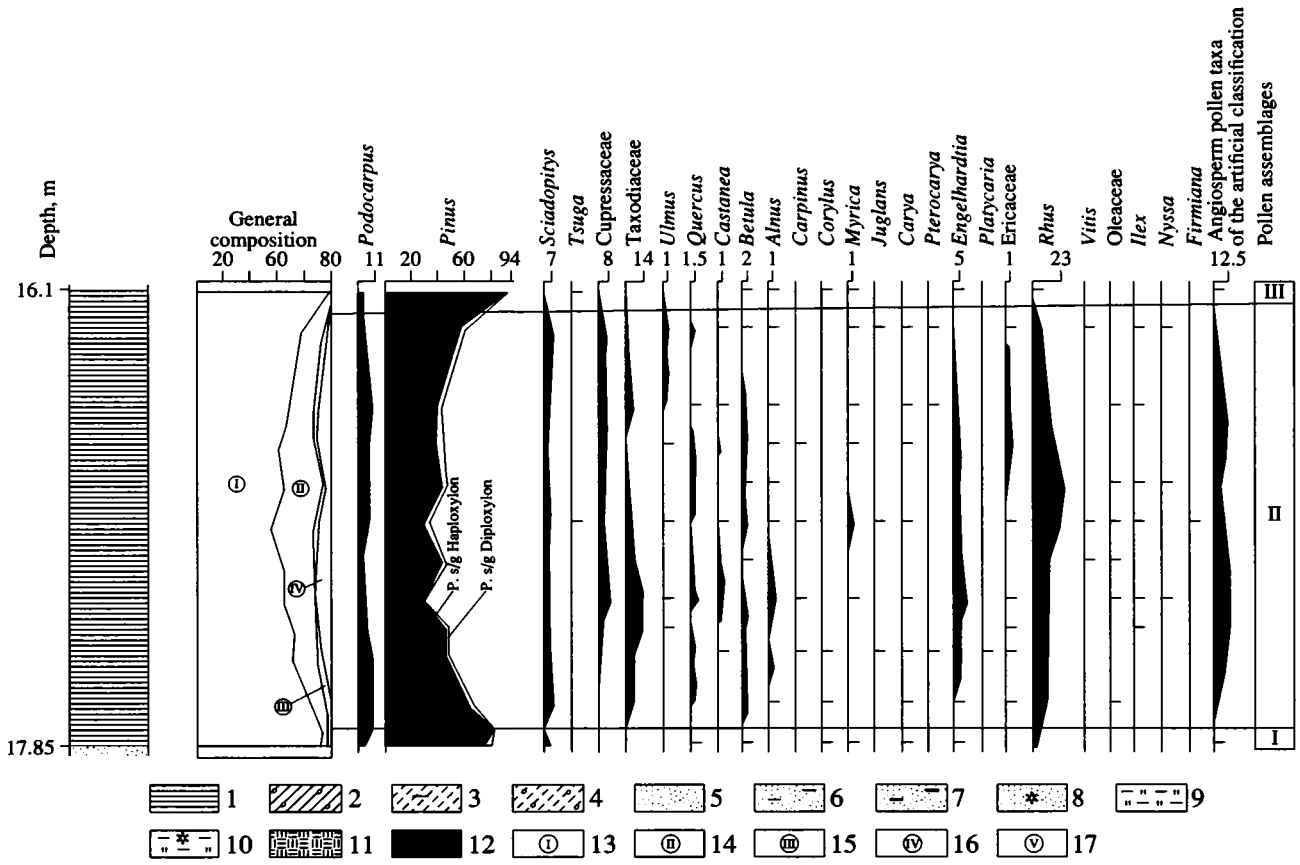

Fig. 2. Palynological diagram for the Oligocene deposits recovered near the village of Starodubka: (1) clay; (2) morainal loam; (3) coaliferous sandy loam; (4) morainal sandy loam; (5) sand; (6) coaliferous sand; (7) sand with brown coal seams; (8) glauconite–quartz sand; (9) silt; (10) glauconite–quartz silt; (11) peat; (12) brown coal; (13) pollen of gymnosperms; (14) pollen of arboreal angiosperms; (15) pollen of herbaceous and fruticose plants; (16) artificially classified taxa of angiosperms; (17) spores.

and fruticose taxa. The Starodubka flora is a first example of the deciduous spermatophyte and carpogenous flora of the Turgai ecotype from Belarus. It is similar to the present subtropical vegetation in the Appalachian and Japanese refugiums.

Unraveling paleoclimatic conditions with method of Grichuk *et al.* (1987), we obtained the following results: temperature of the warmest month was fluctuating around 24–25°C and during the coldest season it varied from 8 to 12°C. These value show that climate of that time was as warm as subtropical at present. Tropical (P_1) to subtropical (P_2) elements were really significant in the composition of this paleoflora, which mainly consisted of moderately thermophilic arctic-tertiary components (A_1).

Assemblage III (Starodubka-III) is typical of the upper clay beds of the formation exposed near the villages of Starodubka and Peredelka. It is similar to Assemblage I and predominantly consists of coniferous pollen (94–98%) mainly representing *Pinus* s/g *Haploxylon* and *Podocarpus* associated with less abundant *Sciadopitys, Taxodium,* and *Tsuga* specimens. Angiosperm taxa, such as *Quercus, Juglans, Engelhardtia, Rhus, Myrica, Ulmus, Betula, Alnus,* and *Corylus,* contributed only single pollen grains to the assemblage. Spores and herbaceous pollen are missing.

Sediments of the Starodubka Formation show genetic relations with white monomineral quartz sands, whose lenses up to 15.7 m in thickness are widespread in the Bragin–Loev saddle (the Loev sand deposit), over the buried Gremyach salient (Lenino, Dobrush, Chertyanka, Vysokopol'e and other localities), and also in the Polesye lowland and northwestern slopes of the Ukrainian crystalline massif (Gorodnoe, Berezhnoe, Stolin, and Goryn River localities). Their position in the section along with the character of bedding, spatial distribution, and mineral composition are suggested to be a result of alluvial reworking of underlying marine sediments, and show that these sands represent the oldest continental deposits accumulated in the flow-type basins of the terminal early and initial late Oligocene.

COAL-BEARING DEPOSITS

Coaliferous deposits of the Podlyaska–Brest and Pripyat depressions include diverse facies of alluvial

The upper Oligocene spermatophyte flora of Belarus (after P.I. Dorofeev and T.V. Yakubovskaya)

Fossil plants	Locality							
	Staro-dubka	Simoni-chi-1	Simoni-chi-2	Gresk	Bere-za-13	Bere-za-328	Belo-ozersk	Pruzha-ny
0	1	2	3	4	5	6	7	8
Aldrovanda clavata Dorof.								
A. ex sect. *Aldrovanda* Dorof.								
Aldrovanda sp. nov.								
Alismataceae gen.								
Alnus sp.								
Ampelopsis sp.								
Andromeda sp. sp.								
Aralia sp.								
Azolla aspera Dorof.								
A. cf. *interglacialis* P. Nikit.								
?*Boehmeria majuskula* T.V. Jakub.								
Boehmeria sp. sp.								
Brasenia goretskyi Dorof.								
B. cf. *baltica* Dorof.								
B. cf. *spinosa* Chandl.								
B. ucrainica Dorof.								
Brasenia sp. sp.								
Butomus cf. *umbellatus* L.								
Caldesia antiqua Dorof.								
Caricoidea jugata (P. Nikit.) Chandl.								
?*C.* cf. *ovalis* (Dorof.) Chandl.								
Carpinus sp.								
Carpolithus zytkovieczensis Dorof.								
Carpolithus sp. sp.								
Chamaecyparis sp.								
Cladium macrocarpum Dorof.								
C. ex gr. *reidiorum* P. Nikit.								
Cladium sp.								
Cladiocarya sp.								
Comptonia sp.								
Crataegus sp.								
Cunninghamia heerii Bud. et Swechn.								
Cyperaceae gen.								
Cypressaceae gen.								
Decodon gibbosus (E. Reid) E. Reid								
D. globosus (E. Reid) P. Nikit.								
Eoeuryale sp.								
Evodia nitida (P. Nikit.) Mai								
Epipremnites ornatus (E. Reid et Chandl.) Gregor et Bogner								
Gaultheria europaea Dorof.								
Glyptostrobus borysthenicus Dorof.								
G. langsdorfii (P. Nikit.) Dorof.								
G. cf. *europaea* (Brong.) Unger								
Glyptostrobus sp.								
Cf. *Hippuris* sp.								
Holoragis sp.								
Hypericum sp. sp.								
Isoëtes sp.								
Leucothoe sp.								
Liriodendron europaeum Dorof.								
Lysimachia sp.								
Magnolia borysthenica Dorof.								
Menyanthes sp.								
Microdiptera cf. *boveyana* Chandl.								
Myrica europaea Dorof.								

Table. (Contd.)

0	1	2	3	4	5	6	7	8
M. sphaeroidea T.V. Jakub.								
Myrica sp. sp.								
Cf. *Myriophyllum* sp.								
Nuphar sp.								
Cf. *Nuphar* sp.								
Nymphaea sp.								
Cf. *Nymphaea* sp.								
Nyssa cf. *europaea* Dorof.								
N. cf. *macrocarpa* Dorof.								
Nyssa sp.								
Picea sp.								
Pinaceae gen.								
Pinus cf. *thomasiana* (Goepp.) Rehb.								
Pinus sp.								
Potamogeton gomelianus Dorof.								
P. echinatus Dorof.								
P. ex gr. *corticosus* P. Nikit.								
P. subgen. *coleogeton* Reichenb.								
Protosequoia europaea Dorof.								
Punica natans (P. Nikit.) Mai								
Rubus sp.								
Salvinia turgaica Dorof.								
Salvinia sp.								
Cf. *Sambucus* sp.								
Saururus bilobatus (P. Nikit.) Mai								
Sciadopitys sp.								
Scirpus ragozinii Dorof.								
S. ex gr. *longispermus* Dorof.								
Scirpus sp. sp.								
Selaginella sp.								
Cf. *Selaginella* sp.								
Sequoia sp.								
Sparganium camenzianum Kirchh.								
S. cf. *costatum* Dorof.								
S. cf. *pusillum* Dorof.								
Sparganium sp.								
Spirimatospermum wetzlerii (Heer) Chandl.								
Stratiotes websterii (Br.) Zinndorf.								
Taxodium distichum–miocenum Heer								
T. cf. *tavdense* Dorof.								
Taxodium sp.								
Taxodiaceae gen.								
Tournfortia sp.								
Tubela cf. *baltica* Dorof.								
T. lidiae T.V. Jakub.								
Typha latissima (A. Br.) E Reid et Chandl.								
Typha sp. sp.								
Urospathites borysthenicus (Dorof.) Gregor et Bogner								
Urticaceae gen.								
Viola cf. *rimosa* P. Nikit.								
Viola sp.								
Vitis sp.								

(waterway and floodplain types), lacustrine, and palustrine (stagnant to flow-type marshes) origin. They occur in the following types of sections:

(1) intercalated glauconite–quartz and gray quartz sandy to silty beds with interlayers of coaly sand (wells 107 and 157 of the Antopol area);

(2) horizontally interbedded thin layers of platy coaly silt and white coaly silt (wells 3, 63, and 67 of the Krasnaya Sloboda area; wells 292, 299, 476, 492, 502, and 571 of the Zhitkovichi area; Well 97 near the village of Borki; Well 189 near the village of Grushevo; wells 6765 and 6781 of the Simonichi area; and wells of the Malishev, Glushkovichi, and Skorodnoe coal occurrences);

(3) beds of coaly quartz sand with interlayers of brown coal (wells 110 and 119 of the Glushkovichi area; wells 3 and 13 of the Smolyarka area; wells 15, 50, and 169 of the Antopol area; wells 62, 231–235, 264, 283, 489, and 494 of the Zhitkovichi area; Well 5526 and others of the Gresk coal occurrence; and wells of the Kossovo, Bereza, Ruzhany, Pruzhany, Volkovysk, and Tonezh localities);

(4) brown coal with sand, silt, and clay interbeds (wells 220, 226, 266, 565–568, 579, and 591 of the Zhitkovichi area, and wells of the Simonichi, Skorodnoe, and Valavsk coal occurrences);

(5) highly humified sands and black clays (wells 12, 45, and others near the Orshitsa water station).

The most complete sections may include various combinations of these members. Their composition and structure point to the dynamic hydrologic state of ancient water basins. The thickness of deposits varies from 3–4 to 77.6 m (Well 7045 of the Tonezh locality).

The coaliferous deposits are coeval with the upper Oligocene Krupeiki Formation. All their units represent an integral sedimentation cycle related to the past activity of the river system that comprised of the Dnieper, Oressa, and Pripyat rivers along with their tributaries. This complex of deposits demonstrates a succession of alluvial facies (from instratified to perstratified) corresponding to different phases of erosion-accumulation cycle. Persistent lithologic features of the complex are traced over a vast territory. Sediments of the Krupeiki Formation are notably altered and crowned with the sialic weathering crust presumably corresponding in age to the late Oligocene–early Miocene. Sections of this type are naturally unfavorable for preservation of paleontological remains.

Synchronism of barren and fossiliferous coal-bearing deposits, genetic interrelations between them, and common paleogeographic settings of their accumulation allow us to include these sediments into the Krupeiki Formation.

Deposits with brown coal seams yielded several spore–pollen assemblages.

Assemblage IV (Simonichi) was distinguished in the depth interval of 19.8–32.9 m penetrated by Well 6765 in the Turov depression (Azhgirevich *et al.*, 1990; Fig. 3). Gymnosperms, mainly *Pinus,* Taxodiaceae, Cupressaceae, *Podocarpus,* and *Sciadopitys* prevail in its composition (60–80%). Components rather abundant among angiosperms are represented by taxa of the artificial classification system (up to 16%) and also by thermophilic *Nyssa, Rhus, Myrica,* Cyrillaceae, *Engelhardtia, Liquidambar,* and others. As compared to the Starodubka assemblages, this one is more rich in the arctic-tertiary representatives, such as *Betula* and *Alnus.* In addition, the assemblage persistently contains pollen of *Corylus, Ulmus, Celtis, Quercus, Fagus, Carpinus, Ostrya, Salix, Juglans, Carya, Pterocarya, Platycarya, Vitis, Ilex, Cornus, Symplocos,* Sapotaceae, Sterculiaceae, and some other taxa. Herbaceous pollen constitutes less than 8% of the assemblage also containing up to 4% of spores.

This assemblage is clearly similar to the late Oligocene palynoflora described by Manykin (1966) in southern Belarus.

Spermatophyte flora (Simonichi-1) from the coaliferous clay bearing spores and pollen of Assemblage IV was sampled in the aforementioned Well 6765 (depth interval of 27.6–33.1 m) and also in Well 6781 (depth interval of 32.3–37.7 m) located near the village of Shugalei. This flora includes 28 species (see the table). Some of them are of the extinct type, and four of 17 genera (23%) are of this type as well, whereas three genera (18%) represent a group of exotic foreign and regional taxa. Several forms, such as *Taxodium distichum-miocenum, Caricoidea jugata, Urospathites borysthenicus, Saururus bilobatus, Stratoites websteri,* and coexisting *Tubela* species suggest a certain similarity between this and Starodubka floras. Nevertheless, its distinct features are evident from the presence of archaic *Aldrovanda* forms and some genera of unclear affinity (cf. *Selaginella,* cf. *Hippuris,* cf. *Myriophyllum,* and others), and also from abundant megaremains of Pinaceae and a lower content of subtropical elements (P_2). On the basis of dominant taxa, we refer the paleocarpological flora Simonichi-1 to the Pinaceae–*Typha–Caricoidea* type.

Assemblage V (Gresk) is macerated from the brown coal bed recovered by Well 5526 in the depth interval of 80.8–85.8 m (Fig. 4 in Rylova, 1991) and by Well 6765 at the depth of 17.7–17.85 m (see Fig. 3 in this work). Being quite similar to Assemblage IV (Simonichi), this one differs from it by a higher content of Taxodiaceae, *Rhus,* and *Corylus* pollen, and also by the appearance of *Itea* specimens, whereas *Podocarpus, Alnus,* and *Betula* are less abundant here. Assemblage V is correlative with the spermatophyte flora Simonichi-2 obtained from brown coal beds penetrated by wells 6765 (depth interval of 17.7–19.1 m) and 6781 (depth interval of 20.3–22.6 m), and also with Gresk flora known from Well 23 of the Stepkovo locality (data of 1977 for the depth interval of 106.0–106.8 m) and from wells 5526 (depth of 77.5–82.4 m) and 5522

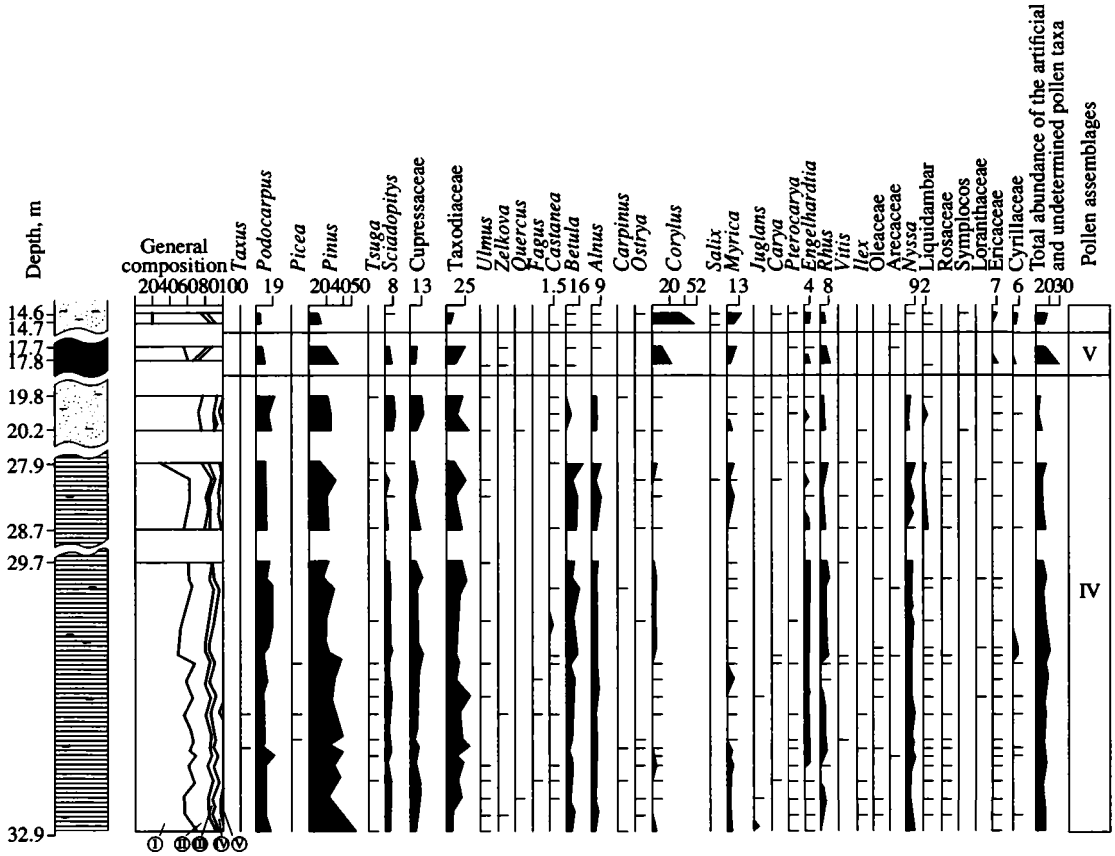

Fig. 3. Palynological diagram for the upper Oligocene deposits recovered by Well 6765 at the Simonichi coal occurrence (symbols as in Fig. 2).

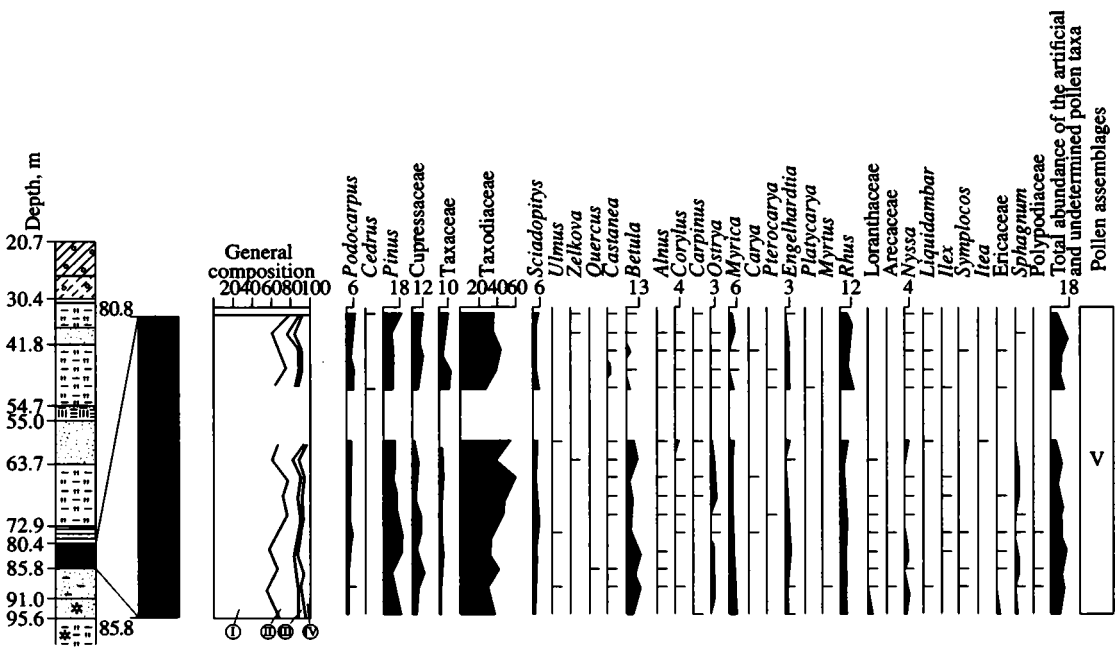

Fig. 4. Spore–pollen diagram for the upper Oligocene deposits recovered by Well 5526 at the Gresk coal occurrence (symbols as in Fig. 2).

(depth of 73.6–75.6 m) of the Shugalei locality (data of 1983).

Flora Simonichi-2 includes 20 extinct genera. In addition, we conditionally attributed to this group several organ genera, such as *Cladiocarya, Tubela*, and *Urospathites* (14%). Eleven genera of this flora (53%) currently occur in North America, Southeast Asia, and the Mediterranean region, whereas, seven genera (33%) survived in the forest flora of Belarus. Flora Simonichi-2 includes several forms characteristic of the Starodubka assemblage (*Aldrovanda* cf. *clavata, Urospathites borysthenicus, Glyptostrobus borysthenica,* and *Taxodium distichum-miocenum*), however it additionally incorporates new genera *Chamaecyparis, Punica,* and *Cladiocarya,* which were typical of the Neogene time in Belarus. As compared to flora Simonichi-1, flora Simonichi-2 is more rich in subtropical elements (up to 50% of genera), and this allows us to relate its origin with a stage of climatic warming. The *Taxodium–Glyptostrobus–Tubela* and *Brasenia–Boehmeria* assemblages of this flora represent the dominant communities of arboreal and lacustrine–palustrine plants, respectively.

In the Gresk flora, there are the late Oligocene species, such as *Caldesia autigua, Urospathites borysthenicus, Tubela cf. baltica, Scirpus ragozinii, Caricoidea jugata,* and some others; they all are also present in the Starodubka flora. *Tubela* cf. *baltica* from the Gresk flora and *Glyptostrobus borysthenica* from the Starodubka flora are the most archaic species of respective genera (Dorofeev, 1974). The northernmost occurrences of *Tubela* forms in Belarus suggest that spermatophyte floras in this country and southern Baltic areas were interrelated during the Oligocene. *Andromeda, Decodon,* and *Hypericum* forms of the Gresk flora are unknown in later Cenozoic floras of Belarus and substantiate the Oligocene age of associated plant remains. On the basis of carpological remains dominant in the oryctocoenosis from the brown coal beds recovered by Well 23, we identified the *Glyptostobus–Tubela* and *Azolla–Caricoidea–Urospathites* assemblages of arboreal and lacustrine–palustrine (coastal) plant communities in this paleoflora, whereas Taxodiaceae and *Salvinia* are recognized as taxa preponderate in the assemblage from Well 5526. Similar palynofloras and assemblages of carpolites were recovered from several brown coal deposits in the karst holes located in the structural zone separating the Brest depression from the Polesye saddle and Belarussian anteclise. They also were recognized in borehole sections situated in the Bereza and Pruzhany areas of the Brest region.

Spores and pollen correlative in composition with Assemblage V (Gresk) were also obtained from two localities near the village of Smolyarka, the Bereza area of the Brest region (Fig. 5), namely from the lower brown coal beds recovered by Well 13 (depth of 102.4–108.3 m; Rylova, 1987, 1993; Yakubovskaya and Rylova, 1992) and from coaly sand and silt deposits underlying the 20-m-thick bed of brown coal penetrated by Well 3 (depth interval of 108.7–114.0 m). The lowermost among seven assemblages (from Sm-1 to Sm-7) identified in Well 3 consists of equally abundant pollen of gymnosperms and angiosperms. Taxodiaceae constitute up to 30% of the assemblage and include *Glyptostrobus, Taxodium, Cunninghamia, Sequoia, Cryptomeria,* and *Metasequoia* genera. Other conifers are represented by Cupressaceae (up to 7%), *Pinus* [up to 30%, including the most abundant *Pinus tertiaria* (Moreva) Anan. and *P. mirabilis* (Rudolph) Anan. from the group of *Pinus* s/g *Haploxylon*], *Podocarpus* (up to 6%), and *Sciadopitys* (up to 7%), and also by single pollen grains of *Picea, Cedrus,* and *Tsuga.* Dominant angiosperms are *Myrica* (up to 12%), *Rhus* (up to 10%), and *Tricolporopollenites pseudocingulum* (up to 7%). Their pollen coexists with less frequent specimens of *Betula, Alnus, Corylus, Platycarya, Nyssa,* and Clethraceae represented by *Trocolporopollenites bruhlensis* (Thomson) Grabowska, *T. cingulum* ssp. *oviformis, T. cingulum* ssp. *pusilis, Tricolpopollenites liblarensis* and other formal species. Single pollen grains of *Magnolia, Celtis,* Myrtaceae, *Staphylea,* Sapotaceae, and *Araliaceoipollenites edmundi* are also present. The total content of formal pollen taxa is 17%. Pollen of herbaceous plants is rare. Sporiferous taxa are represented by *Sphagnum, Lycopodium, Osmunda,* Polypodiaceae, and, what is more important, by Gleicheniaceae, Cyatheaceae, and Schizaeaceae with their genera *Lygodium* (including *Leiotriletes maxoides maxoides*), *Mohria,* and *Anemia.*

This assemblage is, in general, correlative with the composite late Oligocene flora of Belarus described by Manykin (1966). Its correlation with West European floras is more problematic, because in this case we deal with different floral provinces of the Paleogene time. Anyway, our palynoflora is similar in certain aspects to spore–pollen assemblages characteristic of the Dabrova Beds in the Polish Lowland and Glagow Beds in western Poland, where both units are correlated with the Lusation Bed IV. Polish researchers refer these beds either to the upper Oligocene (Ciuk, 1970, 1974; Dyjor, 1978, 1986; Odrzywolska-Bienkowa *et al.*, 1979), or to the lower Miocene (Piwocki, 1986).

The carpolite assemblage from the lower (depth interval of 94.3–108.4 m) brown coal beds of Well 13 located near the village of Smolyarka in the Bereza area (see Bereza-13 flora in the table) is archaic in composition and includes 16 taxa. One group of its species is well known in spermatophyte Oligocene floras of the Pripyat depression (*Caricoidea jugata, Glyptostrobus borysthenica,* and *Scirpus ragozinii*). Other specimens either represent new Oligocene–Miocene forms (*Tubela lidiae, ? Boehmeria majuskula,* and *Myrica sphaeroidea*), or belong to the Neogene genera poorly studied in Belarus (*Cladiocarya*). The archaic character of this flora is testified by *Carpolithus* forms present in its composition. *Caricoidea* and *Tubela* represent two extinct genera (20%) of the flora. The *Glyptostrobus–*

Tubela–Myrica and *Caricoidea–Boehmeria* assemblages exemplify respectively its arboreal and aquatic palustrine communities. The late Oligocene age is also assigned to floras distinguished by Dorofeev in brown coal beds, which were penetrated by wells 328 (the Bereza area, depth of 74 m), 318 (near the village of Yurchiki, depth of 84.5 m), 397 (near the village of Khorevo, depth of 72.5 m), and 383 (close to the village Shereshevo of the Pruzhany area, depth interval of 83.0–87.5 m).

Another interesting Oligocene flora was recovered from the lower brown coal bed of Well 12a (depth interval of 68.6–69.0 m) located in the suburbs of Beloozersk (Yakubovskaya, 1981). The bed was deposited in a coastal setting of the karst lake that was formed above the Cretaceous rocks and accumulated silt and clay in its central part; these sediments are presumably correlative with the Starodubka Formation. Taxa of this flora are listed in the table and show that dominant carpolites belong to the *Glyptostrobus–Aldrovanda* assemblage.

All the carpolite assemblages known from the Bereza, Beloozersk, and Pruzhany districts of the Brest region constitute an integral *Glyptostrobus* flora of the Oligocene time. It is typical of brown coal beds occurring in the upper part of continental Oligocene deposits of the Podlyaska–Brest depression and can be correlated with the flora Simonichi-2 from the Pripyat depression and with the Gresk flora from the southern margin of the Belarussian anteclise.

Paleoclimatic characteristics estimated on the basis of Simonichi and Gresk floras are similar to those obtained for the Starodubka Formation (Assemblage II). However, a greater abundance of *Nyssa, Betula, Alnus,* and Taxodiaceae (especially of *Glyptostrobus* and *Taxodium*) suggests that these floras developed under a similarly warm, but more humid climate than that of the accumulation period of the Starodubka Formation.

Assemblage VI (Sm-2 in Fig. 5) is distinguished for the first time in Belarus. It is characteristic of coaly sand and silt beds recovered by Well 3 near the village of Smolyarka from the depth interval of 100.0–108.7 m. This assemblage differs from the previous one by the lower content of thermophilic tropical and subtropical elements in the flora composition enriched in the arctic-tertiary taxa of the temperate climatic zone. *Betula* (up to 24%) is the dominant taxon among angiosperms represented in addition by *Alnus, Myrica, Corylus, Carpinus, Carya, Quercus, Nyssa, Ilex,* and Cyrillaceae. Pollen of conifers corresponds to that of *Pinus,* Taxodiaceae, Cupressaceae, and occasional *Picea.* Pollen of Ericaceae is also rather abundant, whereas herbaceous taxa are often represented by Poaceae, Cyperaceae, and *Artemisia.* Taxa are irregularly distributed in the section, and inside it there is an interval of a higher diversity of thermophilic elements reflecting the relative climatic warming. Accordingly, this flora is divided into three subassemblages. Characteristics of more cryophilic lower and upper subassemblages is outlined above, and the intermediate palynoflora separating them shows a higher abundance of Taxodiaceae, *Myrica, Engelhardtia, Rhus, Tricolporopollenites pseudocingulum, T. cingulum* ssp. *oviformis, Araliaceoipollenites edmundi, Pterocarya, Carya, Platycarya, Quercoidites microhenrici,* and some other taxa, which are missing or are very rare in the lower and upper beds. At the same time, this interval is considerably depleted in pollen of *Betula, Alnus, Quercus, Ulmus, Zelkova,* and *Corylus.*

Assemblage VI corresponds to the climatic cooling of the terminal Oligocene, which was interrupted by a short, but significant warming episode. In general, these events may be correlative with the cooling phase at the time of Oligocene–Miocene boundary in the Atlantic Ocean and North Sea that is recognized with the help of isotopic data.

Two assemblages (Sm-3 and Sm-4) from the basal portion of the brown coal interval in Well 3 near the village of Smolyarka are distinguished on the basis of few pollen spectra.

Assemblage VII (Sm-3) is confined to the depth interval of 99.0–100.0 m. It shows the peak abundance of *Myrica* pollen constantly associated with that of *Quercus, Castanea, Alnus, Betula, Corylus, Carya, Engelhardtia, Platycarya, Rhus,* Araliaceae, Cornaceae, *Nyssa,* and *Quercoidites henrici* (R. Pot.) R. Pot., Thoms. et Thierg. Taxodiaceae prevail here among coniferous taxa.

Assemblage VIII (Sm-4) is distinguished at the depth interval of 98.5–99.0 m. Conifers, mainly *Pinus* (54%) and *Podocarpus* (12%) dominate in its composition. Angiosperms of this level are represented by *Ulmus, Quercus, Myrica, Alnus, Liquidambar, Tricolporopollenites pseudocingulum,* and by rare pollen grains of *Castanea, Betula, Pterocarya, Engelhardtia, Staphylea,* Arecaceae, *Nyssa, Quercoidites henrici,* and some other taxa.

OLIGOCENE–MIOCENE BOUNDARY DEPOSITS

Studies on paleoflora from coaliferous deposits in karst depressions revealed the transitional Oligocene–Miocene and definite Miocene beds. For instance, in Well 3 near the village of Smolyarka, there were established several spore–pollen assemblages of the transitional type.

Assemblage Sm-5 is from the depth interval of 96.0–98.5 m. Its characteristic feature consists in a sharply decreased abundance of coniferous pollen. At the same time, the assemblage reveals an increased content of *Ulmus–Zelkova* group (up to 5%), *Quercus* (up to 6%), *Fagus* (up to 1.5%), *Liquidambar* (up to 7%), *Itea* (up to 4%), *Rhus* (up to 8%), *Tricolporopollenites pseudocingulum* (up to 9%), *Tricolpopollenites liblarensis* (up to 2%), *Quercoidites henrici* (up to 6%), *Q. microhenrici* (up to 7%), and some other taxa. The

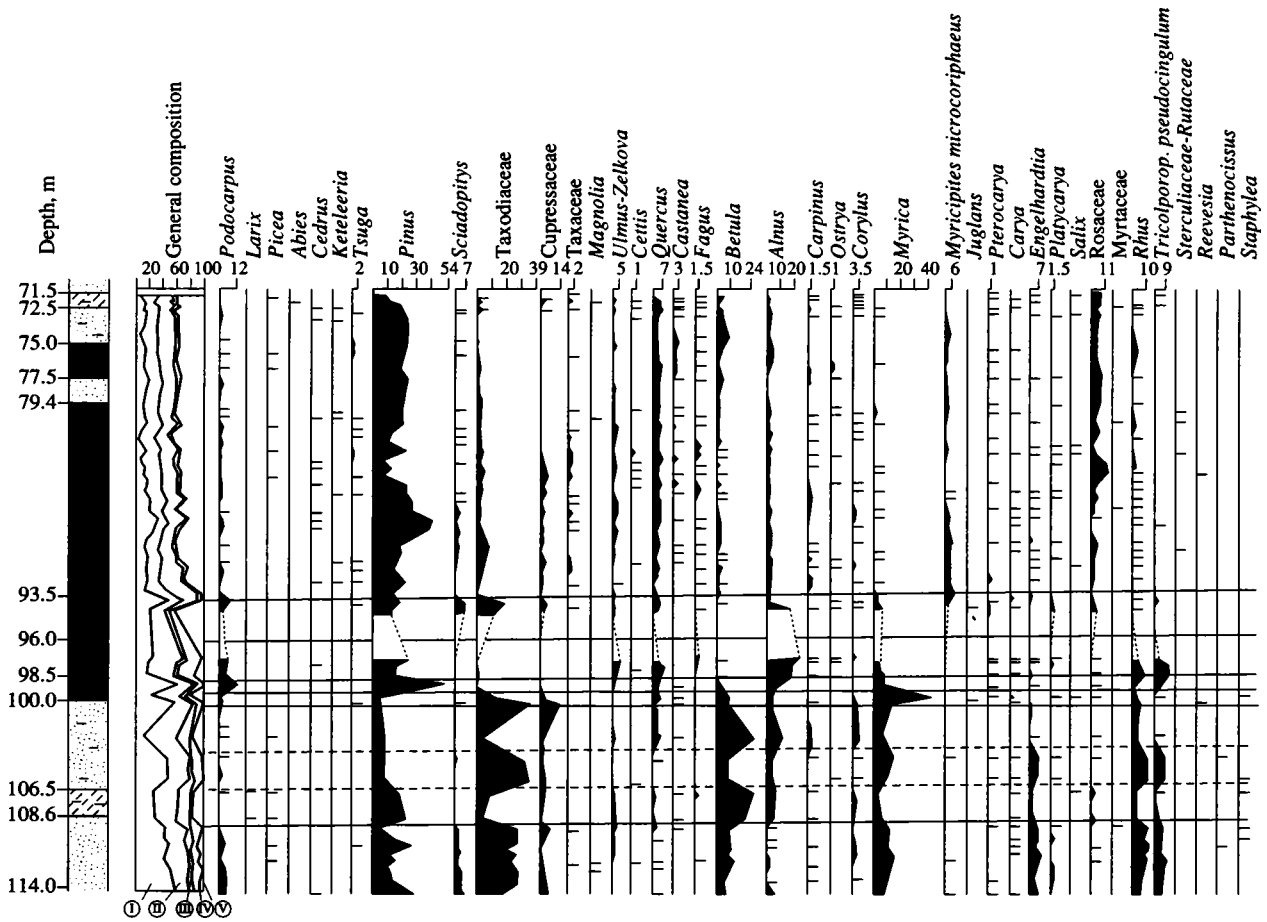

Fig. 5. Spore–pollen diagram for the Oligocene–Miocene deposits recovered by Well 3 near the village of Smolyarka, the Bereza district of the Brest region (symbols as in Fig. 2).

interval is quite rich in *Alnus* pollen (up to 20%). Conifers are mainly represented here by pollen of *Pinus* and *Podocarpus,* the latter as abundant as pollen of *Myrica* and *Rhus*. The last feature and considerable abundance of formal taxa (32% in sum) make the assemblage similar to other late Oligocene floras. Nonetheless, the preponderance of angiosperm pollen and increased abundance of arctic-tertiary elements in the pollen spectra may suggest the early Miocene age of the assemblage.

Assemblage Sm-6 was recovered from the depth interval of 93.5–96.0 m. It demonstrates the further growth of conifers, especially of *Sciadopitys,* Taxodiaceae, and Cupressaceae, which were almost missing below. The arctic-tertiary elements are also more abundant here. *Alnus* (up to 15%) again is dominant among them, whereas *Rhus* (0.5%) and formal taxa (up to 10%) are less significant at this level. The *Alnus*-bearing horizon with impoverished flora composition reflects the new stage of climatic cooling recorded in many localities of central Europe. It is correlative with the following units: with Level III of the Scinawa and Rawicz beds in Poland; with Level III of the Lusation Group in Germany, where it marks the *Alnipollenites verus* Phase; and with the Zone III established by D. Mai in Poland (Ziembińska-Tworzydlo and Wazyńska, 1981; Dyjor and Sadowska, 1986). Accordingly, this horizon should be assigned to the basal Miocene.

The overlying main portion of brown coal beds (depth interval of 71.5–93.5 m) bears an integral Assemblage Sm-7. This is the predominance level of angiosperm pollen (up to 85%) and spores (up to 51%) mainly produced by *Sphagnum.* Angiosperms are very diverse. Ericaceae, Poaceae, Rosaceae, and Cyrillaceae, including *Cyrillaceaepollenites exactus* (R. Pot.) R. Pot., are dominant in this group and always coexist with *Quercus,* Araliaceae, Cornaceae, *Ulmus, Castanea, Fagus, Carpinus, Arceuthobium, Itea, Ilex, Nyssa,* and sometimes with *Celtis, Myrica, Engelhardtia, Platycarya,* Oleaceae, *Symplocos,* and *Liquidambar. Magnolia,* Myrtaceae, Sterculiaceae, Rutaceae, and Sapotaceae are represented among them by single pollen grains. In contrast, Arecaceae are exemplified by several species, including *Monocolpopollenites pararreolatus* W. Kr. and *M. tranquillus* (Pot.) Thoms. et Pf. Other formal taxa of angiosperms are *Myricipites microcoryphaeus* (Pot.) Slodk., *Tricolpopollenites liblarensis, Tricolporopollenites cingulum* ssp. *oviformis, T. cingulum* ssp. *pusillus, Quercoidites henrici, Q.*

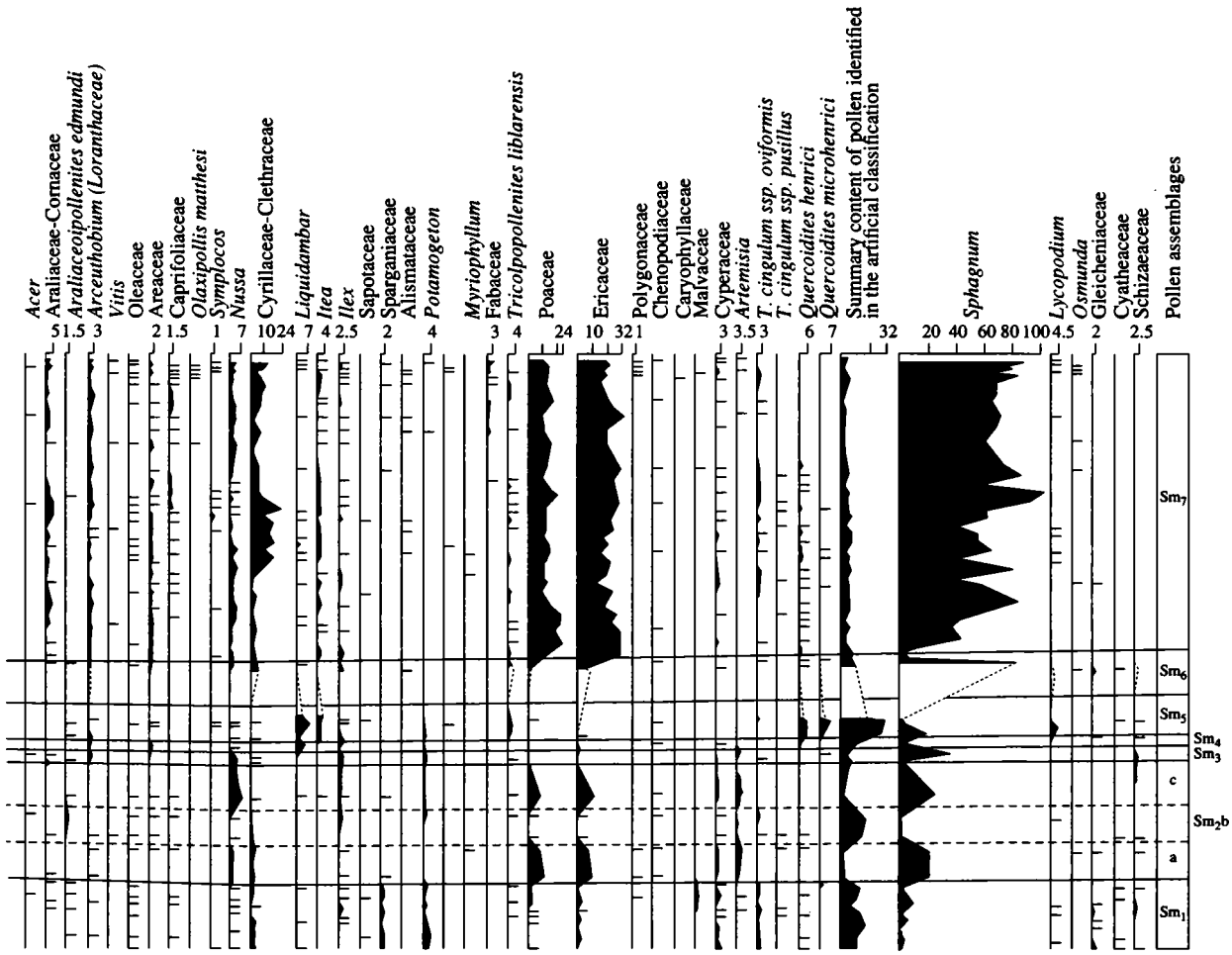

Fig. 5. (Contd.)

microhenrici, and some others. *Pinus* is dominant among gymnosperms, however abundance of Cupressaceae and Taxodiaceae (mostly *Sequoia* and *Cryptomeria*) is insignificant, and their pollen almost disappears in upper beds. *Tsuga* (up to 1%) and Taxaceae (up to 2%) atypical of the older assemblages are constantly present at this level, whereas *Podocarpus, Picea, Cedrus, Keteleeria,* and *Sciadopitys* are not abundant here. In general, this assemblage is similar to palynoflora from Well 13 near the village of Smolyarka, where it is confined to the depth interval of 72.4–80.6 m, and has been formerly referred to the middle Miocene.

The described assemblage from the brown coal beds corresponds to a part of the well-known climatic optimum of the early Miocene time. Its interval may be correlative with the *Monocolpopollenites parareolatus* Palynozone of Poland, which also includes diverse representatives of palm trees and other thermophilic elements, including several characteristic taxa, such as *Cyrillaceaepollenites exactus, Quercoidites henrici, Spinaepollis spinosus* (R. Pot.) W. Kr., *Araliaceoipollenites edmundi,* and *A. euphorii* (R. Pot) R. Pot., characteristic of the megaflora Zone IV of D. Mai in Germany (Ziembińska-Tworzydlo and Wazyńska, 1981).

Spermatophyte flora of the early Miocene consists of assemblages Rozhok-4 and Rozhok-5 (Yakubovskaya, 1993, 1994), the latter formerly considered to be the middle Miocene in age.

The Oligocene and early Miocene carpolite assemblages are quite distinct, because some transitional elements are missing from the chronological succession of these floras. For instance, the late Oligocene marks the last occurrence level of the following carpolite taxa: *Brasenia goretskyi, Caldesia antiqua, Cunninghamia heeri, Evodia nitida, Urospathites borysthenicus, Glyptostrobus borysthenica, Liriodendron borysthenica, Magnolia borysthenica, Microdiptera boveyana, Potamogeton gomelianus, P. echinatus, Protosequoia europeae, Saururus bilobatus, Stratoites websteri, Tubela* cf. *baltica,* and *T. lidiae.* Extinction of these elements mainly representing group P_2 may be interpreted as a consequence of climatic cooling. Moreover, the early Miocene was a period of appearance of new forms in some of the aforementioned genera, e.g., *Brasenia*

bresciana Dorof., *B. dorofeevii* T.V. Yakub., *Caldesia proveutitia* P. Nikit., *Epipremnites reniculus* (Ludw.) Mai, and *Po-tamogeton carbonatus* Dorof. A considerable group of neophytes from other genera also was generated in this period, for instance, *Melastonites tertiaria* Dorof., *Cladium trilobatum* (Mai) Mai, *Ceratophyllum spinulosum* Dorof., *Proserpinaca pterocarpa* Dorof., *Punica natans* (P.N. Nikit.) Mai, *Palaeoeuryale, Trapa* (?) and diverse *Nyssa* forms.

In contrast to Oligocene assemblages, oryctocoenoses of carpolites from the Miocene brown coals permanently include assemblages of *Brasenia* and *Pinus* taxa (*Pinus–Athrotaxis–Brasenia bresciana–Boehmeria pusilla–Caricoidea ovalis; Pinus–Brasenia dorofeevii; Pinus–Brasenia bresciana + B. dorofeevii–Caricoidea ovale–Trapa;* and *Pinus–Epipremnites reniculus–Brasenia bresciana–Caricoidea ovale*).

When correlating our and late Oligocene–early Miocene floras from brown coal beds of Germany, Poland, and Slovakia, we met two principal inconveniences. First, being chiefly recovered from core samples obtained by drilling, Belarussian floras are less representative than European analogues rich in arboreal plant remains. Secondly, many species originally described in Belarus have never been identified in other countries. Nevertheless, our floras still may be correlative with the Tagebau Borna, Borna Ost, Witznitz III, and Witznitz IV floras of the "Floreuzona I," and also with other assemblages of the "Floreuzona II" in classification of Mai and Walther (1991). The latter persistently include *Alnus lusatica* Mai and several other taxa typical of the Belarussian floras (*Taxodium dubium, Athrotaxis, Epipremnites ornatus, Decodon gibbosus, Saururus bilobatus,* and *Caricoidea jugata*). The early Miocene floras of "Floreuzona III" in the Mokrena, Biterfeld Hauptfloz, Langenreicheubach, and some other localities of Saxony contain many species inherited from the Oligocene time. Dominant genera in respective oryctocoenoses are *Taxodium, Alnus, Trapa* (?) and some others.

MINERAL COMPOSITION OF SEDIMENTS

Quartz, glauconite, and feldspar constitute 85–99% of continental Oligocene deposits also containing admixture of clay and accessory authigenic minerals derived from the underlying Paleogene sediments of the marine genesis. Rocks of the Starodubka Formation are most closely related to the latter. These rocks contain 87.6 % of quartz, 6.2% of glauconite, and 3.4 % of feldspar. Their light mineral fraction also includes chalcedony and muscovite. Heavy minerals of sands are mainly represented by ilmenite (49.1%), leucoxene (13.3%), zircon (10.4%), and rutile (10.0%) associated with accessory disthene, sillimanite, staurolite, tourmaline, and single grains of amphibole, garnet, epidote, andalusite, and pyroxene. In clay beds of the Starodubka Formation, leucoxene (14.2%) and zircon (18.6%) are more abundant than ilmenite (12.8%), whereas garnet, epidote, and amphibole disappear from their mineral composition, because these mineral tend to be concentrated only in certain grain-size fractions.

Clay fractions of the rocks consist of the polymineral hydromica–kaolinite–montmorillonite association with an insignificant admixture of mixed-layer minerals and hydrogoethite; the latter is especially typical of the upper part of the Starodubka Formation. Content of siderite, the main authigenic mineral of this formation, is 4.5 % in sands and 14.6% in clays. Marine deposits rich in pyrite, glauconite, and jarosite apparently served as the source rocks of components for siderite formation.

The white sand lenses differ by mineral composition from all other rock types. They consist of well rounded mineral grains very monotonous in granulometric parameters (over 85% of grains range in size from 0.1 to 0.25 mm). The light mineral fraction of these rocks consists of quartz (100%) and lacks the clay admixture. Accessory minerals are represented by zircon (14%), tourmaline (17.4%), rutile (16.0%), staurolite (14.2%), and disthene (12.6%), which are very resistant against weathering. Other guide minerals of Cenozoic rocks, such as ore and authigenic compounds, amphibole, pyroxene, and epidote are missing. Such a peculiar composition of studied sands suggests them to be accumulated under specific hydrodynamic, physical, and chemical conditions of sedimentation in the ancient flow-type lakes (Murashko, 1993).

Coal-bearing deposits display a series of characteristic features of their mineral composition, and first of all, the very wide concentration ranges of many minerals. For instance, the estimated abundance varies from single grains to 31.8% of the rock volume for glauconite, or in the heavy mineral fraction, it changes from 14.2 to 59.6% for ilmenite, from 0.2 to 56.4% for leucoxene, and from 5.2 to 30.6% for zircon. Second, the upward decreasing diversity of mineral composition and simultaneously increasing degree of weathering, that is characteristic of many Oligocene rocks, are not manifested in the coaliferous deposits. Unstable minerals, such as feldspar, garnet, epidote, and amphibole, may be concentrated at various levels of the latter. Third, these sediments are very rich in organic remains (brown coal seams, lignite fragments, and well-preserved spores, pollen, and carpolites), because the sedimentation conditions in deep lake depressions were favorable for accumulation and conservation of this material. Fourth, mineral associations in the coaliferous and related Paleogene to Cretaceous rocks often are identical and suggest that stages of the normal lacustrine–alluvial sedimentation alternated with the diluvial phases and collapse events in walls of the gradually deepening karst holes. Fifth, precisely these Oligocene sediments are devoid of authigenic limonite, whose content in other rocks may be as high as 37.9%. We studied several borehole sections in the Tonezh coaliferous area in order to elucidate mineralogical differ-

ence between the Oligocene coal-bearing and overlying Miocene deposits.

The results obtained on the sandy to silty rock fractions show that, relative to the Miocene sediments, the Oligocene deposits have in average a higher percentage of the heavy mineral fraction (4.8 versus 1.6%), ilmenite (35.5 versus 23.3%), and sillimanite (7.1 versus 1.6%). At the same time, they have a lower content of garnet (0.6 versus 6.6%), amphibole (0.6 versus 2.2%), and staurolite (0.6 versus 3.3%). Authigenic minerals from these two levels are also different (limonite in the Oligocene beds and pyrite in the Miocene deposits). In addition, brown coal beds of the Oligocene and Miocene are again different in composition (Azhgirevich, 1979).

Thus, paleobotanical and lithologic studies on the upper Oligocene deposits in Belarus allow us to conclude the following:

(1) Sedimentation of that time proceeded in the continental environments.

(2) The recurrent climatic fluctuations resulted in changes in the flora composition, which became depleted in tropical elements, but enriched in subtropical and especially in arctic-tertiary plants. This trend corresponds to the cooling and aridization of the continental seasonal climate.

(3) Eight spore–pollen assemblages distinguished in sediments are correlative with coeval floras of Ukraine and western Europe. The carpolite flora of Belarus includes more than 110 fossil species.

(4) According to paleobotanical data from Belarus, the upper Oligocene boundary is inside the coal-bearing deposits filling karst depressions here.

(5) Coaliferous deposits of the Brest and Pripyat depressions are correlative with the Krupeiki Formation in both the genetic and age aspects, and therefore they may be considered as constituents of the latter.

Reviewer M.A. Akhmet'ev

REFERENCES

Azhgirevich, L.F. and Levkov, E.A., The Karst Type of Coal Accumulation in Byelorussia, *Dokl. Akad. Nauk BSSR,* 1979, vol. 23, no. 3, pp. 265–268.

Azhgirevich, L.F., Rylova, T.B., and Yakubovskaya, T.V., Position of the Krupeiki Formation in the Cenozoic Section of the Turov Depression, *Dokl. Akad. Nauk BSSR,* 1990, vol. 34, no. 10, pp. 936–940.

Ciuk, E., Schematy litostratygraficzne trzeciorzedu Nizu Polskiego, *Kwart. Geol.,* 1970, vol. 14, no. 4, pp. 754–771.

Ciuk, E., Schematy litostratygraficzne paleogenu Polski poza Karpatami i zapadieskiem przedkarpackim, *Biul. Inst. Geol.,* 1974, vol. 281, no. 7, pp. 7–48.

Dorofeev, P.I., Data on History of the Genus *Glyptostrobus* Ende, *Bot. Zh.,* 1974, vol. 59, no. 1, pp. 3–13.

Dorofeev, P.I., Taxonomy of the Neogene *Potamogeton* from Byelorussia, *Dokl. Akad. Nauk BSSR,* 1977, vol. 21, no. 8, pp. 736–738.

Dorofeev, P.I., Data on History and Taxonomy of the Genus *Brasenia* (Cabombaceae), *Bot. Zh.,* 1984, vol. 69, no. 2, pp. 137–148.

Dorofeev, P.I., *Miotsenovye flory Tambovskoi oblasti* (Miocene Floras of the Tambov Region), Leningrad: Nauka, 1988.

Dorofeev, P.I. and Manykin, S.S., Oligocene Flora from the Village of Starodubka at the Dnieper River, *Dokl. Akad. Nauk BSSR,* 1969, vol. 13, no. 5, pp. 464–466.

Dyjor, S., Litostratigrafia neogenu Ziemli Lubuskiej: Surowce Mineralne Ziemli Lubuskiej, *Przew. 50 Zjazdu Pol. Tow. Geol.,* 1978, pp. 210–214.

Dyjor, S., Sedimentary Succession and Paleogeographic Evolution of Border Zones of the Silesian Part of Paratethys and of the Tertiary Polish-German Basin, *Zesz. Nauk AqH "Geologia",* 1986, no. 12, pp. 7–23.

Dyjor, S. and Sadowska, A., Proba korelacji wydzielen stratygraficznych i litostratygraficznych trzeciorzedu zachodniej czesci Nizu Polskiego i slaskiej czesci Paratetydy w nawiazaniu do Projektu IGCP NR 25, *Prz. Geol. (Warszawa),* 1986, no. 34, pp. 380–386.

Geologiya SSSR, T. 3: Belorusskaya SSR (Geology of the USSR, vol. 3: Byelorussian SSR), Moscow: Nedra, 1971.

Grichuk, V.P., Zelikson, E.M., and Borisova, O.K., Reconstructed Climatic Indices of the Early Cenozoic Based on Data of Paleobotany, in *Klimaty Zemli v geologicheskom proshlom* (Climates of the Earth in the Geological Past), Moscow: Nedra, 1987, pp. 69–77.

Iskopaemye tsvetkovye rasteniya SSSR (Fossil Flowering Plants of the USSR), 2 vols., Leningrad: Nauka, 1982.

Mai, D. and Walther, H., Die oligozanen und untermiozanen Floren Nordwest-Sachsens und des Nitterfelder Raumes, *Abh. Staat. Mus. Mineral. Geol. Dresden,* 1991, vol. 38, pp. 1–230.

Manykin, S.S., *Stratigrafiya tretichnykh otlozhenii Belorussii* (Stratigraphy of the Tertiary Deposits in Byelorussia), Minsk: Akad. Nauk BSSR, 1959.

Manykin, S.S., Pollen from the Upper Oligocene and Neogene Deposits of Byelorussia and Its Stratigraphic Significance, in *Paleontologiya i stratigrafiya BSSR* (Paleontology and Stratigraphy of the BSSR), Minsk: Nauka i Tekhnika, 1966, pp. 144–297.

Manykin, S.S., *Paleogen Belorussii* (The Paleogene of Byelorussia), Minsk: Nauka i Tekhnika, 1973.

Materialy po stratigrafii Belorussii (Materials Concerning the Stratigraphy of Belarus), Minsk: Nauka i Tekhnika, 1981.

Murashko, L.I., The Oligocene of Belarus (Structure, Composition, and Sedimentation Environment), *Cand. Sci. (Geol.–Min.) Dissertation,* Minsk: Inst. Geosciences, Belarussian Acad. Sci., 1993.

Odrzywolska-Bieńkowa, E., Kosmowska-Ceranowicz, B., *et al.,* Syntetyzny profil stratygraficzny trzeciorzedu polskiej czesci polnocno-zachodniego basenu trzeciorzedowego Europy, *Prz. Geol.* (Warszawa), 1979, no. 9, pp. 159–161.

Okinshevich, A.E., Coal Reserves of the Upper Oligocene–Miocene Deposits in the Pripyat Depression, *Cand. Sci. (Geol.-Min.) Dissertation,* Moscow: Moscow State Univ., 1973.

Piwocki, M., Charakterystyka chemiorno-technologiczna glownych grup trzeciorzedowych weglu brunatnych w Polsce, *Biul. Inst. Geol.,* vol. 357, pp. 41–60.

Resheniya mezhvedomstvennogo regional'nogo stratigraficheskogo soveshchaniya po razrabotke unifitsirovannykh stratigraficheskikh skhem Belorussii (Resolutions of the Interdepartmental Stratigraphic Conference on Elaboration of the Unified Stratigraphic Scheme for Byelorussia), Leningrad: Vses. Geol. Inst., 1983.

Rylova, T.B., New Palynological Data Characterizing the Lower Brown-Coal Formation in the Southwestern Byelorussia, *Dokl. Akad. Nauk BSSR,* 1987, vol. 31, no. 10, pp. 912–915.

Rylova, T.B., Age of Brown Coal Occurrence near the Gresk, *Dokl. Akad. Nauk BSSR,* 1991, vol. 35, no. 3, pp. 270–273.

Rylova, T., Paleofloristic and Paleoclimatic Changes in the Oligocene of Belarus, *Proc. Int. Symp.: Paleofloristic and Paleoclimatic Changes during Cretaceous and Tertiary,* Bratislava, 1993, pp. 93–97.

Yakubovskaya, T.V., Age of the Poltava Group Deposits near the Beloozersk, in *Geologicheskie issledovaniya kainozoya Belorussii* (Geological Investigations of the Cenozoic in Byelorussia), Minsk: Nauka i Tekhnika, 1981, pp. 165–176.

Yakubovskaya, T., Evolution of Flora and Climate in the Miocene of Belarus, *Proc. Int. Symp.: Paleofloristic and Paleoclimatic Changes during Cretaceous and Tertiary,* Bratislava, 1993, pp. 153–158.

Yakubovskaya, T.V., Problems of the Neogene Stratigraphy in Belarus, *Litosfera,* 1994, no. 1, pp. 56–66.

Yakubovskaya, T.V. and Rylova, T.B., Late Cenozoic Floras from the Neogene Karst Area near Bereza, in *Flora i fauna kainozoya Belorussii* (Cenozoic Flora and Fauna from Belarus), Minsk: Nauka i Tekhnika, 1992, pp. 76–94.

Ziembińska-Tworzydlo, M. and Wazyńska, H., Palynological Subdivisions of the Neogene in Western Poland, *Bull. Acad. Polon. Sci., Ser. Sci. de la Terre,* 1981, vol. 34, no. 1, pp. 29–43.

Zinova, R.A. and Burlak, A.F., New Data on Correlation of the Upper Oligocene Deposits near Loev, the Dnieper River Region, in *Problemnye voprosy geologii antropogena i neogena Belorussii* (Vital Problems of the Anthropogene and Neogene Geology of Byelorussia), Minsk: Nauka i Tekhnika, 1980, pp. 20–28.

Zinova, R.A. and Rylova, T.B., Correlation between the Oligocene Starodubka Formation of Byelorussia and the Bereka Formation of Ukraine, in *Geologiya i gidrogeologiya kainozoya Belorussii* (Cenozoic Geology and Hydrogeology of Byelorussia), Minsk: Nauka i Tekhnika, 1985, pp. 77–85.

Zosimovich, V.Yu., The Upper Eocene, Oligocene, and Miocene of the Sub-Paratethys, *Doctoral. (Geol.-Min.) Dissertation,* Kiev: Inst. Geosciences, Ukrainian Acad. Sci., 1992.

Zosimovich, V.Yu. and Rotman, R.N., Zmievka Beds in the Southeastern Pripyat Depression, *Geol. Zh. Akad. Nauk Ukr. SSR,* 1976, vol. 36, no.6, pp. 120–125.

Stratigraphy and Geological Correlation, Vol. 6, No. 4, 1998, pp. 397–407. Translated from Stratigrafiya. Geologicheskaya Korrelyatsiya, Vol. 6, No. 4, 1998, pp. 81–91.
Original Russian Text Copyright © 1998 by Logachev, Rasskazov, Ivanov, Misharina, Chernyaeva.
English Translation Copyright © 1998 by МАИК Наука/Interperiodica Publishing (Russia).

Stratigraphy of the Upper Cenozoic Volcanosedimentary Sequence in the East Sayan Mountains Adjacent to the Baikal Region

N. A. Logachev, S. V. Rasskazov, A. V. Ivanov, V. A. Misharina, and G. P. Chernyaeva

Institute of the Earth's Crust, Siberian Division, Russian Academy of Sciences, ul. Lermontova 128, Irkutsk, 664033 Russia

Received January 10, 1996

Abstract—The large-scale geological mapping in the southeastern area of the East Sayan Mountains permitted the subdivision of the Upper Cenozoic volcanosedimentary sequence into three units: the Sorok (lower–middle Miocene, 24–12 Ma), Khirpisa (upper Miocene, 11–6 Ma), and Khirbes (Pliocene, 5–1.6 Ma) formations. The K-Ar dates for basaltic lavas are in agreement with the age determinations by palynological assemblages recovered from the sedimentary lenses intercalated with lavas. The factorial analysis of spore and pollen spectra revealed two stages in the evolution of vegetal assemblages: first, the stage of gradual degradation of the Turgai-type flora during the warm humid climate of the Miocene and, second, the stage of the boreal flora evolution that succeeded the former after a sudden cooling and aridization of climate. This crisis in flora development occurred in the late Miocene 10 to 5 Ma ago.

Key words: *Neogene deposits, basaltic lavas, spores, pollen, diatomaceous algae, K-Ar dates, Interior Asia*

INTRODUCTION

In the past several decades, the palynological and diatom analyses were the most reliable methods for stratigraphic subdivision of continental Cenozoic deposits in Interior and East Asia. Owing to a sudden climatic change, the difference between the compositionally contrasting palynological and diatom spectra from the Miocene and Pliocene sequences is fairly distinct (Logachev *et al.*, 1964; *Litologiya...*, 1972; Belova, 1985; Popova *et al.*, 1989). Extensive studies on the Late Cenozoic stratigraphy were carried out in inner parts of the continent to subdivide the rock sequences in detail. In the continental Neogene deposits of the Far East, four biostratigraphic zones were identified on the basis of diatoms in the interval between the terminal lower and upper Miocene. These zones are of an interregional rank for their correlation, for example, with those of the Baikal region (Moiseeva, 1995). The Late Cenozoic paleoclimatic reconstructions are now based on the results of a study of malacofauna and buried soils (Popova, 1994; Vorob'eva *et al.*, 1994; 1995). The stratigraphic data on the Baikal region, however, should be verified by data of isotopic geochronometry.

In Interior Asia, the first attempt to compare the biostratigraphic and absolute age data was realized for the early–middle Miocene of the Vitim Plateau and the Pliocene of Central Mongolia, where palynological assemblages, recovered from the sedimentary lenses in basaltic lavas were studied concurrently with the K-Ar dating of the latter (Logachev *et al.*, 1982; Bazarov *et al.*, 1984). In the course of a large-scale geological mapping in the southeastern part of Eastern Sayan, the Upper Cenozoic volcanosedimentary sequence was divided into three units: the Sorok (lower–middle Miocene), Khirpisa (upper Miocene), and Khirbes (Pliocene) formations. These units displaying different localization in the relief can be mapped because of variations in their composition and on the basis of K-Ar dating (Rasskazov, 1993).

In the present paper, the results of the study of the spore, pollen and diatom assemblages recovered from the sedimentary lenses of the aforementioned formations are summarized, and the obtained results are compared with the K-Ar dates for volcanic rocks.

STRATOTYPES OF THE FORMATIONS

The Sorok Formation of the lower–middle Miocene is composed mainly of lavas. Its stratotype is located upstream of the estuary of the Sorok River, which is the right-hand tributary of the Oka River (Fig. 1). In this locality, a pile of basaltic lavas more than 120-m thick was accumulated in a deep fluvial paleovalley. The thalweg of the filled paleovalley rises only 50–60 m above the present-day thalweg.

The Khirpisa Formation of the upper Miocene is composed of sedimentary–volcanic beds. Its stratotype is located at the Mt. Dozoroi-Urda-Khirpisa on the right-hand wall of the Tissa River valley near the Dozor-Nur Lake. The section and its parts are described in the works by Obruchev (1946), Grosval'd (1965), Kiselev and Medvedev (1969), Kiselev *et al.*, (1979), and others. The scarp with exposed rocks is about 300 m high. The lower 100 meters of the section include flows of black olivine–phyric and aphyric

basalts with lenses of coal-bearing sediments and pyroclastic material. Upsection, there are the 30-m-thick lens of fine-clastic deposits and numerous rather thin flows of ashy-gray lavas.

The Pliocene Khirbes Formation was named after the picturesque Khirbes Cliff composed of basaltic rocks on the left-hand wall of the Oka River valley below the Bokson River estuary. The section begins with a lens of shingle and consists of highly vesicular basalts. The total thickness of lava flows reaches 100 m.

SEDIMENTARY LENSES IN THE VOLCANOSEDIMENTARY SEQUENCE

The sedimentary lenses in the Sorok Formation are rare. The largest (100-m thick) is on the left-hand bank of the Urik River near the Yankhor River source. The lens is composed of homogeneous gray fine-laminated shales, in the upper part of gritstones, and is overlain by a packet of basaltic lavas 100 m thick.

Sediments in the upper reaches of the Ekhe-Kheiregte River (the right-hand tributary of the Oka River) also form a part of the Sorok Formation; they rest above the basement surface exposed near the 1970-m elevation mark at the southern foot of the Renchin-Khumba Mountain. The sediments were recovered by a series boreholes located along a transect more than 0.5 km long. The thickness of sediments varies from 10 to 15 m. Sandstones of the section are variable in the grain-size parameters (medium- to fine-grained); they are intercalated with siltstone beds and locally cross-laminated. There are horizons of sooty-black carbonaceous rocks and lignites. The thalweg of the Ekhe-Kheiregte paleovalley, buried under the Sorok basaltic lavas, is 200 m below the base of the sediments. The upper lava flows of the paleovalley overlie the sedimentary deposits.

The Khirpisa and Khirbes formations are penetrated by drilling along a transect of boreholes 4.2 km long in the Tabin-Zurta River valley (the left-hand tributary of the Urdo-Bokson River in the Oka River basin). The transect crosses the sublatitudinal part of the valley in the middle course of the river (Fig. 2; location of the section is shown in Fig. 1).

In the Khirpisa Formation of the Tabin-Zurta section, beds of light and greenish gray, often fine-laminated shales are intercalated with the light gray and light brown coarse- to fine-grained sands and with flows of black massive aphyric and olivine–phyric basalts. The basaltic flows locally discontinuous in the lateral direction are missing in two boreholes. The share of basalts in individual core sections is not greater than 50%. Claystone interbeds locally contain numerous fragments of fossil wood and are enriched in the coalified organic matter. One of the boreholes, drilled in the Khirpisa Formation, penetrated through a lens of boulder–shingle deposits. The lens is rich in basaltic pebbles deposited on the erosion surface of the lava flow. It is overlain by the light brown coarse-grained sand with occasional inclusions of well rounded pebbles. The exposed part of the Khirpisa Formation is 20 to 35-m thick.

The accumulation of sediments and lavas of the Khirpisa Formation was followed by the development of an erosion paleovalley that cut into the basement rocks and then was buried by clastic deposits and lavas of the Khirbes Formation. In the erosion paleovalley, the sedimentary sequence begins with a lens of greenish gray medium-grained sand 12 m thick and enclosing soil interbeds and wood remains. Upsection, the bed of well sorted sand–shingle material is covered by the bed of boulder, shingle, and unsorted coarse-grained material. This bed includes interbeds of loosely cemented greenish gray siltstones and sandstones. The sedimentary detritus that filled the paleovalley was mostly derived from basalt, and the thickness of the coarse-grained lens is 20 m. It is overlain by a horizon of fine-grained sediments, which were deposited in the following succession: coarse-grained sands, greenish gray fine-laminated silty sandstones, silty sandstones with indistinct disrupted lamination, homogeneous silty sandstones, and light gray medium-grained fine-laminated sands with inclusions of basaltic pebbles. The thickness of the horizon of fine-grained sediments is 10 m. The total thickness of the exposed deposits in the erosion paleovalley is 32 m. At the southern end of the transect, the borehole entered the upper part of the sedimentary sequence of another paleovalley.

Sediments of the Khirbes Formation are overlain by a packet of vesicular ashy-gray basaltic lavas with visible crystals of olivine. At the base of the lava packet, almost all boreholes reached a horizon of brown shingle. Volcanic eruptions were preceded by deposition of yellow clastic tuffs and hyaloclastites overlain by the dark red bed of pyroclastic material.

Inside the upper lava packet of the Khirbes Formation, the sedimentary lenses are scarce and not more than 2 m thick. One of these lenses is composed of well sorted shingle and yellowish brown gravely sand. Some of the lenses consist of loosely cemented greenish gray siltstones. According to drilling data, the total thickness of basaltic flows of the Khirbes Formation in the Tabin-Zurta section is not more than 60 m.

Deposits of the Khirbes Formation are eroded and covered by the Quaternary, mainly coarse-grained loose sediments. Two boreholes drilled in the lower part of the valley, north of the river thalweg, reveal the laminated structure of the Quaternary part of the section. The 5-m-thick bed of fluvial rounded pebbles overlies here the Khirbes Formation sediments. In the next 9 meters of the section, the boulder–shingle beds show three intercalated interbeds of yellow-green and green-gray shales with sparsely distributed well rounded pebbles. The coalified trunk of a tree was found in the middle of the horizon. The upper part of the section is composed of coarse clastic morainal deposits. At the northern wall of the Tabin-Zurta valley,

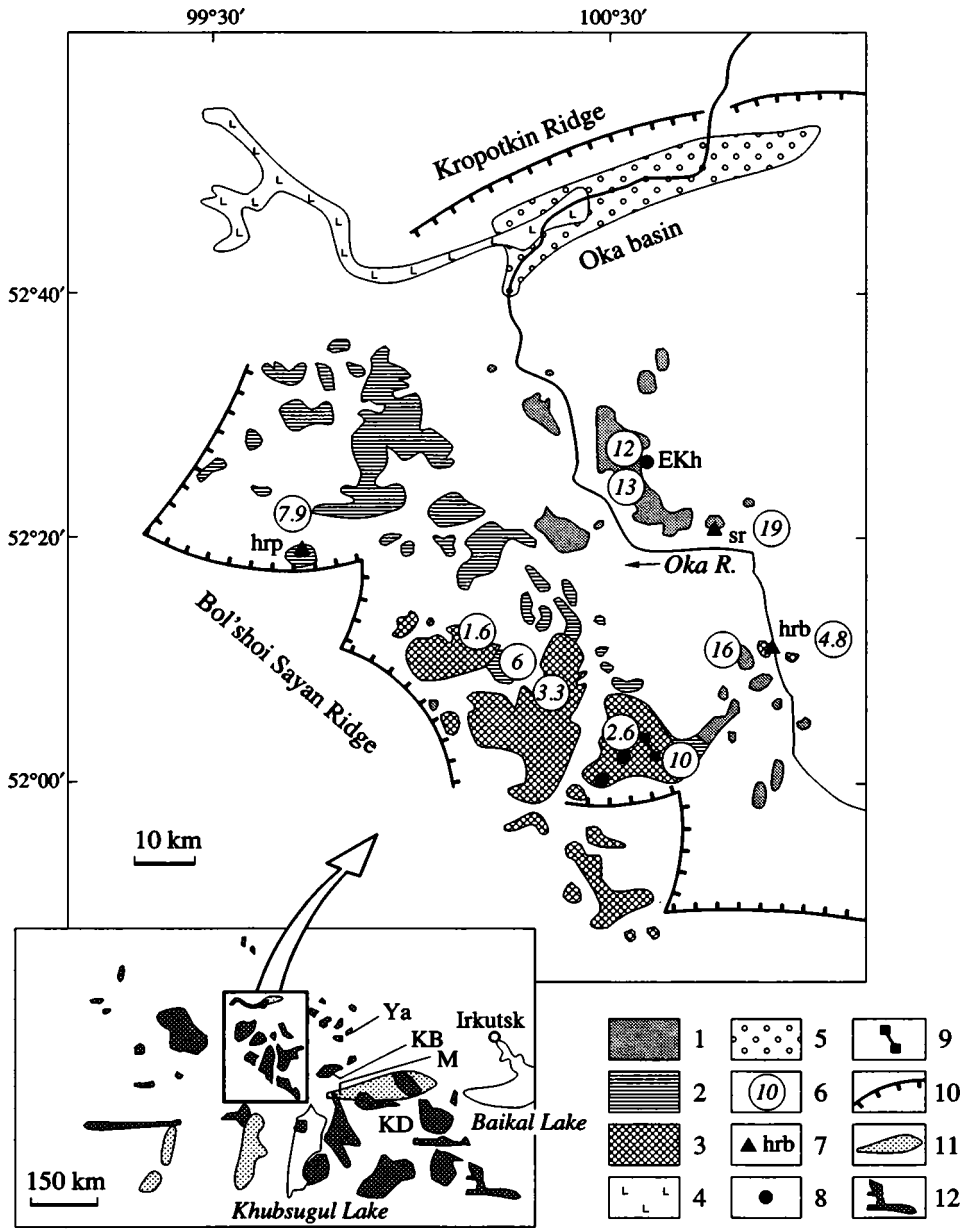

Fig. 1. Scheme of spatial distribution of formations of the volcanosedimentary sequence in the eastern part of the East Sayan Mountains: (1) Sorok Formation (sr); (2) Khirpisa Formation (hrp); (3) Khirbes Formation (hrb); (4) Holocene basalts; (5) Quaternary deposits in the depression; (6) K-Ar dates for basalts, Ma; (7) stratotype localities; (8) localities of some reference sections with dated sedimentary lenses; (9) Tabin-Zurta transect (see Fig. 2); (10) most steep frontal scarps of ridges framing the Oka plateau; (11) depression of the Baikal Rift Zone; (12) basalts; reference sections of volcanosedimentary rocks: (Ya) Yankhor, (M) Mondi basin, (KB) Kitoi Bald Mts., (KD) Khamar-Daban, (EKh) Ekhe-Kheiregte.

their thickness reaches 30 m. At the southern wall, the bed of morainal deposits is only 5 m thick.

The volcanosedimentary sequence exposed in the Tabin-Zurta valley is deformed. The largest amplitudes of vertical displacements of skew rock block at the southern wall of the valley are, apparently, the result of the recent activation of the ancient fault zone in the pre-Cenozoic basement.

The Khirpisa and Khirbes formations were traced by other transects of boreholes located 5 km west of the described section in the upper reaches of the Tabin-Zurta River, and 6 km further southwest in a valley connecting the Mongol-Daban River (the left-hand tributary of the Urdo-Bokson River) with the Altyn-Zhalga River (the right-hand tributary of the Dibi River).

THE AGE OF BASALT LAVAS BY K-Ar DATINGS

The K-Ar dating of basalt lavas was performed by A.S. Batyrmurzaev at the Institute of Geothermal Prob-

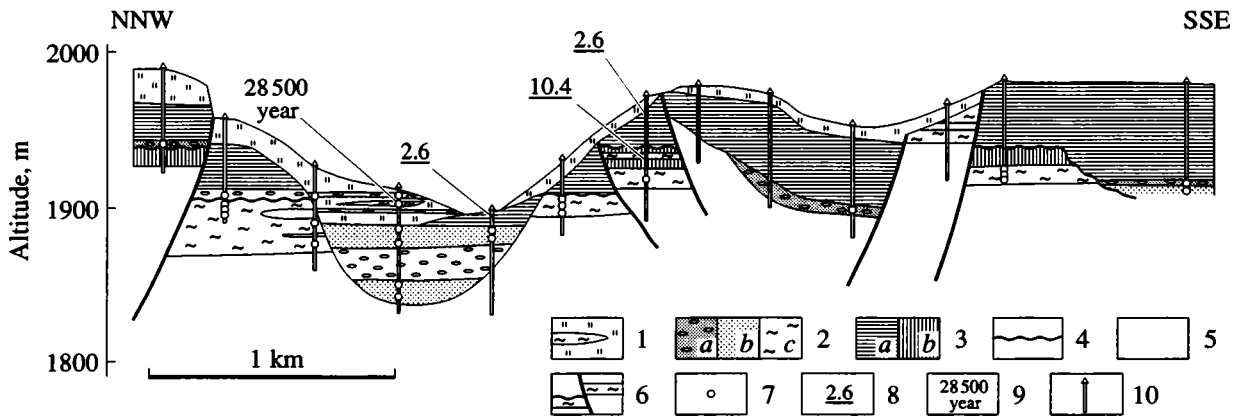

Fig. 2. The Tabin-Zurta reference section (see location in Fig. 1): (1) Quaternary post-basalt coarse-grained deposits with claystone lenses; (2) Pliocene, Khirbes shingle beds of boulder (*a*) or sandy (*b*) types and upper Miocene Khirpisa claystones, siltstones, and silty sandstones (*c*); (3) basalts (*a*) Khirbes, (*b*) Khirpisa; (4) upper boundary of the Khirpisa Formation covered with lavas and the Khirbes Formation sediments; (5) pre-Cenozoic basement rocks; (6) faults; (7) sampling localities for palynological and diatom analyses; (8) K-Ar dates for basaltic lavas, Ma; (9) radiocarbon date for coalified wood; (10) boreholes.

lems of the Dagestan Scientific Center of the Russian Academy of Sciences and by G.G. Mehnert at the Denver Federal Center of the US Geological Survey. The results were published in three papers (Rasskazov *et al.*, 1990; 1991; Rasskazov, 1993). The age of lavas in the Sorok Formation was determined to be 24–12 Ma and date of 19.4 ± 1 Ma was obtained for the stratotype. The Sorok Formation lavas that cover the lens of Yankhor sediments were dated as 20.3 ± 1.0 and 20.7 ± 0.8 Ma old. In the Ekhe-Kheiregte River head, deposits are overlain by lavas 12.4 ± 0.6 Ma old.

Lavas of the Khirpisa Formation are attributed to the upper Miocene (11–6 Ma). The K-Ar date of 7.9 ± 0.7 Ma was obtained for basalts in the middle part of the stratotype. A lava flow intercalated with fine-grained sediments in the Khirpisa part of the Tabin-Zurta section is dated as 10.4 ± 1.0 Ma old.

The Khirbes Formation includes the Pliocene lavas and sediments 5–1.6 Ma old. The K-Ar date for basalts from the upper part of the stratotype is 4.75 ± 0.3 Ma. Two identical dates of 2.6 ± 0.5 Ma were obtained for the basalts in the Khirbes part of the Tabin-Zurta section. The dated basalts overlie the sediments of the Pliocene paleovalley (Fig. 2). Taking into account the age of the erosion incision filled with the stratotype lavas, the deposits of the Tabin-Zurta section should be as old as 4.75–2.6 Ma.

The radiocarbon date of 28500 ± 400 years for the coalified wood remains, recovered from a siltstone interbed at the depth of 11 m in the Quaternary deposits of the Tabin-Zurta section (Fig. 2), was obtained by S.N. Litasova at the Institute of Volcanology of the Far East Scientific Center of the Russian Academy of Sciences (sample IVAN-789).

COMPOSITION OF SPORES, POLLEN AND DIATOMS IN THE SEDIMENTARY LENSES

The earlier studies of spore and pollen composition in the sedimentary lenses of the Oka Plateau were restricted mainly to the section of the Mt. Dozoroi-Urda-Khirpisa. Age interpretations of pollen spectra are contradictory. The sample studied by Obruchev (1946) was recovered from the claystone lens at the base of the sequence and, according to A.N. Krishtofovich, it contains the Miocene spore–pollen assemblage. Later, on the basis of palynological data, Grosval'd (1965) identified the Tertiary and Quaternary parts of the section. Kiselev and Medvedev (1969) considered the volcanic flows as constituents of the integrated lower–middle Miocene sequence. The K-Ar date of 7.9 Ma indicates that its sedimentary lenses are not younger than the late Miocene.

From sedimentary lenses intercalated with volcanic beds of the Oka Plateau, 132 samples were collected and analyzed for spores and pollen. The representative spore–pollen spectra were obtained from 44 samples. Other samples either lacked spores and pollen, or yielded single specimens. The results of the palynological analysis are shown in the table of age groupings of spore–pollen spectra distinguished by factorial analysis. Diatoms were found in several samples.

In most thin sedimentary lenses of the Sorok Formation, spores and pollen are missing. Of the 26 samples recovered from the sections in the basins of the Khore, Urik, Ekhe-Kheiregte, and Yankhor rivers, only five samples from the latter two localities produced representative palynological spectra.

In the Yankhor section, a wide spectrum of spores and pollen was obtained from the siltstone–sandstone beds overlain by lavas 20 Ma old. Pollen of gymnosperm plants dominates in the spectrum. These are various *Tsuga*, fir, pine, *Abies*, and *Podocarpus* species.

They coexist with pollen of the Boreal thermophilic flora represented by linden, beech, hornbeam, maple, *Carya, Pterocarya,* walnut, hazel, parvifoliate birch, alder, willow, and Ericaceae. Rare spores mostly belong to ferns of Polypodiaceae, *Botrychium*, sphagnum, and green mosses. Similar spectra from the Tankhoi and Bayandai formations are the early–middle Miocene in age (Logachev *et al.,* 1964; *Litologiya...,* 1972). In sediments of the Yankhor lens, Yu.P. Katyukha found remains of a segment leaf of *Comptonia naumanii* (Nath.) Huzioka sp. dated back to the early Miocene by M.A. Akhmet'ev from the Geological Institute, Russian Academy of Sciences (Rasskazov *et al.,* 1986).

Spectra from sediments of the Sorok Formation in the upper reaches of the Ekhe-Kheiregte River are similar to those of the Yankhor section and, probably, are of the same age. The differences between these spectra revealed by the multi-component factorial analysis will be discussed below.

The sedimentary lenses of the Khirpisa Formation are more enriched in spores and pollen than the lens in the Sorok Formation. Of 21 claystone, siltstone and sand samples from the two Tabin-Zurta sections and one Altyn-Zhalga section, 19 samples yielded similar spectra of abundant and diverse spore–pollen taxa, which compose a unified upper Miocene assemblage with prevalence of gymnosperm plants (45.3–76.5%). In this group, the most abundant are the dark coniferous species: *Picea* sect. *Eupicea, Picea* sect. *Omorica, and Picea* cf. *obovata* (22.0–49.0%). The different *Tsuga* species represent from 6.7 to 17.6% of the assemblage. Pollen grains of *Podocarpus* sp. and *Abies* sp. are less frequent. The presence of *Cedrus* sp. is sporadic (up to 0.5%), and proportion of Taxodiaceae is up to 2.5%. Single pollen grains of *Ephedra* sp. were discovered, and two samples yielded the relict pollen of *Ginkgo* sp.. Pollen of the light coniferous species belongs to various groups of *Pinus* s/g *Haploxylon* (*Pinus* sect. *Strobus, Pinus* sect. *Cemrae*) and to *Pinus* s/g *Diploxylon*. In the last case, it resembles pollen of *Pinus silvestris.*

Pollen of angiosperms (19.9–60.0%) is often represented by specimens of broad-leaved Juglandaceae: *Carya* sp., *Pterocarya* sp., *Juglans* sp., and *Platycarya* sp., which associate with *Engelhardtia* sp., *Carpinus* sp. (in five samples), *Quercus* sp., *Magnolia* sp., *Liriodendron* sp. (in five samples), *Rhus* sp. (in one sample), *Ilex* sp. (in six samples), *Acer* sp., *Tilia* sp., and *Nyssa* sp. (in one sample). The less abundant pollen of small-leaved plants belongs to *Betula* sp., *Alnus* sp., *Corylus* sp., *Salix* sp., *Diervilla* sp., and *Ericales.*

Pollen of herbaceous plants (Compositae, Cypraceae, Gramineae, Liliaceae, Valerianae, and others) was recovered as individual specimens. Sporophytes (1.3–23.8%) are represented by various *Lycopodium* spp. and Polypodiaceae; less frequent are *Botrychium* sp., *Leiotriletes, Osmunda* sp., *Sphagnum* sp., green mosses, Hepaticeae, *Measea,* and *Riccia.* Almost all spectra from the upper Miocene assemblage include unidentified tricolpate and triporate pollen grains, spores, and hyphae of fungi.

The diatomaceous algae were discovered in sediments of the Khirpisa Formation as single specimens. The valves of several species were identified: *Cyclotella* aff. *baicalensis* Skv., *Tetracyclus lacustris* Ralfs var. *lacustris, Actinocyclus gorbunovii* (Sheshuk.) Moiss. et Sheshuk., and *Cocconeis placentula* Ehr..

Before proceeding to the palynological characteristic of sediments in the Khirbes Formation, we should note that in the section of the Tabin-Zurta middle course these sediments are less productive with respect to spores and pollen than those of the Khirpisa Formation. For example, the conditioned spore–pollen spectra were established only in five of the sixteen preparations from sediments that accumulated in this paleovalley before the lava eruptions 2.6 Ma ago. In seven samples of siltstone lenses from two other borehole sections in the upper reaches of the Tabin-Zurta and on the Altan-Zhalga rivers, all palynological determinations were successful. The studied spectra have many similar features and compose a single spore–pollen assemblage.

The gymnosperms compose the larger part of the assemblage. The share of *Pinus* s/g *Dyploxylon* varies from several fractions of percent to 19.7%; *Pinus* s/g *Haploxylon* is as abundant as 3.4 to 23.6%, and Pinaceae pollen grains represent 19% of the assemblage. The exotic pollen of *Pinus* sect. *Strobus* (0.5 and 2.0%) and *Larix* sp. (0.5 and 0.7%) was observed in two samples. The dark conifers are represented by *Picea* sect. *Eupicea* (up to 19.7%) and *Picea* sp. (up to 32%). The share of the exotic and more thermophilic relic *Picea* sect. *Omorica* is 1.9%, whereas various species of *Tsuga* pollen make up 27.9%. Three samples yielded 0.5, 0.7 and 2.0% of the *Abies* sp. pollen grains.

Angiosperms are represented by small- and broad-leaved trees and herbaceous plants. In the assemblage, the share of this group is so small that only their species can be listed. These are the small-leaved Betulaceae (*Betula* sp., *Salix* sp., *Alnus* sp.), broad-leaved Juglandaceae (*Juglans* sp., *Juglans polyporata, Pterocarya* sp.), *Corylus* sp., *Quercus* sp., *Fagus* sp., Ulmaceae, *Diervilla* sp., *Tilia* sp., and others. The herbaceous group includes Gramineae, Cyperaceae, Compositae, *Artemisia* sp., Ranuncluaceae, Caryaphyllaceae, Chenopodiaceae, Onagraceae, and *Thalictrum*. There is a small amount of spores of *Sphagnum* sp., Polypodiaceae, *Lycopodium* sp., *Botrychium* sp., and *Osmunda* sp.

Only two of six samples recovered from the lens of lacustrine deposits underlying lavas 2.6 Ma old yielded the diatom assemblage of *Ellerbeckia arenaria* var. *teres* (Bun.) Crawford with less abundant *Ellerbeckia arenaria* (Moore ex Ralfs) var. *arenaria,* and *Eunotia clevei* Grun. From one to three specimens, we macerated other species, such as *Eunotia clevei* var. *hispida* Skv., *Campylodiscus* sp., *Pinnularia borealis* Ehr., *Stauroneis anceps* Ehr., *Aulacosira* aff. *baicalensis*

(K. Meyer) Sim., and *Actinocyclus gorbunovii* (Sheshuk.) Moiss. et Sheshuk.. The brown shingle bed below basalts produced single valves of diatoms *Actinocyclus gorbunovii* (Sheshuk.) Moiss. et Sheshuk. and *Cyclotella* aff. *baikalensis* Skv.

The spore–pollen spectra of claystones overlying the basalts (28.500 years old) largely differ from the Pliocene spectra of the underlying formations. Its composition is as follows: gymnosperms 2%, angiosperms 60%, and miospores 19%. A sample collected 4 m higher yielded valves of *Ellerbeckia arenaria* (Moore ex Ralfs) var. *arenaria* (five specimens), *Cyclotella baicalensis* Skv. (two specimens), and *Cyclotella* sp. (two specimens).

THE FACTORIAL ANALYSIS OF AGE VARIATIONS IN THE SPORE AND POLLEN COMPOSITION

By processing the spore–pollen spectra in the factorial analysis, we used percentages of all pollen and spore grains (45 forms) determined in the preparations. In addition to 44 spectra from the Oka Plateau sediments, we included in analysis the spectra from volcanic lenses sampled in the adjoining regions south of the Oka Plateau (Fig. 1; inset map). Two spectra characterize samples obtained by M.E. Medvedev from lava sequence of the Khulugaisha River (16.5 ± 0.8 Ma), the Mondi basin, and one spectrum from the lens at the base of the volcanic sequence (12.9 ± 0.7 Ma) of the Margasan Hill in the Khamar-Daban Range. Five spectra were identified in the samples obtained by V.G. Skopintsev from the sequence of the Samarta–Arlyk-Gol waterdivide, the bald peaks of the Kitoi Ridge, where the absolute age of lavas was not determined yet.

Figures 3 and 4 graphically show the results of the factorial analysis. In the vector diagram of families and species, where the coordinates depict values of the first and second factors (Fig. 3), spores and pollen are discriminated into four groups (see table). The first group of hydrophilic and thermophilic plants differs from the three others by the higher values of the second factor indicating a greater age. With the range of low values of the second factor, the second, third and fourth groups of spores and pollen represent the main components of the first factor. The direction of the latter reflects the distribution of forms typical of the warm and humid climate (group 2) and of the cold dry climate (group 4). The third group of forms is intermediate and characterizes, as a rule, the temperate climatic conditions (see table).

The factorial diagram of sample vectors distinctly discriminates the spectra of five age groups. The first and second factors indicate tendencies of vegetation changes in different time intervals. A consecutive displacement of spectra, which are 20, 16–12 and 11–10 Ma old, takes place along the axis of the second factor, and then, in the interval of low values of this factor, the displacement of spectra 11–10, 4.8–2.6 and 0.03 Ma old is oriented along the axis of the first factor.

The data point for spectra from the sedimentary lenses of the Kitoi Bald Mountains plot in the variation field of samples 16–12 and 11–10 Ma old. One spectrum is similar in its parameters with the Late Pleistocene spectrum.

THE PALEOCLIMATIC INTERPRETATION

Due to the limited occurrence of diatoms, the paleoclimatic environments are reconstructed mainly on the basis of data of palynological analysis. Along with results of the radiological dating, these data are used to subdivide the volcanosedimentary sequence into three formations applicable for geological mapping. In addition, the presented factorial diagrams of spores and pollen from sedimentary lenses, with due regard for the K-Ar ages of basaltic lavas, do not eliminate the possibility of elaboration of a more detailed stratigraphic scheme. Another important result of our research is the conclusion that there were two stages in the flora evolution and a sudden change in its composition after the accumulation of sediments 11–10 Ma ago, but before the deposition of beds 4.8–2.6 Ma old.

In the Miocene, during the deposition of the Sorok and Khirpisa formations, the climate in the Oka Plateau was warm and humid. *Tsuga* pollen abundant and diverse in the spectra dated back to 20 Ma ago suggests a considerable dissection of relief even in the early Miocene. *Tsuga,* the so-called "tree of mists", grows on watersheds, while *Picea, Tilia, Acer, Juglans,* and *Platycarya* prefer to colonize the valleys. Judging from the hypsometric position of the Sorok lavas, the magnitude of relative elevations in the early Miocene topography probably was close to 700 m. The broad-leaved–coniferous taiga of the Miocene time consisted of dark conifers spruce, *Abies,* and *Tsuga* associated with relict *Podocarpus,* cedar, swamp cypress, ginkgo, and accessory gnetaceous plants. The light coniferous group of flora included the exotic species of pines and *Pinus* aff. *silvestris,* the latter closely related with the current forest pine. A considerable part of the taiga was composed of various broad-leaved plants: Juglandaceae, *Carya, Pterocarya, Engelhardtia,* hornbeam, oak, beech, chestnut, elm, magnolia, tulip tree, *Rhus, Ilex,* maple, linden, and nyssa. The small-leaved birch, alder, hazel, willow, various species of Ericaceae, and diervilla grew in the underwood. A restricted amount of herbs was represented by Compositae, Liliaceae, velerian, *Scabiosa,* Chenopodiaceae, Gramineae, and Cyperaceae. Sporophytes included *Licopodium, Polypodiaceae, Botrychium,* rare *Osmunda* sp., sphagnum, Hepaticeae, and green mosses. A relatively slight cooling and adaptation of flora to arid conditions during the deposition of the Khirpisa Formation are indicated by the presence of pollen of *Pinus* aff. *silvetris, Ephedra* sp. (single specimens), and herbaceous plants. The

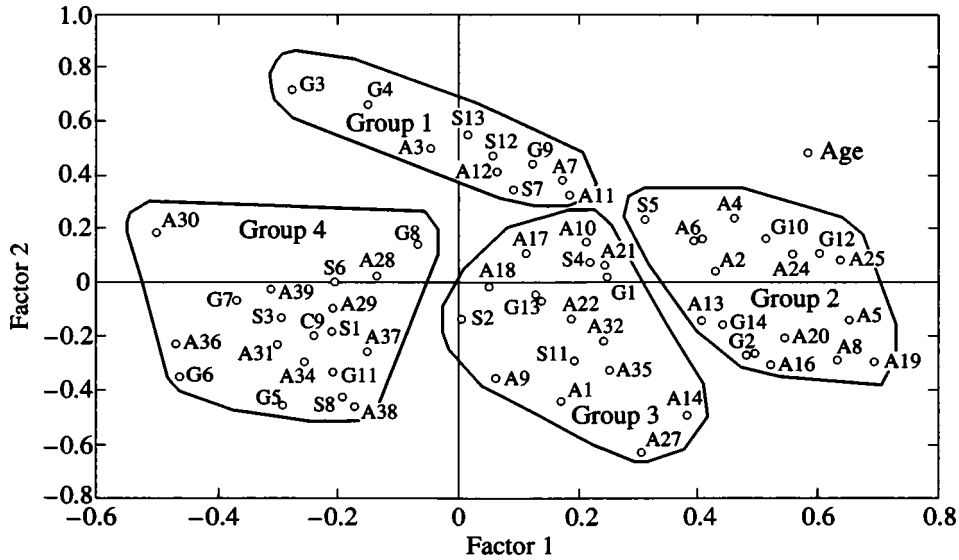

Fig. 3. Factorial diagram of spore and pollen vectors (composition of groups see in table; S—spores; G—gymnosperms; A—angiosperms).

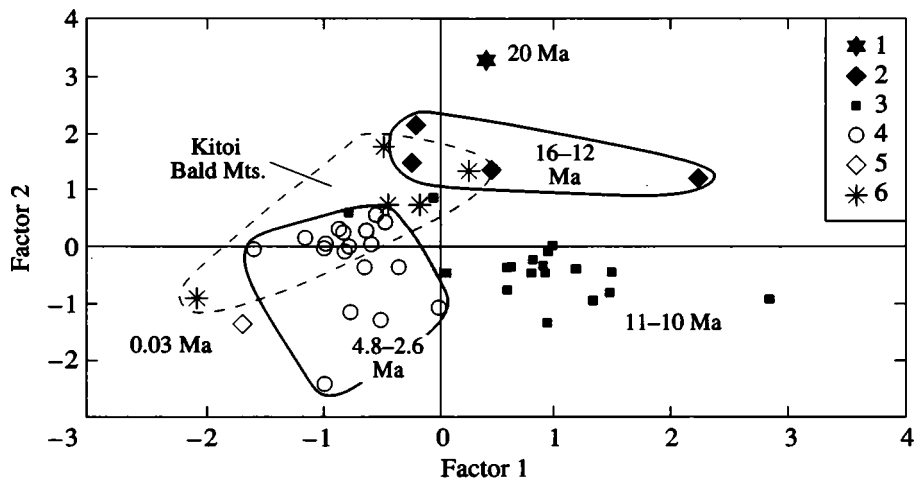

Fig. 4. Factorial diagram of vectors of palynological spectra (structure of factors see in Fig. 3): (1) spectrum of the lower part of Sorok Formation, the Yankhor section; (2) spectra for the upper part of the Sorok Formation, the Ekhe-Kheiregte section, the Mondi basin and Khamar-Daban; (3) spectra for sedimentary lenses of the Khirpisa Formation, the Oka Plateau; (4) spectra for sedimentary lenses of the Khirbes Formation; (5) spectra for Quaternary deposits of the late Karga climatic optimum, the Tabin-Zurta section; (6) spectra for deposits different in age, the Kitoi Bald Mts.

composition of diatoms in this time interval implies a relatively low water temperature in the past lakes.

In the Pliocene, during the second stage of flora development, the Oka Plateau was covered with taiga forests composed of different pine species with an admixture of exotic species *Pinus* sect. *Strobus,* diverse spruces, *Tsuga, Abies*, larch, birch, alder, willow, Juglandaceae, oak, elm, and linden. The underbrush consisted of hazel, honeysuckle, sporadic *Carya,* and magnolia. The herbaceous cover was scarce and contained representatives of Gramineae, Osmundaceae, Compositae, Caryophyllaceae, Chenopodiaceae, Onagraceae, Rosaceae, and Ranunculaceae. There were also ferns (Polypodiaceae, Osmundaceae, *Botrychium*), *Licopodium,* and mosses. The diatom assemblage, recovered from the fine-laminated lacustrine siltstones of the Tabin-Zurta section, developed in the riparian zone of a rather large oligotrophic lake.

A comparison of spore–pollen assemblages from the Khirpisa and Khirbes formations testifies that the Pliocene climate was cooler than before. Although there were still the taiga forests with *Tsuga,* the vegetal

Results of spore–pollen spectra grouping by age in the factorial diagram (see Fig. 3)

Groups and symbols on the factorial diagram		Groups of plants	Spores and pollen	Climatic conditions					20	16–12	11–10	4.8–2.6	0.03
				W	H	T	C	A	Content, %		Age, Ma		
1	S7	Spores	*Leiotriletes* sp.	+	+				0.7	0–3	0–0.4		
	S12		*Polypodium*	+	+				0.7				
	S13		*Polytrichum* sp.	+	+				0.4	0–0.4			
	G3	Gymno-sperms	*Picea* sect. *Eupicea*	+	+				28.7	0–47.8	0–28.8	0–19.7	
	G4		*Picea* sect. *Omorica*	+	+				4.6	0–2.8	0–3.0	0–1.9	
	G9		*Tsuga* sp.	+	+				24.1	0.6–10.7	6.7–17.6	0–27.9	4.9
	A3	Angio-sperms	*Juglans polyporata*	+					3.2	0–1.1	0–1.5	0–0.4	
	A7		*Platycarya* sp.	+					1.8	0–3.1	0–1.7	0–0.3	
	A11		*Corylus* sp.	+					3.9	0–7.3	1.5–10.5	0–5.3	1.4
	A12		*Carpinus* sp.	+					0.7	0–3	0–1.5	0–0.7	
2	S5	Spores	*Osmunda* sp.	+						0.8–3.4	0–2.3	0–3.5	0.3
	G2	Gymno-sperms	*Picea* sp.	+	+				1.1	0.6–11.9	1.9–40	0–32	3.0
	G10		Taxodiaceae	+	+				0.7	0–3.0	0–2.5	0–0.4	0.8
	G12		*Podocarpus* sp.	+	+				1.1	0–0.4	0–1.6	0–0.2	
	G14		*Ginkgo* sp.	+							0–0.6		
	A2	Angio-sperms	Juglandaceae	+						0–3	0.2–3.8	0–2.7	
	A4		*Caya* sp.	+					2.5	0–12.9	0.2–2.4	0–0.6	1.1
	A5		*Pterocarya* sp.	+						0–0.9	0–1.2	0–0.6	
	A6		*Juglans* sp.	+						0–9	0–1.4	0–1.6	
	A8		*Engelhardtia* sp.	+							0–1.2		
	A16		Castanea	+							0–1.1		
	A19		*Magnolia* sp.	+	+					0–0.6	0–3.0	0–0.7	
	A20		*Liriodendron* sp.	+							0–1.2		
	A24		*Acer* sp.	+					0.7	0–0.6	0–1.5	0–0.3	
	A25		*Tilia* sp.	+					0.7	0–0.6	0–0.8	0–0.2	
3	S2	Spores	*Lycopodium* sp.			+				0–6	0.2–6.3	0–8.5	0.3
	S4		Polypodiaceae			+			8.5	0–16.8	0–10.8	0–11.6	0.8
	S11		Bryales			+					0–2.6	0–2.4	
	G1	Gymno-sperms	*Abies* sp.	+					1.1	0–1.1	0.3–1.8	0–3.2	
	G3		*Cedrus* sp.			+					0–0.5	0–0.4	
	A1	Angio-sperms	*Salix* sp.			+			0.4	0–1.2	0–1.9	0–1.8	1.1
	A9		*Betula* sp.			+			2.8	3.8–8.5	1.8–18.7	0.3–18.1	7.7
	A10		*Alnus* sp.			+			1.1	0.6–16.3	0.6–4.9	0.7–9.7	0.8
	A14		*Quercus* sp.	+	+					0.7–3	0.5–3.1	0–5.1	0.8
	A17		*Ulmus* sp.	+	+				1.1	0.6–3	0.4–6.0	0–4.6	
	A18		*Zelkova* sp.	+	+						0–0.6	0–0.2	
	A21		*Rhus* sp.	+	+					0–0.2	0–0.6		
	A22		Leguminosae	+							0–0.3		
	A27		*Ericales* sp.	+					1.4	0–27.6	0–0.4	0–26.3	12.6
	A32		Liliaceae	+							0–0.5		
	A35		Chenopodiaceae			+				0–0.6	0–4.0	0–3.4	

Table. (Contd.)

Groups and symbols on the factorial diagram		Groups of plants	Spores and pollen	Climatic conditions					20	16–12	11–10	4.8–2.6	0.03
				W	H	T	C	A	Content, %		Age, Ma		
4	S1	Mosses	*Sphagnum* sp.				+		0.7	0.9–2.2	0–6.5	1.1–34	1.6
	S6		*Botrychium* sp.				+		1.8	0–0.6	0–0.6	0–2.4	0.6
	S8		Meesea			+						0–2.7	0.6
	S9		Riccia			+							7.4
	G6	Gymno-sperms	*Pinus* s/g *Diploxylon*				+	+		0–3.0	3.1–15.8	2.1–19.7	4.9
	G5		*Pinus* s/g *Haploxylon*				+	+	5.3	0.8–9.6	7.7–22	3.4–23.6	7.1
	G7		*Pinus pumila*				+	+				0–2.7	
	G8		*Pinus* sp.				+	+		0–0.6			
	G11		*Ephedra* sp.			+					0–0.5	0–1.2	
	A36	Angio-sperms	Cyperaceae			+						0–2.3	0.8
	A39		Caryophyllaceae			+				0–0.6	0–0.4	0–3.3	
	A31		*Artemisia* sp.			+					0–0.2		
	A34		*Thalictrum* sp.			+					0–1.1	0–3.3	18.1
	A29		Compositae			+				0–3.0	0–10.1	0–1.6	9.0
	A37		Graminear			+					0–1.4	0–1.6	6.9
	A38		Nuphar	+	+						0–0.6	0–3.3	
	A28		*Diervilla* sp.			+				0–0.5	0–1.8	0–2.5	

Note: Crosses indicate the favorable climatic conditions: W – warm; H – humid; T – temperate; C – cold; A – arid.

cover included the less thermophilic broad-leaved exotic species. Apparently, they grew in places protected from cold winds. The diatom species became more diverse owing to the appearance of stenothermic species of *Eunotia* and *Ellerbeckia* genera. The percentage of extinct species among diatoms is very low, and this indicates their relatively recent burial in sediments.

The studied spore–pollen spectra from the Quaternary deposits overlying the basaltic sequence characterize the floral assemblages of meadows and swamps. Pollen of Compositae, Gramineae and Cyperaceae prevail in these assemblages with a rareness of miospores and scarce pollen of gymnosperms. Pollen of broad-leaved plants is extremely scarce in them. It seems obvious that this vegetation was formed under a relatively cool climate. The obtained date of 28550 years ago implies that the deposits were, evidently, formed during the late Karga climatic optimum (Belova, 1985; and others).

TIME OF RENEWAL IN THE LATE CENOZOIC FAUNAL ASSEMBLAGES

The Late Cenozoic change of climate was conditioned by two factors: the recent formation of mountains and the general Late Cenozoic cooling in the northern hemisphere.

In the Miocene, the Alpine mountain ranges were formed and stretched from western Europe to southeastern Asia. This uplift hindered the free air circulation over Eurasia from the equator to the north and promoted the formation of an arid belt (Akhmet'ev, 1993). In the Eocene–Miocene, the southern part of Tibet rose at a low (0.1–0.4 mm/year) average rate (Xiao and Li, 1995). In the middle Miocene (16–13 Ma ago), the rise of the mountain structures was relatively more rapid (Hodges *et al.*, 1994). By the late Miocene, the mountain ridges of the Alpine belt already rose up the first few kilometers.

The general Late Cenozoic cooling and aridization in the northern hemisphere were accompanied by brief climatic oscillations. The fossil mollusk assemblages testify that the relatively cold Oligocene period was followed by a warming, which reached its maximum in the middle Miocene and was succeeded by a period of progressive cooling in the late Miocene–Pliocene (Gladenkov, 1978). Under the warm and humid climate of the Boreal region, the Eocene–Oligocene flora of dominant pines and Taxodiaceae also included a wide spectrum of genera of deciduous arboreal and fruticose dicotyledons. This Boreal flora is known in the literature as the "Turgai-type" flora. In the terminal middle and initial late Miocene, the distribution of floral provinces in Siberia and northeastern Russia was similar to that of the early Miocene time and did not show any sign of climate deterioration. The new vegetal assemblages of the hypo-Arctic and Arctic appeared in response to a sudden aridization and cooling in the second half of the late Miocene (Akhmet'ev, 1993). The general cooling in the northern hemisphere caused the appearance of the first mountain glaciers in Iceland as early as about 10 Ma ago (Gladenkov, 1978).

The estimated average annual temperatures in the Baikal region were, as it follows from the malacofauna composition, in the intervals from +15 to +20°C during the Oligocene–early Miocene, and from +10 to +15°C during the middle–late Miocene. The water reserves were decreasing and, by the end of the Miocene and in the early Pliocene, the average annual temperatures fell to +10 ... +12°C (Popova, 1994). The same range of annual temperatures (+9 to +12°C) is implied by the reddish brown and brown soils and vertisoils occurring in the lower Pliocene part of the section. At that time, the temperature in January probably varied from +10 to –3°C. The relics of red ferrosialic soils in the Miocene–Pliocene boundary sediments, however, imply a higher range of average annual temperatures: +15 to +17°C (Vorob'eva and Mats, 1994). The temperature decrease is assumed to occur only in the last half of the Pliocene, in the interval of 2.4–1.6 Ma (Vorob'eva *et al.*, 1995). Meanwhile, as the palynological data indicate, the noticeable cooling and aridization that caused the complete degradation of the Turgai flora were already manifested in the late Miocene (Belova, 1985). Data on marine planktonic foraminifers suggest for the late Miocene and Pliocene the relatively cold intervals with a phase of warming in-between (Gladenkov, 1978).

The established renewal of floral assemblages in the southeastern part of Eastern Sayan, which took place after 10 Ma, indicates a transition from the Miocene Turgai flora to the Boreal Pliocene–Quaternary flora in response to the deterioration of climate. The absence of palynological data for sediments 10–5 Ma old precludes so far the determination of the exact time of the beginning of paleoclimatic changes in the Baikal region.

CONCLUSION

The large-scale geologic mapping of volcanosedimentary sequences in the southeastern part of the East Sayan Mountains revealed three stratigraphic units: the Sorok (lower–middle Miocene, 24–12 Ma), Khirpisa (upper Miocene, 11–6 Ma), and Khirbes formations (Pliocene, 5–1.6 Ma). This scheme of subdivision is substantiated by the K-Ar dating of lavas and by the palynological analysis. Valves of diatomaceous algae, recovered from the studied sediments in the southeastern part of the East Sayan Mountains, are scarce and cannot be used for reliable stratigraphic correlations.

The factorial analysis of spore and pollen assemblages from sedimentary lenses different in age revealed two stages in the evolution of flora: first, the stage of gradual degradation of the Miocene Turgai flora in the time interval from 20 to 10 Ma ago and, second, the replacement of this flora with the Boreal vegetation in the time interval from 10 to 5 Ma ago.

The dating of climatic oscillations of the Late Cenozoic time in the Baikal region obviously requires a further study of concrete composite sections. The most interesting in this respect are the Tunka depression and the Vitim Plateau, where sedimentary deposits containing diatoms and other biostratigraphic indicators alternate with the Miocene, Pliocene and lower Pleistocene lavas.

ACKNOWLEDGMENTS

We are grateful to V.M. Klimanova and M.M. Odintsova for their assistance in the spore and pollen determinations. This work was partly supported by the Russian Foundation for Basic Research, project no. 95-05-14277.

Reviewer M.A. Akhmet'ev

REFERENCES

Akhmet'ev, M.A., *Fitostratigrafiya kontinental'nykh otlozhenii paleogena i miotsena vnetropicheskoi Azii* (Phytostratigraphy of the Paleogene and Miocene Continental Deposits of the Extratropical Asia), Moscow: Nauka, 1993.

Bazarov, D.B., Savinova, V.V., Rasskazov, S.V., *et al.*, On the Upper Cenozoic Stratigraphy and Palynoassemblages of the Vitim Upland, in *Morfostruktura i stratigrafiya kainozoiskikh otlozhenii Pribaikal'ya* (Cenozoic Morphostructure and Stratigraphy of the Baikal Region), Ulan-Ude: Geol. Inst. Bur. Fil. Sibir. Otd. Akad. Nauk SSSR, 1984, pp. 67–88.

Belova, V.A., *Rastitel'nost' i klimat pozdnego kainozoya yugo-vostochnoi Sibiri* (The Late Cenozoic Vegetation and Climate of Southeastern Siberia), Novosibirsk: Nauka, 1985.

Gladenkov, Yu.B., *Morskoi verkhnii kainozoi severnykh raionov* (Marine Upper Cenozoic of Northern Regions), Moscow: Nauka, 1978.

Grosval'd, M.G., *Razvitie rel'efa Sayano-Tuvinskogo nagor'ya* (Relief Development in the Sayany–Tuva Upland), Moscow: Nauka, 1965.

Hodges, K.V., Hames, W.E., Olszevski, W., Burchfiel, B.C., Royden, L.H., and Chen, Z., Thermobarometric and $^{40}Ar/^{39}Ar$ Geochronologic Constraints on Eohimalayan Metamorphism in the Dinggye Area, Southern Tibet, *Contrib. Mineral. Petrol,* 1994, vol. 117, no. 2, pp. 151–163.

Kiselev, A.I. and Medvedev, M.E., Cenozoic Volcanism of the Oka Region (Eastern Sayan), in *Voprosy geologii Pribaikal'ya i Zabaikal'ya* (Problems of the Geology of the Baikal and Trans-Baikal Regions), Chita: Chita Izd., 1969, pp. 77–83.

Kiselev, A.I., Medvedev, M.E., and Golovko, G.A., *Vulkanizm Baikal'skoi riftovoi zony i problemy glubinnogo magmoobrazovaniya* (Volcanism of the Baikal Rift Zone and Problems of the Endogenic Magma Formation), Novosibirsk: Nauka, 1979.

Litologiya tretichnykh otlozhenii vpadin yugo-zapadnoi chasti Baikal'skoi riftovoi zony (Lithology of the Tertiary Deposits in the Southwestern Baikal Rift Zone), Moscow: Nauka, 1972.

Logachev, N.A., Devyatkin, E.V., Malaeva, E.M., *et al.*, The Cenozoic of the Taryat Depression and Chulutu River Valley (Central Khangai), *Izv. Akad. Nauk SSSR, Ser. Geol.*, 1982, no. 8, pp. 76–86.

Logachev, N.A., Lomonosova, T.K., and Klimanova, V.M., *Kainozoiskie otlozheniya irkutskogo amfiteatra* (Cenozoic

Deposits in the Irkutsk Amphitheater), Moscow: Nauka, 1964.

Moiseeva, A.I., Subdivision Continental Neogene Deposits of the Far East on Diatoms, *Stratigr. Geol. Korrelyatsiya,* 1995, vol. 3, no. 5, pp. 92–103.

Obruchev, S.V., Relief Development in the Eastern Sayan, *Tr. Inst. Geogr.,* 1946, no. 37, pp. 115–123.

Popova, S.M., Cenozoic Paleoclimates of the Baikal Region and their Secular Variations, in *Baikal—prirodnaya laboratoriya dlya issledovanii izmenenii okruzhayushchei sredy i klimata* (Baikal as a Laboratory for Investigating Environmental and Climatic Changes), vol. 2, Irkutsk: LISNA, 1994, p. 36.

Popova, S.M., Mats, V.D., Chernyaeva, G.P., *et al., Paleolimnologicheskie rekonstruktsii (Baikal'skaya riftovaya zona)* (Paleolimnologic Reconstructions: The Baikal Rift Zone), Novosibirsk: Nauka, 1989.

Rasskazov, S.V., *Magmatizm Baikal'skoi riftovoi sistemy* (Magmatism of the Baikal Rift System), Novosibirsk: Nauka, 1993.

Rasskazov, S.V., Batyrmurzaev, A.S., and Magomedov, Sh.A., K-Ar Dating of Cenozoic Basalts from the Oka Upland (Eastern Sayan), *Geol. Geofiz.,* 1990, no. 3, pp. 100–105.

Rasskazov, S.V., Batyrmurzaev, A.S., and Magomedov, Sh.A., K-Ar Dating of Cenozoic Basalts from the Southwestern Framing Zone of the Siberian Platform, *Sov. Geol.,* 1991, no. 3, pp. 82–85.

Rasskazov, S.V., Rogachev, A.M., Nemchinov, V.G., and Katyukha, Yu.P., The Neogene of the Eastern Sayan, in *Biostratigrafiya—geolkarte 50* (Biostratigraphy: Contribution to the Geological Map-50), Irkutsk: Vost.-Sibir. Otd. Vses. Paleontol. Ob-va, 1986, pp. 74–75.

Vorob'eva, G.A. and Mats, V.D., The Late Miocene–Quaternary Climates of the Baikal Region, in *Baikal—prirodnaya laboratoriya dlya issledovanii izmenenii okruzhayushchei sredy i klimata* (Baikal as a Natural Laboratory for Investigating Environmental and Climatic Changes), vol. 2, Irkutsk: LISNA, 1994, p. 57.

Vorob'eva, G.A., Mats, V.D., and Shimaraeva, M.K., The Late Cenozoic Climates of the Baikal Region, *Geol. Geofiz.,* 1995, vol. 36, no. 8, pp. 82–96.

Xiao, X. and Li, T., Tectonic Evolution and Uplift of the Qinghai-Tibet Plateau, *Episodes,* 1995, vol. 18, nos. 1–2, pp. 31-35.

Stratigraphy and Geological Correlation, Vol. 6, No. 4, 1998, pp. 408–415. Translated from Stratigrafiya. Geologicheskaya Korrelyatsiya, Vol. 6, No. 4, 1998, pp. 92–105.
Original Russian Text Copyright © 1998 by Solov'ev, T. Palechek, R. Palechek.
English Translation Copyright © 1998 by МАИК Наука/Interperiodica Publishing (Russia).

Tectonostratigraphy of the Northern Olyutor Zone (Anastasiya Bay area of Koryak Highland)

A. V. Solov'ev, T. N. Palechek, and R. M. Palechek

Institute of the Lithosphere, Russian Academy of Sciences, Staromonetnyi per. 22, Moscow, 109180 Russia

Received May 29, 1996

Abstract—Volcanogenic-siliceous and sedimentary–volcanogenic rock complexes are distinguished in the Anastasiya Bay area (the Koryak Highland) in the western coast of the Aleutian Basin. The age of siliceous beds in these complexes was inferred from radiolarian finds. The volcanogenic–sedimentary complex incorporates layers of the Campanian–Maastrichtian age. By lithology, it is correlated with the "Vatyna" Group, which previously was attributed to the Albian–Campanian. According to our data, the stratigraphic range of these deposits should also include the Maastrichtian. The sedimentary–volcanogenic rock complex is subdivided into three units: the volcanogenic (lower), volcanogenic–terrigenous (middle or transitional), and siliceous–terrigenous (upper) subcomplexes. The siliceous–terrigenous subcomplex contains radiolarians, which allow the host rocks to be dated as the Campanian–Maastrichtian. The sedimentary–volcanogenic complex is correlated with the Machevna complex or "Achaivayam Formation." The volcanogenic–siliceous complex was probably formed within a marginal sea basin and the sedimentary–volcanogenic complex in an island-arc and its slope settings. The data obtained allow us to reconstruct the hypothetical lateral succession of the Campanian–Maastrichtian paleogeographic settings: the continental margin–marginal sea–island arc–oceanic basin.

Key words: *tectonostratigraphy, radiolarians, Late Cretaceous, paleotectonic reconstructions, Olyutor zone, Koryak Highland.*

INTRODUCTION

Several objective obstacles complicate the stratigraphic subdivision and correlation of deposits composing the thrust-and-fold accretionary systems framing the Bering Sea. First, volcanogenic–siliceous–terrigenous deposits that are widespread there lack determinable macrofossil remains therefore stratigraphic subdivision is based on microfaunal remnants, extraction and determination of which is a time-consuming process, which does not always bring the desirable results. Second, these deposits are characterized by a significant facial variability. Third, their natural sections are too fragmented and disjointed for an easy reconstruction of paleoenvironments. When studying deposits in the intricate accretion zones, researchers should keep in mind that they are dealing with tectonostratigraphic rock successions formed under tectonic accretion of deposits rather than with normal stratigraphic sections (*Tektonicheskaya rassloennost'*..., 1990). Tectonostratigraphic sections composed of tectonic nappes are bounded by thrust surfaces that may stretch from dozens of meters to several kilometers.

In the methodical respect, the study of tectonostratigraphic rock successions requires the detailed sampling of each tectonostratigraphic unit for the micropaleontological investigations, the careful analysis of relationships between beds, and accurate description of lithological properties of rocks. This paper deals with results on tectonostratigraphic sequences composed of Upper Cretaceous volcanogenic–siliceous terrigenous deposits outcropping in the Anastasiya Bay area of the western coast of the Aleutian basin.

The material was obtained in summer 1994. Rock samples from the distinguished tectonostratigraphic units were subjected to petrographic and lithologic analyses. The fluoric (2–10%) or acetic (10–30%) acid etching was used to extract the volumetric radiolarian skeletons from these rocks. Acid concentration and etching exposure time were experimentally defined. Radiolarian microphotographs were made using the scanning electron microscope.

As a result of our study, the primary relationships between deposits now composing the thrust sheets were reconstructed. The principal possibility of such reconstructions is shown in the paper using the thrust-and-fold structures of the Koryak Highland as an example.

GEOLOGY OF THE REGION

The area in question is located in the Anastasiya Bay on the western coast of the Aleutian Basin of the Bering Sea (Fig. 1). The tectonic structure of the area is determined by its position between the Olyutor and Ukelayat zones. The Olyutor zone, which is characterized by the

intricate thrust-and-fold structure was investigated by many scientists from different geological organizations: A.A. Aleksandrov and others from the Northeast Complex Geological Research Institute; E.S. Alekseev from "Aerogeologiya;" N.P. Mitrofanov from the All-Russia Institute of Mineral Resources; A.D. Kazimirov, O.V. Astrakhantsev, and others from Geological Institute, Russian Academy of Sciences; and scientists from the Institute of the Lithosphere, Russian Academy of Sciences (Bogdanov, 1970; Bogdanov *et al.*, 1982; *Geologiya yuga...*, 1987). The frontal part of the Olyutor zone includes a series of Cretaceous oceanic and island-arc complexes composing large allochthonous nappes (Astrakhantsev *et al.*, 1987; Chekhovich, 1993), which were obducted onto deposits of the Ukelayat trough along the Vatyna–Vyvenka thrust (Mitrofanov, 1977). Astrakhantsev *et al.* (1987) distinguished the following structural units in the northern part of the Olyutor zone: (1) relative autochthon represented by tuffaceous–terrigenous deposits of the Upper Cretaceous–lower Paleogene Koryak Group (the Ukelayat zone); (2) paraautochthon composed of the Maastrichtian olistostrome sequence; the matrix of the latter is represented by flysch facies, and olistoliths are mainly composed of rocks of the Vatyna Group affinity; (3) the allochthon represented by volcanogenic–siliceous deposits of the Albian–Campanian Vatyna Group; and (4) neoautochthon composed of lavas and tuffs of the andesite–dacite and dacite–liparite series, and of plateau basalts of the Neogene–Quaternary age. In this paper, tectonostratigraphy of the allochthonous rock complexes is considered.

GEOLOGICAL STRUCTURE

The geological structure of the peninsula located between the Anastasiya Bay and Nerpich'e Ozero Lagoon was investigated (Fig. 1). As a result, the volcanogenic–siliceous and sedimentary–volcanogenic rock complexes were distinguished using differences in their lithologic characteristics and composition. The lower structural boundary of the volcanogenic–siliceous complex is represented by the Vatyna–Vyvenka thrust, along which these deposits were obducted onto the flyschoid deposits of the Ukelayat zone. Upward the sequence, rocks of the sedimentary–siliceous complex are replaced by the volcanogenic–siliceous complex. The contact between these two complexes in the region is of the subhorizontal thrust type in some areas and of the steep upthrow fault type in others.

THE VOLCANOGENIC–SILICEOUS COMPLEX

Deposits of the volcanogenic–siliceous complex outcropping only in coastal sections of the peninsula occupy the lowest hypsometric position (Fig. 2). In this case, we deal with the tectonostratigraphic, but not stratigraphic section. The volcanogenic–siliceous complex is composed of pillow basalts, hyaloclastites, and dolerites intercalated with subordinate siliceous rocks and aleuropelites. Different tectonic slices are characterized by different paragenetic rock associations: (a) pillow basalts, hyaloclastites, and red-brown jaspers; and (b) black auleropelites and green to gray siliciliths.

The red-brown jasper member with clasts of the inoceram shells represents a good marker horizon and is a characteristic feature of the first association. The jaspers have baking contacts with basalt flows, and both rock types compose tectonic slices. The jaspers show turbidite textures and a disharmonic folding in some layers. The latter is a result of synsedimentary deformations, most likely of the slumping origin.

The second association occurs in tectonic slices bounded by thrust surfaces at both sides. Black aleuropelites incorporate strongly deformed lenses and interbeds of green and gray siliceous rocks. Black aleuropelites are characterized by thin platy jointing.

Radiolarians from Siliceous Rocks of the Complex

Samples for the radiolarian analysis were collected from siliceous and terrigenous rocks of different tectonostratigraphic units (Fig. 2). About 100 samples from the volcanogenic–terrigenous complex were studied, and only nine of them collected from red-brown jasper (samples 4, 12, 29, 43/a, 44/c, A10, A12, A14, T28) yielded the determinable radiolarians. Radiolarian assemblages are of a low taxonomic diversity and abundance (Table 1). The maximum diversity amounts to 10–13 species whose abundance is as high as a few dozens of specimens per sample. Most common among radiolarians are *Praestylosphaera pusilla* (Campbell et Clark), *Amphipyndax stocki* (Campbell et Clark), *Stichomitra livermorensis* (Campbell et Clark), *Dictyomitra densicostata* Pessagno, *D. multicostata* Zittel, *Clathrocyclas tintinnaeformis* Campbell et Clark, and various species of the *Phaseliforma* genus (*P.* ex gr. *carinata*, *P.* cf. *subcarinata*). In addition, single specimens of *Cornutella californica* Campbell et Clark, *Stichomitra* cf. *shirshovica* Vishnevskaya, *Xitus* cf. *asymbatos* (Foreman), and *Phaseliforma* cf. *meganosensis* Pessagno are also present. Such composition of the radoiolarian assemblage (Table 1, Plates 1, 2) allows the volcanogenic–siliceous complex of the Anastasiya Bay to be attributed to the Campanian–Maastrichtian (Table 2). The radiolarian assemblage of sample 29 from the upper tectonic slice of section I (Fig. 2) indicates the middle Campanian–early Maastrichtian age of red-brown jaspers baked by overlying pillow basalts. This fact is important because it suggests that basalt eruption occurred in submarine environments at that time.

The Sedimentary–Volcanogenic Complex

The main part of the peninsula between the Anastasiya Bay and Nerpich'e Ozero Lagoon is composed of rocks of the sedimentary–volcanogenic complex (Fig. 1).

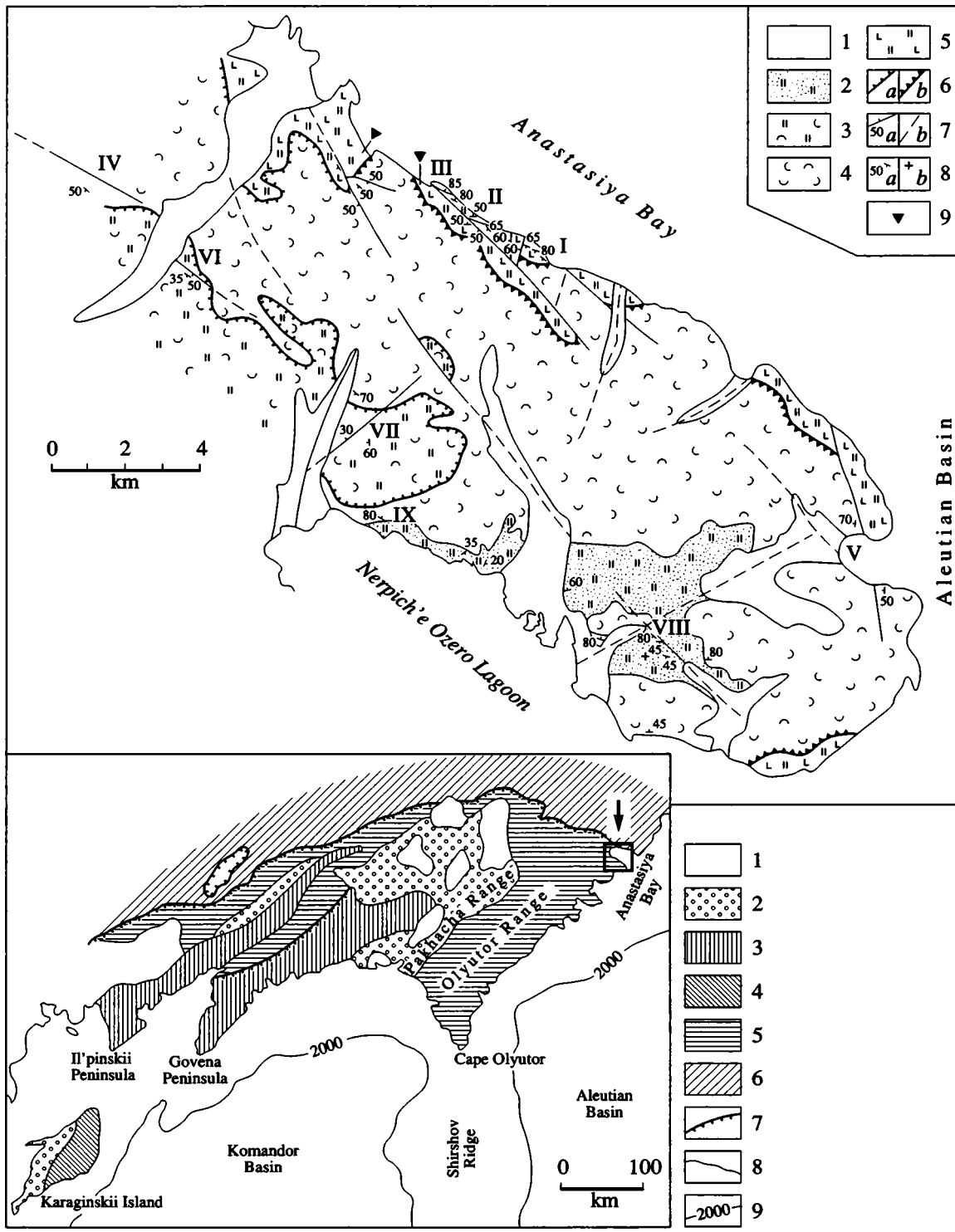

Fig. 1. Schematic geological structure of the Anastasiya Bay area (including data from the appendix to *Tektonicheskaya rassloennost'...*, 1990): (1) Quaternary loose deposits; (2–4) sedimentary–volcanogenic complex: (2) siliceous–terrigenous subcomplex (Campanian–Maastrichtian), (3) volcanogenic–terrigenous subcomplex, (4) volcanogenic subcomplex; (5) volcanogenic–siliceous complex (late Turonian–Maastrichtian); (6) reversed fault: (6*a*) subhorizontal thrust, (6*b*) steep reversed fault; (7) nonclassified faults: (7*a*) proven, (7*b*) assumed; (8) occurrence of bedding surface: (8*a*) slopping, (8*b*) vertical; (9) location of samples from collection of N.A. Bogdanov and K.A. Savel'ev; determination of radiolarians by V.S. Vishnevskaya (Table 3). Roman number indicate location of studied sections shown in Figs. 2, 3. Inset map shows the study area and schematic geological structure of the southwestern framing of the Bering Sea: (1) Pliocene–Quaternary volcanics; (2–6) complexes: (2) Neogene, (3) Paleogene, flyschoid and volcanogenic, (4) Upper Cretaceous, undivided, (5) Cretaceous, siliceous–volcanogenic, (6) Cretaceous–Paleogene, flyschoid, the Ukelayat trough; (7) thrusts; (8) stratigraphic contacts; (9) isobaths, m.

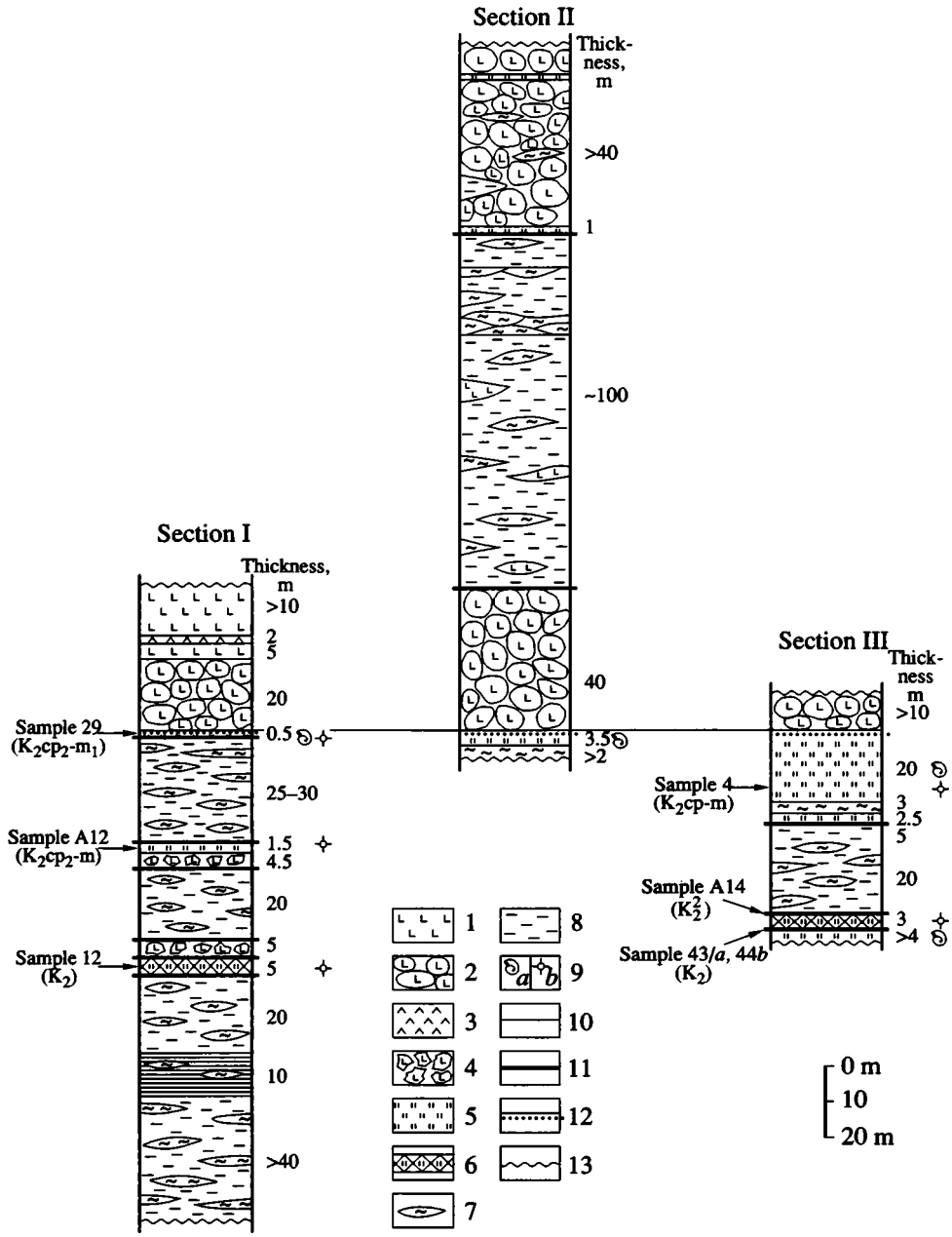

Fig. 2. Tectonostratigraphic sections of the volcanogenic–siliceous complex: (1) massive basalt; (2) pillow-basalts; (3) hyaloclastites of the basaltic composition; (4) red jaspers; (6) fractured zones; (7) red and gray siliceous rocks (beds and lenses); (8) black aleuropelites; (9) fossils: (*9a*) inocerams (indeterminable), (*9b*) radiolarians; (10) stratigraphic contact; (11) tectonic contact; (12) quenched contacts; (13) boundary of exposed section.

Fragmentary sections of the sedimentary–volcanogenic complex were studied along trubutaries of the Ushchel'nyi, Obkhodnoi, and Bolotnyi creeks, in the northern coast of the Nerpich'e Ozero Lagoon, on the southwestern slope of Mt. Krutaya, and in coastal outcrops of the Malaya Bight (Fig. 3). Tectonostratigraphic units are bounded by thrust surfaces. Columns in the figure show the hypsometric position of thrust sheets and stratigraphic contacts within the distinguished units.

The sedimentary–volcanogenic complex is somewhat arbitrarily subdivided into three units: (1) volcanogenic (lower); (2) volcanogenic–terigenous (middle or transitional), and (3) siliceous–terrigenous (upper) subcomplexes.

The volcanogenic subcomplex is composed of porphyry amygdaloid basalts, volcanic breccia basaltic in composition, and subordinate lavaclastites with the graywacke matrix, as well as interbeds and lenses of

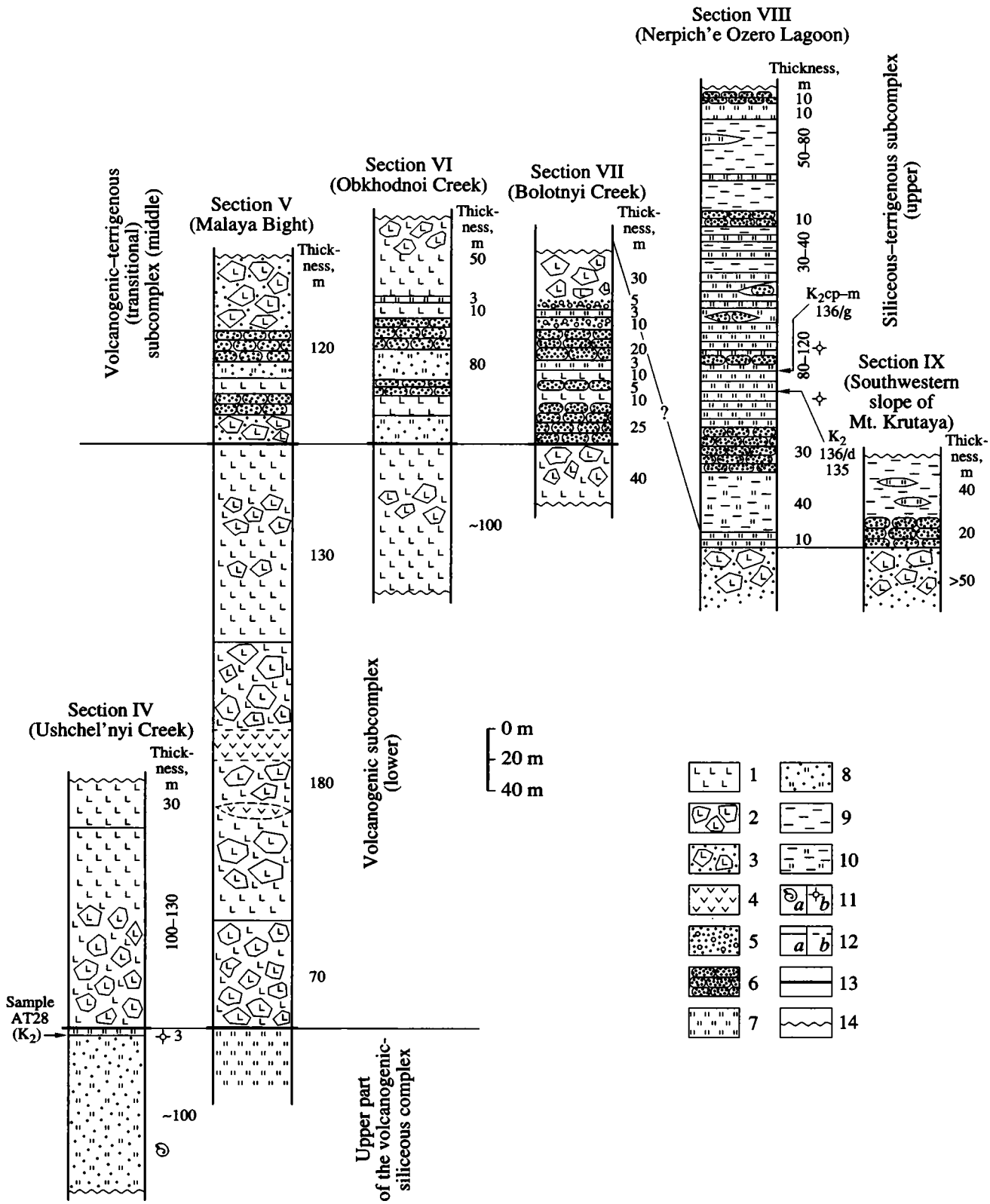

Fig. 3. Tectonostratigraphic sections of the sedimentary–volcanogenic complex: (1) massive amygdaloid porphyry basalt; (2) volcanic basaltic breccia; (3) basaltic blocks in the graywacke matrix; (4) basaltic andesites; (5) volcanomictic lithocrystalline graywacke; (6) volcanomictic graywacke sandstone with a tuffaceous admixture; (7) siliceous rocks; (8) siliceous rocks with an admixture of terrigenous material; (9) aleuroprlite; (10) siliceous aleuropelite; (11) fossils: (11*a*) inocerams (indeterminable), (11*b*) radiolarians; (12) stratigraphic contact: (12*a*) proven, (12*b*) assumed; (13) tectonic contact; (14) boundary of visible section.

basaltic andesites (Fig. 3). The characteristic constituents of the subcomplex are the amygdaloid basalts with large clinopyroxene phenocrysts (to 2 cm) and volcanic breccias with the ataxic (brecciated–taxic) texture (*Struktura gornykh...*, 1948). The ataxic texture is characterized by inclusions (to 10–50 cm across) of both rounded and irregular forms submerged into matrix with the fine-porphyry texture. The matrix and inclusions are identical in composition. The volcanogenic subcomplex overlies with the tectonic contact the volcanogenic–siliceous complex. The tectonic contact was observed along the Ushchel'nyi Creek tributaries and in coastal outcrops of the Malaya Bight. Structurally higher, the volcanogenic–terrigenous complex is thrust along the low-angled plane over the volcanogenic subcomplex of the southwestern part of the peninsula and represents an autonomous tectonic nappe.

The volcanogenic–terrigenous subcomplex is locally exposed and composed of graywacke sandstones, monovolcanic lithocrystalloclastic basaltic breccia, basalts, lavabreccia, and siliceous rocks with a substantial admixture of terrigenous material (Fig. 3). Its upper horizons include submarine slump deposits: large (to 10 m) blocks of basalts and lavabreccia submerged into the graywacke sandy matrix. The position of this subcomplex in the structure of the peninsula is unclear because it was detected only in isolated allochthonous thrust sheats (Fig. 1). The transitional character of the volcanogenic–terrigenous subcomplex is evident from its composition: it includes both the volcanic rocks typical of the volcanogenic subcomplex (lower) and terrigenous deposits characteristic of the siliceous–terrigenous (upper) subcomplex.

The siliceous–terrigenous subcomplex is widespread in the southern part of the peninsula and consists of grawacke sandstones, aleuropelites, silicified siltstones, and green to black cherts. The subcomplex conformably rests upon the rocks of the volcanogenic subcomplex. The gradual transition from volcanic breccia to fine-grained sandstones was observed on the southwestern slope of Mt. Krutaya and the conformable contact between black cherts and underlying volcanic breccia was described in the Nerpich'e Ozero Lagoon area.

Radiolarians from Siliceous Rocks of the Complex

Over 50 samples from the siliceous–terrigenous subcomplex were subjected to the radiolarian analysis. Three samples yielded radiolarian assemblages that were sufficiently well preserved and diverse in the sample 136/g only (Fig. 3, Table 1, Plate III). The assemblage includes *Praestylosphaera pusilla* (Campbell et Clark), *Cornutella californica* Campbell et Clark, *Clathrocyclas* cf. *tintinnaeformis* Campbell et Clark, *C.* cf. *hyronia* Foreman, *Theocampe* cf. *altamontensis* (Campbell et Clark), *Lithostrobus* cf. *rostovzevi* Lipman, *Phaseliforma* sp., *Stichomitra* sp., *Dictyomitra* sp., and prevalent *Theocampe yaoi* Taketani. This assemblage suggests the Campanian–Maastrichtian age of host rocks of the siliceous–terrigenous subcomplex (Table 2).

DISCUSSION

The frontal part of the Olyutor zone in the Anastasiya Bay area is chracterized by the thrust-and-fold structure and comprises two units: the volcanogenic–siliceous and sedimentary volcanogenic complexes.

The volcanogenic–siliceous complex is composed of oceanic (*sensu lato*) pillow basalts, as well as of pelagic and hemipelagic siliciliths and aleuropelites. Volcanics of the volcanogenic–siliceous complex are represented by aphyric and plagioclase–clinopyroxene–porphyry basalts and dolerites. All the rocks are variably spilitizied. The prevalence of lavas and absence of pyroclastic rocks indicate that eruptive centers were of the fracture or central types located below the pressure compensation level (Fisher, 1987). According to estimates, this level is 200 m and deeper below sea level for basic lavas. Siliceous rocks and aleuropelites contain an admixture of the graywacke material derived by erosion from the ensimatic crust. The presence of turbidity and slump textures testifies to the existence of the differentiated relief during the formation of the complex.

Siliciliths from tectonic slices of the tectonostratigraphic section of the volcanogenic–siliceous complex are dated back to the Campanian–Maastrichtian. Correlation of radiolarian assemblages from these deposits with radiolarian zonation elaborated for the Bering Sea region (Vishnevskaya, 1985) shows that they appear to be coeval with the late Vatyna and early Innetyvayam assemblages.

Previously, deposits of the volcanogenic–siliceous complex of the Anastasiya Bay area were studied by N.A. Bogdanov and K.A. Savel'ev. From samples collected by these reasearchers, Vishnevskaya (1985) determined radiolarian assemblages of the late Turonian–early Campanian and Coniacian–middle Campanian ages (Table 3), which were correlated with the early–middle Vatyna assemblages. L.G. Bragina determined radiolarians of the Santonian–Campanian age correlative with the middle–late Vatyna assemblages from jaspers of the Snegovaya nappe (Astrakhantsev *et al.*, 1987) probably representing rocks of the volcanogenic–siliceous complex.

The history of stratigraphic studies of volcanogenic–siliceous deposits in the Koryak Highland was considered earlier (*Geologiya yuga...*, 1987). The "Vatyna Group" was attributed to the Cretaceous at the end of the 1950s (Lipman, 1959), to the Late Cretaceous at the beginning of the 1970s (Zhamoida, 1972), and to the Albian–Campanian in the mid-1980s (Vishnevskaya, 1985). In lithologic and petrographic properties, the volcanogenic–siliceous complex of the Anastasiya Bay area is identical to deposits previously included in the "Vatyna Group." Based on the latter evi-

Table 1. Taxonomic composition and abundance of radiolarians from the Anastasiya Bay area

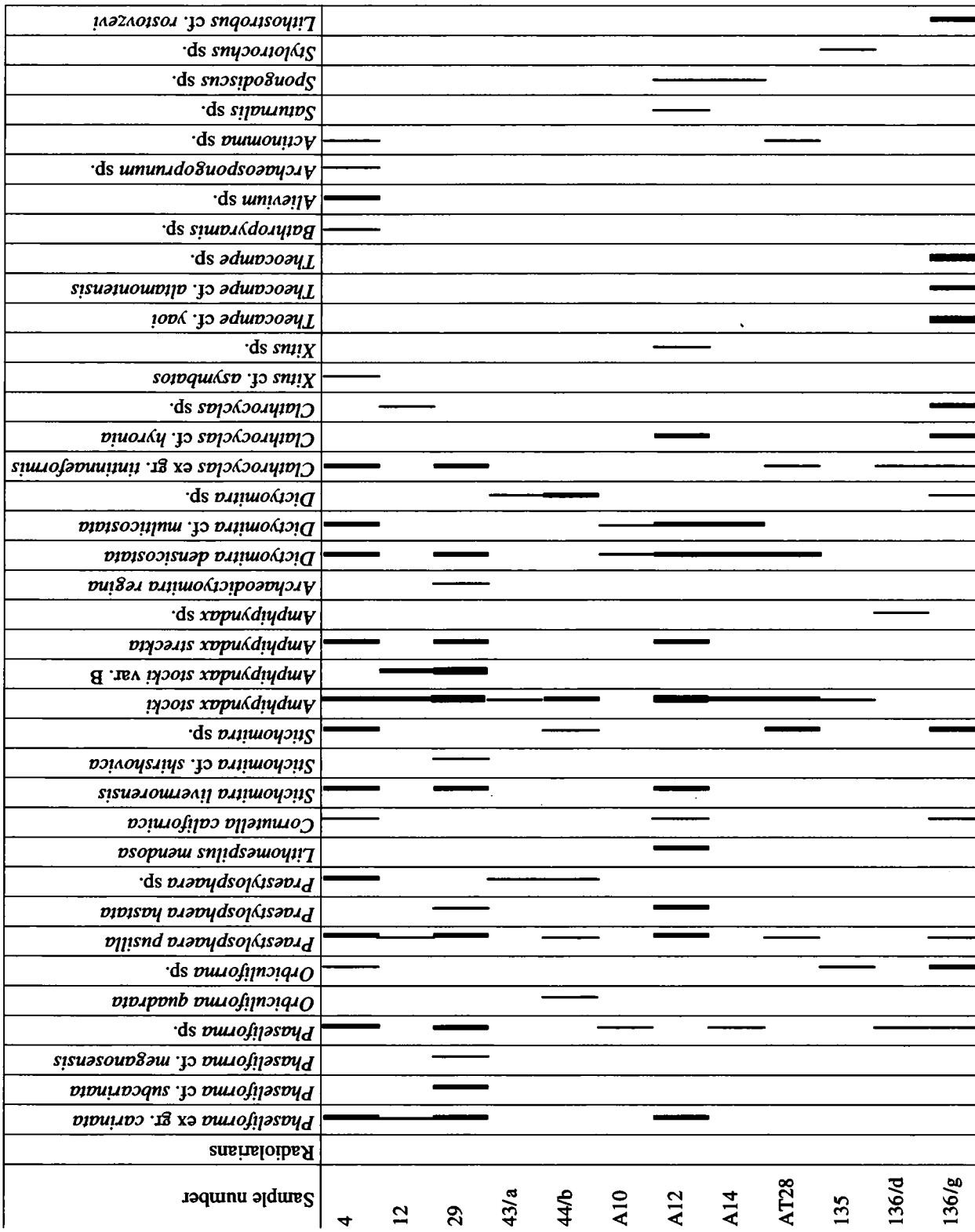

Plate I

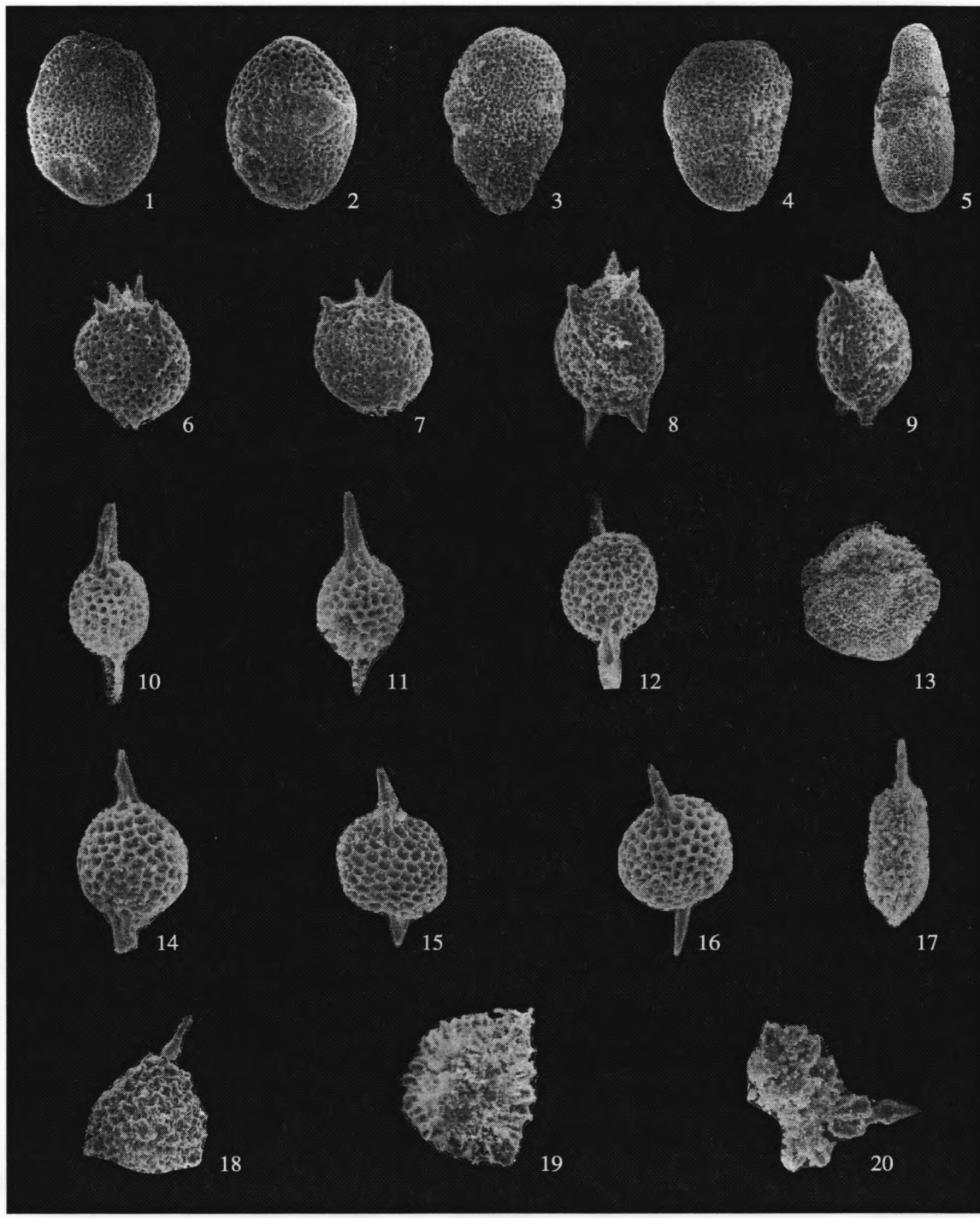

Plate 1. Radiolarians from rocks of the volcanogenic–siliceous complex.

(1, 2) *Phaseliforma* ex gr. *carinata* Pessgno, ×100, Sample A12 (1), Sample 12 (2); (3, 4) *Phaseliforma* cf. *sucarinata* Pessagno, ×100, Sample 29; (5) *Phaseliforma* cf. *meganosensis* Pessagno, x50, Sample 29; (6–9) *Lithomespilus mendosa* (Krasheninnikov), ×150 (6, 8, 9), x120 (7), Sample A12; (10–12) *Praestylosphaera pusilla* (Campbell et Clark), ×100, Sample 29; (13) *Orbiculiforma* sp., ×90, Sample 4; (14–16) Praestylosphaera hastata (Campbell et Clark), ×100, Sample 29 (14), ×110, Sample A12 (15, 16); (17) *Archaeospongoprunum* sp., ×150, Sample 4; (18–20) *Alievium* sp., ×90 (218), ×100 (19, 20), Sample 4.

Plate II

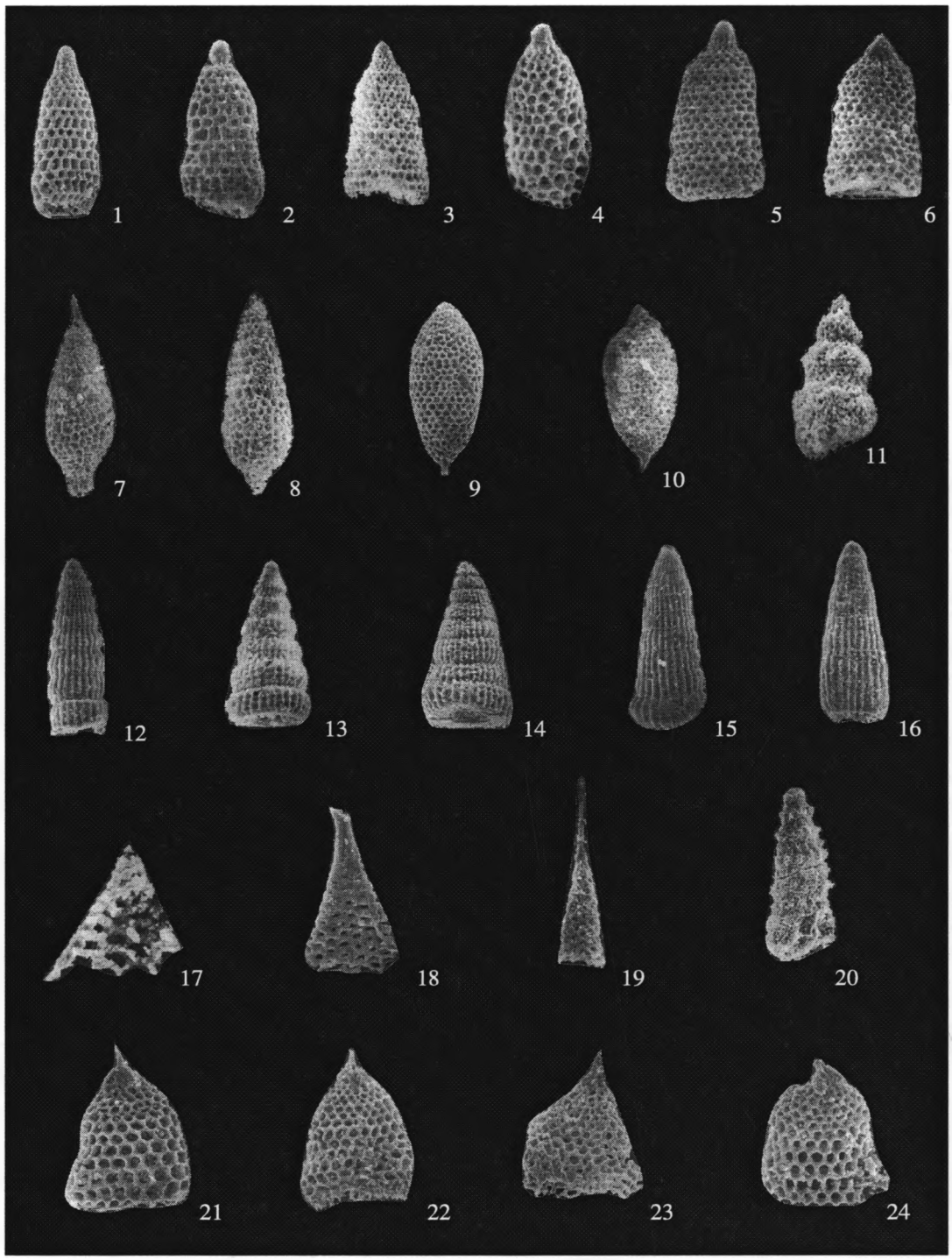

Plate II. Radiolarians from rocks of the volcanogenic–siliceous complex.

(1, 2) *Amphipyndax streckta* Empson-Morin, ×100, Sample A12 (1), Sample 29 (2); (3) *Amphipyndax stocki* (Campbell et Clark), ×100, Sample 29; (4) *Amphipyndax stocki* var. B Vishnevskaya, ×100, Sample 29; (5, 6) *Amphipyndax? stocki* (Campbell et Clark), ×100, Sample 29; (7, 8) *Stichomitra livermorensis?* (Campbell et Clark), ×100, Sample 4; (9, 10) *Stichomitra* cf. *shirshovica* Vishnevskaya, ×100, Sample 29; (11) *Stichomitra* sp., ×110, Sample 4; (12) *Archaeodictyomitra regina* (Campbell et Clark), ×100, Sample 29; (13, 14) *Dictyomitra densicostata* Pessagno, ×100, Sample 29 (13), Sample 4 (14); (15, 16) *Dictyiomitra multicostata* Zittel, ×100, Sample A12; (17) *Bathropyramis* sp., ×100, Sample 4; (18) *Cornutella* cf. *californica* Campbell et Clark, ×110, Sample A12; (19) *Cornutella californica* Campbell et Clark, ×100, Sample 4; (20) *Xitus* cf. *asymbatos* (Foreman), ×100, Sample 4; (21, 22) *Clathrocyclas hyronia* Foreman, ×120 (21), ×110 (22), Sample A12; (23, 24) *Clathrocyclas* ex gr. *hyronia* Foreman, ×110 (23), ×100 (24), Sample A12.

Plate III

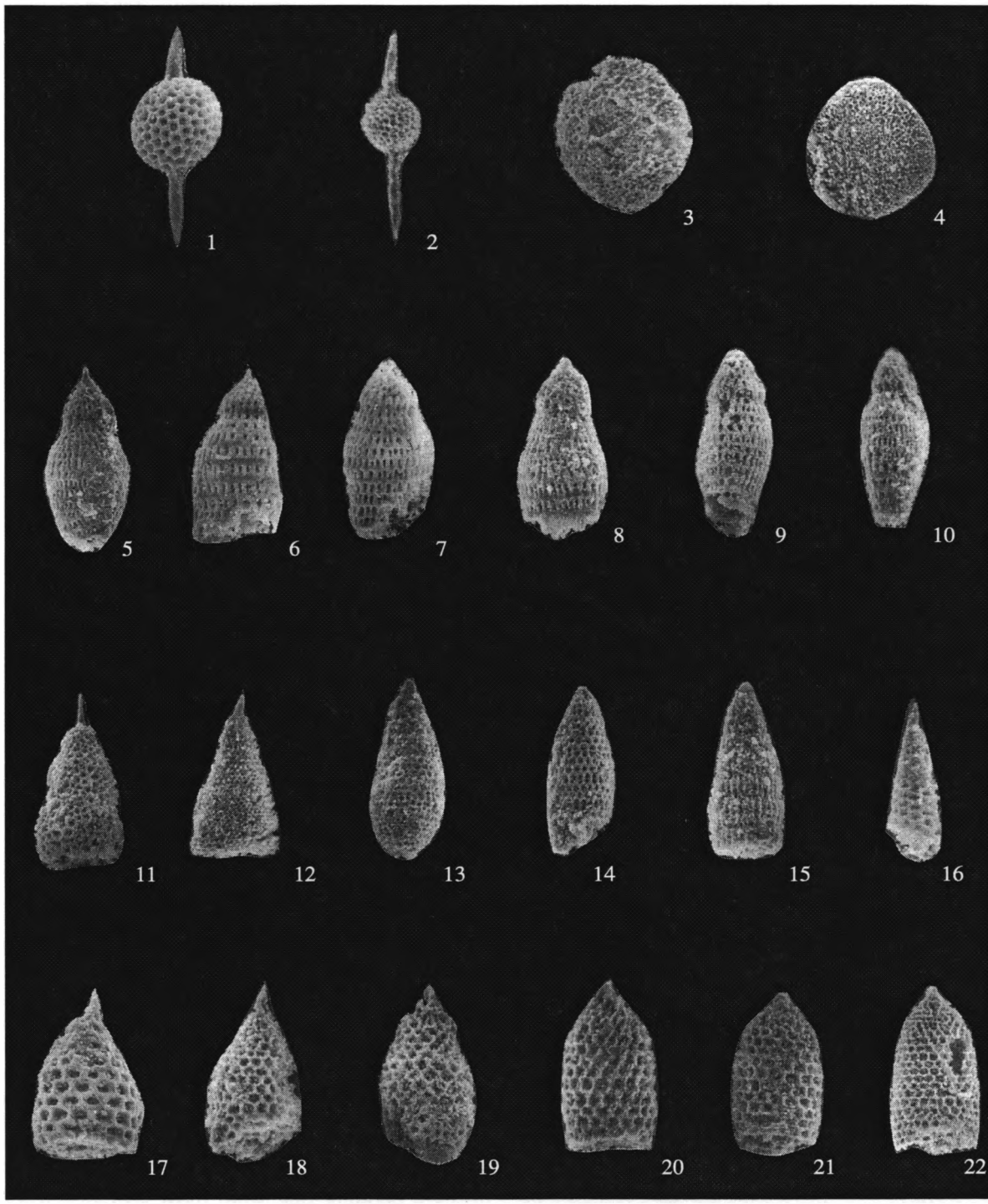

Plate 3. Radiolarians from rocks of the siliceous–terrigenous subcomplex of the sedimentary–volcanogenic complex (Sample 136/g). (1, 2) *Praestylosphaera pusilla* (Campbell et Clark), ×150 (1), ×100 (2); (3, 4) *Orbiculiforma* ? sp., ×100; (5–8) *Theocampe* cf. *yaoi* Taketani, ×100; (9, 10) *Theocampe* cf. *altamontensis* (Campbell et Clark), ×110; (11, 12) *Lithostrobus* cf. *rostovzevi* Lipman, ×100; (13, 14) *Stichomitra* sp., ×100; (15) *Dictyomitra* sp., ×110; (16) *Cornutella californica* Campbell et Clark, ×150; (17–19) *Clathrocyclas* cf. *hyronia* Foreman, ×100; (20–22) *Clathrocyclas* cf. *tintinnaeformis* Campbell et Clark, ×100.

Table 2. Stratigraphic range of radiolarian species

Radiolarians	K_2							P_1^1
	cn	st	cp			m		
			e	m	l	e	l	
Phaselifroma ex gr. *carinata* Pessagno			—	—	—	—	?		
Phaseliforma cf. *subcarinata* Pessagno			—	—	—	—			
Phaseliforma cf. *meganosensis* Pessagno		—	—	—	—	—			
Orbiculiforma quadrata Pessagno				—	—				
Praestylosphaera pusilla (Campbell & Clark)			?	—	—	—		—	
Praestylopshaera hastata (Campbell & Clark)			—	—	—	—	—		
Ltihomespilus mendosa (Krasheninnikov)								—	—
Cornutella californica (Cambell & Clark)			—	—	—	—	—	—	—
Stichomitra livermorensis Campbell & Clark	—	—	—	—	—	—	—	—	—
Stichomitra cf. *shirchovica* Vishnevskaya					—	—			
Amphipyndax stocki (Campbell & Clark)								—	
Amphipyndax stocki var. B. Vishnevskaya		—	—	—	—	—			
Amphipyndax streckta Empson–Morin				—	—	—			
Archaeodictyomitra regina (Campbell & Clark)				—	—		—	—	—
Dictyomitra densicostata Pessagno	—	—	—	—	—				
Dictyomitra cf. *multicostata* Zittel								—	
Clathrocyclas tintinnaeformis Campbell & Clark			—	—	—	—	—		
Clathrocyclas cf. *hyronia* Foreman					—	—	—		
Xitus cf. *asymbatos* (Foreman)								—	
Theocampe yaoi Taketani					—	—	—	—	
Theocampe cf. *altamontensis* (Campbell & Clark)					—	—	—	—	
Lithostrobus cf. *rostovzevi* Lipman		—	—	—	—				

dence and our dating, we believe that the "Vatyna Group" incorporates also younger Maastrichtian horizons.

Rocks of the "Vatyna Group" were previously interpreted as representing: (1) deposits of the eugeosynclinal Late Cretaceous depression on the oceanic crust (Alekseev, 1979); (2) deposits of a deepwater basin (Bogdanov *et al.*, 1982); (3) a fragment of the upper oceanic crust (Astrakhantsev *et al.*, 1987); (4) the basaltic layer of the oceanic crust detached from the basement or fragments of oceanic volcanic plateaus (Kazimirov *et al.*, 1987); (5) heterogenous complex of deposits originated in the mid-ocean ridge and abyssal plains (the Albian–Turonian), intraoceanic undersea rises (the Coniacian–Campanian), and marginal seas (Campanian) (Sokolov, 1992); and (6) deposits of a marginal sea (Chekhovich, 1993).

The sedimentary–volcanogenic complex is subdivided into three units: volcanogenic, volcanogenic–terrigenous (transitional), and siliceous–terrigenous subcomplexes. Some inferences concerning formation environments of the complex can be based on classification of volcanoclastic sedimentation setting proposed by Fisher (1987) in accordance with lithologic properties of sections. The volcanogenic subcomplex is composed of thick flows of massive basalt and basaltic andesite with subordinate beds of coarse tuffs and explosive breccia. These features allows us to suggest that the volcanogenic subcomplex was formed in subaerial environments. The volcanogenic–terrigenous subcomplex is represented by basalts, volcanic breccias, and thick poorly sorted terrigenous deposits with obscure bedding that were most probably formed in shallow submarine environments as a result of reworking of subaerial volcanics with subsequent transportation of the reworked material by gravity flows. The siliceous–terrigenous subcomplex incorporates thin layers of fine-grained sorted material displaying the graded bedding that indicates their accumulation in sufficiently deep submarine settings. According to the model of volcanogenic sedimentation (Cary and Sigurdsson, 1987), two latter subcomplexes probably rep-

Table 3. Age of some siliceous rocks from the Anastasiya Bay area (collection by N.A. Bogdanov and K.A. Savel'ev, 1985; determinations by V.S. Vishnevskaya)

Sample number	Age / Relative abundance	al	cm	t	cn	st	cp_1	cp_2	m
8/6, 8/7	*Acanthocircus* cf. *ichikawai* (Foreman)					?			
	Euchitonia triradiata Lipman								
	Dictyomitra ex gr. *multicostata* Zittel	—	—						
	Archaeodictyomitra regina (Campbell & Clark)						—	—	—
	Stichomitra? *livermorensis* (Campbell & Clark)				—	—	—	—	—
	Lithostrobus rostovzevi Lipman								
	Theocapsomma ex gr. *comys* Foreman					—	—	—	—
	Amphipyndax stocki var. A Vishnevskaya						—	—	
	A. stocki var. B. Vishnevskaya					—	—	—	—
7/2	*Pseudoaulophacus floresensis* Pessagno	—	—	—	—	—	—	—	
	Orbiculiforma quadrata Pessagno			—					
	Amphipyndax stocki var. A. Vichnevskaya						—	—	
	Archaeodictyomitra squinaboli Pessagno								
3/6	*Phaseliforma carinata* Pessagno						—	—	?
	P. concentrica (Lipman)							—	
	Stylodruppa bifascicula Kazintsova								
	Amphipyndax stocki var. A. Vishnevskaya							—	—
	Lithostrobus zhamoidae Kazintsova						?	—	—
1/1	*Cromyosphaera vivenkensis* Lipman								
	Orbiculiforma quadrata Pessagno								
	Alievium superbum (Squinabol)		—	—	—	—	—	—	
	Theocapsomma? *amphora* Campbell & Clark							—	—
	Neosciadiocapsa diabloensis Pessagno					—	—	—	—
	Amphipyndax stocki var. A Vishnevskaya						—	—	
	A. stocki var. B. Vishnevskaya					—	—	—	—
	A. conicus Nakaseko & Nishimura			—					
	Archaeodictyomitra squinaboli Pessagno								

resenting different facies of the volcanoclastic apron on the slope of an island arc with subaerial volcanic eruptions.

Siliciliths from the siliceous–terrigenous subcomplex are dated as the Campanian–Maastrichtian. The radiolarian assemblages from these deposits are correlative with the late Vatyna and early Inetyvayam assemblages (Vishnevskaya, 1985). In lithology and structure, the sedimentary–volcanogenic complex can be correlated with three units: with the "Achaivayam Formation" (Zhamoida, 1972; Astrakhantsev *et al.*, 1987), volcanogenic complex (Bogdanov *et al.*, 1982), and Machevna complex (Sukhov, 1983; *Geologiya yuga...*, 1987).

The "Achaivayam Formation" was considered as representing deposits of an island-arc system (Bogdanov *et al.*, 1982; Astrakhantsev *et al.*, 1987; Kazimirov *et al.*, 1987). The Machevna complex was interpreted to be a relict of the incipient or remnant island arc of a westward orientation in its frontal part (Sukhov, 1983; *Geologiya yuga...*, 1987).

Thus, three main structural–formational complexes formed in different geodynamic settings can by recognized in the Anastasiya Bay area: flysch deposits of the continental rise or deep-sea trench (the Ukelayat zone; Kazimirov *et al.*, 1987; Chekhovich, 1993); volcanogenic–siliceous deposits of the marginal sea (the "Vatyna Group" of the Olyutor zone; Chekhovich, 1993); and sedimentary–volcanogenic deposits of the ensimatic island-arc system and its slope (the Machevna complex or "Achaivayam Formation"; *Geologiya yuga...*, 1987). As was shown above, some horizons of volcanogenic–siliceous and sedimentary–volcanogenic complexes were formed simultaneously, in the Campanian–Maastrichtian. Deposits of the Cam-

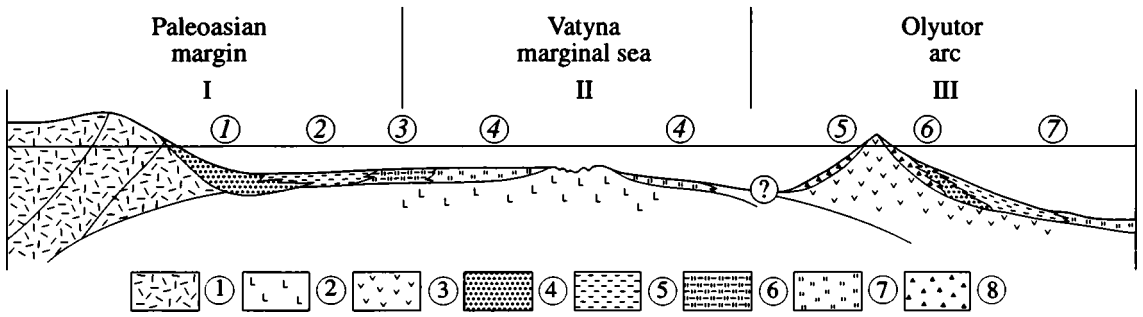

Fig. 4. Hypothetical lateral succession of the Campanian–Maastrichtian settings inferred from the analysis of tectonostratigraphic sections of the Anastasiya Bay area and published data (Chekhovich, 1993): (I) Ukelayat flysch complex with (*1*) proximal and (*2*) distal fan facies; (II) volcanogenic–siliceous complex (the "Vatyna Group") with (*3*) transitional facies (aleuropelites and siliceous rocks) and (*4*) basalts with siliceous rocks; (III) sedimentary–volcanogenic complexes (the "Achaivayam Formation") with (*5*) volcanogenic, (*6*) volcanogenic–terrigenous, (*7*) siliceous–terrigenous subcomplexes. Symbols in boxes: (1) accretion complexes of the Koryak Highland; (2) marginal-sea crust, (3) island-arc crust; (4) terrigenous and volcanogenic psammites; (5) aleuropelites of a variable genesis; (6) clayey–siliceous facies; (7) siliceous facies; (8) coarse volcanogenic rocks.

panian–Maastrichtian age were also recorded in the flyschoid complex of the Ukelayat zone (Kazimirov *et al.*, 1987). All these structural–formational complexes are close in the formation time and tectonically juxtaposed in the modern structure. Accordingly, we reconstruct the following lateral succession of depositional settings during the Campanian–Maastrichtian: the continental slope–marginal sea basin–island arc–deepwater oceanic basin (Fig. 4). Presence of aleuropelites in the tectonostratigraphic sections of the volcanogenic–siliceous complex allows the latter to be referred to transitional facies between the continental rise (Ukelayat facies) and marginal sea basin (the "Vatyna Group" of the Olyutor zone). Transitional facies were also described in sections of the Ukelayat zone, where siliceous–clayey rocks and high-titanium basalts occur among flysch deposits (Sokolov, 1992).

The Analysis of Radiolarian Assemblages

The presence of cancellate radiolarian skeletons, along with cyrtoid forms, in radiolarian assemblages and sponge remains in rocks of the volcanogenic–siliceous complex (Samples 12, 29) suggest that this community inhabited waters of a marginal sea. The burial of the assemblage most likely occurred in relatively shallow environments, which is evident indirectly from a rather high percentage of sponge forms, almost complete absence of spines, and strong fragmentation of skeletons.

The radiolarian assemblage from the siliceous–terrigenous subcomplex is dominated by cyrtoid forms (sponge/cyrtoid forms ratio is 1: 10). Most common are representatives of the *Theocampe* genus typical of basins with a depth close to the abyssal one (Empson-Morin, 1984). The above-described assemblage probably inhabited an open sea basin, where the burial depth was greater as compared with that of radiolarians from the volcanogenic–siliceous complex.

Radiolarians from tectonostratigraphic sections of the Anastasiya Bay area are akin to those from Upper Cretaceous deposits of California (Campbell and Clark, 1944; Pessagno, 1976) and Japan (Taketani, 1982), as well as to assemblages from DSDP Site 275 in the southern high-latitude Pacific (Pessagno, 1975). Empson-Morin (1984) noted that the high-latitude radiolarian assemblages are characterized by presence of orbiculiformids and phaseliformids with the reduced height/width ratio of skeletons. This value in phaseliformids from our collection is 1.42–1.59.

The low diversity, smoothed forms, presence of massive thick-walled shells, low percentage of spiny forms, and small dimensions allow the described radiolarians to be referred to the high-latitude assemblage.

CONCLUSION

(1) Two structural–formational complexes are established in the Anastasiya Bay area: volcanogenic–siliceous and sedimentary–volcanogenic. In the modern structure, deposits of these complexes occur in tectonostratigraphic sections.

(2) The volcanogenic–siliceous complex incorporates rock members dated as the late Turonian–early Campanian and Coniacian–middle Campanian (determinations by V.S. Vishnevskaya). The Campanian–Maastrichtian members are established in the complex for the first time. By lithology, the complex is correlative with the "Vatyna Group" (*Geologiya yuga...*, 1987; Astrakhantsev *et al.*, 1987). Previously, it was believed that the "Vatyna Group" was formed in the Albian–Campanian (*Geologiya yuga...*, 1987). According our data, it also includes Maastrichtian rocks.

(3) The sedimentary–volcanogenic complex is subdivided into three units: the volcanogenic (lower), volcanogenic–terrigenous (middle or transitional), and siliceous–terrigenous (upper) subcomplexes. The siliceous–terrigenous subcomplex contains radiolarians,

which allow the host deposits to be dated as the Campanian–Maastrichtian. The sedimentary–volcanogenic complex is correlated with the Machevna complex (*Geologiya yuga...*, 1987) or "Achaivayam Formation" (Astrakhantsev *et al.*, 1987).

(4) The volcanogenic–siliceous complex was likely formed in a marginal sea basin, whereas the sedimentary–volcanogenic complex was accumulated in an island arc and its slope setting. The data obtained allow the succession of paleosettings to be reconstructed as follows: continental slope–marginal sea basin–island arc–oceanic basin.

ACKNOWLEDGMENTS

We express our sincere gratitude to N.A. Bogdanov and V.S. Vishnevskaya for their constructive advice and samples that supplemented our collection. We also thank V.V. Bernard for the radiolarian images photographed under the scanning electron microscope.

The work was supported by the Russian Foundation for Basic Research (projects 97-05-65566 and 98-05-64525).

Reviewers S.D. Sokolov and N.A. Bogdanov

REFERENCES

Alekseev, E.S., Main Features of the Development and Structure of the Southern Koryak Highland, *Geotektonika*, 1979, no. 1, pp. 85–95.

Astrakhantsev, O.V., Kazimirov, A.D., and Kheifets, A.M., Tectonics of the Northern Olyutor Zone, in *Ocherki po geologii severo-zapadnogo sectora Tikhookeanskogo tektonicheskogo poyasa* (Assays on Geology of the Northern Segment of the Pacific Tectonic Belt), Moscow: Nauka, 1987.

Bogdanov, N.A., Some Peculiarities of Tectonics of the Eastern Koryak Highland, *Dokl. Akad. Nauk SSSR*, 1970, vol. 192, no. 3, pp. 607–610.

Bogdanov, N.A., Chekhovich, V.D., Sukhov, A.N., and Vishnevskaya, V.S., Tectonics of the Olyutor Zone, in *Ocherki po geologii severo-zapadnogo sectora Tikhookeanskogo tektonicheskogo poyasa* (Assays on Geology of the Northern Segment of the Pacific Tectonic Belt), Moscow: Nauka, 1987.

Campbell, A. and Clark, B., Radiolaria from Upper Cretaceous of Middle California, *Spec. Pap. Geol. Soc. Am.*, 1944, no. 57, pp. 1–61.

Chekhovich, V.D., *Tektonika i geodinamika skladchatogo obramleniya malykh okeanicheskikh basseinov* (Tectonics and Geodynamics of the Fold Framing of Minor Oceanic Basins), Moscow: Nauka, 1993.

Cary, S. and Sigurdsson, Ch., A Model of Volcanogenic Sedimentation in Marginal Basins, in *Marginal Basin Geology*, Oxford: Blackwell, 1984, pp. 37–59. Translated under the title *Geologiya okrainnykh basseinov*, Moscow: Mir, 1987, pp. 65–101.

Empson-Morin, K., Depth and Latitude Distribution of Radiolaria in Campanian (Late Cretaceous) Tropical and Subtropical Oceans, *Micropaleontology*, 1984, vol. 30, no. 1, pp. 87–115.

Fisher, R.V., Submarine Volcaniclastic Rocks, in *Marginal Basin Geology*, Oxford: Blackwell, 1984, pp. 5–28. Translated under the title *Geologiya okrainnykh basseinov*, Moscow: Mir, 1987, pp. 9–51.

Kazimirov, A.D., Krylov, K.A., and Fedorov, P.I., Tectonic Evolution of Marginal Seas, the Koryak Highland as an Example, in *Ocherki po geologii severo-zapadnogo sectora Tikhookeanskogo tektonicheskogo poyasa* (Assays on Geology of the Northern Segment of the Pacific Tectonic Belt), Moscow: Nauka, 1987.

Lipman, R.Kh., Importance of Radiolaria for Stratigraphic Subdivision of Sedimentray Rocks, *Byul. Mosk. O-va Ispyt. Prir., Otd. Geol.*, 1959, vol. 34, issue 6, pp. 67–88.

Mitrofanov, N.P., The Vatyna Tectonic Nappe in the Central Koryak Fold Zone, *Geol. Geofiz.*, 1977, no. 4, pp. 144–149.

Pessagno, E., Upper Cretaceous Radiolaria from DSDP Site 275, *Initial Rep. Deep Sea Drill. Project*, Kennett, J.P. and Houtz, R.E., Eds., Washington: U.S. Govt. Print. Office, 1975, vol. 29, pp. 1011–1029.

Pessagno, E., Radiolarian Zonation and Stratigraphy of the Upper Cretaceous Portion of the Great Valley Sequence, California Coast Range, *Micropaleontology, Spec. Publ.*, 1976, no. 2, pp. 1–95.

Sokolov, S.D., *Akkretsionnaya tektonika Koryakskо-Chukotskogo segmenta Tikhookeanskogo poyasa* (Accretionary Tectonics of the Koryak–Chukchi Segment of the Pacific Belt), Moscow: Nauka, 1992.

Struktury gornykh porod. Tom 1. Magmaticheskie porody (Textures of Rocks. Volume 1. Magmatic Rocks), Leningrad: Gosgeolizdat, 1948.

Sukhov, A.N., Volcanogenic Complex of the Olyutor Range, *Izv. Akad. Nauk SSSR, Ser. Geol.*, 1983, no. 10, pp. 12–28.

Taketani, Y., Cretaceous Radiolarian Biostratigraphy of the Urakawa and Obira Areas, Hokkaido, *Tohoku Univ. Sci. Repts., 2nd Ser. (Geol.)*, 1982, vol. 52, nos. 1–2. pp. 1–76.

Tektonicheskaya rassloennost' litosfery i regional'nye geologicheskie issledovaniya (Tectonic Layering of the Lithosphere and Regional Geological Investigations), Moscow: Nauka, 1990.

Vishnevskaya, V.S., Biostratigraphy of the Upper Cretaceous Volcanogenic–Siliceous Deposits of the Bering Sea Region Based on Radiolarians, *Tikhookean. Geol.*, 1985, no. 4, pp. 84–93.

Zhamoida, A.I., *Biostratigrafiya mezozoiskikh kremnistykh tolshch Vostoka SSSR* (Biostratigraphy of Mesozoic Siliceous Sequences of the Eastern USSR), Leningrad: Nedra, 1972.

Stratigraphy and Geological Correlation, Vol. 6, No. 4, 1998, pp. 422–428. Translated from Stratigrafiya. Geologicheskaya Korrelyatsiya, Vol. 6, No. 4, 1998, pp. 106–112.
Original Russian Text Copyright © 1998 by Mogucheva.
English Translation Copyright © 1998 by МАИК Наука/Interperiodica Publishing (Russia).

On the Taimyr Stage of the Continental Permian Deposits in Siberia

N. K. Mogucheva

Siberian Research Institute of Geology, Geophysics, and Mineral Resources, Siberian Division, Russian Academy of Sciences, Krasnyi pr. 67, Novosibirsk, 630104 Russia

Received May 29, 1996; in final form, October 1, 1996

Key words: *Stratigraphy, correlation, Permian, Triassic, Korvunchana flora, "Taimyr Stage," Induan Stage.*

In central Siberia, the Permian-Triassic boundary sediments are largely represented by continental sequences. According to the adopted point of view, the Permian-Triassic boundary is defined here by the contact of Permian gray-colored coal deposits bearing the paleophytic Cordaites flora with the overlying volcanogenic and tuffaceous–sedimentary, mainly variegated sediments bearing the mesophytic lepidophytic flora in the coastal margins of the Siberian platform and the mesophytic coniferous–ferny Korvunchana flora on the rest of the territory, correspondingly. This boundary corresponds to the radical transformation and differentiation of paleogeographical environments, to the replacement of the humid climate by semiarid, to the cessation of coal accumulation, to wide manifestations of the trap volcanism, and to drastic changes in the plant formations, when the paleophytic floras gave way to the mesophytic assemblages.

On the basis of flora, the uppermost Permian horizons in Siberia are customary assigned to the upper Tatarian Substage. In central Siberia, they are overlain by volcanogenic and tuffaceous–sedimentary deposits, whose lowermost beds correspond to the Induan Stage, like in the Tunguska syneclise (Mogucheva, 1986; Dobruskina and Mogucheva, 1987; Kukhtinov and Neustrueva, 1986; Saidakovskii, 1990; and others). However, there is an opinion that the volcanogenic sequences of the Tunguska syneclise and Taimyr characterized by the Korvunchana flora, are not Triassic but Permian in age. The lower Tutonchana Horizon is attributed in this case to the Tatarian Stage, whereas the Dvurogii and Putorana horizons are distinguished as the so-called "Taimyr Stage terminal in the continental Permian" and supposedly corresponding to the Dzhulfinian and Dorashamian stages of the Tethys and to the hiatus between the Permian and Triassic in the Russian platform (Sadovnikov and Orlova, 1994). Seeking the stratotype of the new stage, the cited authors chose "the most complete", but actually fragmentary section of volcanogenic and volcano-terrigenous sediments of the Kiryaka-Tas Range in southeastern Taimyr studied previously (Sadovnikov and Orlova, 1990). The section was described in isolated, widely separated outcrops in northeastern and southwestern parts of the Kiryaka-Tas Range. It is unclear what part of the section was distinguished as the Taimyr Stage. Stratigraphic considerations of Sadovnikov and Orlova are summarized in Table 1. In their paper of 1990, they placed the "Dorashamian or Induan Stage" (Fig. 2; p. 65) above the Tatarian (?) Stage, to which they attributed the volcanogenic sediments of the Zverinaya Formation. The former subdivision includes the Kholid'e, Betlinga, and Poputnaya formations, but the latter is missing in the Kiryaka-Tas Range. It was distinguished in central Taimyr and, as it is now established by Vavilov *et al.* (1990), this unit is of the Early Jurassic age. In Table 1 of the same paper (pp. 60, 61) in the column "Kiryaka-Tas," only the Betlinga Formation partly entering the Lower Triassic, is shown as a constituent of the "Dorashamian or Induan Stage," whereas the Kholid'e and Zverinaya formations are included in the "Tatarian or Dzhulfinian Stage." The paper in question discusses one more version: "...as the floral assemblages with dominant conifers of the Putorana type occur in the Kiryaka-Tas Range only in the lowermost lava beds, whereas in central Taimyr they are recovered from the Poputnaya Formation overlying the Betlinga lavas, we can suggest that the Betlinga Formation corresponds only to the lower part of the Kiryaka-Tas lavas, whose upper part is younger" (p. 67).

There are some other unclear points concerning the structure of the section. In its previous description, it was noted that in the Kiryaka-Tas Range the Permian coal deposits with Cordaites flora are overlain by the Zverinaya Formation consisting of tuffs, tuffites, and basalts about 300 m thick, then by the Betlinga Formation composed of basalts and mandelstones with *Quadrocladus* remains, and finally, above the hidden contact, by the marine Olenekian sediments (Sadovnikov *et al.*, 1981). In the other paper (Sadovnikov and Orlova, 1990), the Kholid'e Formation, distinguished by the authors in the Kholid'e massif, is shown above the Zverinaya tuffs. This formation is represented by dark- to gray-green sandstones, siltstones, and shales

Table 1. Correlated subdivision schemes of volcanogenic deposits in the Kiryaka-Tas Range

Sadovnikov and Orlova, 1990							Sadovnikov and Orlova, 1994		
System	Stage	Horizon	Central Taimyr	Kiryaka-Tas	Stage	Kiryaka-Tas	System	Stage	Horizon
Triassic	Olenekian	Ust'-Kel'ter	Mamonovo	Kiryaka-Tas	Olenekian	Kiryaka-Tas	Triassic	Olenekian	–
				Tsvetkova Cape		Tsvetkova Cape			Ust'-Kel'ter
	Induan		Fad'yukuda		Induan	Fad'yukuda		Induan	
				Betlinga		?			?
Permian or Triassic	Dorashamian or Induan	Putorana	Poputnaya		Dorashamian or Induan		Triassic	?	Marininskii
						Betlinga	Permian	Dorashamian	Putorana
			Gofmana						
			Betlinga			Kholid'e			Khungtukun
Permian	Tatarian or Dzhulfinian	Lebed'	Zverinaya	Kholid'e	Tatarian ?	Zverinaya		Dzhul'finian	Lebed'
		Tutonchana		Zverinaya ?				Tatarian	Tutonchana
	Tatarian	Gagarii Island							Gagarii Island

Table 2. Comparison of floral assemblages from the Keshi, Kholid'e, Syurbelyakh formations, and Tutonchana Horizon, the Tunguska and Kuznetsk basins

Keshi Formation T_1 ind	1	2	3	4	5
Mesenteriophyllum sp.	+			+	+
Pleuromeia sp.	+				
Tomiostrobus migayi (Schved.)		+		+	+
Neokoretrophyllites annularioides Radcz.			+	+	+
Paracalamites triassica Radcz.	+	+	+	+	+
Equisetites sixteliae Mog.			+		
Cladophlebis parvus Mog.				+	+
C. borealis Pryn.			+	+	+
C. cf. kirjamkensis Pryn.	+		+	+	+
Sphenopteris kirjamkensis Pryn.	+		sp.		
Kchonomakidium cf. *tunguscanum* (Pryn.) Schved.				+	+
K. cf. *srebrodolskae* Schved.			+	+	+
Lepidopteris arctica Mog.	+	+			
Peltaspermum sp.	+			+	+
Taeniopteris tajmyrica Mog.		sp.	sp.		
Glossophyllum sp.				+	+
Rhipidopsis sp.				+	+
Carpolithes zwetkoviensis Mog.		+			
C. ex gr. *minor* Pryn.	+			+	+

Note: (1) Kholid'e Formation; (2) lavas of the Kiryaka-Tas Range; (3) Syurbelyakh Formation of the Verkhoyansk region; (4, 5) Tutonchana Horizon in the Kuznetsk (4) and Tunguska (5) basins.

enclosing conglomerate beds. Its total thickness is about 450 m.

A.Yu. Egorov, who later studied the sections in the Kiryaka-Tas and Tulai-Kiryaka regions, distinguished at the base of the section of the Kholid'e Uplift only the undivided Zverinaya-Betlinga formations about 1000 m thick and composed of various basalts intercalated with basaltic tuff beds in the lower half of the sequence and enclosing scarce interbeds of shales with plant remains (Egorov and Kulikova, 1989). The terrigenous sequence 450 m thick is not mentioned in this work. Without the detailed layer-by-layer description of the section, it is impossible to understand if the Kholid'e Formation really exists.

It also remains unclear what is the Kiryaka-Tas Formation supposedly distinguished by Egorov and Bogomolov in the Kiryaka-Tas Range. Neither the given reference to Dagis *et al.* (1989), nor the paper by Egorov and Kulikova (1989) from the same collection of articles, which describe the Kiryaka-Tas section, contain any data on the recognition of this formation in the Kiryaka-Tas Range.

The paper about the "new stage" (Sadovnikov and Orlova, 1994) is devoid of explanations concerning the structure and stratigraphic range of its stratotype excluding the reference to its previous description in the Kiryaka-Tas Range. In the table supplementing the paper, the Taimyr Stage includes only units distinguished in the Tunguska basin, namely, the Lebed', Khungtukun, and Putorana horizons, while their correlation with the stratotype is not presented. However, the paper of 1990 states that "...the Lebed' Horizon is almost unknown in the northern Siberian platform and Taimyr..." (Sadovnikov and Orlova, 1990, p. 69). As it follows from the paper, the age of the Putorana Horizon is unclear, but "...the almost complete absence of Permian ostracodes and conchostracans in this unit but a wide distribution of *Falsisca* in the Lower Triassic and, especially, in the Marininskii Formation, as well as the occurrence of Triassic *Gerdalia* in the central and southern Tunguska syneclise, suggest the Early Triassic age of the unit" (the aforementioned paper, p. 70). Thus, it turns out that the Triassic horizon is attributed to the Permian stage (?).

It should be also pointed out that the Lebed' and Khungtukun horizons, distinguished instead of the Dvurogii Horizon, are biostratigraphic but not regional units like the Tutonchana, Dvurogii, and Putorana horizons. The indicated two horizons were distinguished in different structural–facies zones and in the sections of different formations not correlated with each other, and, as a result, their relationships are obscure. Both units are of local occurrence and, at best, can be considered as beds bearing flora (Lebed' "Horizon") and/or conchostracans (Khungtukun "Horizon") typical of the regional Dvurogii Horizon. Thus, they cannot substitute the Dvurogii Horizon and be considered as equal in rank to the Tutonchana and Putorana regional horizons.

Let us consider now the paleontologic characteristics and age substantiation of the stratotype of the Taimyr Stage. The authors did not draw inferences about these issues. They only listed the plant and conchostracan remains. In the Kholid'e Formation, the following plant remains were recorded: *Neokoretrophyllites* (?) cf. *triassica* (Radcz.), *Lepidopteris* cf. *arctica* Mog., scarce cf. *Pleuromeia taimyrica* Sad., *Boweria?* sp., *Marattiopsis?* sp., *Todites?* sp., *Acrostichides* cf. *kirjamkensis* Pryn., *Peltaspermum* sp., *Ginkgo* sp., *Carpolithes* ex gr. *cinctus* Nath., *C.* ex gr. *minor* Pryn., and *Elatocladus?* sp. The lower part of lava beds yielded remains of coniferous *Quadrocladus pachyphyllus* (Pryn.), whereas the second lava sequence contains rare *Neokoretrophyllites?* sp., *Neocalamites?* cf. *triassic* (Radcz.), *Equisetites?* sp., *Radicites* sp., *Tomiostrobus belozerovii* Sadovn. = *T. migayi* (Schved.), *Cladophlebis?* sp., *Lepidopteris* cf. *arctica* Mog., *Taeniopteris* sp., *Carpolithes* ex gr. *cinctus* Nath., *C.* cf. *zwetkoviensis* Mog. and conchostracan remains. According to Sadovnikov, a similar assemblage was recovered from the undivided Zverinaya and Betlinga formations in the Kiryaka-Tas section (Egorov and

Kulikova, 1989). Floral assemblages from the "Kholid'e" Formation and the lava sequence are similar in composition.[1] They are composed of representatives of the Early Triassic lepidophytic and Korvunchana floras. I should mention that *Tomiostrobus* and *Pleuromeia*, universally characteristic of the Lower Triassic sediments and never occurring in the Permian, dominate in the lepidophytic flora of central Siberia. The occurrence of both genera in the Kiryaka-Tas section indicates only the Early Triassic age of the deposits distinguished as a new Permian stage. The floral assemblage from the Kholid'e Formation is closely similar to that from the stratotype of the Keshi Formation in the Triassic section of the Tsvetkova Cape in eastern Taimyr, where the Induan foraminifers were recorded. All species of the Kholid'e assemblage, excluding forms identified in the open nomenclature with the question-mark, occur not only in the Keshi Formation, but also in the Syurbelyakh Formation of the Verkhoyansk region and in the lowermost Tutonchana Horizon of the volcanogenic sequence in the Tunguska basin (Table 2). This indicates the identical level of these sediments and their Induan age (Mogucheva, 1986). Remains of coniferous *Quadrocladus* in the lower lava bed of the Kiryaka-Tas Range permit the correlation of this part of the section most likely with the lower part of the Dvurogii Horizon overlying the Tutonchana Horizon. Finally, *Tomiostrobus* remains from the second lava sequence underlying the Fad'yukuda Formation with Induan bivalves *Promyalina schamarae* Bitt., indicate that this sequence is attributable to the Induan stage as well. The underlying Zverinaya Formation bearing the Korvunchana plant remains (Vladimirov *et al.*, 1990), is of the same age.

Therefore, the stratotype of the so-called Permian Taimyr Stage is of the Early Triassic, exactly Induan age. It corresponds to the Tutonchana and, most likely, to the lower part of the Dvurogii horizons of the Tunguska basin. The Induan age of these horizons was established on the basis of ostracode and charophyte remains (Kukhtinov and Neustrueva, 1986; Saidakovskii, 1990).

In the Tunguska basin, the Dvurogii and Putorana horizons were assigned to the Taimyr stage. This means that the "Taimyr Stage" is of different age in the Taimyr and Tunguska syneclise and corresponds to different stratigraphic intervals of the volcanogenic sequence.

In Taimyr, the stratotype of the stage appears to be older than in the Tunguska basin. Such unit can hardly be accepted as a valid subdivision, especially because there are no grounds to distinguish a new Permian stage. Moreover, none of the intervals of the section with the Korvunchana and lepidophytic floras could be Permian in age, even if it would be younger than the Tatarian Stage.

Table 3. Comparison of the Tutonchana flora with the Late Permian, Triassic, and Jurassic floras of Eurasia

Tutonchana flora	1	2	3	4	5	6	7	8
Mesenteriophyllum			+	+	+	+		
Tomiostrobus			+	+	+			
Neokoretrophyllus			+					+
Gamophyllites		+						
Tschernovia		+						
Paracalamites		+	+	+	+	+	+	
Neocalamites			+		+	+	+	+
Schizoneura			+		+	+	+	+
Prynadaia						+		
Equisetites				+	+	+	+	+
Osmundopsis							+	+
Todites		+	+			+	+	+
Lobifolia			+				+	+
Cladophlebis		+	+	+	+	+	+	+
Pecopteris?		+	+		+	+	+	
Sphenopteris		+	+	+		+	+	+
Kchonomakidium			+	+				
Prynadaeopteris		+	+					
Korvunchania			+					
Katasiopteris			+					
Tersiella–Tatarina	+		+				+	
Peltaspermum	+					+	+	
Taeniopteris			+	+	+	+	+	+
Ctenopteris							+	+
Yavorskyia		+	+					
Tomia		+	+					
Leuthardtia	+					+		
Clossophyllum			+			+	+	
Ginkgo						+	+	+
Rhipidopsis		+	+					
Yuccites			+		+	+	+	

Note: (1) *Tatarina* flora from the Russian platform; (2) Late Permian flora of Siberia; (3) Mal'tsevo flora from the Kuznetsk basin; (4) lepidophytic flora from central Siberia; (5) Buntsandstein flora from Western Europe; (6) Keuper floras; (7) Late Triassic floras; (8) Early Jurassic floras.

The considered data contradict the statement about the evident similarity between the Vyatka and Tutonchana floras and about the late Tatarian age of the latter (Sadovnikov and Orlova, 1990; 1994). Table 3 shows the comparison of the generic composition of the Korvunchana flora with the Permian, Triassic, and Jurassic floras of Eurasia. It is evident from the table that the similarity of the Vyatka and Tutonchana floras is lim-

[1] There are some incorrect identifications in the assemblages cited above. The species *Paracalamites triassica* Radcz. was listed for unknown reasons under different generic names: *Neokoretrophyllites?* and *Neocalamites?*. *Sphenopteris kirjamkensis* Pryn. was incorrectly defined as *Acrostichides*, the Late Triassic genus now discredited.

Table 4. Distribution of major plant species in the volcanogenic sequence of the Tunguska Basin and in the Mal'tsevo Formation of the Kuznetsk basin

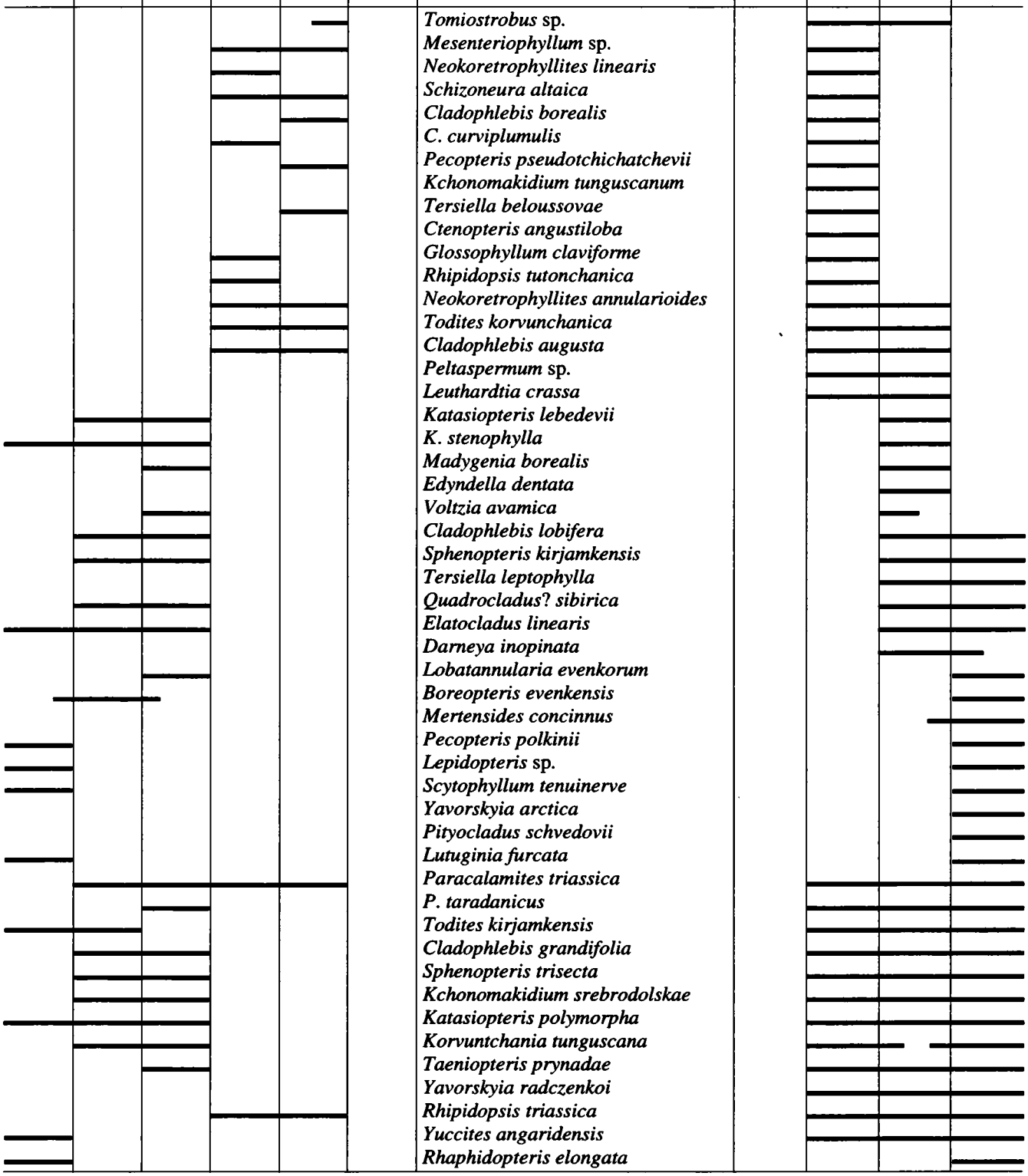

Note: (1) Tarakanikha Beds, (2) Barsuch'ya Beds; (3) Kedrovka Beds; (4) Ryaboi Kameshek Beds of the Mal'tsevo Formation, (5) Sosnovka Formation, (6) Tutonchana Horizon, (7) Dvurogii Horizon, (8) Putorana Horizon.

ited to three transitional genera. The floras are totally different in composition, have not common species, and "...the miospore assemblages of enclosing sediments sufficiently differ as well" (Goman'kov and Meyen, 1986, p. 154). The Tutonchana and the Korvunchana flora as a whole contain many genera characteristic of the Triassic (from 6 to 16 genera) and even of the Jurassic (11 genera) floras. The Korvunchana flora is most similar to the Early Triassic flora of the Mal'tsevo Formation from the Kuznetsk basin. This similarity is evident at both the generic (about 30 common genera) and specific (about 40 species) levels. It is manifested as well in similar stages of evolution (Tables 3 and 4). The Tutonchana assemblage includes 20 genera and 15 species identical to taxa of the Tarakanikha–Barsuch'ya assemblage from the Mal'tsevo Formation of the Kuznetsk basin. This is obviously more important and decisive evidence substantiating the age of the Tutonchana and Korvunchana flora as a whole than the doubtful similarity to the Vyatka flora.

In the light of these data, the correlation of the Mal'tsevo Formation with the volcanogenic sequence of the Tunguska basin (Goman'kov and Meyen, 1986), when "...the Tarakanikha Beds should be correlated... and attributed to the Upper Putorana Subhorizon" (Sadovnikov, 1981, p. 80), is unjustified and invalid. The following statements seem particularly astonishing: "...there is no evidence in favor of the Induan age of the Tutonchana Horizon..." and "...almost all the available data on bivalve mollusks, ostracodes, and insects also argue for the Permian age of the Tutonchana Horizon..." (Sadovnikov and Orlova, 1990, p. 69). Actually, the Early Triassic age of the horizon is supported by the data on bivalves (Betekhtina and Mogucheva, 1984), and its Induan age is confirmed by data on ostracodes (Kukhtinov and Neustrueva, 1986) and on charophyte–ostracode assemblages (Saidakovskii, 1990).

Charophytes have been collected from the lower part of the Tutonchana Formation in the outcrop at the Nizhnyaya Tunguska River opposite the Gagarii Island and from the lowermost Marininskii Formation in eastern Taimyr. They were studied by Saidakovskii (1990). In the Tutonchana Formation, he identified the charophyte assemblage typical, in his opinion, of the *Vladimiriella karpinskyi* Zone I of the Lower Triassic, and associated with ostracodes *Gerdalia* and *Darwinula*. The index species of the same zone was recorded in the Marininskii Formation. According to Saidakovskii, the Tutonchana and Marininskii formations are of the early Induan age.

The Marininskii Formation distinguished by G.P. Kochetkov in 1944 near the Tsvetkova Cape on the Marininskii Creek we consider following the conclusion of Migai (1952) as a part of the extrusive tuffite sequence in the section of the Tsvetkova Cape in eastern Taimyr, which is now termed the Keshi Formation. These formations are exposed on different flanks, northern and southern, of the same anticline, and their floral assemblages are very similar. In the section on the Marininskii Creek, I detected *Mesenteriophyllum* sp., *Tomiostrobus migayi* (Schved.), *Paracalamites* sp., *Cladophlebis* ex gr. *parvus* Mog., *C.* spp., *Sphenopteris* cf. *kirjamkensis* Pryn., *Kchonomakidium* sp., *Lepidopteris arctica* Mog., *Peltaspermum* sp., *Nilssonia* sp. nov., *Glossophyllum* sp., *Yuccites* sp., *Samaropsis* sp. nov., and *Carpolithes* sp. Most forms of the assemblage also occur in the Keshi Formation.

The data of Saidakovskii are of a great importance. They indicate that the lower Induan deposits occur in Taimyr and Tunguska basin, and confirm the Induan age of the Tutonchana Horizon and its correlation with the Induan sediments of the Taimyr and Verkhoyansk regions. They substantially and reliably prove that the Permian–Triassic boundary in the Tunguska basin is at the base, but not at the top of the volcanogenic sediments.

CONCLUSION

The considered data permit the following conclusions:

(1) Sediments distinguished as a stratotype of the new Permian stage are Triassic in age and correspond to the Induan Stage. They are correlative with the Tutonchana and, most likely, with the lowermost part of the Dvurogii Horizon. In the Tunguska syneclise the "Taimyr Stage" includes sediments of a higher stratigraphic level: the Dvurogii and Putorana horizons. Therefore, the diachronous Triassic sediments of different regions were attributed to the Taimyr Stage.

(2) The Tutonchana Horizon corresponds not to the Vyatka Horizon of the Russian platform, but to the lower part of the Mal'tsevo Formation of the Kuznetsk basin in the range of the Tarakanikha and Barsuch'ya beds. Their floral assemblages are almost identical. According to Neustrueva, the ostracode assemblages from the Tarakanikha Beds are very close to those from the Tutonchana Horizon. The Induan age of these deposits is established by their correlation with the sections of the Verkhoyansk and eastern Taimyr regions, and on the basis of charophytes typical of the lower Induan zone and coexisting ostracodes.

(3) The position of the Induan volcanogenic and tuffaceous sedimentary deposits above the Permian coal-bearing sediments with the cordaitean flora of the Tatarian Stage shows that any pre-Triassic beds between the known Permian and Triassic units are missing. The suggested "Taimyr Stage" has no valid ground and its recognition is senseless.

(4) All the discussed data undoubtedly suggests the Triassic but not Permian age of the volcanogenic deposits of the Tunguska syneclise and Taimyr. The position of the Permian-Triassic boundary is at the base of these deposits but not at their top.

Reviewers M.V. Durante and M.A. Akhmet'ev

REFERENCES

Betekhtina, O.A. and Moguchevа, N.K., On the Age of the Volcanogenic Sequence of the Tunguska Syneclise, in *Stratigrafiya, fauna i flora triasa Sibiri* (Triassic Stratigraphy, Fauna, and Flora of Siberia), Moscow: Nauka, 1984, pp. 4–8.

Dagis, A.S., Egorov, A.Yu., Kazakov, A.M., *et al.*, Triassic Stratigraphy of Southeastern Taimyr, in *Verkhnii paleozoi i trias Sibiri* (The Upper Paleozoic and Triassic of Siberia), Novosibirsk: Nauka, 1989, pp. 71–91.

Dobruskina, I.A. and Moguchevа, N.K., On the Age of the Volcanogenic Deposits in the Tunguska Syneclise, *Geol. Geofiz.*, 1987, no. 1, pp. 29–36.

Egorov, A.Yu. and Kulikova, L.I., Stratigraphic Position of the Early Triassic Traps in Taimyr, in *Verkhnii paleozoi i trias Sibiri* (The Upper Paleozoic and Triassic of Siberia), Novosibirsk: Nauka, 1989, pp. 91–103.

Goman'kov, A.V. and Meyen, S.V., *Tatarinovaya flora* (The *Tatarina* Flora), Moscow: Nauka, 1986.

Kukhtinov, D.A. and Neustrueva, I.Yu., Stratigraphic Significance of Ostracods, in *Parastratigraficheskie gruppy flory i fauny triasa* (Parastratigraphic Groups of the Triassic Flora and Fauna), Leningrad: Nedra, 1986, pp. 162–170.

Migai, I.M., Geological Structure of the Mys Tsvetkova Area, Eastern Taimyr, *Tr. Nauch.-Issled. Inst. Geol. Arktiki Glavsevmorputi*, 1952, vol. 36, p. 60.

Moguchevа, N.K., Correlation of the Lower Triassic Deposits in Central Siberia Using Floral Data, in *Regional'nye i mestnye stratigraficheskie podrazdeleniya dlya krupnomasshtabnogo geologicheskogo kartirovaniya* (Regional and Local Stratigraphic Units for the Large-Scale Geological Mapping), Novosibirsk: Sovm. Nauch.-Issled. Inst. Geol. Geofiz. Mineral. Syr'ya, 1986, pp. 89–97.

Sadovnikov, G.N. and Orlova, E.F., Age of the Continental Volcanogenic Sequences in the North of Central Siberia, *Izv. Akad. Nauk SSSR, Ser. Geol.*, 1990, no. 3, pp. 58–70.

Sadovnikov, G.N. and Orlova, E.F., The Taimyr Stage as a Terminal One in the Continental Permian, *Dokl. Akad. Nauk*, 1994, vol. 338, no. 5, pp. 658–661.

Sadovnikov, G.N., Orlova, E.F., and Belozerov, V.P., A Transition from the Permian to Triassic in the Continental Deposits of Taimyr and Western Verkhoyansk Region, *Izv. Akad. Nauk SSSR, Ser. Geol.*, 1981, no. 5, pp. 53–64.

Sadovnikov, G.N., Upper Permian and Lower Triassic Regional Stratigraphic Subdivisions of Siberian Platform and Adjacent Regions, *Sov. Geol.*, 1981, no. 6, pp. 74–84.

Saidakovskii, L.Ya., *Biostratigraficheskaya korrelyatsiya triasovykh otlozhenii Evrazii po kharofitam* (Biostratigraphic Correlation of Triassic Deposits in Eurasia on the Basis of Charophytes), Syktyvkar: Inst. Geol. Komi Nauch. Tsentr, Ural. Otd. Akad. Nauk SSSR, 1990, pp. 60–62.

Vavilov, M.N., Kulikova, N.K., and Golovin, S.V., The Triassic Stratigraphy of Central Taimyr, in *Bio- i litostratigrafiya mezozoya neftegazonosnykh raionov SSSR* (Mesozoic Bio- and Lithostratigraphy of the Oil- and Gas-bearing Areas of the USSR), Leningrad: Vses. Nauch.-Issled. Geol.-Razved. Inst., 1990, pp. 4–14.

Vladimirov, A.E., Moguchevа, N.K., Nikulov, L.P., and Romanov, A.P., On Subdivision of the Permian–Triassic Volcanogenic Deposits in Western Taimyr, in *Trias Sibiri* (The Triassic of Siberia), Novosibirsk: Nauka, 1990, pp. 4–13.

Subscribe to the journals from the Russian Academy of Sciences

Translated and Published by МАИК Наука/Interperiodica Publishing

Distributed Worldwide by INTERPERIODICA

Copy this form to mail or fax your order today

	TITLE	Volume	ISSN	ISSUES	RATE IN US DOLLARS US/CAN	INTERNATIONAL	YOUR ORDER
❑	**Agricultural Chemistry**	2	Pending	4	$514	$593	$ _____
❑	**Biophysics**	43	0006-3509	6	$2265	$2355	$ _____
❑	**Computational Mathematics and Mathematical Physics**	38	0965-5425	12	$1979	$2409	$ _____
❑	**Doklady Mathematics**	57/58	1064-5624	6	$1198	$1378	$ _____
❑	**Entomological Review**	78	0013-8738	9	$1857	$2136	$ _____
❑	**Environmental Geoscience**	1	Pending	4	$520	$590	$ _____
❑	**Eurasian Soil Science**	31	1064-2293	12	$1756	$2020	$ _____
❑	**Geochemistry International**	36	0016-7029	12	$1980	$2277	$ _____
❑	**Geology of Ore Deposits**	40	1075-7015	6	$839	$964	$ _____
❑	**Geotectonics**	32	0016-8521	6	$487	$529	$ _____
❑	**Herald of the Russian Academy of Sciences**	68	1019-3316	6	$1138	$1446	$ _____
❑	**Izvestiya, Atmospheric andOceanic Physics**	34	0001-4338	6	$678	$728	$ _____
❑	**Izvestiya, Physics of the Solid Earth**	34	1069-3513	12	$714	$786	$ _____
❑	**Journal of Communications Technology and Electronics**	43	1064-2269	12	$2300	$2645	$ _____
❑	**Journal of Computer and Systems Sciences International**	37	1064-2307	6	$1837	$2113	$ _____
❑	**Journal of Ichthyology**	38	0032-9452	9	$1596	$1835	$ _____
❑	**Laser Physics**	8	1054-660X	6	$953	$1150	$ _____
❑	**Oceanology**	38	0001-4370	6	$603	$650	$ _____
❑	**Paleontological Journal**	32	0031-0301	6	$1192	$1371	$ _____
❑	**Pattern Recognition & Image Analysis**	8	1054-6618	4	$599	$688	$ _____
❑	**Petroleum Chemistry**	38	0965-5441	6	$2478	$2578	$ _____
❑	**Petrology**	6	0869-5911	6	$839	$964	$ _____
❑	**Polymer Science. Series A**	40	0965-545X	12	$2265	$2609	$ _____
❑	**Polymer Science. Series B**	40	Pending	6	$859	$989	$ _____
	Both Series A & B. $200 discount				$2924	$3398	$ _____
❑	**Proceedings of the Steklov Institute of Mathematics**	220-223	0081-5438	4	$880	$1014	$ _____
❑	**Russian Forest Sciences**	32	1068-669X	4	$460	$530	$ _____
❑	**Russian Journal of Inorganic Chemistry**	43	0036-0236	12	$2345	$2697	$ _____
❑	**Russian Journal of Physical Chemistry**	72	0036-0244	12	$2345	$2697	$ _____
❑	**Russian Journal of Zoology**	2	Pending	4	$504	$577	$ _____
❑	**Stratigraphy and Geological Correlation**	6	0869-5938	6	$839	$964	$ _____
❑	**Studies on Russian Economic Development**	9	1075-7007	6	$604	$695	$ _____
❑	**The Physics of Metals and Metallography**	85/86	0031-918X	12	$2045	$2353	$ _____
❑	**Thermophysics and Aeromechanics**	5	0869-8643	4	$559	$670	$ _____
❑	**Thermal Engineering**	45	0040-6015	12	$1306	$1502	$ _____
❑	**Doklady Earth Sciences**	358-363A	1028-334X	9	$2515	$2893	$ _____
						TOTAL	_____

❶ Name _____

Institution _____

Address _____

_____ State _____

City _____ Country _____

Zip/Postal Code _____

Telephone(_____)

Delivery is not made until payment is received

To order by phone call **1 800 633-4931**

or (205) 995-1567 outside the US and Canada

❷ ❑ My payment for $_____ is enclosed.

OR

❑ Bill me. My library's purchase order number is _____

❸ Send this order and payment to:

INTERPERIODICA

P.O. Box 1831

Birmingham, AL 35201-1831

Or fax this order form to (205) 995-1588

Order now for immediate delivery. All journals will be published in 1998!

МАИК НАУКА/INTERPERIODICA PUBLISHING

is pleased to present to the international scientific community simultaneous Russian- and English-language publication of the journals of the Russian Academy of Sciences

МАИК НАУКА (NAUKA International Academic Publishing Company), in cooperation with the Russian Academy of Sciences, publishes the results of research in all fields of modern science performed by leading scientists and scientific institutions from Russia, the CIS, and other countries. Simultaneous English translation of the journals is provided by INTERPERIODICA Publishing, the translation division of МАИК НАУКА. Today, scientists around the world have direct access to the most significant Russian research at the time it is first published in Moscow – at the time it is most relevant to the worldwide scientific community. In addition to more timely publication, readers benefit from more precise translations of each journal, provided by a carefully chosen team of scientific translators with direct access to the authors and editors. English versions of the journals published by МАИК НАУКА/INTERPERIODICA PUBLISHING are distributed worldwide by INTERPERIODICA, Plenum/Consultants Bureau, and the American Institute of Physics.

МАИК НАУКА 1998 volumes include the following titles:

- *Agricultural Chemistry*
- *Biophysics*
- *Computational Mathematics and Mathematical Physics*
- *Doklady Mathematics*
- *Entomological Review*
- *Environmental Geoscience*
- *Eurasian Soil Science*
- *Geology of Ore Deposits*
- *Geochemistry International*
- *Geotectonics*
- *Herald of the Russian Academy of Sciences*
- *Izvestiya, Atmospheric and Oceanic Physics*
- *Izvestiya, Physics of the Solid Earth*
- *Journals of Communications Technology and Electronics*
- *Journal of Computer and Systems Sciences International*
- *Journal of Ichthyology*
- *Laser Physics*
- *Oceanology*
- *Paleontological Journal*
- *Pattern Recognition and Image Analysis*
- *Petroleum Chemistry*
- *Petrology*
- *Polymer Science, Series A*
- *Polymer Science, Series B*
- *Proceedings of the Steklov Institute of Mathematics*
- *Russian Forest Sciences*
- *Russian Journal of Inorganic Chemistry*
- *Russian Journal of Physical Chemistry*
- *Russian Journal of Zoology*
- *Stratigraphy and Geological Correlation*
- *Studies on Russian Economic Development*
- *The Physics of Metals and Metallography*
- *Thermophysics and Aeromechanics**
- *Thermal Engineering*
- *Doklady Earth Sciences*

Please direct all inquiries about the above journals to: **INTERPERIODICA**, P.O. Box 1831, Birmingham, AL 35201-1831. For faster service call toll-free (800) 633-4931 or (205) 995-1567 (outside US and Canada). Fax: (205) 995-1588.
* *Thermophysics and Aeromechanics*: Only distributed by МАИК НАУКА/Interperiodica

- *Applied Biochemistry and Microbiology*
- *Biochemistry (Moscow)*
- *Biology Bulletin*
- *Colloid Journal*
- *Cosmic Research*
- *Doklady Biochemistry*
- *Doklady Biological Sciences*
- *Doklady Biophysics*
- *Doklady Botanical Sciences*
- *Doklady Chemical Technology*
- *Doklady Chemistry*
- *Doklady Physical Chemistry*
- *Glass Physics and Chemistry*
- *High Energy Chemistry*
- *High Temperature*
- *Human Physiology*
- *Inorganic Materials*
- *Instruments and Experimental Techniques*
- *Journal of Evolutionary Biochemistry and Physiology*
- *Journal of Analytical Chemistry*
- *Kinetics and Catalysis*
- *Lithology and Mineral Resources*
- *Microbiology*
- *Molecular Biology*
- *Programming and Computer Software*
- *Protection of Metals*
- *Radiochemistry*
- *Russian Journal of Applied Chemistry*
- *Russian Journal of Bioorganic Chemistry*
- *Russian Journal of Coordination Chemistry*
- *Russian Journal of Developmental Biology*
- *Russian Journal of Ecology*
- *Russian Journal of Electrochemistry*
- *Russian Journal of General Chemistry*
- *Russian Journal of Genetics*
- *Russian Journal of Marine Biology*
- *Russian Journal of Organic Chemistry*
- *Russian Journal of Plant Physiology*
- *Russian Microelectronics*
- *Solar System Research*
- *Theoretical Foundations of Chemical Engineering*
- *Water Resources*

Please direct all inquiries about the above journals to: **Plenum/Consultants Bureau**, 233 Spring Street, New York, NY 10013. Phone: (212) 620-8467. Fax: (212) 807-1047.

- *Acoustical Physics*
- *Astronomy Reports*
- *Astronomy Letters*
- *Crystallography Reports*
- *Optics and Spectroscopy**
- *Doklady Physics*
- *Physics of Atomic Nuclei*
- *Plasma Physics Reports*

Please direct all inquiries about the above journals to: **American Institute of Physics**, Circulation and Fulfillment Services, 500 Sunnyside Boulevard, Woodbury, NY 11797-2999 USA. Tel. (516) 576-2270, (800) 344-6902. Fax: (516) 349-9704.
* *Optics and Spectroscopy*: Optical Society of America, 2010 Massachusetts Ave., NW, Washington, DC 20036-1023, Attn.: Publications Department. Tel. (202) 223-8130, (800) 582-0416. Fax: (202) 223-1096.

МАИК Наука/Interperiodica Publishing (International Academic Publishing Co. "Nauka")
Profsoyuznaya ul., 90, Moscow, 117864, Russia, Phone: 7 (095) 3361600; Fax: 7 (095) 336 0666, E-mail:compmg@maik.rssi.ru